UNCLASSIFIED

AD NUMBER
ADB130470
LIMITATION CHANGES
TO: **Approved for public release; distribution is unlimited.**
FROM: **Distribution authorized to DoD only; Software Documentation; MAR 1988. Other requests shall be referred to Air Force Wright Aeronautical Laboratories, Attn: FIBRA, Wright-Patterson AFB, OH 45433-6553. This document contains export-controlled technical data.**
AUTHORITY
WL/DOOS ltr dtd 19 Sep 1991

THIS PAGE IS UNCLASSIFIED

AFWAL-TR-88-3028
Volume III

AUTOMATED STRUCTURAL OPTIMIZATION SYSTEM (ASTROS)

VOLUME III - APPLICATIONS MANUAL

E. H. JOHNSON
D. J. NEILL
Northrop Corporation, Aircraft Division
Hawthorne, California 90250

December 1988

FINAL REPORT FOR PERIOD JULY 1983 - JULY 1988

Distribution authorized to DOD components only; software documentation, March 1988. Other requests for this document must be referred to AFWAL/FIBRA, WPAFB OH 45433-6553. Requests must include a Statement of Terms and Conditions--Release of Air Force-Owned or Developed Computer Software Packages. (See block 16 of DD Form 1473 herein.)

<u>WARNING</u> - This document contains technical data whose export is restricted by the Arms Export Control Act (Title 22, U. S. C., Section 2751, <u>et seq</u>.) or The Export Administration Act of 1979, as amended, Title 50, U. S. C., App. 2401, <u>et seq</u>. Violations of these export laws are subject to severe criminal penalties. Disseminte in accordance with the provisions of AFR 80-34. (Include this statement with any reproduced portion.)

<u>DESTRUCTION NOTICE</u> - Destroy by any method that will prevent disclosure of contents or reconstruction of the document.

FLIGHT DYNAMICS LABORATORY
AIR FORCE WRIGHT AERONAUTICAL LABORATORIES
AIR FORCE SYSTEMS COMMAND
WRIGHT-PATTERSON AIR FORCE BASE, OHIO 45433-6553

NOTICE

When Government drawings, specifications, or other data are used for any purpose other than in connection with a definitely Government-related procurement, the United States Government incurs no responsibility or any obligation whatsoever. The fact that the Government may have formulated or in any way supplied the said drawings, specifications, or other data, is not to be regarded by implication, or otherwise as in any manner, as licensing the holder or any other person or corporation; or as conveying any rights or permission to manufacture, use, or sell any patented invention that may in any way be related thereto.

This technical report has been reviewed and is approved for publication.

R. A. Canfield

ROBERT A. CANFIELD, Capt, USAF
Aerospace Engineer
Design & Analysis Methods Group

Nelson D. Wolf

NELSON D. WOLF, Technical Manager
Design & Analysis Methods Group
Analysis & Optimization Branch
Structures Division

FOR THE COMMANDER

John T. Ach

JOHN T. ACH, Chief
Analysis & Optimization Branch
Structures Division
Flight Dynamics Laboratory

"If your address has changed, if you wish to be removed from our mailing list, or if the addressee is no longer employed by your organization please notify AFWAL/FDSRA, WPAFB, OH 45433-6553 to help us maintain a current mailing list".

Copies of this report should not be returned unless return is required by security considerations, contractual obligations, or notice on a specific document.

UNCLASSIFIED

SECURITY CLASSIFICATION OF THIS PAGE

REPORT DOCUMENTATION PAGE

1a. REPORT SECURITY CLASSIFICATION UNCLASSIFIED	1b. RESTRICTIVE MARKINGS
2a. SECURITY CLASSIFICATION AUTHORITY 2b. DECLASSIFICATION / DOWNGRADING SCHEDULE	3. DISTRIBUTION / AVAILABILITY OF REPORT Distr. autb. t DOD components only; software documentation, March 88. Other requests for this doc. shall referred to AFWAL/FIBRA, WPAFB, OH 45433-655
4. PERFORMING ORGANIZATION REPORT NUMBER(S) NOR 88-14	5. MONITORING ORGANIZATION REPORT NUMBER(S) AFWAL-TR-88-3028, Volume III
6a. NAME OF PERFORMING ORGANIZATION Northrop Corporation Aircraft Division 6b. OFFICE SYMBOL (If applicable) 3854/82	7a. NAME OF MONITORING ORGANIZATION Flight Dynamics Laboratory (AFWAL/FIBR) Air Force Wright Aeronautical Laboratories
6c. ADDRESS (City, State, and ZIP Code) Hawthorne, California 90250-3277	7b. ADDRESS (City, State, and ZIP Code) Wright-Patterson Air Force Base, Ohio 45433-6553
8a. NAME OF FUNDING / SPONSORING ORGANIZATION 8b. OFFICE SYMBOL (If applicable)	9. PROCUREMENT INSTRUMENT IDENTIFICATION NUMBER F33615-83-C-3232
8c. ADDRESS (City, State, and ZIP Code)	10. SOURCE OF FUNDING NUMBERS PROGRAM ELEMENT NO 62201F; PROJECT NO. 2401; TASK NO 02; WORK UNIT ACCESSION NO 57

11. TITLE (Include Security Classification)
AUTOMATED STRUCTURAL OPTIMIZATION SYSTEM (ASTROS)
VOLUME III - APPLICATIONS MANUAL

12. PERSONAL AUTHOR(S)
Johnson, E.H., and Neill, D.J.

13a. TYPE OF REPORT	13b. TIME COVERED	14. DATE OF REPORT (Year, Month, Day)	15. PAGE COUNT
Final	FROM 7/83 TO 7/88	1988, December	253

16. SUPPLEMENTARY NOTATION Copies of Statement of Terms and Conditions -- Release of Air Force - Owned or Developed Computer Software Packages will be furnished upon request to AFWAL/IST WPAFB, OH 45433-6553, Export Control Restrictions.

17. COSATI CODES		
FIELD	GROUP	SUB-GROUP
01	03	03
01	01	03

18. SUBJECT TERMS (Continue on reverse if necessary and identify by block number)
AUTOMATED DESIGN, STRUCTURAL ANALYSIS, MULTIDISCIPLINARY ANALYSIS, FLUTTER ANALYSIS, DYNAMIC ANALYSIS. (JES)

19. ABSTRACT (Continue on reverse if necessary and identify by block number)

The ASTROS (Automated STRuctural Optimization System) procedure provides a multidisciplina analysis and design capability for aerospace structures. The engineering analysis capabil ities in the system include structural analysis (static and dynamic), aeroelastic analysis (static and dynamic) and automated design. A specifically designed data base and executiv system were implemented to maximize the system's efficiency, flexibility, and maintainability.

The final report consists of four volumes:

Volume I - ASTROS Theoretical Manual
Volume II - ASTROS User's Manual
Volume III - ASTROS Applications Manual
Volume IV - ASTROS Programmer's Manual

(Continued on the reverse side of this form)

20. DISTRIBUTION / AVAILABILITY OF ABSTRACT ☐ UNCLASSIFIED/UNLIMITED ☐ SAME AS RPT. ☒ DTIC USERS	21. ABSTRACT SECURITY CLASSIFICATION UNCLASSIFIED	
22a. NAME OF RESPONSIBLE INDIVIDUAL Capt. R.A. Canfield	22b. TELEPHONE (Include Area Code) (513) 255-6992	22c. OFFICE SYMBOL AFWAL/FIBRA

19. (Continued)

This report is the Applications Manual for the ASTROS system. As such, it provides documentation sources, as well as guidelines and examples for the use of ASTROS. The guidelines emphasize aspects of data preparation that are unique to ASTROS, such as the definition of the design model and the steady aerodynamics input. A series of examples provides further definition of key ASTROS features and clarifies input requirements. An Appendix contains an example of the insertion of a new module into ASTROS.

FOREWORD

Contract F33615-83-C-3232, entitled "Automated Strength-Aeroelastic Design of Aerospace Structures," was initiated by the Analysis and Optimization Branch (FIBR) of the Air Force Wright Aeronautical Laboratories. The objective of this contract was to develop a computer procedure which can assist significantly in the preliminary automated design of aerospace structures. This report, which is one of a four volume final report, is the Applications Manual for the delivered computer procedure.

Northrop Corporation, Aircraft Division, was the primary contractor for this program with Dr. E. H. Johnson, the Program Manager, and Mr. D. J. Neill, the Project Co-Principal Investigator. Subcontractors for the program were Universal Analytics, Incorporated (UAI), with Mr. D. L. Herendeen the UAI Project Manager, and Kaman AviDyne, with Dr. J R. Ruetenik, the Project Manager. At the Air Force, Capt. R. A. Canfield was the Project Manager while Dr. V. B. Venkayya initiated the program and provided overall program direction.

TABLE OF CONTENTS

TABLE OF CONTENTS

SECTION I

INTRODUCTION

This Applications Manual is one of four manuals documenting the ASTROS (Automated STRuctural Optimization System). The other three manuals are the Theoretical Manual, the User's Manual and the Programmer's Manual. The Theoretical Manual provides an overview of the technology that has been incorporated into this multidisciplinary design procedure while the User's Manual describes the input requirements and output features of the procedure. The Programmer's Manual provides details on the internal workings of the engineering modules. The primary purpose of this Applications Manual is to provide guidelines and examples for the use of ASTROS.

Section II of this report identifies source material that provides details on the various disciplines that have been incorporated into ASTROS. Many of these sources are also identified in the ASTROS Theoretical Manual, but this manual is more comprehensive in its citations and in its descriptions of the referenced documents. Section III offers modeling guidelines for the development of ASTROS input. Since NASTRAN formats were adapted for the ASTROS input data and since NASTRAN based methodologies were implemented extensively in ASTROS, the guidelines provided in this manual emphasize aspects of the data preparation that are unique to ASTROS. In particular, data required in the definition of the design model is described in detail. The steady aerodynamics capability in ASTROS is also unique and is therefore fully described. Other areas represent perturbations on the NASTRAN formulations so that details are provided in this report that are intended to complement extensive existing NASTRAN documentation.

Section IV contains a series of sample cases. The numerous options in ASTROS makes it impossible, both in terms of the manpower required and in terms of the amount of documentation that would be required, to present a comprehensive set of examples. Instead, an attempt has been made to address key options and provide examples that a potential user can refer to for help in modeling more extensive cases. The test cases given in this document are,

for the most part, quite small. This provides the user with the essence of the ASTROS capabilities, but they may be deficient in terms of physical meaningfulness. The test cases presented here have also been included in the delivery of the software to the Air Force and should therefore be available electronically to interested parties.

SECTION II

DOCUMENTATION RESOURCES

The multidisciplinary design procedure developed for ASTROS involves itself, by definition, with a number of technologies, each of which has a large body of literature associated with it. The documentation provided for ASTROS, while seemingly extensive, cannot begin to give a comprehensive description of each of the disciplines it contains. This fact is recognized throughout the ASTROS documentation by reference to related documentation that provides more detailed descriptions. The primary motivation for including a documentation subsection in this manual is to bring this information together, while providing added detail on the information contained in each of the cited documents. A secondary motivation is that a discussion of these documents can provide insight into the development of ASTROS, since the documents that are cited are essentially the ones that were used to develop the engineering technologies that have been integrated into this procedure. The remainder of this section is divided into subsections that relate to the ASTROS engineering disciplines in a format that basically follows the discussion of these disciplines that is contained in the Theoretical Manual.

2.1 STRUCTURAL ANALYSIS

The impact of the NASTRAN procedure on the development of ASTROS should be obvious. There are a number of alternative structural analysis procedures that could have provided a departure point for this program, but the NASTRAN procedure is widely accepted by the aerospace community at large, and the Northrop Corporation in particular, as the premier finite element structural analysis tool for aerospace structures. Once the decision had been made to emulate the NASTRAN formats for data entries, it was a logical next step to follow the NASTRAN terminology and basic programming structure in the development of the ASTROS procedure. It must be stressed, however, that ASTROS can in no way be considered a modification or enhancement to the NASTRAN procedure. It is, instead, a completely new system that started with no preconceptions or restraints for its development. From a programming standpoint,

NASTRAN served primarily as a model and it was found that many of the NASTRAN constructs were unnecessary, given the ASTROS data base system, or were unworkable in a multidisciplinary analysis and design context.

The term NASTRAN is used here to encompass all the related procedures that have as their roots the NASA sponsored effort to develop a general structural analysis tool given the acronym NAsa STRuctural ANalysis. Since the development of this code into the late 1960s, it has expanded into a widely used and maintained procedure with a number of versions available. The government sponsored version is now generally identified as COSMIC/NASTRAN, reflecting the fact that it is available from the Computer Software Management and Information Center located at the University of Georgia. COSMIC acts as a clearing house for the NASA Scientific and Technical Information Office and provides NASTRAN documentation and computer codes. Ongoing maintenance and enhancement of this procedure is performed by government funded contractors. Manuals that are available on this procedure include: (1) The NASTRAN Theoretical Manual, NASA SP-221 (06), 1981; (2) The NASTRAN User's Manual, NASA SP-222 (06), 1983; (3) The NASTRAN Programmer's Manual, NASA SP-223 (04), 1977; and (4) The NASTRAN Demonstration Problem Manual, NASA SP-224 (05), 1983.

These manuals undergo constant maintenance and are updated periodically. In the context of ASTROS development, the Theoretical and Programmer's Manuals were consulted extensively while the other two manuals were not used.

Commercial versions of the NASTRAN code have become available in recent years and two of these versions played a role in ASTROS development. The first is marketed by the MacNeal-Schwendler Corporation (MSC) of Pasadena, California and is referred to as MSC/NASTRAN. It is this version of NASTRAN that is used most extensively at Northrop and that was therefore emulated, to the extent possible, when matching the ASTROS code to NASTRAN. Extensive documentation for this code is available from the MacNeal-Schwendler Corporation that parallels the COSMIC/NASTRAN manuals listed above. In addition, a number of handbooks have been developed by MSC to aid in the use of specialized analyses within the procedure. Several of these handbooks are discussed in subsequent subsections. A textbook, based on MSC/NASTRAN, but that has general applicability in terms of the structural analysis methods it describes is:

Schaeffer, H.G., MSC/NASTRAN Primer: Statics and Normal Modes Analysis, Schaeffer Analysis, Inc., Mont Vernon, New Hampshire, 1979.

This text and the MSC/NASTRAN User's Manual were used extensively in the development of ASTROS.

The second commercial version is marketed by Universal Analytics, Inc. of Playa del Rey, California. Since UAI was a subcontractor to Northrop in the development of ASTROS, UAI/NASTRAN also influenced the development of ASTROS. Documentation available for this code includes a User's and a Demonstration Problem Manual.

In addition to the NASTRAN procedure, certain other texts were consulted for special purpose needs. For finite element analysis, the text:

Przemieniecki, J.S., Theory of Matrix Structural Analysis, McGraw-Hill Book Company, 1968

provided information basic to understanding these powerful techniques. Two texts:

Jones, R.M., Mechanics of Composite Materials, Scripta Book Co., Washington, D.C., 1975

Tsai, S.W. and Hahn, H.T., Introduction to Composite Materials, TECHNOMIC Publishing Co., Inc., Westport, CT, 1980

provided an entry into the area of composite materials.

2.2 STEADY AERODYNAMICS

The discipline of aerodynamics does not contain an industry standard procedure comparable to the NASTRAN procedure for structural analysis. Instead, a variety of procedures are in use throughout the industry based on government sponsored or in-house research. The USSAERO (Unified Subsonic and Supersonic Aerodynamics) procedure was selected for incorporation into ASTROS primarily, as discussed in Subsection 8.1 of the Theoretical Manual, because it was a code with which the Northrop developers had familiarity. Before citing sources for USSAERO, it is perhaps useful to discuss alternative procedures.

The trend in the calculation of aerodynamic response is toward the use of sophisticated computational fluid dynamics (CFD) techniques that solve the partial differential equations governing the flow at a large number of

discrete grid points in a manner somewhat analogous to the finite element method employed for structural analysis. These techniques are inappropriate for ASTROS since (1) the computing costs associated with these techniques would dwarf the remaining ASTROS disciplines and make the procedure prohibitively expensive at the preliminary design level and (2) the incorporation of elastically deforming structures into a CFD code is an area of ongoing research that has not matured to the extent that it could be incorporated into ASTROS. The CFD field is a very active area, with the following text a useful introduction to the topic:

> Anderson, D.A., Tannehill, J.C., and Fletcher, R.H., Computational Fluid Mechanics and Heat Transfer, Hemisphere Publishing Company, New York, New York, 1984

The primary alternative to CFD methods are methods based on solving for the pressure distribution on the air vehicle at a number of discrete panels. USSAERO is one of these panel procedures while PAN AIR

> Sidwell, K.W., Baruah, P.K., and Bussoletti, J.E., "PAN AIR, A Computer Program for Predicting Subsonic or Supersonic Linear Potential Flows about Arbitrary Configurations Using a Higher Order Panel Method," NASA CR-3252, May 1980.

and VSAERO

> Maskew, B., "Program VSAERO, A Computer Program for Calculating the Nonlinear Aerodynamic Characteristics of Arbitrary Configurations," NASA CR-166476, November 1982.

are available alternatives. PAN AIR is significantly more complex than USSAERO while the VSAERO code is proprietary. The USSAERO code was developed sequentially by several organizations and this is reflected in both the code and the documentation. The basic USSAERO procedure is documented in

> Woodward, F.A., "An Improved Methods for the Aerodynamic Analysis of Wing-Body-Tail Configurations in Subsonic and Supersonic Flow, Part I - Theory and Applications, Part II - Complete Program Description," NASA CR-2228, May 1973.

Part II was consulted extensively in incorporating this code into the ASTROS procedure since it contains the most comprehensive description of the USSAERO computer code.

An enhanced version of the code, identified as USSAERO-C, is described in:

Woodward, F.A., "USSAERO Computer Program Development, Versions B and C," NASA CR-3227, 1980

Modeling guidelines for applying the procedures that are discussed in Subsection 3.2.3 were obtained, in part, from this latter report.

2.3 UNSTEADY AERODYNAMICS

The calculation of unsteady aerodynamics used in flutter, gust and blast response analyses is performed in ASTROS by use of the Doublet Lattice Method (DLM) for subsonic Mach numbers and by the Constant Pressure Method (CPM) for supersonic Mach numbers. The selection of these codes were relatively straightforward in that the DLM is widely recognized as a standard in the aerospace industry while the CPM has been developed at Northrop under internal and contracted research to complement the DLM at supersonic speeds. A useful, although somewhat dated, discussion of methods available for unsteady aerodynamics analysis is given in

Woodcock, D.L., "A Comparison of Methods Used in Lifting Surface Theory," AGARD R-583-71, June 1971

The ASTROS development used test cases provided in this report to judge the correctness of the CPM procedure as it has been installed into ASTROS. The original theoretical formulation of the DLM method is given in:

Albano, E. and Rodden, W.P, "A Doublet-Lattice Method for Calculating Lift Distributions on Oscillating Surfaces in Subsonic Flows," AIAA Journal, Volume 7, February 1969, pp 279-285, and Volume 7, November 1969, page 2142

while the DLM codes typically used by industry are described in

Giesing, J.P., Kalman, T.P., and Rodden, W.P., "Subsonic Unsteady Aerodynamics for General Configurations," Air Force Flight Dynamics Laboratory Report No. AFFDL-TR-71-5,

Volume I, Part I, - Direct Application of the Nonplanar Doublet-Lattice Method, November 1971

Volume I, Part II - Computer Program H7WC, November 1971

Volume II, Part I - Application of the Doublet-Lattice Method and the Method of Images to Lifting Surface/Body Interference, April 1972

Volume II, Part II - Computer Program N5KA, April 1972.

The N5KA code of Volume II of this report has been implemented in ASTROS and it can be characterized as having an improved treatment of body elements relative to the H7WC version of Volume I.

The CPM code is a substantially modified version of the Potential Gradient Method (PGM) described in

Jones, W.P. and Appa, K., "Unsteady Supersonic Aerodynamic Theory by the Method of Potential Gradients," NASA CR-2898, October 1977.

Among the enhancements made in the CPM code relative to PGM is an improvement in the results at relatively high reduced frequencies and a structuring of the code that allows models developed for the DLM code to be applied using the CPM code as well. Two papers describe these developments and show extensive correlations with available data:

Appa, K., "Constant Pressure Panel Method for Supersonic Unsteady Airloads Analysis," Journal of Aircraft, Volume 24, October 1987, pp 696-702.

Appa, K. and Smith, M.J.C., "Evaluation of the Constant Pressure Panel Method (CPM) for Unsteady Air Loads Prediction," presented as paper AIAA-88-2282 at the AIAA/ASME/ASCE/AHS 29th Structures, Structural Dynamics and Materials Conference, Williamsburg, Virginia, April 1988.

The CPM code has also been installed by Northrop under a contract from NASA/Ames-Dryden Flight Research Center in a code used at that center:

Appa, K. and Smith, M.J.C., "Integration of A Supersonic Unsteady Aerodynamic Code into the NASA FASTEX System," NOR 88-10, December 1987.

2.4 STATIC AEROELASTIC ANALYSIS

The static aeroelastic analysis contained in ASTROS primarily relates to the determination of the external loads acting on an aircraft structure during a trimmed maneuver. This entails coupling the steady aerodynamics with the structural model and solving carefully formulated equations of motion. The textbook

Bisplinghoff, R.L., Ashley, H., and Halfman, R.L., Aeroelasticity, Addison-Wesley Publishing Co., Inc., Reading, Massachusetts, 1955.

continues to be a relevant source for a discussion of the concepts of static aeroelasticity. In particular, the ASTROS definition of aileron effectiveness constraint is based directly on the formulation provided in Chapter 8 of this

text. The equations of motion used in ASTROS for the trim analysis are based closely on those used for static aeroelasticity in MSC/NASTRAN and are described in

> Rodden, W.P., Editor, MSC/NASTRAN Handbook for Aeroelastic Analysis, The MacNeal-Schwendler Corporation, Pasadena, California, 1987.

An Air Force contract to Northrop in the area of maneuver loads was also a resource for ASTROS. Reports from this contract are contained in

> Appa, K. and Yamane, J.R., "Update Structural Design Criteria, Design Procedures and Requirements for Fighter Type Airplane Wing and Tails - Volume I. Nonlinear Maneuver Loads Analysis of Flexible Aircraft: MLOADS Theoretical Development," AFWAL TR-82-3113, Volume I, May 1983.

The TSO procedure, discussed in greater detail in Subsection 2.8 of this report also provided basic concepts related to the integration of static aeroelastic results in an automated design procedure.

2.5 FLUTTER ANALYSIS

Concepts and methods of flutter analysis continue to evolve, but the basics are discussed in the textbook cited in the previous subsection. The methods used for flutter analysis in ASTROS are, as discussed in Subsection 10.1 of the Theoretical Manual, a synthesis of methods used in NASTRAN and the FASTOP procedure. The NASTRAN technique is described in the handbook referenced in Subsection 2.4 while a description of the FASTOP methodology is given in:

> Markowitz, J. and Isakson G., "FASTOP-3: A Strength Deflection and Flutter Optimization Program for Metallic and Composite Structures," AFFDL-TR-78-50, Volumes I and II, May 1978.

A report prepared by Lockheed for NASA/Langley Research Center:

> O'Connell, R.F., Hassig, H.J., and Radovich, N.A., "Study of Flutter Related Computational Procedures for Minimum Weight Structural Sizing of Advanced Aircraft," NASA CR-2607, March 1976.

presents a number of methods for performing flutter analysis and also discusses a number of ways to address the flutter design task. The p-k method of flutter analysis has been implemented in ASTROS, primarily because this method has the attractive feature that flutter behavior is assessed only at the velocities of interest in the analysis. The alternative V-g, or k, method

obtains flutter results over a range of velocities that can not be predetermined and therefore requires sophistication in the algorithm to assess whether the results are relevant to the task at hand.

The flutter constraint formulation developed for ASTROS and discussed in Subsection 10.2 of the Theoretical Manual is considered to be an ASTROS innovation. This constraint was developed based on experience in the use of the flutter constraint formulation developed for TSO. Again, the TSO code is discussed is greater detail in Subsection 2.8.

2.6 DYNAMIC ANALYSIS

Dynamic Analysis in ASTROS relates to the computation of transient and frequency response information. The development of this capability in ASTROS was based heavily on the comparable capability contained in NASTRAN. The COSMIC/NASTRAN Theoretical and Programmer's Manuals provided the details required to develop this capability while a MSC/NASTRAN handbook:

> Gockel, M.A., Editor, MSC/NASTRAN Handbook for Dynamic Analysis, The MacNeal-Schwendler Corporation, Pasadena, California, 1987.

provided a concentrated resource for understanding and applying these disciplines. The Newmark-Beta method utilized to perform coupled transient response analysis in ASTROS and NASTRAN may be somewhat out-dated, but (1) it was deemed adequate for the anticipated ASTROS applications, (2) a strong alternative candidate did not present itself, and (3) the implementation of an alternative procedure for performing transient response analysis is extremely straightforward due to the highly modular implementation of the Newmark-Beta method.

2.7 BLAST ANALYSIS

Methodology to compute an aircraft's response to nuclear blasts has undergone development since the 1950s. Two alternative methods for performing these analyses have been developed. The first is described in

> Giesing, J.P., et al, "Modification to VIBRA-6 Nuclear Blast Response Computer Program," AFWL-TR-81-166, Parts 1 through 4, August 1983.

and solves for the response in the frequency domain while the second:

> Webster, B.E., "VIBRA-12-Documentation and User's Manual," DNA-TR-84-390, October 1984

employs a time domain response. This latter method was applied in ASTROS, primarily because this method is more amenable to the insertion of nonlinear effects and secondarily because Kaman AviDyne, the subcontractor on the ASTROS program who supplied the blast response methodology, was very experienced in the time response calculations. Nonlinear effects have not been included in the ASTROS procedure, but a report prepared by Kaman AviDyne

> Lee, W.N. and Mente, L.J., "NOVA-2-A Digital Computer Program for Analyzing Nuclear Overpressure Effects on Aircraft," AFWL-TR-75-26, Part 1 - Theory, August 1976.

describes an algorithm that does so.

2.8 AUTOMATED DESIGN

The primary contribution of the ASTROS procedure is its ability to perform automated structural design while considering a multiplicity of design conditions. Extra attention is therefore given in this section to automated design concepts relative to that given to the technologies of the preceding subsections. This discussion first presents the background for automated design of aerospace structures and then addresses the specific areas of approximation concepts and optimization techniques.

2.8.1 Automated Design of Aerospace Structures

The ASTROS procedure has as its roots two other procedures developed under Air Force contract to perform automated structural design. The first of these is TSO (Aeroelastic Tailoring and Structural Optimization) which was developed for the Air Force by the General Dynamics Corporation:

> Lynch, R.W., et al, "Aeroelastic Tailoring of Advanced Composite Structures for Military Aircraft," AFFDL-TR-76-100
>
> Volume I, April 1977.
>
> Volume II - Wing Preliminary Design, April 1977.
>
> Volume III - Modifications and User's Guide to Procedure TSO, February 1978.

This procedure couples a plate model of the aircraft structure with steady aerodynamic loads, unsteady aerodynamic loads and mathematical programming techniques to perform automated design while considering constraints on strength, stiffness, flutter and aeroelastic performance; in other words, many

of the same capabilities that have been included in the ASTROS procedure. Despite its simplicity, this code has played a significant role in the development of concepts of aeroelastic tailoring and was key in early studies which demonstrated the capability of composite materials to permit the design of forward swept wings:

> Krone, N.J., "Divergence Elimination with Advanced Composites," AIAA Paper No. 75-1009, Aircraft Systems and Technology Meeting, Los Angeles, California, August 1975.

The second procedure is FASTOP (Flutter and Strength Optimization Procedure), which was developed for the Air Force by the Grumman Aerospace Corporation and is cited in Subsection 2.5. The FASTOP procedure permits the use of a detailed finite element model, has a rudimentary static airloads analysis capability and a variety of unsteady aerodynamic and flutter analysis capabilities; in other words, it too has many of the features contained in ASTROS. The FASTOP redesign algorithm uses fully stressed design concepts for strength conditions and employs an analogous condition to satisfy flutter criteria: the structure is redesigned to achieve equal energy in all the elements. This procedure has been applied throughout the industry and at the Air Force to perform preliminary design studies. It can be extremely useful as a supplement to a designer's judgment when there is a requirement to simultaneously satisfy strength and flutter conditions while using composite materials.

As the citations indicate, both of these procedures were developed over ten years before ASTROS and their differences from ASTROS must also be listed:

(1) Like FASTOP, ASTROS uses a finite element formulation, but like TSO, a multiplicity of design conditions can be considered simultaneously. FASTOP's requirement that strength and flutter conditions be treated sequentially, rather than in parallel, is felt to be the major drawback of this procedure. On the other hand, TSO's use of a Rayleigh-Ritz analysis of a plate model for the aircraft structure is felt to limit the utility of the procedure to the early stages of an aircraft design.

(2) Unlike the other two procedures, ASTROS is not limited to one boundary condition or a single flight condition (in fact, there is no limit in ASTROS on these numbers).

(3) The NASTRAN compatibility of the input data deck makes the data preparation for ASTROS consistent with the existing environment at many companies and laboratories.

(4) Computer science aspects, such as the data base, executive system and its high order programming language, the modular programming methods and the extensive use of FORTRAN 77, should ease maintenance and enhancement tasks relative to the other procedures.

(5) TSO utilizes relatively expensive finite difference techniques to obtain gradient information while ASTROS uses analytical sensitivity methods. (The optimality criteria employed by the FASTOP procedure and the fully stressed design option in ASTROS make it unnecessary to compute gradients.)

(6) Numerous limits imposed by the other procedures, such as in the number of layers of composite materials (three in TSO and six in FASTOP), the number of panels in the Doublet-Lattice model, the number of load cases allowed, etc., have been eliminated in ASTROS through the use of Dynamic Memory Allocation and open core concepts.

There are a large number of other differences, many of them quite subtle, that combine to provide the user with substantially more capability when using the ASTROS procedure relative to TSO and FASTOP.

As a final note on automated design techniques, it is recognized that TSO, FASTOP and ASTROS are not the only procedures than can perform automated structural design. NASA/Langley has been very active in the development of these procedures and practically every aerospace company in the United States and Europe has its own procedure. The unique feature of the three procedures discussed in this subsection is that they can be thought of as being in the "public domain." Two surveys on the use of these methods are given in

Ashley, H., "On Making Things the Best - Aeronautical Uses of Optimization," Journal of Aircraft, Volume 19, No. 1, January 1982, pp 5-28.

Venkayya, V.B., "Structural Optimization: A Review and Some Recommendations," International Journal for Numerical Methods in Engineering, Volume 13, 1978, pp 203-228.

2.8.2 Approximation Concepts

As discussed in Subsection 13.1 of the Theoretical Manual, the specification of an approximate problem for solution by the optimizer is a key feature in converting an imposing structural design task into one of tractable size. All the concepts applied in ASTROS, including constraint deletion, design variable linking, inverse design variables and the solution of the approximate problem are discussed in

> Schmit, L.A., Jr. and Miura, H., "Approximation Concepts for Efficient Structural Syntheses," NASA CR-2552, March 1976.

2.8.3 Optimization Techniques

Numerous techniques to optimize a given function, with or without considering constraints, have been developed for a wide variety of applications. Any library of general purpose mathematical algorithms is likely to contain a number of these techniques and the literature that addresses these topics is vast. A general discussion of these techniques is, therefore, beyond the scope of this manual. Two textbooks in this area that were consulted in the development of ASTROS are

> Fox, R.A., Optimization Methods for Engineering Design, Addison-Wesley, Reading, Mass., 1971.

> Vanderplaats, G.N., Numerical Optimization Techniques for Engineering Design, McGraw-Hill Book Co., New York, New York, 1984.

The latter text can be considered a theoretical manual for the ADS procedure:

> Vanderplaats, G.N., "ADS - A FORTRAN Program for Automated Design of Synthesis," NASA CR-172460, October 1984.

which is a package of optimization techniques, with the user selecting the algorithm that is most applicable to a particular problem. Early versions of ASTROS utilized the ADS code, but only one option was being selected and this option is contained in the MICRO-DOT algorithm that is used in the ASTROS procedure:

> Vanderplaats, G.N., "An Efficient Feasible Directions Algorithm for Design Synthesis," AIAA Journal, Volume 22, No. 11, November 1984, pp 1633-1640.

ASTROS has been constructed so that users who have use for the ADS procedure can link it to ASTROS with minimal difficulty.

SECTION III

MODELING GUIDELINES

The multidisciplinary nature of ASTROS makes it likely that the general user is unfamiliar with some of the conceptual and input requirements for the procedure. This section addresses this shortcoming by providing guidance in the use of the more specialized features. The assumption is made that the user is either familiar with basic structural modeling or has access to handbooks or colleagues that can provide this material. Therefore, this section does not deal with such issues as recommended structural modeling techniques, material allowables, reduction of the solution set or the development of mass models. The primary emphasis in this section is instead placed on the development and exercising of the design model. Secondary emphasis is placed on the steady aerodynamics modeling which prepares geometric input for the USSAERO procedure that has been integrated into ASTROS. This modeling can be quite complex and there are a number of limitations im-posed by USSAERO that have been retained in this integration. Finally, Sub-sections 3.3 and 3.4 discuss unsteady aerodynamics (including flutter) and dynamic response analyses, respectively. These areas receive less emphasis partially because NASTRAN documentation already provides some assistance in these areas. Finally, Subsection 3.5 provides a checklist for converting bulk data packets generated for the NASTRAN procedure to ASTROS formats.

3.1 THE DESIGN MODEL

The term design model refers to the collection of bulk data information that is required to define the design task to the ASTROS system. This section discusses the preparation of input data for the design variables, the design constraints and, optionally, the parameters for the optimization algorithm.

3.1.1 Design Variables

As discussed in Subsection 2.2.1 of the Theoretical Manual, ASTROS makes a distinction between local and global design variables and links the two types through a relationship of the form

$$\{t\} = [P]\{v\} \qquad (3\text{-}1)$$

where t is a vector of physical properties of the structural model while v is a vector of global design variables. It is the user's responsibility to provide the information required to assemble the P matrix and the initial value of the v vector. The automated design task works directly with the v vector while the t vector is determined indirectly and the P matrix is invariant.

Subsection 2.2.1 of the Theoretical Manual also identifies three available linking options. The user is allowed to intermix these three types of linking, but should be aware that the use of any shape function linking precludes the use of inverse design variables even for global variables that are unlinked or that are linked physically.

The unique linking feature is invoked using the DESELM entry of **Figure 1**. The DVID value for this entry must be unique with respect to the remaining DESELM and DESVAR entries. The VINIT field defines the initial value of a term in the v vector of Equation 3-1 while the single non-zero column of the P matrix is given by the property entry for the element specified by EID and ETYPE. The LAYRNUM field refers to an associated PCOMP, PCOMP1 or PCOMP2 entry, where layer number one is associated with the T1 and TH1 fields of the PCOMP entry and the ith layer refers to the Ti and THi fields. The LABEL field on the DESELM entry is for user convenience only and does not affect processing in any way. Examples of DESELM input are given in Subsections 4.1 and 4.2.

The physical and shape function linking options are invoked by the DESVAR data entry of **Figure 2**. The EID and ETYPE fields of the DESELM entry are not present in this case while the meaning of the remaining, shifted fields are unchanged. A subtlety in the shape function linking for this entry is that the user may wish to set the initial value of the global design variable to zero (VINIT = 0.0) and that this, coupled with the use of the VMIN default, will cause an error because VINIT < VMIN. The user is required to input a value of VMIN that is less than zero in this case. Further, as remark 2 of **Figure 2** indicates, this VMIN value is subsequently overridden in the code by a large negative number.

For the physical linking option, the PLIST entry of **Figure 3** provides the linking information. The concept is that a column of the P matrix

Input Data Entry DESELM

Description: Designates design variable properties when the design variable is uniquely associated with a single finite element.

Format and Examples:

1	2	3	4	5	6	7	8	9	10
DESELM	DVID	EID	ETYPE	VMIN	VMAX	VINIT	LAYERNUM	LABEL	
DESELM	5	10	CROD	0.01	10.0	1.0			

Field	Contents
DVID	Design variable identification (Integer > 0).
EID	Element identification (Integer > 0).
ETYPE	Element type.
VMIN	Minimum allowable value of the design variable (Real > 0) (Default = .001).
VMAX	Maximum allowable value of the design variable (Real > 0) (Default = 1000.)
VINIT	Initial value of the design variable (Real, VMIN $\leq$ VINIT $\leq$ VMAX).
LAYERNUM	The layer number if a composite element is to be designed.
LABEL	Optional user-supplied label to define the design variable (Text)

Remarks:

1. Valid ETYPE's are CROD, CONROD, CBAR, CSHEAR, CTRMEM, CQDMEM1, CQUAD4, CMASS1, CMASS2 and CONM2.
2. The initial element size used in the structural analysis is the product of the VINIT value and the element size on the associated property entry.

Figure 1. The DESELM Bulk Data Entry

Input Data Entry DESVAR

Description: Designates design variable properties.

Format and Examples:

1	2	3	4	5	6	7	8	9	10
DESVAR	DVID	VMIN	VMAX	VINIT	LAYERNUM	LABEL			
DESVAR	1	0.01	2.0	1.0	13	INBDTOP			

Field	Contents
DVID	Design variable identification (Integer > 0).
VMIN	Minimum allowable value of the design variable (Real > 0) (Default = 0.001).
VMAX	Maximum allowable value of the design variable (Real > 0) (Default = 1000.0).
VINIT	Initial value of the design variable (Real, VMIN $\leq$ VINIT $\leq$ VMAX).
LAYRNUM	Layer number if referencing composite element(s).
LABEL	Optional user supplied label to define the design variable (Text).

Remarks:

1. The elements linked to the DESVAR are specified using either a PLIST or an ELIST data entry.
2. Shape function linking (using ELIST entries) will override VMIN and VMAX with large negative and positive values, respectively.

Figure 2. The DESVAR Bulk Data Entry

Input Data Entry PLIST

Description: Defines property entries associated with a design variable.

Format and Examples:

1	2	3	4	5	6	7	8	9	10
PLIST	DVID	PTYPE	PID1	PID2	PID3	PID4	PID5	PID6	CONT
PLIST	6	PROD	12	14	22				

CONT	PID7	PID8	PID9	-etc-					

Alternate Form:

PLIST	DVID	PTYPE	PID1	THRU	PID2				
PLIST	25	PROD	8	THRU	25				

Field	Contents
DVID	Property list identifier (Integer).
PTYPE	Property type associated with this list (e.g., PROD).
PID1,PID2, PID3	Property entry identifications.

Remarks:

1. Allowable PTYPES are: PROD, PSHEAR, PCOMP, PCOMP1, PCOMP2, PSHELL, PMASS, PELAS, PTRMEM, PQDMEM1, and PBAR.
2. If the alternate form is used, PID2 must be greater than or equal to PID1.
3. All elements using properties listed as PLIST entries for a particular DVID, will be designed by (linked to) that design variable.

Figure 3. The PLIST Bulk Data Entry

is defined using thicknesses specified on the referenced property entries and that all other columns for the rows controlled by this PLIST entry must be zero (i.e., a property ID/layer number combination cannot be referenced by more than one PLIST entry). As Equation 3-1 indicates, the physical thickness is the product of the initial thickness specified by VINIT and the value on the property entry. Note also, that a DESVAR/PLIST combination referring to a single element is functionally identical to the DESELM option.

Typically, this linking option would be used to force all the finite elements in a given zone to vary simultaneously and would therefore require a single PIDi entry. Note that, if two different property types are to be linked to the same DVID, a separate PLIST entry is required for each property type. Subsections 4.4, 4.6 and 4.7 present examples of the use of the PLIST data entry.

For the shape function linking option, the ELIST entry of Figure 4 provides the linking information. The concept is that the ELIST data define a single column of the P matrix but that other columns of the P matrix can contribute to the calculation of the local variable t (i.e., the ETYPE and EIDi values need not and, most likely, will not be unique across ELIST entries). In a typical example, one global design variable might control a shape that is uniform across a number of elements while a second variable would control a shape that is linear in the chordwise coordinate for the same set of elements. The P matrix is determined completely by the PREFi data on the ELIST entry in this case and that values on the property entries that correspond to the element size (e.g., element thickness) are ignored. An information message to this effect is written for each element type which is involved in shape function design variable linking. Subsection 4.8 contains an example of the use of the ELIST linking.

The generation of data for shape function linking is tedious and users who employ this option will most likely set about automating the process. The Appendix to this report which discusses the insertion of a module into ASTROS, has an example which can assist in the generation of the ELIST bulk data entries.

In the case of layered composites, if the same shape function applies to a number of layers, the user would like to reference a single

Input Data Entry ELIST

Description: Defines element connectivity entries associated with a design variable.

Format and Examples:

1	2	3	4	5	6	7	8	9	10
ELIST	DVID	ETYPE	EID1	PREF1	EID2	PREF2	EID3	PREF3	CONT
ELIST	10	CROD	12	12.0	22	1.0			

CONT	EID4	PREF4	EID5	PREF5	-etc-				

Field	Contents
DVID	Design variable identification (Integer).
ETYPE	Element type associated with this list (e.g., CROD).
EID1,EID2, EIDi	Element identification numbers.
$PREF_i$	Linking factor for the associated EID.

Remarks:

1. Allowable ETYPES are: CROD, CONROD, CSHEAR, CQDMEM1, CQUAD4, CTRMEM, CBAR, CMASS1 and CMASS2.

2. The design variable identification must match that of a design variable defined as a DESVAR entry.

3. The linking factors define a shape function to be used as the global design variable.

4. Designed properties (e.g., thicknesses) of elements listed on ELIST entries will be set to unity to ensure proper shape function definition.

Figure 4. The ELIST Bulk Data Entry

shape function more than once. This is not possible and the user must duplicate the shape function and assign the separate layers unique DVID's. This results in a large input data packet, but does not affect performance significantly.

3.1.2 Limits on Design Variables

The specification of limits on the physical and global design variables is a crucial aspect of the design model. For the unique and the physical linking this is a straightforward task in that the VMIN and VMAX values of the DESELM and DESVAR data entries provide all the information used to define limits on the global design variables and, by extension, the physical design variables. The physical variable and gauge limits are a combination of V, VMIN or VMAX and the initial property values.

For shape function linking the task is somewhat more complex. The VMIN and VMAX values have little physical meaning in this case and are, in fact, replaced in ASTROS with very large negative and positive numbers so that there are no effective limits on the global design variables. The minimum thickness limits for the local variables are given on the associated property bulk data entry and the maximum thickness limits are given on the associated connectivity bulk data entry. This construction is based on the fact that minimum thicknesses are typically specified by the material properties and are therefore properly placed on the property entry while maximum thickness limits are typically specified by geometry, which is associated with the connectivity data.

The VMIN and VMAX values associated with unique and physical linking and are side constraints on the design variables while the TMIN and TMAX values used in conjunction with the shape function linking are converted into additional regular constraints, as discussed in Subsection 2.2.2.3 of the Theoretical Manual. The use of shape functions for large design tasks presented two problems with respect to thickness constraints. The first was that, if the approximate problem did not retain an adequate set of these constraints, the optimizer could direct the design to points where the physical values were very small or even negative and the subsequent reanalysis would be invalid. The second problem was that many of these constraints could become active simultaneously (e.g., when a composite layer went to its minimum allowable gauge across a large number of elements) and swamp the design task. In order to avoid these problems the DCONTHK entry of Figure 5 was developed.

Input Data Entry DCONTHK Thickness constraints

Description: Defines a list of elements (linked using ELIST entries) for which thickness constraints are to be retained on all design iterations.

Format and Examples:

1	2	3	4	5	6	7	8	9	10
DCONTHK	ETYPE	EID	EID	EID	EID	EID	EID	EID	CONT
DCONTHK	QDMEM1	100	101	200	205				

CONT	EID	EID	-etc-						

Alternate Form:

1	2	3	4	5	6	7	8	9	10
DCONTHK	ETYPE	EID	"THRU"	EID					
DCONTHK	QDMEM1	100	"THRU"	200					

Field	Contents
ETYPE	Character input identifying the element type. One of the following: BAR CONM2 ELAS MASS QDMEM1 QUAD4 ROD SHEAR TRMEM
EID	Element identification number (Integer > 0 or blank)

Remarks:

1. The purpose of this bulk data list is to ensure that adequate physical move limits are retained in optimization with shape function design variable linking without requiring retention of all move limits. For problems with large numbers of local variables using shape functions, the move limits often cause too many minimum thickness constraints (see Remark 2) to be retained in the optimization task. Using this bulk data entry to name "critical" minimum guage constraints (see Remark 3) will cause only the named elements' thickness constraints to be computed and retained.

   NOTE that an element with a violated minimum gauge constraint will always be computed irrespective of the DCONTHK entries, but may be deleted in the constraint deletion.

Figure 5. The DCONTHK Bulk Data Entry

2. The global design variable in shape function linking is non-physical and no reasonable restriction for a global move limit (side constraint) can be defined; therefore, constraints on the local design variables controlled by shape functions are generated by ASTROS to ensure that the design is reasonable (ie, non-negative thicknesses).

3. The DCONTHK entry should select a minimum number of elements linked to shape functions that will enable the optimizer to select physically reasonable designs without retaining all the minimum thickness constraints (potentially a very large number). Typically, this means N+1 elements spread over the range of the shape function (e.g. span or chord) where N is the order of the shape (N=0, UNIFORM: N=1, LINEAR, etc.)

Figure 5. The DCONTHK Bulk Data Entry (Concluded)

This entry is used only for shape function linking and requires the user to explicitly define the elements whose thickness constraints are always retained in the approximate problems. The remaining thickness constraints are retained only if the they are violated. A burden is placed on the user to select those elements that are sufficient to limit the overall shape. The reader can envision that, for simple functions, elements at the corners of the area over which the shape is defined are logical elements to select. These elements can sometimes only be determined in an iterative fashion by selecting an initial set and then adding to it when unselected elements are driven to a negative thickness. The remarks that accompany **Figure 5** further explain the use of this feature.

3.1.3 <u>Design Constraints</u>

Compared to the design variables, the specification of constraints is relatively straightforward. Strength constraints are specified using the DCONSTR data entry of **Figure 6**. The constraints are specified for the materials, implying that these limits are independent of the applied loading and/or boundary condition. Strength constraints are computed for all elements that reference a constrained material, irrespective of whether the elements are

Input Data Entry <u>DCONSTR</u>

<u>Description</u>: Defines stress/strain constraints.

<u>Format and Examples</u>:

1	2	3	4	5	6	7	8	9	10
DCONSTR	MID	CRIT	MID	CRIT	MID	CRIT	MID	CRIT	
DCONSTR	1	VMISES	10	VMISES					

<u>Field</u>	<u>Contents</u>
MID	Material identification number for the constrained elements.
CRIT	Failure criterion to be used (Text)

<u>Remarks</u>:

1. Allowable constraint criteria (CRIT) are: VMISES, TSAIWU, STRAIN

   (A) von Mises stress constraint. Yield values are given by ST, SC and SS values on a MAT1 or MAT2 data entry.

   (B) Tsai-Wu stress constraint. Yield values are given on the MAT8 data entry.

   (C) Maximum strain constraint. Strain allowables for tension, compression and shear are given defined in the ST, SC and SS fields of a MAT1, MAT2 or MAT8 data entry. The shear strain allowable is used only for the shear element and is ignored for other element types.

Figure 6. The DCONSTR Bulk Data Entry

designed. Conversely, it is not necessary to apply strength constraints to an element that is designed.

Displacement constraints are specified using the DCONDSP entry of Figure 7. Although the user may impose very complex shapes that the deformed structure must achieve, satisfaction of such a constraint may be costly and difficult.

Frequency constraints are specified using the DCONFRQ entry of Figure 8. For this constraint, and for the DCONDSP, DCONALE and DCONCLA constraints as well, it is possible to specify equality constraints by placing nearly identical upper and lower limits on the variable. Also, these constraints can be used to increase the flexibility, as opposed to their conventional use where the goal is to increase the stiffness. Aileron and lift effectiveness constraints are specified using the DCONALE and DCONCLA constraints. Lift effectiveness constraints are discussed in Subsections 2.2.2.1 and 9.2.2 of the Theoretical Manual while aileron effectiveness constraints are discussed in Subsections 2.2.2.1 and 9.3 of the Theoretical Manual.

Constraints on the flutter behavior are specified using the DCONFLT entry of **Figure** 9. Subsection 10.2 of the Theoretical Manual contains an extensive discussion of this constraint. The default value of GFACT=0.1 is usually adequate, but it can be increased to force the retention of a flutter constraint in the approximate optimization task.

There are a number of guidelines for performing the flutter analysis and design. Experience has shown that the flutter solution may sometimes have difficulty in getting started. In this case, we recommend that the first velocity for the flutter analysis be reduced. In this way, the initial guess that the flutter roots approximate the natural frequencies of the structure is more nearly satisfied and convergence is more likely.

In some cases, a natural mode does not participate in the aeroelastic response. For example, a mode that vibrates in the plane of the wing does not produce significant aerodynamic forces. This is manifested by the flutter root associated with this mode having a frequency equal to its natural frequency and its damping essentially zero. The design process cannot distinguish this type of behavior from a mode which is fluttering and will futilely

Input Data Entry <u>DCONDSP</u>

Description: Defines a deflection constraint of the form:

$$A_j u_j \le \delta_{all} \text{ (UPPER BOUND) or } A_j u_j \ge \delta_{all} \text{ (LOWER BOUND)}$$

Format and Examples:

1	2	3	4	5	6	7	8	9	10
DCONDSP	CTSET	DCID	CTYPE	DALL	LABEL	G	C	A	CONT
DCONDSP	1	10	LOWER	-2.3	TIP	32	3	2.0	ABC

CONT		G	C	A	G	C	A		etc
+BC		7	3	-4.0					

Field	Contents
CTSET	Constraint set identification number (Integer).
DCID	Constraint identification number (Integer).
CTYPE	Constraint type, either UPPER or LOWER bound (Text, Def = UPPER).
DALL	Allowable displacement (Real).
LABEL	User specified label to identify constraint.
G	Grid identification.
C	Component number - any one of digits 1-6.
A	Real coefficient.

Remarks:

1. Both upper and lower bounds on the deflections can be specified by this entry. E.g., if constraints of the form $|u| \le 2.0$ are to be imposed, one DCONDSP entry would use CTYPE = UPPER, DALL = 2.0, G = 32, C = 3, A = 1.0 while a second entry would use CTYPE = LOWER, DALL = -2.0, G = 32, C = 3, A = 1.0.

2. Twist constraints can be specified by differencing two displacements while camber constraints can be expressed as a weighted sum of three displacements.

3. Any number of continuation cards are permitted.

4. A LOWER bound constraint excludes all values to the left of DALL on a real number line, while an UPPER bound constraint excludes all values to the right, irrespective of the sign of DALL.

Figure 7. The DCONDSP Bulk Data Entry

Input Data Entry DCONFRQ

Description: Defines a frequency constraint of the form:

$$f \leq f_{all} \quad \text{or} \quad f \geq f_{all}$$

Format and Examples:

1	2	3	4	5	6	7	8	9	10
DCONFRQ	SID	MODE	CTYPE	FRQALL					
DCONFRQ	3	1	LOWER	6.0					

Field	Contents
SID	Constraint set identification (Integer).
MODE	Modal number of the frequency to be constrained (Integer).
CTYPE	Constraint type, either UPPER for upper bounds or LOWER for lower bounds (Text, Def = LOWER).
FRQALL	Frequency constraint (in Hz.). (Real > 0.0)

Remarks:

1. More than one constraint can be placed on a mode.

Figure 8. The DCONFRQ Bulk Data Entry

Input Data Entry DCONFLT

Description: Defines a flutter constraint in the form of a table:

$$(\gamma - \gamma_{REQ})/(GFACT) \leq 0.0$$

Format and Examples:

1	2	3	4	5	6	7	8	9	10
DCONFLT	SID	GFACT	V1	GAM1	V2	GAM2	V3	GAM3	CONT
DCONFLT	2		100.0	-.01	1000.0	0.0	1500.0	0.0	+ABC

CONT	V4	GAM4	V5	-etc-					
+BC									

Field	Contents
SID	Constraint set identification, the constraints are referenced by the design constraint id in solution control.
GFACT	Constraint scaling factor (Real > 0.0, D = 0.10).
V_i	Velocity value (Real).
GAM_i	Required damping value (Real).

Remarks:

1. A negative value of GAMi refers to a stable system.
2. The V_i must be in either ascending or descending order.
3. Linear interpolation is used to determine GAMA for a given velocity.
4. At least two pairs must be entered.
5. Jumps between two points ($V_i = V_{i+1}$) are allowed, but not at the end points.

Figure 9. The DCONFLT Bulk Data Entry

attempt to stabilize this mode. This can be avoided by omitting this mode from the flutter solution process by using the MLIST field on the FLUTTER bulk data entry.

3.1.4 Modification of Default MICRO-DOT Parameters

Unless the Fully Stressed Design option is exercised, an approximate design problem is generated at each iteration and passed to the MICRO-DOT procedure for solution by mathematical programming methods. The process of generating this approximate problem is described in Section 13 of the Theoretical Manual. MICRO-DOT, in turn, utilizes an iterative procedure to solve the approximate problem. Several internal MICRO-DOT parameters affect both the efficiency of the procedure and the quality of the answer obtained. All internal parameters are provided with defaults which, experience has shown, provide for robust performance. For the large, practical design problems for which ASTROS was designed, these defaults should be adequate to obtain a good "optimal" design. The researcher or interested user may, however, want to modify the MICRO-DOT parameters to enhance the optimization algorithm for a particular application.

The MICRO-DOT algorithm within ASTROS has been implemented in such a way as to provide the ability to fine tune the procedure through modification of the internal parameters. The MPPARM bulk data entry is the mechanism provided to communicate the changes to the MICRO-DOT procedure. When each approximate problem is generated, the MPPARM data are utilized to override the initial values of the named parameters prior to initiating the MICRO-DOT procedure. These parameters establish constraint tolerance parameters, search direction parameters, termination criteria and many others. A list of available parameters is given on the MPPARM bulk data entry documentation Appendix E of the User's Manual.

The most common changes are to the termination criteria and scaling parameters: DABOBJ, DABOBM, DELOBJ, DELOBM, STOL, ITRMOP, ITMAX and ISCAL. The default values tend to favor early termination, whereas overall efficiency considerations suggest that the relatively inexpensive (in-core) approximate optimization problem should be solved rigorously to get as much as possible out of each global iteration. Also, experience has shown that the global optimization problem may converge to a "better" design if, at each iteration,

the MICRO-DOT algorithm rescales the approximate problem at intervals equal to the number of design variables. Although highly problem dependent, better performance can sometimes be obtained if more frequent rescaling is done.

Other common changes are to the constraint tolerance parameters, CTxxx, which are used in performing constraint deletion within MICRO-DOT. The initial values are chosen (for efficiency considerations) such that relatively few constraints are considered active or violated by the MICRO-DOT procedure. Particular optimization problems may, however, require retention of more constraints to adequately define the constraint boundaries in computing the search direction.

Not only are many other parameters provided by the MICRO-DOT algorithm, but each particular application can generate a slightly different set of "optimal" algorithm parameters. The default operation has been very robust but it is also true that substantial improvement in results has occurred through the judicious modification of the MICRO-DOT parameters (notably the intermediate complexity wing examples of Subsections 4.7 and 4.8). The user is therefore encouraged to investigate the effects of the optimization parameters on the results of particular cases.

3.2 USSAERO MODELING

The USSAERO procedure has been incorporated into the ASTROS code. USSAERO (Unified Subsonic and Supersonic Aerodynamics) computes steady pressure loading on arbitrary wing-body-tail configurations that are subdivided into a large number of aerodynamic panels. This subsection provides guidance in the use of USSAERO in ASTROS. This is followed by a listing of the modeling limitations that USSAERO has imposed and then specific guidelines in the development of the models are provided.

3.2.1 Input Description

From the ASTROS application standpoint, the primary change made to USSAERO was the way input data were entered. The original USSAERO code uses formatted input with flags and counters directing the flow of the input. ASTROS uses the bulk data format established in NASTRAN and this required extensive revisions in the ASTROS module which develops the geometric data. A summary of the bulk data entries developed for steady aero-elastic analysis is given in **Figure 10**.

FUNCTION			
CONFIGURATION	PANELING	REFERENCE DATA	TRIM
AIRFOIL BODY AXSTA AEFACT	CAERO6 PAERO6 AESURF AEFACT	AEROS	TRIM

Figure 10. Bulk Data Entries for Aerodynamic Paneling

This figure helps in making a key point: USSAERO makes a distinction between modeling the configuration (i.e., defining the shapes of the aerodynamic surfaces) and defining the panels used in the discretization of the surfaces. This distinction is necessary to permit the detailed description of the surfaces in terms of airfoil thicknesses and cambers, and arbitrary fuselage shapes. The guidelines in this manual are intended primarily to assist in preparing the input data entries once the aerodynamic configuration has been defined. This initial definition is typically a major task that requires an experienced modeler.

Each aerodynamic surface is classified as being either a lifting surface or a body. A lifting surface, in turn, can be either a WING, FIN or CANARD. The primary lifting surface is designated by WING and only one WING can be defined for a given model. CANARDs are distinguished from FINs by the fact that the CANARDs have a corresponding surface across the plane of symmetry while FINs do not. In addition the lift forces for CANARDs are carried through to the y = 0 plane as shown in the following sketch:

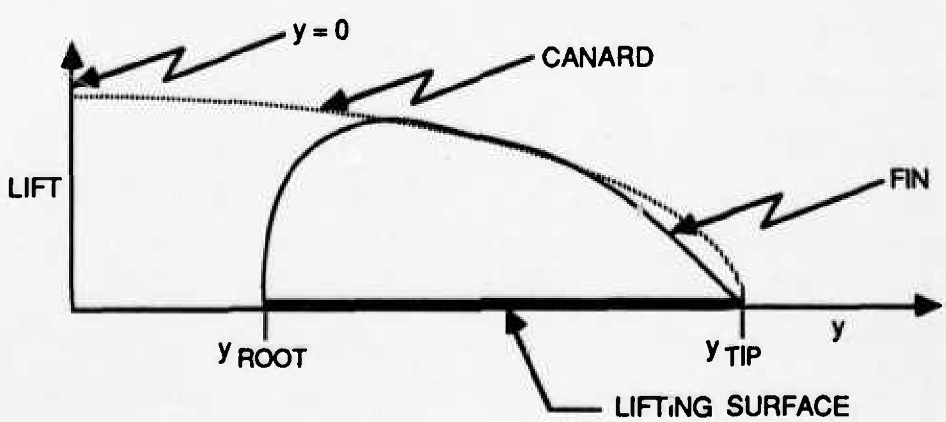

Lifting surfaces on pods should always be modeled as fins so as to avoid the lift carry through behavior.

Configuration data for lifting surfaces are given by the AIRFOIL entry of **Figure 11** plus any associated AEFACT entries. Information provided with the AIRFOIL data entry is expanded upon in the following items:

(1) The aerodynamic coordinate system must be the basic coordinate system (i.e., CP must be either 0 or blank). This option is available for enhancement.

(2) Chordwise division points are expressed in terms of percent chord. The first value must be 0.0 and the last value 100.0 with intermediate points input in ascending order.

(3) Thickness and camber distributions are input with AEFACT lists designated by IUST, ILST and ICAM. These values are input in percent chord and measured relative to coordinate Z1. Two options are available for describing the coordinates for a general airfoil such as the one shown in **Figure 12**:

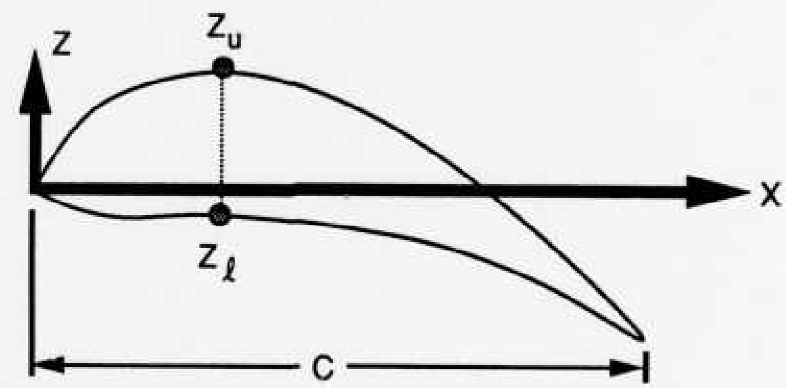

Figure 12. Airfoil Thickness and Camber

In the first option, upper and lower thickness surface values are input with:

Upper = $100\ z_u/c$

Lower = $-100\ z_\ell/c$

These definitions require, for the airfoil shown in the sketch, that some z_u coordinates be negative while all the z_ℓ values are positive.

Input Data Entry **AIRFOIL**

Description: Defines airfoil properties for USSAERO.

Format and Examples:

1	2	3	4	5	6	7	8	9	10
AIRFOIL	ACID	CMPNT	CP	ICHORD	IUST	ILST	ICAM	RADIUS	CONT
AIRFOIL	1	WING	1	10	20		30		abc

CONT	X1	Y1	Z1	X12	IPANEL				
+BC	0.0	0.0	0.0	50.					

Field	Contents
ACID	Associated aircraft component ID (Integer > 0).
CMPNT	Type of aircraft component (Text).
CP	Coordinate system for airfoil (Integer).
ICHORD	ID of an AEFACT data entry containing a list of division points (in terms of percent chord) at which airfoil data are specified (Integer).
IUST, ILST	ID of an AEFACT data entry containing a list of airfoil half thicknesses in percent chord at the chordwise cuts for the upper and lower surfaces, respectively (Integer).
ICAM	ID of an AEFACT data entry containing a list of airfoil camber values (z-ordinates expressed in percent chord) at the chordwise cuts (Integer).
RADIUS	Radius of the leading edge, expressed in percent chord (Real).
X1, Y1, Z1	Location of airfoil leading edge in coordinate system CP (Real).
X12	Airfoil chord length in coordinate system CP. (Real > 0).
IPANEL	ID of an AEFACT data entry containing a list of chordwise cuts for wing panelling.

Remark:

1. Allowable components are WING, FIN and CANARD.
2. ILST and ICAM present redundant information so that, at most, only one can be non-zero.
3. ICAM cannot be defined for FIN and CANARD components. ILST cannot be defined for FIN components.

Figure 11. The AIRFOIL Bulk Data Entry

4. If the RADIUS field is blank, a round leading edge of radius zero is used.

5. IPANEL is optional and is used when different chordwise cuts on each end of the panel are desired.

Figure 11. The AIRFOIL Bulk Data Entry (Concluded)

In the second option, camber values and the half thicknesses are input as:

$$\text{Upper} = 100\,(z_u - z_\ell)/c$$

$$\text{Lower} = 100\,(z_u + z_\ell)/c$$

Fin airfoils must be symmetric, which implies that ILST and ICAM fields are blank in this case.

(4) The leading edge radius is an optional input. In the ASTROS implementation of USSAERO, the option of a sharp leading edge has been disabled for the fins and canards. If the ARADIUS field is blank or zero, the program assumes a round leading edge of zero radius. It is recommended that the appropriate nonzero value be determined for input for all airfoils.

(5) As its name implies, the IPANEL data entry is paneling, rather than configuration input. It is used in the situation where different percent chord cuts are required at the inboard and outboard edges of a panel. **Figure 13** shows an example of this.

In the sketch, the trailing edge panels may represent a control surface whose hinge line is perpendicular to the wing centerline.

(6) The wing can be defined by two or more airfoils while the fin and canards are modeled using exactly two airfoils.

(7) USSAERO imposes limits on a number of configuration and paneling parameters. Subsection 3.2 summarizes these limits.

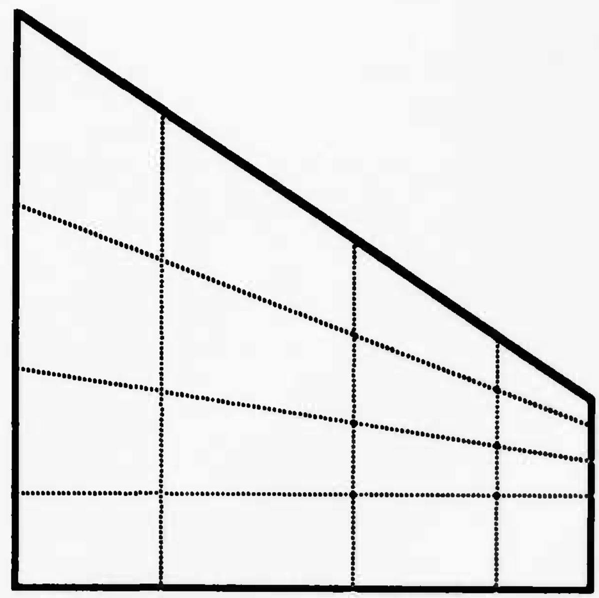

Figure 13. Paneling Using Cuts that are not a Constant Percent Chord

Paneling data for lifting surfaces are given by CAERO6 entries of Figure 14. Some guidelines for this entry include:

(1) The IGRP data field refers to the group with which the panel is associated. The wing/body/tail combination is one group while a pod and its associated fins represent a second group. PODS cannot be input in the same group as a wing or fuselage. The wing and fuselage must be in the same group, and canards are typically in this group as well.

(2) If the panel chordwise division points are the same as the ICHORD points on the AIRFOIL entry, ICHORD must still be specified on the CAERO6 entry. If ICHORD is zero, IPANEL must be nonzero for all the wing AIRFOIL data entries.

(3) The LSPAN division points are listed in dimensional form, <u>not</u> percent span.

Input Data Entry CAERO6

Description: Defines an aerodynamic macroelement (panel) for steady aeroelasticity.

Format and Examples:

1	2	3	4	5	6	7	8	9	10
CAERO6	ACID	CMPNT	CP	IGRP	LCHORD	LSPAN			
CAERO6	1	WING		1	20	30			

Field	Contents
ACID	Component ID (Integer > 0)
CMPNT	Aircraft component (Text)
CP	Coordinate system (Integer)
IGRP	Group number for this component (Integer)
LCHORD	ID of AEFACT data entries containing a list of division points in percent chord for chordwise boxes for aerodynamic surface. If LCHORD is zero, the chordwise divisions are identified by the IPANEL entry on the AIRFOIL bulk data entry (Integer $\geq$ 0, or blank).
LSPAN	ID of an AEFACT data entry containing a list of division points in terms of dimensional span stations for spanwise boxes. If this is zero or blank, the y locations from the AIRFOIL bulk data entries for the component ACID are used (Integer $\geq$ 0, or blank).

Remarks:

1. Allowable components are WING, FIN and CANARD.
2. The IGRP field allows related components to be processed together for interference effects; e.g., one group could be a wing/body/tail combination while a second group would be a pod/fin combination.
3. Note that chordwise cuts are in percent while spanwise cuts require physical coordinates. For spanwise cuts, y-coordinates are input for wings and canards while z-coordinates are input for fins.

Figure 14. The CAERO6 Bulk Data Entry

(4) LSPAN division points for WINGS and CANARDS are given in terms of the y coordinate while FIN division points are given in terms of z.

A final input for the lifting surfaces relates to control surfaces. The AESURF data entry identifies the aerodynamic boxes that panel the control surface. The panel numbering starts from the inboard leading edge and proceeds to the outboard trailing edge. **Figure 15** gives an example of the box numbering for a surface with component ID 200 and a control surface represented by the shaded panels. For this example, FBOXID1 = 203 and LBOXID1 = 214.

Each body surface is classified as being either a fuselage (FUSEL) or a pod (POD). There is a maximum of one fuselage per model, although it may be composed of up to six segments. By definition, a fuselage is on the aircraft centerline and only the right half of the fuselage is modeled. Pods can be on the centerline, but more typically are off the centerline, requiring that the complete pod be modeled. In the special case of twin fuselages, the fuselage must be modeled as a pod. Up to nine pods can be modeled.

Configuration data for bodies are given by a combination of BODY, AXSTA and AEFACT data. Cross sectional properties can be defined as either circular or arbitrary in nature. Circular cross sections are defined using

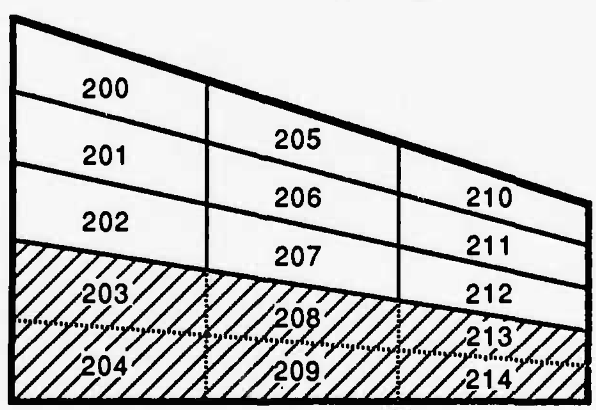

Figure 15. Specification of Control Surface Panels

the ABOD field on the AXSTA data entry and the NRAD field on the BODY data entry. For arbitrary cross sections, the LYRAD and LZRAD parameters of the AXSTA data entry are used. Circular and arbitrary cross sections cannot be

combined in a single body. Pods cannot have camber. The number of radial cuts can be varied for different fuselage segments as shown in **Figure 16**. Pod geometry is specified relative to a location given on the BODY data entry while fuselage geometry is in the basic coordinate system.

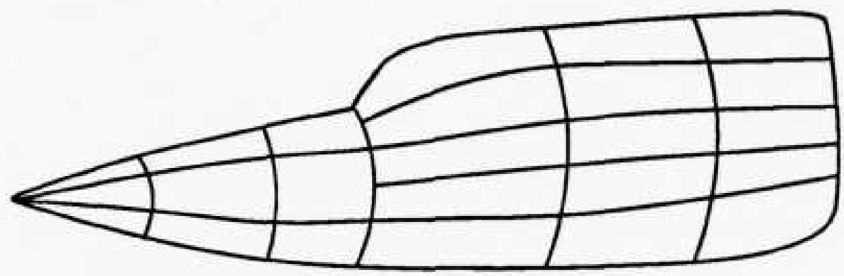

Figure 16. Body Configuration Example Showing Different Radial Cuts for Body Segments

Paneling data for bodies are given by PERO6 data entries of **Figure 17**. For each POD, the IGRP field must be unique. With the configuration already defined, it is only necessary to specify axial and radial cuts. If the divisions specified in the configuration input are adequate, KRAD, LRAD, and LAXIAL are left blank. Equal radial cuts are specified using KRAD while arbitrary cuts are given on an AEFACT card identified by LRAD. The LAXIAL parameter is used only for FUSEL components.

By convention, the bottom centerline is at a meridian angle of 0° while the top centerline is at 180°. For fuselage segments and pods on the centerline, the angles must be input in ascending order from 0 to 180°. For pods not on the centerline, the angles must vary from 0 to 360°.

The AEROS entry of **Figure 18** provides reference lengths and areas that are used in determining stability information. The specification of reference properties is somewhat arbitrary, but we recommend that total aircraft span and the total wing reference area be used for REFB and REFS, respectively. The coordinate system ID's have no meaning at present so that fields ACSID and RCSID must be zero or blank. The GREF entry identifies a grid point about which pitching moment derivatives are calculated. If this field is left blank, the calculations are made about the origin of the basic coordinate system.

Input Data Entry PAERO6

Description: Defines body analysis parameters for steady aerodynamics.

Format and Examples:

1	2	3	4	5	6	7	8	9	10
PAERO6	BCID	CMPNT	CP	IGRP	NRAD	LRAD	LAXIAL		
PAERO6	10	FUSEL	0	3	4				

Field	Contents
BCID	Body component ID (Integer > 0)
CMPNT	Component type (FUSEL for the fuseIage or POD for a POD)
CP	Coordinate system of the geometric input (Integer)
IGRP	Aerodynamic group flag (Integer > 0)
NRAD	Number of equal radial cuts used to define the body panels (Integer ≥ 0.0 or blank)
LRAD	ID of an AEFACT data entry which defines the angular locations in degrees of the body panels (Integer ≥ 0.0 or blank).
LAXIAL	ID of an AEFACT data entry which defines the axial locations of the body panels (Integer ≥ 0.0 or blank).

Remarks:

1. LRAD is required only if NRAD is zero or blank.
2. LAXIAL is used only for FUSEL components. Inputs on the AEFACT entry are the dimensional fuselage stations.
3. If LAXIAL is blank, the axial locations are the same as those given by AXSTA data entries for the component.

Figure 17. The PAERO6 Bulk Data Entry

Input Data Entry <u>AEROS</u> Static Aero Physical Data

<u>Description</u>: Gives basic parameters for static aeroelasticity.

<u>Format and Examples</u>:

1	2	3	4	5	6	7	8	9	10
AEROS	ACSID	RCSIO	REFC	REFB	REFS	GREF	REFD	REFL	
AEROS	10	20	10.	100.	1000.	1			

Field	Contents
ACSID	Aerodynamic coordinate system identification (Integer > 0). See Remark 2.
RCSID	Reference coordinate system identification for rigid body motions (Integer > 0).
REFC	Reference chord length (Real > 0.0)(D - 1.0)
REFB	Reference span (Real > 0.0)(D - 1.0)
REFS	Reference wing area (Real > 0.0)(D - 1.0)
GREF	Reference grid point for stability derivative calculations.
REFD	Fuselage reference diameter (Real > 0)(D - 1.0)
REFL	Fuselage reference length (Real > 0)(D - 1.0)

<u>Remarks</u>:

1. This entry is required for static aeroelasticity problems. Only one AEROS entry is allowed.

2. The ACSID must be a rectangular coordinate system. Flow is in the positive x-direction.

3. The RCSID must be a rectangular coordinate system. All degrees of freedom defining trim variables will be defined in this coordinate system.

Figure 18. The AEROS Bulk Data Entry

The trim entry of **Figure 19** is used to specify the flight maneuver that is to be analyzed. Subsection 7.2.5 of the User's Manual discusses the output from various trim options while Subsection 9.2 through 9.4 of the Theoretical manual provide a basic description of these options.

3.2.2 Modeling Limits

A valuable property of the NASTRAN procedure is that it imposes virtually no problem size limits. There are limits imposed by integer word sizes and, of course, a user is strongly motivated to restrict the problem size to retain physical insight and to minimize computer resource expenditures. ASTROS has attempted to retain this freedom to model arbitrarily large models and, in most cases, this has been done. The USSAERO code was originally developed with fixed upper limits on all the model parameters and these were not removed within the scope of the ASTROS program. In most cases, these limits are sufficiently generous that they do not limit the ability to accurately model an aircraft for preliminary design purposes. The user does need to be aware of these limits and that is the purpose of this section. If the limits are exceeded, ASTROS, in most cases, terminates with a specific error message identifying the offending exceeded limits. **Tables 1 and 2** list these limits, the relevant data entries, and the relevant fields.

3.2.3 Modeling Guidelines

The quality of the aerodynamics can be strongly affected by the nature of the paneling. This subsection provides suggestions for preparing this input based on user experience and USSAERO documentation.

Because the USSAERO module makes linearized assumptions with respect to the individual panels, increasing the number of panels necessarily improves accuracy. Paneling meshes should be made finer in areas where substantial pressure gradients may be expected, such as lifting surface leading edges. In general, lifting surface results converge with a smaller number of panels than bodies. Simple trapezoidal wings may give excellent results with as few as 100 panels. The modeling of bodies typically requires a larger number of panels to best reflect the contours and thereby minimize the change in slope between adjacent panels.

Input Data Entry TRIM   Trim Variable Constraint

Description: Specifies conditions for aeroelastic trim analysis.

Format and Example:

1	2	3	4	5	6	7	8	9	10
TRIM	TID	MACH	QDP	SYMXZ	TRMTYP	NZ	QRATE	VO	
TRIM	1	.9	100.	1	1	1.0	0.0	0.0	

Field	Contents
TID	Trim set identification number (Integer > 0)
MACH	Mach number (Real > 0.0)
QDP	Dynamic pressure (Real > 0.0)
SYMXZ	Symmetry key for aero coordinate xz plane (Integer) (+1 for symmetry, 0 for no symmetry, -1 for antisymmetry).
TRMTYP	Type of trim required (0 = No trim, 1 = trim lift forces only, 2 = trim lift and pitching moment)(Integer)
NZ	Load factor or acceleration (Real)
QRATE	Aircraft pitch rate (rad/sec)(Real)
VO	Aircraft velocity (Real)

Remarks:

1. The TRIM entry is selected in solution control by "TRIM = TID."

2. Units on the inputs are:

   QDP - Force/unit area.
   NZ - This input is dimensioned with units of length/sec^2 unless a MASS conversion factor has been given, in which case NZ is non-dimensional. Acceleration used by the program is equal to NZ/MASS, where MASS is input on the CONVERT data entry or is defaulted to 1.0.
   QRATE - Rad/sec

$$q_{rate} = \frac{g(NZ-1.0)}{VO}$$

   VO - Length/sec

where the length, area and force units must be consistent with the remaining bulk data entries.

Figure 19. The TRIM Bulk Data Entry

3. QRATE and VO are required only when TRMTYP = 2.

4. Symmetric analyses are for longitudinal motions while anti-symmetric analyses are for lateral motions.

Figure 19. The TRIM Bulk Data Entry (Concluded)

TABLE 1. LIMITS ON CONFIGURATION DATA IN USSAERO

PARAMETER	LIMIT	BULK DATA ENTRY	DATA FIELD	QUANTITY
NWAF	$2 \le$ NWAF ≤ 20	AIRFOIL	N/A	Airfoils on the wing
NFINA & NCANA	NFINA = 2 NCANA = 2	AIRFOIL	N/A	Airfoils on canards and fins
NF	$0 \le$ NF ≤ 6	CAERO6	N/A	Fins in a given group
NCAN	$0 \le$ NCAN ≤ 6	CAERO6	N/A	Canards in a given group
NFUS	NFUS ≤ 6	BODY	N/A	Fuselage segments
NP	$0 \le$ NP ≤ 9	BODY	N/A	Pods
NWAFOR	$3 \le$ NWAFOR ≤ 30	AIRFOIL	ICHORD	Chordwise division points to define a wing airfoil
NFINOR & NCANOR	$3 \le$ NFINOR ≤ 10 $3 \le$ NCANOR ≤ 10	AIRFOIL	ICHORD	Chordwise division points to define a fin or canard airfoil
NFORX	$2 \le$ NFORX ≤ 30	AXSTA	N/A	Axial stations per fuselage segment
NRADX	$3 \le$ NRADX ≤ 20	LYRAD/ BODY	LYRAD/ NRAD	Radial cuts for a given axial station for half the fuselage
NPODOR	$2 \le$ NPODOR ≤ 30	AXSTA	N/A	Axial stations per pod
NTS	$3 \le$ NTS ≤ 21	AXSTA/ BODY	N/A	Radial cuts for a given axial station for a complete pod

TABLE 2. LIMITS ON PANELING DATA IN USSAERO

PARAMETER	LIMIT	BULK DATA ENTRY	DATA FIELD	QUANTITY
NBOX	NBOX $\leq$ 600	N/A		Total number of boxes in model
KWAF	2 $\leq$ KWAF $\leq$ 20	CAERO6	LSPAN	Spanwise division to define wing panel edges
KWAFOR	3 $\leq$ KWAFOR $\leq$ 30	CAERO6	LCHORD	Chordwise divisions to define wing panel edges
KFORX	2 $\leq$ KFORX $\leq$ 30	PAERO6	LAXIAL	Axial panel edges for a fuselage segment
KRADX	3 $\leq$ KRADX $\leq$ 20	PAERO6	LRAD	Radial panel edges for a fuselage segment
KF & KCAN	2 $\leq$ KF $\leq$ 20 2 $\leq$ KCAN $\leq$ 20	CAERO6	LSPAN	Spanwise divisions to define fin (canard) panel edges
KFINOR & KCANOR	3 $\leq$ KFINOR $\leq$ 30 3 $\leq$ KCANOR $\leq$ 30	CAERO6	LCHORD	Chordwise divisions to define fin (canard) panel edges
KPOD	3 $\leq$ KPOD $\leq$ 30	PAERO6	LAXIAL	Axial panel edges for a pod
KTRAD	3 $\leq$ KTRAD $\leq$ 21	PAERO6	LRAD	Radial panel edges per pod

For configurations with coplanar surfaces, the spanwise locations of the panel edges should be aligned to avoid influence from the concentrated vortices trailing in the wakes of upstream surfaces. If perfect alignment is not possible, the worst case occurs when the edge of one panel is aligned exactly with the centroid of another streamwise panel. This guideline should also be followed for non-coplanar surfaces if the vertical separation is on the order of the panel width.

The intersection of lifting and body surfaces must also be modeled with care. The lifting surface should intersect the body surface at a circumferential body panel edge, with an intersection at the centroid of the body panel constituting the worst possible case. Similarly, the streamwise edges on the lifting surface should be aligned so as to avoid the body panel centroids in the longitudinal direction.

For lifting surfaces, the panel aspect ratio (span divided by chord for the panel) should be kept between 0.5 and 5.0 with 1.0 the optimum. Panel sweep angles greater than 60 degrees may be prone to inaccuracy. The body panels should be constructed so as to minimize the change in slope both radially and circumferentially between adjacent panels. For supersonic analysis, if the slope is greater than the Mach angle, USSAERO terminates with an error message.

A modeling technique that addresses the fact that root segments of lifting surfaces are not necessarily along the x axis is to model a portion of what is nominally the lifting surface as a body surface. This is done by using the arbitrary body input option to define the wing root. Body segments are not required to extend completely around the body cross section. This feature can be used in the wing-body intersection region by modeling the upper body portion with one fuselage segment and the lower body portion with a second segment.

A final set of guidelines deals with reasonableness checks that can be made with the USSAERO data. Subsection 7.3.2 of the User's Manual discusses the use of the print parameter that can be set to view intermediate output from the USSAERO calculations. Many common errors will be obvious from scanning the geometry output for unreasonable values of areas, chord lengths and thickness and camber slopes. Stability derivatives, both from the rigid calculations of USSAERO and from the elastic corrections discussed in Subsection 7.2.5 of the User's Manual, can also be compared with estimates from other sources or engineering judgment. The experienced user can extract further information from the pressure and velocity output that is available by increasing the debug print.

3.3 UNSTEADY AERODYNAMIC MODELS AND FLUTTER ANALYSIS

Modeling for the subsonic Doublet Lattice (DLM) and the supersonic Constant Pressure (CPM) unsteady aerodynamics methods is relatively simple compared to the steady aerodynamic methods described in the preceding subsections. Both unsteady methods use the CAERO1 bulk data entries to describe the lifting surface panels. The CPM method does not have a provision for bodies while the DLM method inputs body data using a combination of CAERO2 bulk data entries to identify the body configurations, PAERO1 bulk data entries to identify the body IDs and PAERO2 bulk data entries to identify the body paneling.

The following guidelines were liberally adapted from the MSC/ NASTRAN Handbook for Aeroelasticity cited in Subsection 2.4.

The lifting surfaces are idealized as planes parallel to the flow. The configuration is divided into planar trapezoidal panels (macro-elements), each with a constant dihedral and with sides parallel to the airstream direction. These panels are further subdivided into "boxes" which are similarly configured trapezoids. If a surface lies in (or nearly in) the wake of another surface, then its spanwise divisions should lie along the divisions of the upstream surface. The aspect ratio of the boxes should approximate unity; a range of 1/3 to 3 is acceptable. The chord length of the boxes should be less than 0.08 times the velocity divided by the greatest frequency in (Hz) of interest, i.e., $\Delta x < 0.08V/f$, but no less than four boxes per chord should be used. Boxes should be concentrated near wing edges and hinge lines or any other place where downwash is discontinuous and pressures have large gradients. The chord length of adjacent boxes in the streamwise direction should not change abruptly.

Aerodynamic panels are assigned to interference groups. All panels within a group have aerodynamic interaction. The purpose of the group is to reduce the time to compute aerodynamic matrices when it is known that aerodynamic interference is important within the group but otherwise is negligible, or to allow the analyst to investigate the effects of aerodynamic interference.

Each panel is described by a CAERO1 bulk data entry. A property card PAERO1 may be used to identify associated interference bodies. A body should be identified as a member of the group if the panel is within one diameter of the surface of the body. The box divisions along the span are determined either by specifying the number of equal boxes, NSPAN, or by using LSPAN to identify the AEFACT data entry which specified a list of division points in terms of fractions of the span. A similar arrangement is used to specify divisions in the chordwise direction by choosing NCHORD or LCHORD. The locations of the two leading edge points are specified in any coordinate system (CP) defined by the user. The lengths of the sides (chords) are specified by the user, and they are in the airstream direction. Every panel must be assigned to some interference group (IGID). If all panels interact, then IGID will be the same for all panels.

The bodies are idealized as either "slender" or "interference" elements. The primary purpose of the slender body elements is to account for the forces arising from the motion of the body, whereas the interference elements are used to account for the interference among all bodies and panels in the same group. This is done by providing a surface through which the boundary condition of no flow is imposed. Bodies are further classified as to the type of motion allowed. In the aerodynamic coordinate system, y and z are perpendicular to the flow. In general, bodies may move in either the y- and z-directions. Frequently, a body (e.g., a fuselage) lies on a plane of symmetry and only z- (or y-) motion is allowed. Thus, any model may contain z-bodies, zy-bodies, and y-bodies. One or two planes of symmetry or antisymmetry may be specified.

The location of a body is specified on a CAERO2 data card. The location of the nose and the length in the flow direction are given. The slender body elements and interference elements are distinct quantities and must be specified separately. At least two slender body elements are required for every body, while interference elements are optional. The geometry is given in terms of the element division points, the associated width and a single height-to-width ratio for the entire body length. The locations of the division points may be given in dimensionless units or, if the lengths are equal, only the number of elements need be specified. The semi-width of the two types of elements may be specified separately and are given in units of length. Usually, the slender body semi-width is taken as zero at the nose and is a function of x. The interference body semi-width is constant. The height-to-width ratio must be constant for each body.

Body elements are intended for use with Doublet-Lattice panels, and there must be at least one panel in the model. The interference elements are intended for use only with panels and/or other bodies, while slender body elements can stand alone.

There are some rules about bodies which have been retained from the NASTRAN code. All z-only bodies must have lower ID numbers than zy bodies, which, in turn, must have lower ID numbers than y-only bodies. The total number of interference bodies associated with a panel is limited to six. The user should be cautious about the use of associated interference bodies since they increase computing time significantly.

There are no built-in limits on the number of panels, slender bodies or boxes in the unsteady aerodynamics model. Computational time is an expotential function of aerodynamic degrees of freedom so that user is motivated to minimize this number.

3.4 DYNAMIC RESPONSE ANALYSIS

As discussed in Section XI of the Theoretical Manual, dynamic response analysis in ASTROS refers to structural analyses that are performed with applied loadings that are a function of time or frequency. This subsection discusses data preparation for these analyses in terms of (1) structural modifications, (2) loads generation, and (3) response point specification.

3.4.1 Modifications to the Structural Model

Dynamic analyses permit a number of special purpose inputs that allow the user considerable flexibility in specifying the equations of motion that are to be solved in the particular analysis. Subsection 11.1 of the Theoretical Manual describes the generation of the mass, damping and stiffness matrices for these analysis. This subsection discusses three special input options that are available for defining these matrices: (1) direct matrix input, (2) extra points, and (3) transfer functions. An innovation in ASTROS is that these inputs are invoked by the BOUNDARY solution control command. This allows the user to exercise a number of dynamic structural models in a single job submittal.

Mass, damping and stiffness matrix modifications are designated using the M2PP, B2PP, and K2PP options of the BOUNDARY solution control command, respectively, to identify DMI or DMIG bulk data entries. This input is in the p-set, implying that any extra point degrees of freedom must be considered in defining these matrices.

Extra points are designated using the ESET option of the BOUNDARY solution control command. This option identifies the extra point set that is to be used in the corresponding boundary condition, and this set identification is included on the EPOINT bulk data entries. Note that NASTRAN does not have a set identifier on the EPOINT bulk data entry.

Transfer functions are designated using the TFL option of the BOUNDARY solution control command. This option identifies the transfer function set that is to be used in the corresponding boundary condition, and this

set identification is included on the TF bulk data entries. This conforms to NASTRAN convention.

3.4.2 Dynamic Loads Generation

The generation of the applied loads in ASTROS is conceptually complex in that it requires a series of bulk data entries to define a given set of loads. The charts given in **Figure 20** for time dependent loads and in **Figure 21** for frequency dependent loads are useful in defining the sequence of data entries.

For the time dependent loads, the DLOAD bulk data entry identifies the component loads and the scale factors that are to be applied to each. The DLOAD entry is referenced by the TRANSIENT solution control entry and it references TLOAD1 or TLOAD2 bulk data entries to define the component loads. The TLOADi entries allow alternative means for specifying the time dependent nature of the loading but both reference the DLAGS bulk data entry to define any prescribed time lags and the spatial loading condition. This loading condition is, in turn, defined by a combination of standard bulk data entries used to define statically applied loads and the special purpose DLONLY bulk data entry. The DLONLY entry is similar to the DAREA bulk data entry of NASTRAN (which ASTROS does not support) and is particularly useful in applying loads to extra points that are in the structural model. Two other NASTRAN entries related to transient loading that are not supported in ASTROS are the DPHASE and the DELAY entries. Equal capability is available from the two systems with the ASTROS implementation streamlined relative to the NASTRAN formulation.

The specification of frequency dependent loads (**Figure 21**) is similar to the transient case in that the DLOAD bulk data entry identifies the component loads and the scale factors that are to be applied to each. In this case, the DLOAD entry is referenced by the FREQUENCY solution control entry, and it references RLOAD1 or RLOAD2 bulk data entries to define the component loads. The RLOADi entries allow alternative means for specifying the frequency dependent nature of the loading, but both reference the DLAGS bulk data entry to define any prescribed time and phase lags and the spatial loading condition. This loading condition is, in turn, defined by a combination of standard bulk data in a manner identical to the transient loading case.

$$P(x, y, z, t) = S(x, y, z)\,F(t)$$

Input Flow

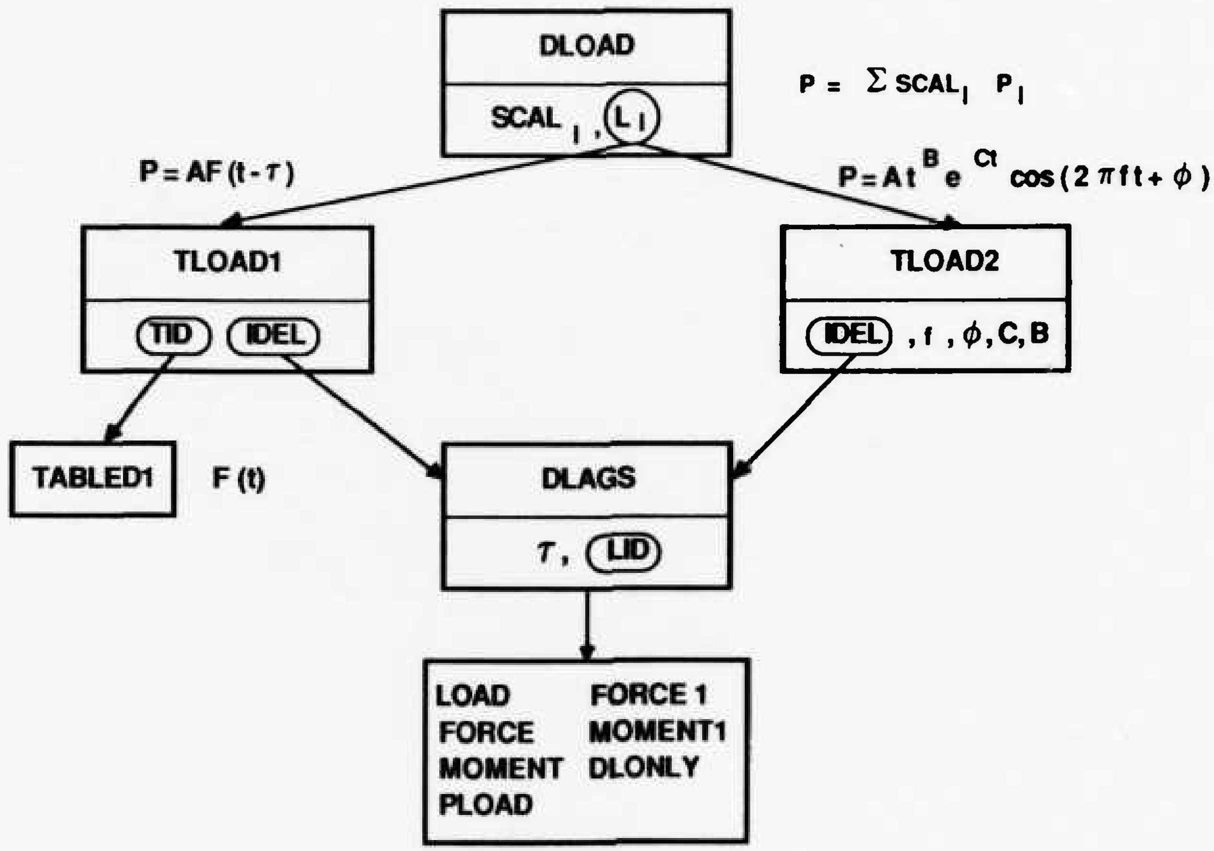

Figure 20. Bulk Data Entries for the Generation of Loads Used in Transient Response Analysis

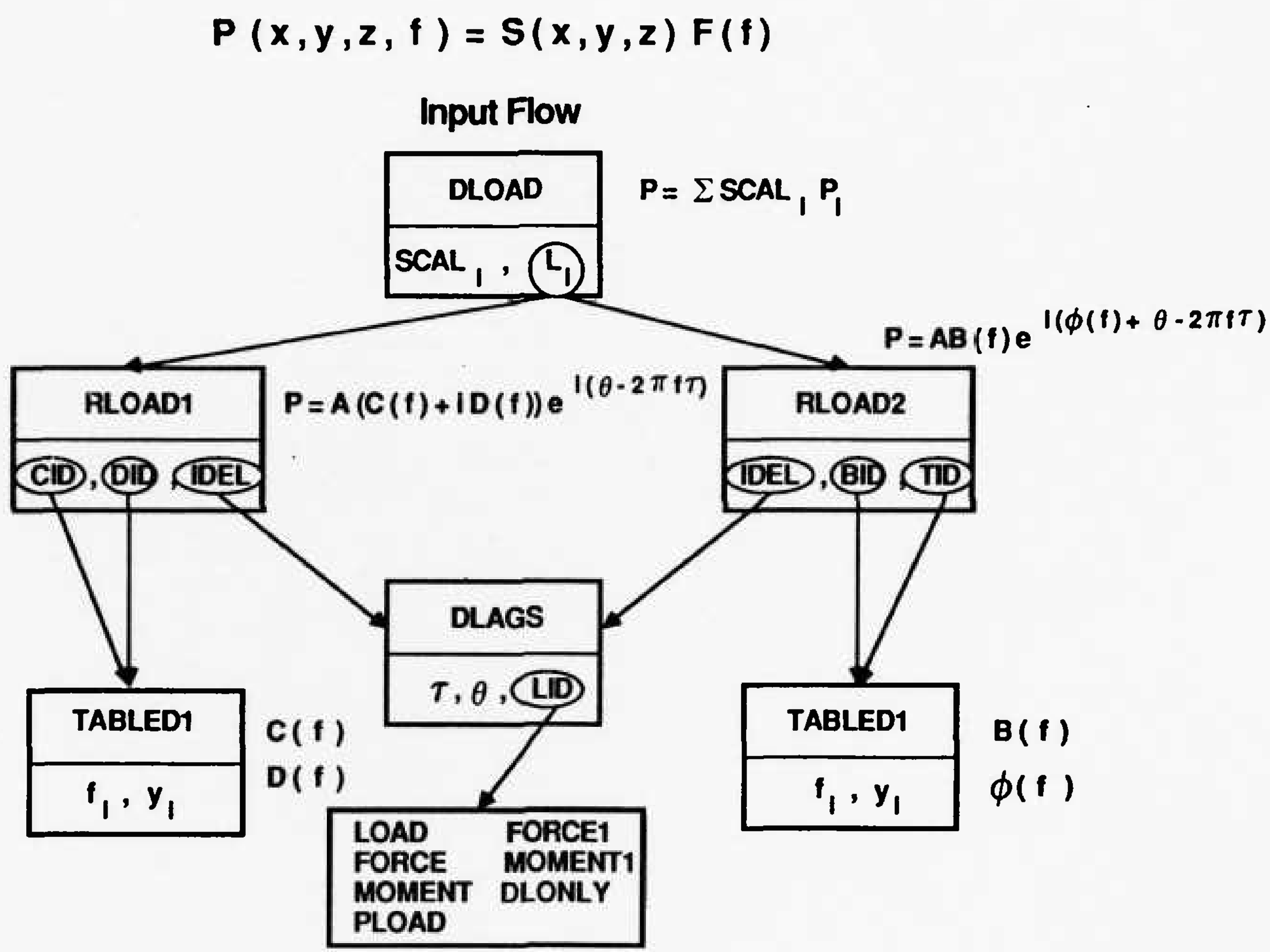

Figure 21. Bulk Data Entries for the Generation of Loads Used in Frequency Response Analysis

The dynamic response analysis of calculating an aircraft's response to atmospheric gust requires specialized inputs that are an improvisation on the FREQUENCY discipline under which the gust option is performed. **Figure 22** shows the input flow for this case and indicates that, in addition to the gust input requirements, there are phantom inputs that are required to satisfy error checking requirements. The gust loads are generated based on the GUST bulk data entry, which is referenced by the GUST option for the FREQUENCY discipline in solution control. The gust bulk data entry defines several gust parameters and identifies an RLOADi bulk data entry which defines a frequency dependent function that is applied to the gust wave (see Subsection 11.2.3 of the Theoretical Manual). These two entries completely specify the gust loading while further entries satisfy error checking requirements. For example, the FREQUENCY discipline always specifies a DLOAD identification for which a corresponding DLOAD entry must exist. If it does not, the error checking routine terminates ASTROS processing. The error checking routine is sufficiently intelligent that it does not require data subsequent to the DLOAD entry as indicated in **Figures 20 and 21**. The RLOADi entry does require phantom inputs in that an RLOADi entry without a DLAGS entry results in a fatal error as does the presence of a DLAGS entry without some corresponding applied load.

3.4.3 Response Point Specification

Dynamic analyses are performed at a user defined set of time or frequency points. For transient analyses, the TSTEP option of the TRANSIENT solution control command identifies the TSTEP bulk data entry that specifies the time steps that are to be used in the analysis. TSTEP bulk data entry also specifies at which time steps the results of the analysis are to stored. User output is specified using the PRINT solution control command. The DISP, VELO and ACCE options of the PRINT request reference a GRIDLIST bulk data entry which specifies the grids at which displacement, velocity and acceleration outputs, respectively, are to be printed. Element response quantities are also available. The TIME option identifies a TIMELIST bulk data entry which defines the times at which the outputs are to be printed. If the TIMELIST requests a time at which results were not computed, the nearest computed time is used to satisfy the output request.

An item related to transient response points is the initial condition specification that can be used with the direct approach for transient

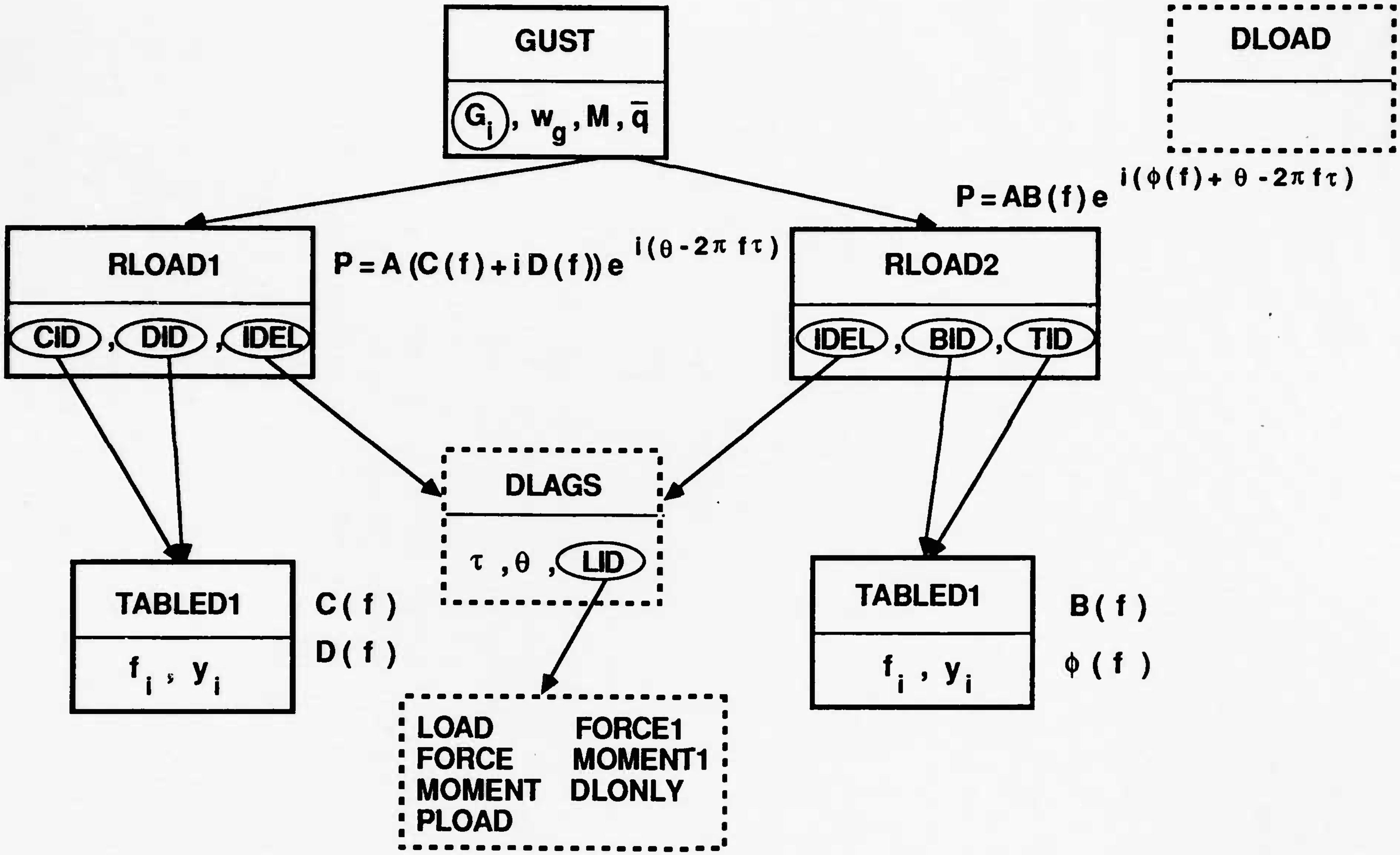

Figure 22. Bulk Data Entries for the Generation of Loads Used in Gust Response Analysis

analysis. The IC option of the TRANSIENT solution control command designates the set identifier of the IC bulk data entries that contain the actual initial conditions. The bulk data entry is identical, except for the name, with the NASTRAN TIC entry.

For frequency analyses, the FSTEP option of the FREQUENCY solution control identifies the FREQ, FREQ1 and FREQ2 bulk data entries that specify the frequency steps that are to be used in the analysis. Frequencies are integrated from all the data entries with the given set identifier and duplicate frequencies are removed. User output is specified using the PRINT solution control command. The DISP, VELO, and ACCE options of the PRINT request reference GRIDLIST bulk data entries which specify the grids at which displacement, velocity, and acceleration outputs, respectively, are to be printed. The FREQ option for the PRINT command identifies a FREQLIST bulk data entry which defines the frequencies at which the outputs are to be printed. If the FREQLIST entry requests a frequency at which results were not computed, the nearest computed frequency is used to satisfy the output request.

3.5 CONVERSION OF NASTRAN BULK DATA PACKETS

As has been stressed, ASTROS has emulated NASTRAN bulk data entries the maximum extent possible. This has been done to ease acceptability of the ASTROS code into the industrial aerospace environment and to minimize the learning required to exercise this new system. The ability of existing preprocessors to generate and depict NASTRAN bulk data packets should be a major facilitator in the development of ASTROS bulk data packets.

Despite this similarity, there are differences in the input requirements and Subsections 6.4 and 6.5 of the User's Manual identify and explain the discrepancies between the two systems. A large number of the differences in the entries are in the connectivity and property entries where maximum and minimum thickness values are input by ASTROS for the shape function linking concept discussed in Subsection 3.1.2. This subsection emphasizes the more substantial revisions that are sometimes required when an existing NASTRAN data packet is converted to ASTROS.

The NASTRAN procedure encompasses a number of capabilities that have not been implemented in ASTROS. Among these are nonlinear, hydroelastic, cyclic symmetry, and superelement analysis. Obviously, data packets that

require these capabilities cannot be converted to ASTROS. In addition, the NASTRAN procedure has several convenience features that have not been implemented in ASTROS. Three notable examples of these are rigid elements, the AUTOSPC feature and automated grid point resequencing.

The rigid element capability allows for a streamlined specification of multipoint constraints. These elements represent kinematic constraints between grid points that are based on the rigid body motion of a rod, bar, plate or higher order member. These elements are very useful in defining NASTRAN models, particularly when simplified dynamics models are being constructed. The absence of these elements in ASTROS can be a serious hindrance because the manual translation of these elements into their equivalent multipoint constraints typically requires painstaking definition. An alternative to this manual translation is to exercise the NASTRAN bulk data deck in NASTRAN and use an alter to the DMAP sequence to print the GM matrix of NASTRAN (TMN in Subsection 6.1 of the Theoretical Manual). This matrix can be directly converted into MPC bulk data entries and inserted into ASTROS.

The AUTOSPC feature of NASTRAN relieves the user of the burden of specifying the single point constraints which remove the unconnected degrees of freedom from the structure. ASTROS does not support this feature. However, if the PARAM,AUTOSPC,YES feature of NASTRAN is utilized, the PARAM, PRGPST, YES feature can be used to print identified singular degrees of freedom and the PARAM,SPCGEN,1 can be used to punch SPC bulk data entries which could then be inserted into the ASTROS bulk data packet.

While ASTROS does not have the automatic bandwidth minimization capability of MSC/NASTRAN, the benefits of good internal connectivity properties are so profound the capability for manual resequencing was included. In order to provide maximum capability with known preprocessors that provide resequencing data for COSMIC/NASTRAN, the same input was chosen for ASTROS. This involves the use of the SEQGP bulk data entry which specified the "sequence id" of a structural node. The default ordering in ASTROS (based on the external id value) can be modified by manual definition of sequence IDs. The internal order is then determined by a sorted list of these sequence identification numbers. As in COSMIC, the sequence number defaults to be 1000 times the external grid point identification number. The SEQGP entry can change this sequence number for any or all grid points with the final internal sort

determined from the resulting list of sequence numbers. This method forces the addition of one restriction to the external grid point id: when SEQGP is used, the value of 1000 time any external grid point id must be less than the machine maximum integer. This restriction is slightly less strict than in COSMIC/NASTRAN where the grid id must be less than 200,000. In ASTROS, there is no such restriction if no SEQGPs are used. The SEQGP entries allow the resequencing of the grid and scalar points (the so-called structural nodes). In COSMIC/NASTRAN, there is an additional capability to reorder the nonstructural "physical" degrees of freedom defined by EPOINT bulk data entries. While extra points are supported in ASTROS for dynamic response disciplines, the resequencing of extra point degrees of freedom is not. These degrees of freedom are always appended onto the end of the a-set structural matrices during dynamic matrix assembly.

ASTROS' SEQGP data can be prepared manually or obtained by running the input deck in MSC/NASTRAN with "PARAM,NEWSEQ,3" and "PARAM,SEQOUT,2" in the bulk data deck. These two parameters invoke the automated resequencer in NASTRAN and punch the results in the form of SEQGP entries directly interpretable by ASTROS. Any other independent source of SEQGP data may also be used.

Experience in converting NASTRAN bulk data packets for use in ASTROS has indicated that the following, relatively simple, modifications are often required:

(1) ASET, ASET1, OMIT, OMIT1 entries all require set identifiers that must be referred to as part of the BOUNDARY solution control command to be used.

(2) For dynamic analyses, EPOINT bulk data entries require set identifiers that must be referenced as part of the BOUNDARY solution control command to be used.

(3) Tabular data (e.g., the TABLED1 data entry) in ASTROS do not recognize the ENDT field and this must be deleted.

(4) There is no CTRIA3 element in ASTROS so that triangular elements must be modeled by a CTRMEM element or replaced by a very irregular CQUAD4 element.

(5) The SPLINE2 bulk data entry has not been implemented in ASTROS. This is the linear spline and it is possible to approximate its

use in ASTROS either by a combination of extra grids, MPCs and the SPLINE1 feature or by the ATTACH bulk data entry.

(6) ASTROS does not use PARAM bulk data entries. The CONVERT, MFORM and VSDAMP bulk data entries in ASTROS perform the function of the WTMASS, VREF, COUPMASS, W3 and W4 PARAMeters in NASTRAN.

(7) ASTROS requires that all continuation bulk data entries immediately follow their parent. Further, the insertion of a comment line between a parent and a child entry is not permitted in ASTROS.

Continuation entries can also be troublesome when converting an ASTROS generated bulk data packet to NASTRAN. This is because ASTROS has no requirement that the data in the continuation field be unique. It is sometimes expedient to use the same continuation indicator for any number of entries in ASTROs and these all have to be made unique before NASTRAN can be exercised.

SECTION IV

SAMPLE CASES

This section presents a series of sample cases that can be used as examples for various modeling options and that also serve as test cases that can be used to check the installation of the ASTROS procedure at a new site. One criteria used in selecting cases for presentation was that they should be relatively small so that the key features would not be overwhelmed by the volume of data required to define the model. A second criteria was that a representative set of cases should be provided with a broad range of capabilities and a minimum of overlap.

4.1 THE TEN BAR TRUSS MODEL

This example illustrates the performance of ASTROS system in minimum weight optimization subject to strength constraints. Secondarily, this problem provides an example of the use of the MPPARM bulk data entry to control the performance of the MICRO-DOT optimization algorithm.

4.1.1 Problem Description

The structural model is the classic ten bar truss defined in, for example,

> Venkayya, V. B., "Design of Optimum Structures," Computers and Structures, Volume 1, pp 265-309, 1971.

The finite element model, shown in **Figure 23**, has six nodes and ten truss elements made of aluminum with a Young's Modulus of 10.0×10^6 psi and a weight density of 0.10 lb/in^3. The initial truss member cross sectional areas are 30.0 in^2, resulting in an initial design weight of 12, 589.4 lb. The design problem minimizes the weight of the structure while limiting the transverse displacements to 2.0 inches and the stress in each truss element to 25 ksi under the loading shown in **Figure 23**. The design variables are the ten truss element cross section areas, each of which has a lower bound side constraint of 0.10 in^2.

P = 100,000 lbs

| σ | ≤ 25 ksi

Vertical Displacement < 2.0 inches

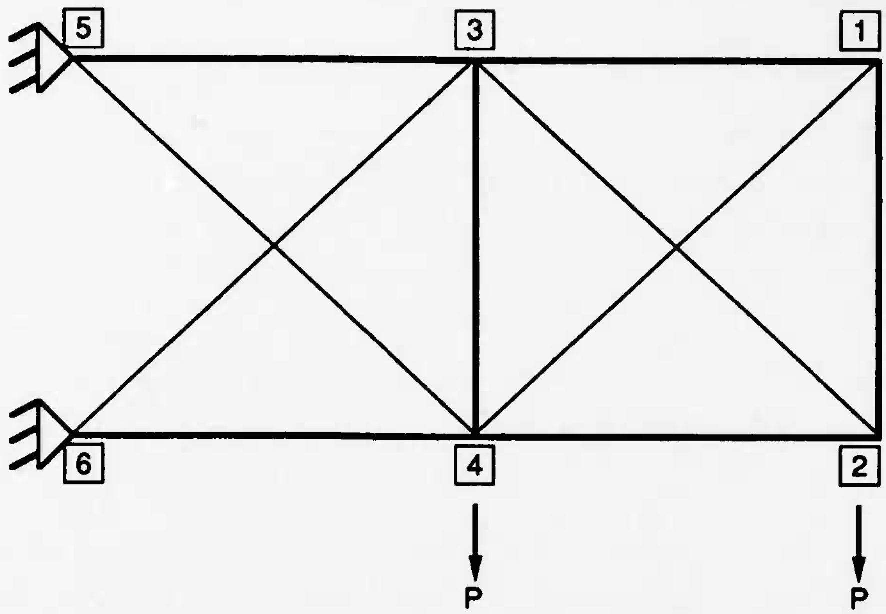

Figure 23. The Ten Bar Truss Model

This classic optimization problem has been thoroughly discussed in numerous places, notably the report cited above. The remaining theoretical aspect of relevance to this example is the discussion of the optimizer, MICRO-DOT, employed in the ASTROS system. Section XIII of the Theoretical Manual presents the theoretical background for mathematical programming methods and lists other sources of information for the particular optimization algorithms used by MICRO-DOT.

4.1.2 <u>Input Description</u>

Figure 24 shows the input for this example. The solution control packet contains both an optimization subpacket, starting with the OPTIMIZE command, and an analysis subpacket, starting with the ANALYZE command. The optimization subpacket contains a single boundary condition with a single static analysis discipline. The STATICS discipline specification includes a design constraint set (DCON = 100) which refers to the DCONDSP bulk data entries in the bulk data packet. These entries specify the limits on the

```
ASSIGN DATABASE TENBAR SHAZAM NEW DELETE
SOLUTION
TITLE = TEN BAR TRUSS
OPTIMIZE STRATEGY = 57
   BOUNDARY SPC = 1
      LABEL = STATIC ANALYSIS
      PRINT DCON
      STATICS (MECH = 1, DCON = 100 )
END
ANALYZE
   BOUNDARY SPC = 1, METHOD = 2
      STATICS ( MECH = 1 )
         LABEL = FINAL STATIC ANALYSIS
         PRINT DISP = ALL
      MODES
         LABEL = FINAL MODAL ANALYSIS
         PRINT DISP = ALL, MODES ALL, ROOT=ALL
END
BEGIN BULK
$
$     ASTROS PILOT SYSTEM SAMPLE PROBLEM 1
$
$            TEN BAR TRUSS MODEL
$            FROM SCHMIT, L.A., JR. AND MIURA, H., " APPROXIMATION
$                    CONCEPTS FOR EFFICIENT STRUCTURAL SYNTHESIS ",
$                    NASA CR-2552, MARCH 1976.
$
$
$        THE STRUCTURAL MODEL
$
GRID,    1,    , 720.0,  360.0,   0.0
GRID,    2,    , 720.0,    0.0,   0.0
GRID,    3,    , 360.0,  360.0,   0.0
GRID,    4,    , 360.0,    0.0,   0.0
GRID,    5,    ,   0.0,  360.0,   0.0
GRID,    6,    ,   0.0,    0.0,   0.0
CROD,    1, 10,     3,      5
CROD,    2, 10,     1,      3
CROD,    3, 10,     4,      6
CROD,    4, 10,     2,      4
CROD,    5, 10,     3,      4
CROD,    6, 10,     1,      2
CROD,    7, 10,     4,      5
CROD,    8, 10,     3,      6
CROD,    9, 10,     2,      3
CROD,   10, 10,     1,      4
PROD,   10,  2,  15.0
$
MAT1,    2,  1.E+7,  ,  0.3,  0.1, , , ,  25000.0,  -25000.0
$
SPC1,    1,  123456,  5,   6
SPC1,    1,  3456,    1,   THRU,  4
$
```

Figure 24. Input Data Stream for the Ten Bar Truss

```
$       STATICS CASE
$
FORCE,  1,  2, , -1.E5,  0.0,   1.0,   0.0
FORCE,  1,  4, , -1.E5,  0.0,   1.0,   0.0
$
$       MODAL ANALYSIS INPUT
$
CONVERT, MASS, 2.59E-3
EIGR,      2,    GIV,  0.0,  700.0,   2,   2,  ,  , ABC, +BC,  MAX
$
$       THE DESIGN MODEL
$
MPPARM, DABOBJ, 0.01, DELOBJ, 0.0001, CTLMIN, 0.0001, STOL, 0.0001, +MP1
+MP1,   ITRMOP, 6, ITMAX, 75
DESELM,  1,  1,  CROD,  6.667E-3,  1000.0,   2.0,  ,  ROD1
DESELM,  2,  2,  CROD,  6.667E-3,  1000.0,   2.0,  ,  ROD2
DESELM,  3,  3,  CROD,  6.667E-3,  1000.0,   2.0,  ,  ROD3
DESELM,  4,  4,  CROD,  6.667E-3,  1000.0,   2.0,  ,  ROD4
DESELM,  5,  5,  CROD,  6.667E-3,  1000.0,   2.0,  ,  ROD5
DESELM,  6,  6,  CROD,  6.667E-3,  1000.0,   2.0,  ,  ROD6
DESELM,  7,  7,  CROD,  6.667E-3,  1000.0,   2.0,  ,  ROD7
DESELM,  8,  8,  CROD,  6.667E-3,  1000.0,   2.0,  ,  ROD8
DESELM,  9,  9,  CROD,  6.667E-3,  1000.0,   2.0,  ,  ROD9
DESELM, 10, 10,  CROD,  6.667E-3,  1000.0,   2.0,  ,  ROD10
$
$       CONSTRAINT DEFINITION
$
DCONSTR,    2, VMISES
DCONDSP,  100,  1,  UPPER, 2.0,   POSNOD1,  1,  2,   1.0
DCONDSP,  100,  2,  UPPER, 2.0,   POSNOD2,  2,  2,   1.0
DCONDSP,  100,  3,  UPPER, 2.0,   POSNOD3,  3,  2,   1.0
DCONDSP,  100,  4,  UPPER, 2.0,   POSNOD4,  4,  2,   1.0
DCONDSP,  100,  5,  LOWER, -2.0,   NEGNOD1,  1,  2,  1.0
DCONDSP,  100,  6,  LOWER, -2.0,   NEGNOD1,  2,  2,  1.0
DCONDSP,  100,  7,  LOWER, -2.0,   NEGNOD1,  3,  2,  1.0
DCONDSP,  100,  8,  LOWER, -2.0,   NEGNOD1,  4,  2,  1.0
ENDDATA
```

Figure 24. Input Data Stream for the Ten Bar Truss (Concluded)

transverse displacements. The stress constraints are imposed through the appearance of a DCONSTR bulk data entry which declares that MATi entry 2 has a von Mises stress criteria associated with it. The MATi entry, in this case, is a MAT1 with the tension and compression stress limits given in the stress allowable field.

The analysis subpacket of the Solution Control packet also selects a statics analysis so that the final displacements may be printed. In addition, a modal analysis is performed to obtain the modal frequencies and the first two eigenvectors of the final design. The Solution Control packet includes the request to print the eigenvalues and eigenvectors for this analysis. Because a modal analysis is performed, the analysis boundary condition definition includes the specification of the eigenvalue extraction method.

The basic structural model is very simple, with standard GRID, CROD, PROD and MAT1 entries used to define the model. The design model is also relatively simple in that unique linking is used: one DESELM entry is supplied for each rod element, resulting in 10 global design variables. The DESELM entry includes a specification of the minimum global variable value, 0.006667, and the initial global design variable value, 2.0. Since the initial property value on the PROD entry is 15.0, the physical variables are limited to 0.01 in^2 and are initially 30.0 in^2.

The CONVERT bulk data entry is used in this example to convert the weight density used on the MAT1 entry to a mass density. This allows the objective function to appear in pounds, but gives the correct mass properties for the modal analysis.

The MPPARM bulk data entry sets a number of MICRO-DOT parameters to ensure that each ASTROS iteration is more fully exploited by the optimizer. These parameters redefine the value of the objective function change that signifies convergence, define stricter parameters indicating active and violated constraints, and decrease the tolerance of components indicating that the Kuhn-Tucker conditions are satisfied. Finally, the number of iterations that MICRO-DOT can perform and the number of cycles that must be repeated to indicate that convergence has occurred are both increased relative to default values.

4.1.3 Results and Output Description

The optimization phase of this example produces minimal output consisting only of the constraint values at each iteration and the default final design output. **Figure 25(a)** shows the design iteration history for the optimization phase. A discussion of the format of this table is given in Subsection 4.2.3. A converged solution was found in 11 redesign cycles and the final objective function value is 5,100 pounds. The lower bound displacement constraints at Nodes 1 and 2 are both exactly satisfied at the optimum. **Figure 25(b)** shows the same data for the case where the MPPARM data are omitted from the input stream. The problem then requires 14 redesign cycles and converges to a weight that is slightly higher than otherwise obtained. The utility of the MPPARM data entry is thus demonstrated for this problem. The convergence behavior of this particular problem, however, has been shown to be very sensitive to the optimization algorithm and thus, no general statements can be made about the "best" optimization parameters for all problems. At best, it indicates that the convergence behavior in any particular optimization problem may be dramatically improved through the judicious selection of MICRO-DOT parameters.

The static displacements for the final design are printed in the second (ANALYZE) boundary condition, as shown in **Figure 26(a)** while **Figure 26(b)** shows the results of the normal modes analysis of the final design which takes place in the same boundary condition.

4.2 THE ACOSS MODEL

This example illustrates the performance of the ASTROS system in minimum weight optimization subject to modal frequency constraints. Secondarily, the example provides a comparison of Guyan Reduction and Generalized Dynamic Reduction (GDR) in normal modes analysis. The structural model is the modified ACOSS-II (Active Control of Space Structures - Model 2) presented in "Structural Optimization with Frequency Constraints" by R.V. Grandhi and V.B. Venkayya, AIAA/ASME/ASCE/AHS 28th Structures, Structural Dynamics and Materials Conference proceedings.

TEN BAR TRUSS　　ASTROS VERSION 1.00　5/12/88　P. 27
ASTROS ITERATION 12

STATIC ANALYSIS

A S T R O S　D E S I G N　I T E R A T I O N　H I S T O R Y

ITERATION NUMBER	OBJECTIVE FUNCTION VALUE	NUMBER FUNCTION EVAL	NUMBER GRADIENT EVAL	NUMBER RETAINED CONSTRAINTS	NUMBER ACTIVE CONSTRAINTS	NUMBER VIOLATED CONSTRAINTS	NUMBER LOWER BOUNDS	NUMBER UPPER BOUNDS	APPROXIMATE PROBLEM CONVERGENCE
1	1.25894E+04	0	0	0	0	0	0	0	NOT CONVERGED
2	7.12562E+03	48	9	18	1	0	0	7	NOT CONVERGED
3	6.35730E+03	57	12	18	1	0	0	3	NOT CONVERGED
4	6.07620E+03	47	12	18	1	0	0	1	NOT CONVERGED
5	5.88243E+03	63	15	18	1	0	0	1	NOT CONVERGED
6	5.73494E+03	53	13	18	1	0	0	1	NOT CONVERGED
7	5.60611E+03	54	14	18	1	0	0	1	NOT CONVERGED
8	5.47428E+03	66	16	18	1	0	0	1	NOT CONVERGED
9	5.32908E+03	97	23	18	1	0	0	1	NOT CONVERGED
10	5.18424E+03	107	27	18	2	0	0	3	NOT CONVERGED
11	5.11367E+03	101	22	18	2	0	0	2	NOT CONVERGED
12	5.10094E+03	113	28	18	2	0	0	1	CONVERGED

THE FINAL OBJECTIVE FUNCTION VALUE IS:

FIXED = 0.00000E+00
+ DESIGNED = 5.10094E+03

TOTAL = 5.10094E+03

(a) MPPARM Data

TEN BAR TRUSS　　ASTROS VERSION 1.00　2/23/88　P. 33
ASTROS ITERATION 15

STATIC ANALYSIS

A S T R O S　D E S I G N　I T E R A T I O N　H I S T O R Y

ITERATION NUMBER	OBJECTIVE FUNCTION VALUE	NUMBER FUNCTION EVAL	NUMBER GRADIENT EVAL	NUMBER RETAINED CONSTRAINTS	NUMBER ACTIVE CONSTRAINTS	NUMBER VIOLATED CONSTRAINTS	NUMBER LOWER BOUNDS	NUMBER UPPER BOUNDS	APPROXIMATE PROBLEM CONVERGENCE
1	1.25894E+04	0	0	0	0	0	0	0	NOT CONVERGED
2	7.12706E+03	32	5	18	1	0	0	8	NOT CONVERGED
3	6.36279E+03	30	6	18	1	0	0	1	NOT CONVERGED
4	6.08679E+03	39	8	18	1	0	0	1	NOT CONVERGED
5	5.89346E+03	47	11	18	1	0	0	1	NOT CONVERGED
6	5.77157E+03	35	9	18	1	0	0	0	NOT CONVERGED
7	5.63784E+03	42	9	18	1	0	0	1	NOT CONVERGED
8	5.52991E+03	31	8	18	1	0	0	0	NOT CONVERGED
9	5.42730E+03	31	7	18	1	0	0	0	NOT CONVERGED
10	5.33242E+03	28	8	18	1	0	0	0	NOT CONVERGED
11	5.24528E+03	20	5	18	2	0	0	0	NOT CONVERGED
12	5.20137E+03	30	6	18	2	0	0	0	NOT CONVERGED
13	5.16791E+03	22	5	18	2	0	0	0	NOT CONVERGED
14	5.14050E+03	16	3	18	2	0	0	1	NOT CONVERGED
15	5.12243E+03	17	4	18	2	0	0	1	CONVERGED

THE FINAL OBJECTIVE FUNCTION VALUE IS:

FIXED = 0.00000E+00
+ DESIGNED = 5.12243E+03

TOTAL = 5.12243E+03

(b) No MPPARM Data

Figure 25. Iteration Histories for the Ten Bar Truss

TEN BAR TRUSS | ASTROS VERSION 1.00 5/12/88 P. 31

FINAL STATIC ANALYSIS | STATICS ANALYSIS: BOUNDARY 2, SUBCASE 1

D I S P L A C E M E N T   V E C T O R

POINT ID.	TYPE	T1	T2	T3	R1	R2	R3
1	G	2.34025E-01	-2.00087E+00	0.00000E+00	0.00000E+00	0.00000E+00	0.00000E+00
2	G	-5.42511E-01	-1.99994E+00	0.00000E+00	0.00000E+00	0.00000E+00	0.00000E+00
3	G	2.35050E-01	-7.32939E-01	0.00000E+00	0.00000E+00	0.00000E+00	0.00000E+00
4	G	-2.98249E-01	-1.47151E+00	0.00000E+00	0.00000E+00	0.00000E+00	0.00000E+00
5	G	0.00000E+00	0.00000E+00	0.00000E+00	0.00000E+00	0.00000E+00	0.00000E+00
6	G	0.00000E+00	0.00000E+00	0.00000E+00	0.00000E+00	0.00000E+00	0.00000E+00

(a) Static Displacements

TEN BAR TRUSS | ASTROS VERSION 1.00 5/12/88 P. 32

FINAL MODAL ANALYSIS | MODES ANALYSIS: BOUNDARY 2, MODE 1

S U M M A R Y   O F   R E A L   E I G E N   A N A L Y S I S

8 EIGENVALUES AND 2 EIGENVECTORS EXTRACTED USING METHOD GIVENS

MAXIMUM OFF DIAGONAL MASS TERM IS 9.700372651E-17 AT ROW 2 AND COLUMN 1

MODE	EXTRACTION ORDER	EIGENVALUE (RAD/S)**2	FREQUENCY (RAD/S)	FREQUENCY (HZ)	GENERALIZED MASS	GENERALIZED STIFFNESS
1	8	1.75766E+04	1.32577E+02	2.11003E+01	3.42760E+00	6.02457E+04
2	7	3.26974E+04	1.80824E+02	2.87791E+01	2.63337E+00	8.61045E+04
3	6	7.39096E+04	2.71863E+02	4.32684E+01	0.00000E+00	0.00000E+00
4	5	1.74786E+05	4.18074E+02	6.65386E+01	0.00000E+00	0.00000E+00
5	4	2.20952E+05	4.70055E+02	7.48115E+01	0.00000E+00	0.00000E+00
6	3	2.98000E+05	5.45894E+02	8.68817E+01	0.00000E+00	0.00000E+00
7	2	3.65539E+05	6.04598E+02	9.62248E+01	0.00000E+00	0.00000E+00
8	1	6.16610E+05	7.85245E+02	1.24976E+02	0.00000E+00	0.00000E+00

(b) Modal Analysis Results

Figure 26. Final Analysis Results for the Ten Bar Truss

4.2.1 Problem Description

The finite element model, shown in **Figure 27** has 33 nodes and 113 truss elements made of a graphite epoxy material with a Young's Modulus of 18.5×10^6 psi and a weight density of 0.055 lb/in^3. The initial truss number cross sectional areas are 10.0 in^2, resulting in an initial design weight of 18,655.1 pounds. An additional 11,217.2 pounds of design invariant mass is placed at the nodes indicated in the paper to represent non-structural components. The first five frequencies are initially 1.21, 2.71, 4.21, 10.34 and 10.49 Hz. The design problem minimizes the weight of the structure while imposing a lower bound frequency constraint of 2.0 Hz on the first mode and 3.0 Hz on the second. The design variables are the 113 truss element cross sectional areas, each of which has a lower bound side constraint of 0.10 in^2.

A theoretical description of the frequency constraint is given in Subsection 7.3 and 7.4 of the Theoretical Manual. This particular sample is a simple, representative example of the application of this constraint. The Generalized Dynamic Reduction in this example uses only approximate mode shapes as the generalized degrees of freedom. A general discussion of the computation of these mode shapes is given in Subsection 7.1 of the Theoretical Manual.

4.2.2 Input Description

Figure 28 shows the input for this sample problem. The solution control packet contains both an optimization subpacket, starting with the OPTIMIZE command, and an analysis subpacket, starting with the ANALYZE command. The optimization subpacket contains a single boundary condition with a single normal modes discipline. The boundary condition definition includes the eigenvalue extraction method, METHOD, and selects the Guyan Reduction set REDUCE. This latter feature is an innovation relative to NASTRAN in that the Guyan Reduction is not selectable in NASTRAN. Finally, the MODES discipline selection includes a specification of the design constraint set (DCONSTRAINT = 2). The DCONSTRAINT refers to the two DCONFRQ bulk data entries in the bulk data packet which specify the two lower bound frequency constraints. The analysis subpacket also selects a modal analysis discipline, to be performed on the converged design obtained following the optimization. In this subpacket, a print of the eigenvalues and eigenvectors is selected to confirm the results of the optimization. Note that the analysis boundary condition selects

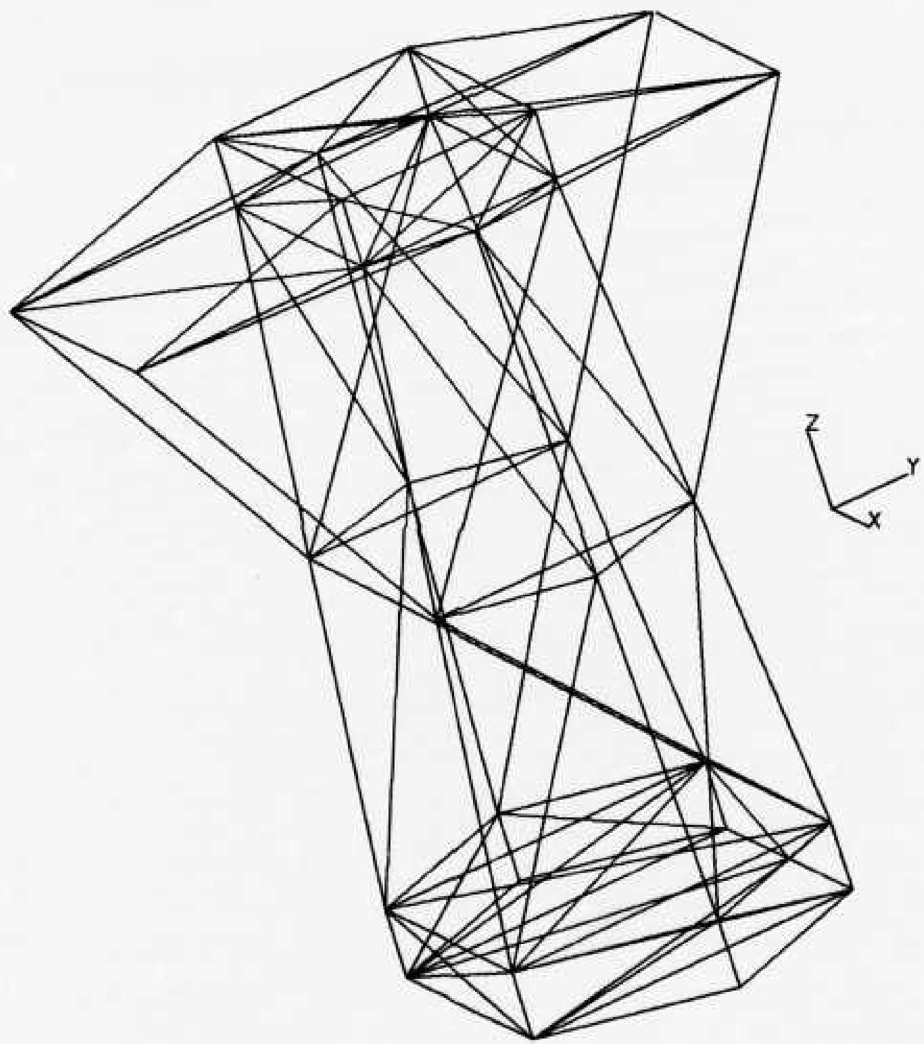

Figure 27. The ACOSS Structural Model

```
ASSIGN DATABASE ACOSS KIMBERLY NEW DELETE
SOLUTION
TITLE = MODIFIED ACOSS II MODEL
OPTIMIZE STRATEGY = 057
   BOUNDARY METHOD=1, SPC=18, REDUCE=10
   PRINT DCONS
   SUBTITLE = NATURAL FREQUENCY DESIGN, FIRST 2 MODES
     MODES ( DCONSTRAINT = 2 )
END
ANALYZE
   BOUNDARY METHOD=1, SPC=18, DYNRED=1
   PRINT DISP=ALL, MODES ALL, ROOT=ALL
   SUBTITLE = MODAL ANALYSIS
     MODES
END
BEGIN BULK
$
$ Eigenanalysis solution parameters.
$
DYNRED, 1, 12.0
EIGR, 1, GIV, 0.0, 12.0, 12, 3, , , +EIGR
+EIGR, MAX
GRIDLIST, 1, 24, THRU, 29
MODELIST, 1, 1
OMIT1, 10, 123, 1, 2, 5, 7, 8
OMIT1, 10, 123, 13, 20, 25
OMIT1, 10, 123, 30, THRU, 33
$
$ Coordinates
$
SPC1, 18, 123, 3, 4, 6
GRDSET,,,,,,,456
GRID            1       -275.591   0.000   0.000
GRID            2       -157.480 196.850   0.000
GRID            3       -157.480-196.850   0.000
GRID            4          0.000 196.850   0.000
GRID            5        157.480 196.850   0.000
GRID            6        157.480-196.850   0.000
GRID            7        275.591   0.000   0.000
GRID            8       -275.591   0.000  78.740
GRID            9       -157.480 196.850  78.740
GRID           10       -157.480-196.850  78.740
GRID           11        157.480 196.850  78.740
GRID           12        157.480-196.850  78.740
GRID           13        275.591   0.000  78.740
GRID           14       -236.220   0.000 472.441
GRID           15       -157.480 157.480 472.441
GRID           16       -157.480-157.480 472.441
GRID           17        157.480 157.480 472.441
GRID           18        157.480-157.480 472.441
GRID           19        236.220   0.000 472.441
GRID           20       -196.850   0.000 866.142
GRID           21       -157.480 118.110 866.142
```

Figure 28. The Input Data Stream for the ACOSS Model

```
GRID           22          -157.480-118.110 866.142
GRID           23           157.480 118.110 866.142
GRID           24           157.480-118.110 866.142
GRID           25           196.850   0.000 866.142
GRID           26          -157.480 393.701 866.142
GRID           27           157.480 393.701 866.142
GRID           28          -157.480-393.701 866.142
GRID           29           157.480-393.701 866.142
GRID           30          -157.480 118.110 944.882
GRID           31          -157.480-118.110 944.882
GRID           32           157.480 118.110 944.882
GRID           33           157.480-118.110 944.882
$
$ Elements.
$
CROD            1   10001         1       2
CROD            2   10001         1       3
CROD            3   10001         2       3
CROD            4   10001         2       4
CROD            5   10001         3       4
CROD            6   10001         4       5
CROD            7   10001         4       6
CROD            8   10001         3       6
CROD            9   10001         5       6
CROD           10   10001         5       7
CROD           11   10001         6       7
CROD           12   10001         1       8
CROD           13   10001         2       9
CROD           14   10001         3      10
CROD           15   10001         5      11
CROD           16   10001         6      12
CROD           17   10001         7      13
CROD           18   10001         3       8
CROD           19   10001         2       8
CROD           20   10001         3       9
CROD           21   10001         4       9
CROD           22   10001         4      11
CROD           23   10001         5      12
CROD           24   10001         5      13
CROD           25   10001         6      13
CROD           26   10001         3      12
CROD           27   10001         6      10
CROD           28   10001         8       9
CROD           29   10001         8      10
CROD           30   10001         9      10
CROD           31   10001         9      12
CROD           32   10001        10      11
CROD           33   10001         9      11
CROD           34   10001        10      12
CROD           35   10001        11      12
CROD           36   10001        11      13
CROD           37   10001        12      13
CROD           38   10001        14      15
```

Figure 28. The Input Data Stream for the ACOSS Model (Continued)

CROD	39	10001	14	16
CROD	40	10001	15	16
CROD	41	10001	17	18
CROD	42	10001	17	19
CROD	43	10001	18	19
CROD	44	10001	8	14
CROD	45	10001	10	14
CROD	46	10001	10	16
CROD	47	10001	9	16
CROD	48	10001	9	15
CROD	49	10001	11	17
CROD	50	10001	8	15
CROD	51	10001	11	18
CROD	52	10001	12	18
CROD	53	10001	12	19
CROD	54	10001	13	19
CROD	55	10001	13	17
CROD	56	10001	14	20
CROD	57	10001	14	22
CROD	58	10001	16	22
CROD	59	10001	16	21
CROD	60	10001	15	21
CROD	61	10001	15	20
CROD	62	10001	17	23
CROD	63	10001	18	23
CROD	64	10001	18	24
CROD	65	10001	19	24
CROD	66	10001	19	25
CROD	67	10001	17	25
CROD	68	10001	15	26
CROD	69	10001	16	28
CROD	70	10001	17	27
CROD	71	10001	18	29
CROD	72	10001	20	21
CROD	73	10001	20	22
CROD	74	10001	21	22
CROD	75	10001	23	24
CROD	76	10001	23	25
CROD	77	10001	24	25
CROD	78	10001	21	23
CROD	79	10001	21	24
CROD	80	10001	22	24
CROD	81	10001	21	30
CROD	82	10001	22	31
CROD	83	10001	24	33
CROD	84	10001	23	32
CROD	85	10001	23	30
CROD	86	10001	21	31
CROD	87	10001	22	33
CROD	88	10001	24	32
CROD	89	10001	30	31
CROD	90	10001	31	33
CROD	91	10001	32	33

Figure 28. The Input Data Stream for the ACOSS Model (Continued)

```
CROD          92   10001       30       32
CROD          93   10001       31       32
CROD          94   10001       20       26
CROD          95   10001       21       26
CROD          96   10001       21       27
CROD          97   10001       23       27
CROD          98   10001       25       27
CROD          99   10001       26       27
CROD         100   10001       20       28
CROD         101   10001       22       28
CROD         102   10001       24       28
CROD         103   10001       24       29
CROD         104   10001       25       29
CROD         105   10001       28       29
CROD         106   10001       26       30
CROD         107   10001       27       32
CROD         108   10001       28       31
CROD         109   10001       29       33
CROD         110   10001       20       31
CROD         111   10001       20       30
CROD         112   10001       25       33
CROD         113   10001       25       32
$
$ Properties and materials.
$
PROD       10001       1    10.0
MAT1           1 1.85E+7 9.25E+6 0.00000 .000142 0.00000 0.00000 0.00000+MT     1
+MT    1 3.00E+4 3.00E+4
$
$ Non-structural masses.
$
CONM2,  9,  9, , 2.855
CONM2, 10, 10, , 2.855
CONM2, 11, 11, , 2.855
CONM2, 12, 12, , 2.855
CONM2, 14, 14, , 0.046
CONM2, 15, 15, , 0.097
CONM2, 16, 16, , 0.097
CONM2, 17, 17, , 0.097
CONM2, 18, 18, , 0.097
CONM2, 19, 19, , 0.046
CONM2, 21, 21, , 2.141
CONM2, 22, 22, , 2.141
CONM2, 23, 23, , 2.141
CONM2, 24, 24, , 2.141
CONM2, 26, 26, , 2.855
CONM2, 27, 27, , 2.855
CONM2, 28, 28, , 1.428
CONM2, 29, 29, , 1.428
$
$ Design variables.
$
DESELM, 1, 1, CROD, 0.01, , 1.0
```

Figure 28. The Input Data Stream for the ACOSS Model (Continued)

```
DESELM, 2, 2, CROD, 0.01, , 1.0
DESELM, 3, 3, CROD, 0.01, , 1.0
DESELM, 4, 4, CROD, 0.01, , 1.0
DESELM, 5, 5, CROD, 0.01, , 1.0
DESELM, 6, 6, CROD, 0.01, , 1.0
DESELM, 7, 7, CROD, 0.01, , 1.0
DESELM, 8, 8, CROD, 0.01, , 1.0
DESELM, 9, 9, CROD, 0.01, , 1.0
DESELM, 10, 10, CROD, 0.01, , 1.0
DESELM, 11, 11, CROD, 0.01, , 1.0
DESELM, 12, 12, CROD, 0.01, , 1.0
DESELM, 13, 13, CROD, 0.01, , 1.0
DESELM, 14, 14, CROD, 0.01, , 1.0
DESELM, 15, 15, CROD, 0.01, , 1.0
DESELM, 16, 16, CROD, 0.01, , 1.0
DESELM, 17, 17, CROD, 0.01, , 1.0
DESELM, 18, 18, CROD, 0.01, , 1.0
DESELM, 19, 19, CROD, 0.01, , 1.0
DESELM, 20, 20, CROD, 0.01, , 1.0
DESELM, 21, 21, CROD, 0.01, , 1.0
DESELM, 22, 22, CROD, 0.01, , 1.0
DESELM, 23, 23, CROD, 0.01, , 1.0
DESELM, 24, 24, CROD, 0.01, , 1.0
DESELM, 25, 25, CROD, 0.01, , 1.0
DESELM, 26, 26, CROD, 0.01, , 1.0
DESELM, 27, 27, CROD, 0.01, , 1.0
DESELM, 28, 28, CROD, 0.01, , 1.0
DESELM, 29, 29, CROD, 0.01, , 1.0
DESELM, 30, 30, CROD, 0.01, , 1.0
DESELM, 31, 31, CROD, 0.01, , 1.0
DESELM, 32, 32, CROD, 0.01, , 1.0
DESELM, 33, 33, CROD, 0.01, , 1.0
DESELM, 34, 34, CROD, 0.01, , 1.0
DESELM, 35, 35, CROD, 0.01, , 1.0
DESELM, 36, 36, CROD, 0.01, , 1.0
DESELM, 37, 37, CROD, 0.01, , 1.0
DESELM, 38, 38, CROD, 0.01, , 1.0
DESELM, 39, 39, CROD, 0.01, , 1.0
DESELM, 40, 40, CROD, 0.01, , 1.0
DESELM, 41, 41, CROD, 0.01, , 1.0
DESELM, 42, 42, CROD, 0.01, , 1.0
DESELM, 43, 43, CROD, 0.01, , 1.0
DESELM, 44, 44, CROD, 0.01, , 1.0
DESELM, 45, 45, CROD, 0.01, , 1.0
DESELM, 46, 46, CROD, 0.01, , 1.0
DESELM, 47, 47, CROD, 0.01, , 1.0
DESELM, 48, 48, CROD, 0.01, , 1.0
DESELM, 49, 49, CROD, 0.01, , 1.0
DESELM, 50, 50, CROD, 0.01, , 1.0
DESELM, 51, 51, CROD, 0.01, , 1.0
DESELM, 52, 52, CROD, 0.01, , 1.0
DESELM, 53, 53, CROD, 0.01, , 1.0
DESELM, 54, 54, CROD, 0.01, , 1.0
```

Figure 28. The Input Data Stream for the ACOSS Model (Continued)

```
DESELM, 55, 55, CROD, 0.01, , 1.0
DESELM, 56, 56, CROD, 0.01, , 1.0
DESELM, 57, 57, CROD, 0.01, , 1.0
DESELM, 58, 58, CROD, 0.01, , 1.0
DESELM, 59, 59, CROD, 0.01, , 1.0
DESELM, 60, 60, CROD, 0.01, , 1.0
DESELM, 61, 61, CROD, 0.01, , 1.0
DESELM, 62, 62, CROD, 0.01, , 1.0
DESELM, 63, 63, CROD, 0.01, , 1.0
DESELM, 64, 64, CROD, 0.01, , 1.0
DESELM, 65, 65, CROD, 0.01, , 1.0
DESELM, 66, 66, CROD, 0.01, , 1.0
DESELM, 67, 67, CROD, 0.01, , 1.0
DESELM, 68, 68, CROD, 0.01, , 1.0
DESELM, 69, 69, CROD, 0.01, , 1.0
DESELM, 70, 70, CROD, 0.01, , 1.0
DESELM, 71, 71, CROD, 0.01, , 1.0
DESELM, 72, 72, CROD, 0.01, , 1.0
DESELM, 73, 73, CROD, 0.01, , 1.0
DESELM, 74, 74, CROD, 0.01, , 1.0
DESELM, 75, 75, CROD, 0.01, , 1.0
DESELM, 76, 76, CROD, 0.01, , 1.0
DESELM, 77, 77, CROD, 0.01, , 1.0
DESELM, 78, 78, CROD, 0.01, , 1.0
DESELM, 79, 79, CROD, 0.01, , 1.0
DESELM, 80, 80, CROD, 0.01, , 1.0
DESELM, 81, 81, CROD, 0.01, , 1.0
DESELM, 82, 82, CROD, 0.01, , 1.0
DESELM, 83, 83, CROD, 0.01, , 1.0
DESELM, 84, 84, CROD, 0.01, , 1.0
DESELM, 85, 85, CROD, 0.01, , 1.0
DESELM, 86, 86, CROD, 0.01, , 1.0
DESELM, 87, 87, CROD, 0.01, , 1.0
DESELM, 88, 88, CROD, 0.01, , 1.0
DESELM, 89, 89, CROD, 0.01, , 1.0
DESELM, 90, 90, CROD, 0.01, , 1.0
DESELM, 91, 91, CROD, 0.01, , 1.0
DESELM, 92, 92, CROD, 0.01, , 1.0
DESELM, 93, 93, CROD, 0.01, , 1.0
DESELM, 94, 94, CROD, 0.01, , 1.0
DESELM, 95, 95, CROD, 0.01, , 1.0
DESELM, 96, 96, CROD, 0.01, , 1.0
DESELM, 97, 97, CROD, 0.01, , 1.0
DESELM, 98, 98, CROD, 0.01, , 1.0
DESELM, 99, 99, CROD, 0.01, , 1.0
DESELM, 100, 100, CROD, 0.01, , 1.0
DESELM, 101, 101, CROD, 0.01, , 1.0
DESELM, 102, 102, CROD, 0.01, , 1.0
DESELM, 103, 103, CROD, 0.01, , 1.0
DESELM, 104, 104, CROD, 0.01, , 1.0
DESELM, 105, 105, CROD, 0.01, , 1.0
DESELM, 106, 106, CROD, 0.01, , 1.0
DESELM, 107, 107, CROD, 0.01, , 1.0
```

Figure 28. The Input Data Stream for the ACOSS Model (Continued)

```
DESELM, 108, 108, CROD, 0.01, , 1.0
DESELM, 109, 109, CROD, 0.01, , 1.0
DESELM, 110, 110, CROD, 0.01, , 1.0
DESELM, 111, 111, CROD, 0.01, , 1.0
DESELM, 112, 112, CROD, 0.01, , 1.0
DESELM, 113, 113, CROD, 0.01, , 1.0
$
$ Design constraints.
$
DCONFRQ, 2, 1, LOWER, 2.001
DCONFRQ, 2, 2, LOWER, 3.001
ENDDATA
```

Figure 28. The Input Data Stream for the ACOSS Model (Concluded)

that GDR be used instead of the Guyan reduction of the previous subpacket. The DYNRED set refers to the DYNRED bulk data entry which requests that the analysis set be composed of sufficient approximate mode shapes to represent the structure up to 12.0 Hz.

The basic structural model is very simple, with standard GRID, CROD, PROD, CONM2 and MAT1 entries used to define the model. The design model is also relatively simple in that unique linking is used: one DESELM entry is supplied for each rod element, resulting in 113 global design variables. The DESELM entry includes a specification of the minimum gage, 0.01, and the initial global design variable value, 1.0. Since the initial property value on the PROD entry is 10.0 and the initial global variable values are unity, the initial local variable values (cross sectional areas) are also 10.0.

The GRIDLIST and MODELIST bulk data entries that appear in the input stream are not referenced and are not used. They could be used to limit the eigenvector print to the specified grid points and the specified normal modes, respectively, by modifying the Solution Control PRINT command and the analysis subpacket.

4.2.3 Results and Output Description

The optimization phase of this example produces minimal output consisting only of the constraint values at each iteration of the default final design output. Figure 29 shows the design iteration history for the optimization phase.

A S T R O S   D E S I G N   I T E R A T I O N   H I S T O R Y

ITERATION NUMBER	OBJECTIVE FUNCTION VALUE	NUMBER FUNCTION EVAL	NUMBER GRADIENT EVAL	NUMBER RETAINED CONSTRAINTS	NUMBER ACTIVE CONSTRAINTS	NUMBER VIOLATED CONSTRAINTS	NUMBER LOWER BOUNDS	NUMBER UPPER BOUNDS	APPROXIMATE PROBLEM CONVERGENCE
1	4.83053E+01	0	0	0	0	0	0	0	NOT CONVERGED
2	3.98657E+01	38	8	2	0	0	12	45	NOT CONVERGED
3	3.13250E+01	72	7	2	1	1	0	22	NOT CONVERGED
4	2.81194E+01	151	25	2	2	0	0	41	NOT CONVERGED
5	2.73324E+01	103	18	2	2	0	0	23	NOT CONVERGED
6	2.64588E+01	102	24	2	2	0	0	9	NOT CONVERGED
7	2.66199E+01	26	6	2	2	0	0	0	NOT CONVERGED
8	2.63344E+01	45	10	2	2	0	0	0	NOT CONVERGED
9	2.63084E+01	26	5	2	2	0	0	0	CONVERGED
10	2.62814E+01	22	[illegible]	2	2	0	0	0	CONVERGED

THE FINAL OBJECTIVE FUNCTION VALUE IS:

FIXED =	2.90300E+01
+ DESIGNED =	2.62814E+01
TOTAL =	5.53114E+01

Figure 29. ACOSS Design Iteration History

This history table contains a wealth of information that can be helpful in assessing the progress of the automated design task. The iteration number and objective function value indicate the rapidity at which a converged design is being approached. The number of function and gradient evaluations at each iteration refers to the approximate problem and provides an indication of the complexity of the design task. The number of retained, active and violated constraints again refers to the approximate problem. ASTROS typically retains many more constraints for consideration by the optimizer than are actually used in the redesign task. The upper and lower bounds column indicate the number of design variables which met prescribed limits during the approximate design task. In this example, inverse design variables are being used so that an upper bound on the design variable is actually a lower bound on the direct variable. The final column indicates whether preliminary criteria for convergence have been specified. For the ninth iteration of Figure 29, the approximate problem was deemed converged, but a further iteration was required when a re-analysis indicated that the frequency constraints were not within prescribed bounds. Subsection 13.1 of the ASTROS Theoretical Manual discusses the approximate optimization task and the termination criteria.

For the ACOSS structure, a converged solution was found in nine redesign cycles and the final objective function value is 10,155.1 pounds.

Both frequency constraints are exactly satisfied at the optimum. The published result obtained a final objective value of 11,820.2 pounds with the first modal frequency at 2.00 Hz and the second modal frequency at 3.72 Hz after 17 redesign cycles. The ASTROS result clearly represents a more fully converged optimal solution.

This ASTROS result is confirmed in the final analysis phase, the results of which are shown in **Figure 30**. These modal frequencies are those resulting from a normal modes analysis using GDR with 17 approximate mode shapes as the generalized coordinates. The first five modal frequencies are 2.00, 3.00, 3.31, 6.68, and 6.96 Hz.

S U M M A R Y   O F   R E A L   E I G E N   A N A L Y S I S

17 EIGENVALUES AND 3 EIGENVECTORS EXTRACTED USING METHOD GIVENS

MAXIMUM OFF DIAGONAL MASS TERM IS 1.298314731E-17 AT ROW 2 AND COLUMN 1

MODE	EXTRACTION ORDER	EIGENVALUE (RAD/S)**2	FREQUENCY (RAD/S)	FREQUENCY (HZ)	GENERALIZED MASS	GENERALIZED STIFFNESS
1	17	1.57922E+02	1.25667E+01	2.00005E+00	1.45179E+01	2.29270E+03
2	16	3.55742E+02	1.88611E+01	3.00184E+00	1.08169E+01	3.84801E+03
3	15	4.33803E+02	2.08279E+01	3.31487E+00	2.02829E+01	8.79878E+03
4	14	1.76352E+03	4.19943E+01	6.68360E+00	0.00000E+00	0.00000E+00
5	13	1.91126E+03	4.37179E+01	6.95793E+00	0.00000E+00	0.00000E+00
6	12	3.47322E+03	5.89340E+01	9.37964E+00	0.00000E+00	0.00000E+00
7	11	3.69198E+03	6.07617E+01	9.67053E+00	0.00000E+00	0.00000E+00
8	10	4.67791E+03	6.83952E+01	1.08854E+01	0.00000E+00	0.00000E+00
9	9	4.96184E+03	7.04403E+01	1.12109E+01	0.00000E+00	0.00000E+00
10	8	5.08197E+03	7.12880E+01	1.13458E+01	0.00000E+00	0.00000E+00
11	7	5.47024E+03	7.39611E+01	1.17713E+01	0.00000E+00	0.00000E+00
12	6	6.30587E+03	7.94095E+01	1.26384E+01	0.00000E+00	0.00000E+00
13	5	6.69441E+03	8.18194E+01	1.30220E+01	0.00000E+00	0.00000E+00
14	4	8.43483E+03	9.18413E+01	1.46170E+01	0.00000E+00	0.00000E+00
15	3	1.12545E+04	1.06087E+02	1.68843E+01	0.00000E+00	0.00000E+00
16	2	1.29622E+04	1.13851E+02	1.81200E+01	0.00000E+00	0.00000E+00
17	1	1.67100E+04	1.29267E+02	2.05735E+01	0.00000E+00	0.00000E+00

Figure 30. Final Modal Analysis Results for the ACOSS Model

4.3 FORWARD SWEPT WING

This subsection describes a test case that has been adapted from the forward swept wing example presented in Subsection 6.1.1 of the MSC/NASTRAN Handbook for Static Aeroelastic Analysis. Two boundary conditions are given in the example. The first duplicates, to the extent possible, the example given in the handbook while the second analyzes the lateral performance of the aircraft, including the effect of an aileron. The brief description which follows has been adapted from that given in the handbook.

4.3.1 Problem Description

The planform of the model is shown in **Figure 31**. The figure shows the aerodynamic model on the left-hand side of the aircraft and the structural model on the right-hand side. This is done for clarity in that the actual input uses only the right-hand side for both models. The wing has an aspect ratio of 4.0, a forward sweep angle of 30 degrees and no taper, twist, camber or incidence relative to the fuselage. The canard has an aspect ratio of 1.0, no sweep, taper, camber, twist or incidence. The chords of both the wing and the canard are 10.0 feet, as is the reference chord. The reference area is 400.0 square feet. The wing is modeled by 32 equal aerodynamic boxes for the steady USSAERO aerodynamic procedure, as shown on the left wing of **Figure 31**. The canard is modeled by eight aerodynamic boxes while aerodynamic forces on the fuselage are neglected. The structural model is made up of beam elements,

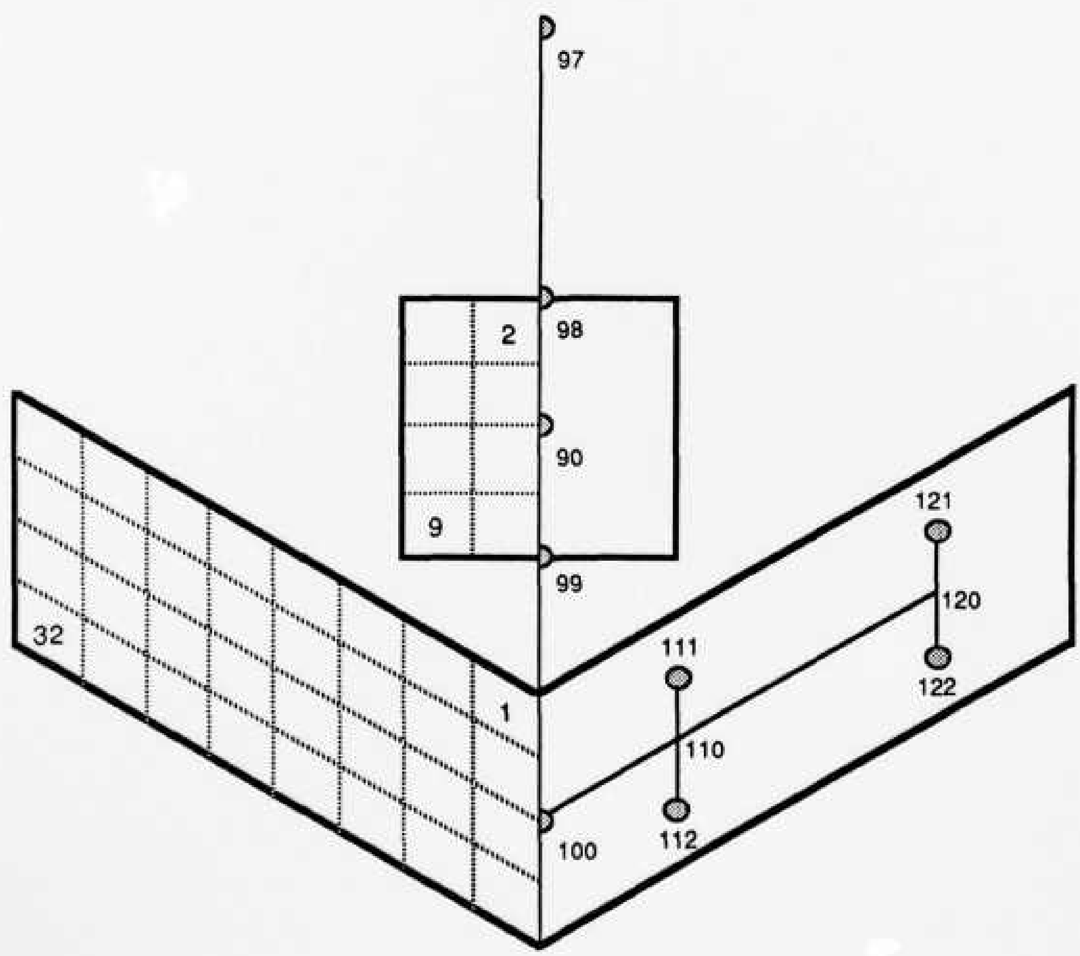

Figure 31. Idealization of FSW Configuration

as shown on the right-hand side of **Figure 31**. The following subsection provides details on the structural model.

The analysis task for this test case is primarily to determine the trim angles and the aircraft stability derivatives for a level flight condition; i.e., $n_z = 1.0$, at a Mach number of 0.9 at sea level. The structural displacements for this trim condition are also determined.

4.3.2 Input

Figure 32 contains the input for this example. GRIDs 111, 112, 121, and 122 have concentrated masses attached to them, but no structure. Instead, multipoint constraints are used to make the motion of these GRIDs dependent on the motion of the structural beams representing the wing elastic axis that extends from GRID 100 to GRIDs 110 and 120.

The fuselage length, from GRID 97 to GRID 100, is 30.0 feet. Bar elements are used between grid points, and a weight of 1,500 pounds is at each fuselage grid point except GRID 90. The wing stiffnesses were assumed equal in bending and torsion, $EI_y = GJ = 25.0 \times 10^7$ pounds-feet^2, so assuming $E = 1.44 \times 10^9$ psf and $G = 5.40 \times 10^8$ psf, leads to $I_y = 0.173611$ ft^4 and $J = 0.462963$ ft^4. Values of cross-sectional area, $A = 1.5$ sq. ft., and chordwise inertia, $I_z = 2.0$ ft^4, are chosen arbitrarily. The wing forward grid points have 600 pounds attached and the aft ones have 400 pounds attached. The fuselage material properties are assumed the same as in the wing with the same vertical cross-section moment of inertia, $I_y = 0.173611$ ft^4. There are two rigid body modes in the model: vertical translation and rotation in pitch. A SUPORT entry defines these rigid body modes on GRID 100, DOFs 3 and 5. Wing grid points 110 and 120 are omitted from the flexibility calculation in order to reduce the problem size. GRID 99 is constrained long-itudinally and all of the fuselage grid points are constrained for symmetry. The CONVERT entry converts weights to masses in slugs.

The aerodynamic data begin with the AEROS entry which defines the reference geometrical data. GRID 100 is specified as the point about which the pitching moment derivatives are calculated. The USSAERO theory for defining the aerodynamic surfaces requires that both configuration and paneling data be input. The AIRFOIL entries define the airfoils at the root and tip of the wing and canard lifting surfaces. Flat plate shapes are used in this

```
ASSIGN DATABASE FSW3 KIMBERLY NEW DELETE
SOLUTION
ANALYZE
  BOUNDARY SPC=1, MPC=10, REDUCE=6, SUPPORT=100
      SAERO (TRIM=9)
      PRINT DISP = ALL, TRIM
BOUNDARY SPC=4, MPC=10, REDUCE=6, SUPPORT=200
      SAERO (TRIM=19)
      PRINT TRIM
END
BEGIN BULK
$$$$$$$$$$$$$$$$$$$$$$$$$$$$$$$$$$$$$$$$$$$$$$$$$$$$$$$$$$$$$$$$$$$$$$$$
$    ASTROS SAMPLE PROBLEM 3A - ADAPTED FROM THE MSC/NASTRAN HANDBOOK
$        FOR AEROELASTIC ANALYSIS - VOLUME II,  SECTION 6.1.1
$
$    STATIC AEROELASTIC ANALYSIS OF A FORWARD SWEPT WING FEATURING:
$        STEADY AEROELASTIC TRIM ANALYSIS
$            GENERATION OF AN AERODYNAMIC MODEL
$            INTERCONNECTION OF AERODYNAMIC AND STRUCTURAL MODELS
$            SPECIFICATION OF A TRIM CONDITION
$        MULTIPOINT AND SINGLE POINT CONSTRAINTS
$        OMIT AND SUPORT
$$$$$$$$$$$$$$$$$$$$$$$$$$$$$$$$$$$$$$$$$$$$$$$$$$$$$$$$$$$$$$$$$$$$$$$$
$
$    THE STRUCTURAL MODEL
$
GRID    90              15.     0.      0.              126
GRID    97              0.      0.      0.
GRID    98              10.     0.      0.
GRID    99              20.     0.      0.
GRID    100             30.     0.      0.
GRID    110             27.113255.      0.
GRID    111             24.613255.      0.
GRID    112             29.613255.      0.
GRID    120             21.3397515.     0.
GRID    121             18.8397515.     0.
GRID    122             23.8397515.     0.
CBAR    100     100     90      99      0.      0.      1.
CBAR    101     100     97      98      0.      0.      1.
CBAR    102     100     98      90      0.      0.      1.
CBAR    103     100     99      100     0.      0.      1.
CBAR    110     101     100     110     0.      0.      1.
CBAR    120     101     110     120     0.      0.      1.
CONM2   97      97      0       1500.0
CONM2   98      98      0       1500.0
CONM2   99      99      0       1500.0
CONM2   100     100     0       1500.0
CONM2   111     111     0       600.0
CONM2   112     112     0       400.0
CONM2   121     121     0       600.0
CONM2   122     122     0       400.0
$
$       PROPERTIES AND MATERIALS
```

Figure 32. Input Data Stream for the Forward Swept Wing Model

```
$
PBAR    100     1       1.+15   25.+7   1.+15   25.+7
PBAR    101     1       1.+15   25.+7   1.+15   25.+7                   +PB1
+PB1    5.      -50.    5.      50.     -5.     50.     -5.     -50.
PBAR    102     1       1.+15   1.+15   1.+15   1.+15
MAT1    1       1.      1.
CONVERT MASS    .031081
$
$       COMMON BOUNDARY CONDITIONS
$
MPC     10      111     1       1.0     110     1       -1.
MPC     10      111     2       1.0     110     2       -1.             +A10
+A10            110     6       2.5
MPC     10      111     3       1.0     110     3       -1.             +A20
+A20            110     5       -2.5
MPC     10      122     6       1.0     120     6       -1.
MPC     10      122     5       1.0     120     5       -1.
MPC     10      122     4       1.0     120     4       -1.
MPC     10      122     3       1.0     120     3       -1.             +D20
+D20            120     5       2.5
MPC     10      122     2       1.0     120     2       -1.             +D10
+D10            120     6       -2.5
MPC     10      122     1       1.0     120     1       -1.
MPC     10      121     6       1.0     120     6       -1.
MPC     10      121     5       1.0     120     5       -1.
MPC     10      112     4       1.0     110     4       -1.
MPC     10      121     4       1.0     120     4       -1.
MPC     10      121     3       1.0     120     3       -1.             +C20
+C20            120     5       -2.5
MPC     10      121     2       1.0     120     2       -1.             +C10
+C10            120     6       2.5
MPC     10      121     1       1.0     120     1       -1.
MPC     10      112     6       1.0     110     6       -1.
MPC     10      112     5       1.0     110     5       -1.
MPC     10      111     4       1.0     110     4       -1.
MPC     10      112     3       1.0     110     3       -1.             +B20
+B20            110     5       2.5
MPC     10      112     2       1.0     110     2       -1.             +B10
+B10            110     6       -2.5
MPC     10      112     1       1.0     110     1       -1.
MPC     10      111     6       1.0     110     6       -1.
MPC     10      111     5       1.0     110     5       -1.
OMIT1   6       4       110     120
$
$       SPECIAL DATA FOR THE SYMMETRIC BOUNDARY CONDITION
$
SPC1    1       246     97      98      100
SPC1    1       1246    99
SPC1    1       4       90
SUPORT  100     100     35
$
$       SPECIAL DATA FOR THE ANTISYMMETRIC BOUNDARY CONDITION
$
```

Figure 32. Input Data Stream for the Forward Swept Wing Model (Continued)

```
SPC1    4       2356    97      98      100
SPC1    4       12356   99
SPC1    4       35      90
SUPORT  200     100     4
$
$     THE AERODYNAMIC MODEL
$
AEROS                   10.0    40.0    400.0   100
AIRFOIL 1       WING            30                                      +ABC1
+ABC1   25.0    0.      0.      10.
AIRFOIL 1       WING            30                                      +DEF1
+DEF1   13.453  20.     0.      10.
AIRFOIL 2       CANARD          30                                      +JKL2
+JKL2   10.0    5.      0.      10.
AIRFOIL 2       CANARD          30                                      +GHI2
+GHI2   10.     0.      0.      10.
AEFACT  30      0.      25.     50.     75.     100.0
CAERO6  1       WING            1       30      40
CAERO6  2       CANARD          1       30      20
AEFACT  20      0.      2.5     5.0
AEFACT  40      0.      2.5     5.0     7.5     10.     12.5    15.     +SBOX
+SBOX   17.5    20.0
AESURF  505     ELEV    2               2       9
AESURF  505     AILERON 1               20      32
$
$     TRIM SPECIFICATION  - SYMMETRIC BOUNDARY CONDITION
$
TRIM    9       0.9     1200.   1       2       1.              980.
$
$     TRIM SPECIFICATION  - ANTISYMMETRIC BOUNDARY CONDITION
$
TRIM    19      1.2     1200.   -1      0       1.              980.
$
$     INTERCONNECTION OF AERODYNAMIC AND STRUCTURAL MODEL
$
SPLINE1 1501            1       1       32      1100
SET1    1100    111     112     121     122
ATTACH  100     2       2       9       90
$
ENDDATA
```

Figure 32. Input Data Stream for the Forward Swept Wing Model (Concluded)

modeling in order to be consistent with the MSC/NASTRAN results which do not allow the consideration of thickness or camber effects. The fuselage is not modeled aerodynamically. CAERO6 entry 1 provides the paneling data for the wing and, by reference to AEFACT entries, specifies that the wing is modeled by four chordwise and by eight spanwise equal boxes. Similarly, CAERO6 entry 2 specifies that the canard is modeled by four chordwise and two spanwise equal boxes. The elevator is defined as the complete canard surface while the aileron surface is made up of the four aerodynamic boxes along the trailing edge extending from the midspan to the tip. Note that SETID for the AESURF entry for these inputs is only used for error messages while the CID1 and CID2 fields are not operational.

The aerodynamic and structural models are connected by the use of SPLINE1 and ATTACH entries. Although the SPLINE1 entry, which defines a surface spline, is not ideally suited to transfer loads to the beam structure, results appear to be adequate for this simple case. The forces of the 32 boxes on the wing are transferred to grids 111, 112, 121, and 122. The ATTACH entry is used to transfer aerodynamic forces of the canard to GRID 90.

The symmetric trim condition of TRIM entry 9 specifies that the aircraft be trimmed for pitch and plunge degrees of freedom at a Mach number of 0.9 and a dynamic pressure or 1200 psf in level flight. The antisymmetric condition of TRIM entry 19 specifies that the lateral analysis be performed at M = 1.2 and a dynamic pressure of 1200 psf, which correspond to an altitude of 15,000 feet.

4.3.2 Output

Key results for the two boundary conditions are shown in **Figures 33** and 34. In **Figure 33**, longitudinal results are presented. The header information prints out the relevant flight conditions and reference areas and this is followed by a listing of lift and pitching moments stability derivatives. Subsection 7.2.5 of the User's Manual provides information that can be used to interpret these numbers. A print of the trim condition in terms of the angle of attack and the elevator setting follows the derivative information. **Table** 3 shows a comparison of ASTROS results and those contained in the MSC/NASTRAN Handbook. The elastic displacements that result from this trim are included in **Figure** 33.

NONDIMENSIONAL LONGITUDINAL STABILITY DERIVATIVES

MACH = 9.0000E-01 QDP = 1.2000E+03 REFERENCE GRID = 100

REFERENCE AREA = 4.0000E+02 REFERENCE CHORD = 1.0000E+01

PARAMETER	LIFT			PITCHING MOMENT		
	RIGID (DIRECT)	RIGID (SPLINED)	FLEXIBLE	RIGID (DIRECT)	RIGID (SPLINED)	FLEXIBLE
THICKNESS AND CAMBER	0.0000	0.0000	0.0000	0.0000	0.0000	0.0000
ALPHA(DEGS)	0.0866	0.0866	0.1320	0.0786	0.0786	0.1139
ALPHA(RADS)	4.9620	4.9628	7.5636	4.5057	4.5057	6.5255
ELEVATOR(DEGS)	0.0047	0.0047	0.0084	0.0165	0.0165	0.0194
ELEVATOR(RADS)	0.2686	0.2686	0.4795	0.9456	0.9456	1.1091
PITCH RATE(DEGS/SEC)	-0.0646	-0.0646	-0.1274	-0.1000	-0.1000	-0.1489
PITCH RATE(RADS/SEC)	-3.7041	-3.7041	-7.3010	-5.7310	-5.7310	-8.5326

TRIM RESULTS

ALPHA = 1.7954E-01 (DEGS) ELEVATOR = 1.1510E+00 (DEGS)

(a) Stability Derivatives

D I S P L A C E M E N T V E C T O R

POINT ID.	TYPE	T1	T2	T3	R1	R2	R3
90	G	0.00000E+00	0.00000E+00	8.86937E-04	0.00000E+00	6.33872E-05	0.00000E+00
97	G	0.00000E+00	0.00000E+00	-5.91225E-03	0.00000E+00	-6.86613E-04	0.00000E+00
98	G	0.00000E+00	0.00000E+00	-4.61262E-05	0.00000E+00	-3.86613E-04	0.00000E+00
99	G	0.00000E+00	0.00000E+00	-4.74109E-04	0.00000E+00	4.82579E-04	0.00000E+00
100	G	0.00000E+00	0.00000E+00	-1.06001E-02	0.00000E+00	1.64882E-03	0.00000E+00
110	G	0.00000E+00	0.00000E+00	-2.57764E-03	7.90333E-04	2.40298E-03	0.00000E+00
111	G	0.00000E+00	0.00000E+00	3.42981E-03	7.90333E-04	2.40298E-03	0.00000E+00
112	G	0.00000E+00	0.00000E+00	-8.58510E-03	7.90333E-04	2.40298E-03	0.00000E+00
120	G	0.00000E+00	0.00000E+00	2.54127E-02	1.40210E-03	3.02482E-03	0.00000E+00
121	G	0.00000E+00	0.00000E+00	3.29747E-02	1.40210E-03	3.02482E-03	0.00000E+00
122	G	0.00000E+00	0.00000E+00	1.78507E-02	1.40210E-03	3.02482E-03	0.00000E+00

(b) Static Displacements

Figure 33. Longitudinal Results for the Forward Swept Wing

NONDIMENSIONAL LATERAL ROLLING MOMENT STABILITY DERIVATIVES

MACH = 1.2000E+00 QDP = 1.2000E+03 REFERENCE GRID = 100

REFERENCE AREA = 4.0000E+02 REFERENCE SPAN = 1.0000E+01

PARAMETER	ROLLING MOMENT RIGID (DIRECT)	RIGID (SPLINED)	FLEXIBLE
AILERON(DEGS)	0.0051	0.0051	0.0045
AILERON(RADS)	0.2937	0.2937	0.2582
ROLL RATE(DEGS/SEC)	-0.0087	-0.0087	-0.0090
ROLL RATE(RADS/SEC)	-0.5005	-0.5005	-0.5160

Figure 34. Lateral Stability Derivative Results for the Forward Swept Wing

TABLE 3. COMPARISON OF ASTROS AND MSC/NASTRAN RESULTS FOR THE FORWARD SWEPT WING

PARAMETER	RIGID		FLEXIBLE	
	ASTROS	NASTRAN	ASTROS	NASTRAN
C_{L_α}	4.96	5.07	7.56	8.11
C_{m_α}	4.51	4.74	6.53	7.20
$C_{L_{\delta e}}$	0.27	0.25	0.48	0.45
$C_{m_{\delta e}}$	0.95	0.94	1.11	1.11
C_{L_q}	-3.70	-3.14	-7.30	-7.48
C_{m_q}	-5.73	-6.05	-8.53	-9.59
α_{trim} (degs)	----	----	0.180	0.270
δe_{trim} (degs)	----	----	1.151	1.061

Lateral results are given in **Figure 34**. As described in Subsection 7.2.5 of the User's Manual, only rolling moment data are computed in this case.

4.4 RECTANGULAR WING

The development of the static aeroelastic capability in ASTROS was validated, in part, through the use of a very simple aircraft system. This system is also an ideal example for describing a number of the static aeroelastic analysis and design features. A series of design tasks were performed on this one basic model and four of them are included in this subsection.

4.4.1 Problem Description

The aerodynamic planform and the paneling is shown in **Figure** 35. The wing is paneled by 12 boxes and the horizontal stabilizer by 6 boxes. The two trailing edge boxes on the stabilizer model the pitch control surface while the roll control surface extends from the wing midspan, and is modeled by two aerodynamic boxes. The aerodynamic reference point, for the calculation of pitching moment stability derivatives, is at the 50 percent station of the root chord. No fuselage model is used in this case.

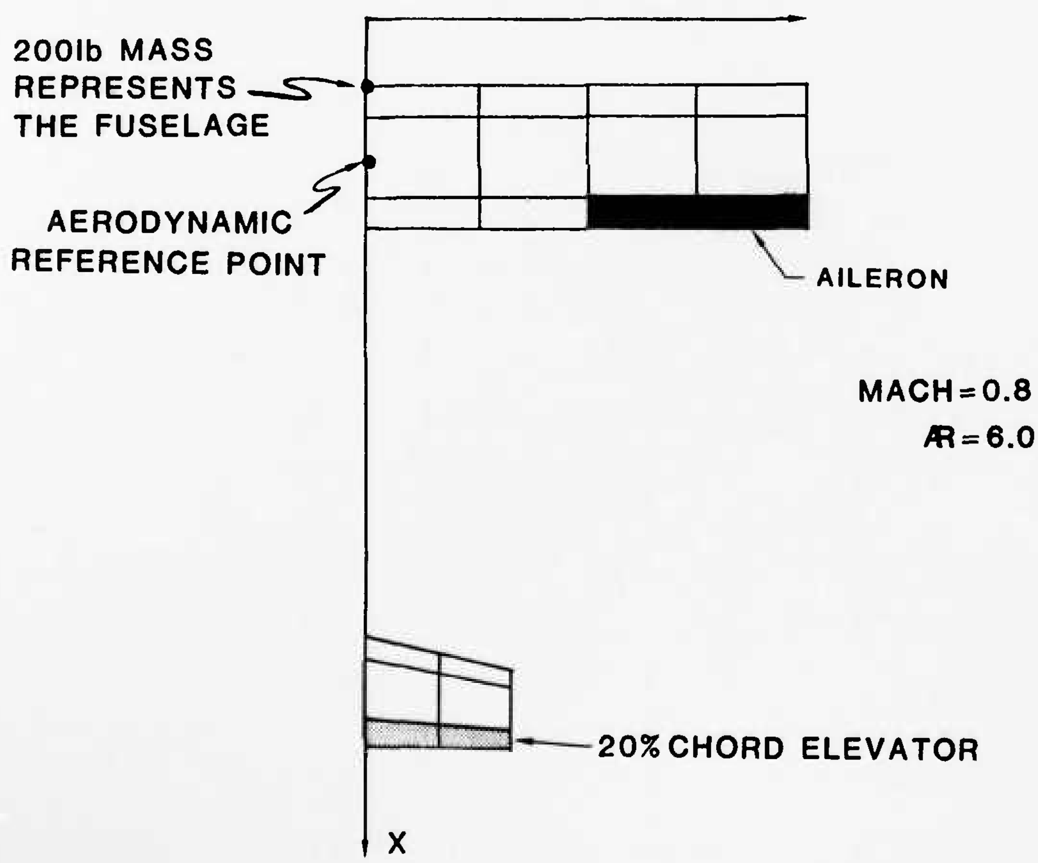

Figure 35. Aerodynamic Planform for the Rectangular Wing

The structural model is shown in **Figure 36**. Only the wing has an underlying structure. As the figure indicates, the structural model is simplified to the extent that it violates good modeling practice for finite element analysis. This is not considered important for the purposes of this example.

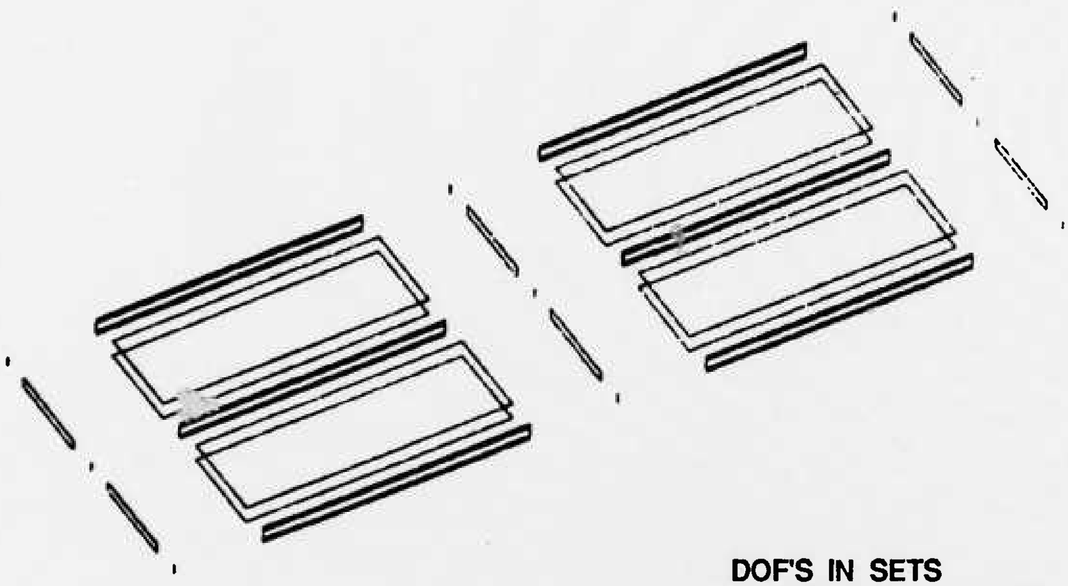

	ELEMENTS
ROD	9
SHEAR	12
QUAD MEMBRANE	6
CONM2	1
TOTAL	28

DOF'S IN SETS	SYMMETRIC	ANTI SYMMETRIC
MPC	4	6
SPC	64	71
SOLUTION	44	36
REFERENCE	2	1
TOTAL	114	114

Figure 36. The Structural Model of the Rectangular Wing

Four different design cases are presented. Each of them designs the upper and lower cover skins of **Figure 36** for fixed values of the substructure. The cases differ only in the design conditions that are imposed, with **Table 4** identifying the imposed conditions. For Case A, stress allowables are applied in the aluminum skin and the aeroelastic twist of the wing tip is restrained to be less than one degree. Case B adds the constraint that the lift effectiveness must be less than 1.6. Because the aerodynamic center is ahead of the elastic axis for this model, the aerodynamic loading tends to twist up the wing tip, thereby providing additional lift. Imposing a limit on the lift effectiveness could therefore be considered an indirect way of providing for structural stiffness. Case C imposes a single design condition that the roll

TABLE 4. DESIGN CONDITIONS FOR THE RECTANGULAR WING

CONSTRAINT	CASE A	CASE B	CASE C	CASE D
Tension Stress Allowable (ksi)	20.0	20.0	---	20.0
Compression Stress Allowable (ksi)	15.0	15.0	---	15.0
Shear Stress Allowable (ksi)	12.0	12.0	---	12.0
Maximum Tip Rotation (Degs)	1.0	1.0	---	1.0
Maximum Lift Effectiveness	---	1.6	---	1.6
Minimum Roll Effectiveness	---	---	0.30	0.30

effectiveness be greater than 0.30. In words, this specifies that the nondimensional steady state roll rate achievable for a unit aileron deflection must be at least 0.30. Subsection 9.3 of the Theoretical Manual describes this roll performance constraint. Case D imposes all the constraints from the previous three cases simultaneously.

4.4.2 Input

The structural bulk data input for the four cases is shown in **Figure 37**, while **Figure 38** shows the bulk data for the aerodynamic modeling. These data are segregated because subsequent examples in this manual share the structural data, but have different aerodynamic properties. These data are incorporated into the input data stream through the use of INCLUDE statements. **Figure 39** shows the controlling packets for the four cases. The RECTS.DAT file of these packets is the bulk data of **Figure 37** while RECTA is given in **Figure 38** data. Cases B and D also include a third INCLUDE file called DCONC.DAT. This is one line of bulk data that specifies the lift effectiveness constraint:

```
DCONCLA     100     UPPER     1.600
```

It is necessary to include this line of data separately because it shares the set identification with the displacement constraint so that it would be imposed in Case A if it were included with the **Figure 37** data. The DCONCLA input imposes an upper bound limit of 1.6 on the lift effectiveness.

```
$
GRID        1              10.0    0.0     0.5
GRID        2              10.0    0.0    -0.5
GRID        3              10.0   30.0     0.5                456
GRID        4              10.0   30.0    -0.5                456
GRID        5              10.0   60.0     0.5                456
GRID        6              10.0   60.0    -0.5                456
GRID        7              20.0    0.0     0.5
GRID        8              20.0    0.0    -0.5
GRID        9              20.0   30.0     0.5                456
GRID       10              20.0   30.0    -0.5                456
GRID       11              20.0   60.0     0.5                456
GRID       12              20.0   60.0    -0.5                456
GRID       13              30.0    0.0     0.5
GRID       14              30.0    0.0    -0.5
GRID       15              30.0   30.0     0.5                456
GRID       16              30.0   30.0    -0.5                456
GRID       17              30.0   60.0     0.5                456
GRID       18              30.0   60.0    -0.5                456
GRID       20              20.0    0.0     0.0
$
CSHEAR     11      199        1        2        4        3
CSHEAR     12      199        3        4        6        5
CSHEAR     15      199       11        5        6       12
CSHEAR     18      199        9        3        4       10
CSHEAR     19      199       15        9       10       16
CSHEAR     22      199       17       11       12       18
CSHEAR     24      199       13       14       16       15
CSHEAR     25      199       15       16       18       17
CSHEAR     27      199        7        8       10        9
CSHEAR     28      199        9       10       12       11
CSHEAR     29      199        1        2        8        7
CSHEAR     30      199        7        8       14       13
$
CROD        1      299        1        2
CROD        2      299        3        4
CROD        3      299        5        6
CROD        4      299        7        8
CROD        5      299        9       10
CROD        6      299       11       12
CROD        7      299       13       14
CROD        8      299       15       16
CROD        9      299       17       18
$
CQDMEM1    13       96        7        1        3        9      0.0
CQDMEM1    20       96       13        7        9       15      0.0
CQDMEM1    14       97        9        3        5       11      0.0
CQDMEM1    21       97       15        9       11       17      0.0
CQDMEM1    17       98        8        2        4       10      0.0
CQDMEM1    26       98       14        8       10       16      0.0
CQDMEM1    16       99       10        4        6       12      0.0
CQDMEM1    23       99       16       10       12       18      0.0
$
```

Figure 37. Data Set RECTS.DAT - Structural Bulk Data for the Rectangular Wing

```
CONM2          10     20           200.0  -10.0                        BC3
+C3        1000.        22500.                      22500.
CONVERT    MASS 2.588E-3
$
MAT1     1      10.E6              0.3      0.1                        CMAT1
+MAT1    20.+5  15.0+5   12.0+5
MAT1     90     10.E6              0.3      0.1                        CMAT90
+MAT90   20.+3  15.0+3   12.0+3
$
PSHEAR   199       1      0.05
PROD     299       1      0.01
PQDMEM1  96       90      0.20
PQDMEM1  97       90      0.20
PQDMEM1  98       90      0.20
PQDMEM1  99       90      0.20
$
$     SYMMETRIC BOUNDARY CONDITION
$
SPC1           10   1246       20
SPC1           10   2456        1      14       8      2      13     7
MPC           200      7        3  1.0     20      3     -1.0
MPC           200      7        1  1.0     20      5     -0.5
MPC           200      8        3  1.0     20      3     -1.0
MPC           200      8        1  1.0     20      5      0.5
SUPORT        100     20       35
$
$     ANTISYMMETRIC BOUNDARY CONDITION
$
SPC1           20   12356      20
SPC1           20   13456       1      14       2      13
SPC1           20   13456       8       7
MPC           400   1       2         1.0     20      4       0.5      +MPC1A
+MPC1A              20      6        10.0
MPC           400   2       2         1.0     20      4      -0.5      +MPC1A
+MPC1A              20      6        10.0
MPC           400   13      2         1.0     20      4       0.5      +MPC1A
+MPC1A              20      6       -10.0
MPC           400   14      2         1.0     20      4      -0.5      +MPC1A
+MPC1A              20      6       -10.0
MPC           400   7       2         1.0     20      4       0.5
MPC           400   8       2         1.0     20      4      -0.5
SUPORT        101   20      4
$
$    DESIGN INFORMATION
$
DESVAR   1        .01              1.0              INBDSKNT
DESVAR   2        .01              1.0              OTBDSKNT
DESVAR   3        .01              1.0              INBDSKNB
DESVAR   4        .01              1.0              OTBDSKNB
PLIST    1      PQDMEM1  96
PLIST    2      PQDMEM1  97
PLIST    3      PQDMEM1  98
PLIST    4      PQDMEM1  99
```

Figure 37. Data Set RECTS.DAT - Structural Bulk Data for the Rectangular Wing (Continued)

```
$
DCONDSP   100      10   UPPER     0.0174TIPTWIST  5        3       0.05  DCO
+CO                17         3   -0.05      20       5      -1.0
DCONALE   200   LOWER    0.30
DCONSTR   90    VMISES
DCONSTR   1     VMISES
```

Figure 37. Data Set RECTS.DAT - Structural Bulk Data for the Rectangular Wing (Concluded)

```
$
$    AERODYNAMIC MODEL
$
AEROS                         20.0      60.0   2400.0   20
$
$    WING DATA
$
CAERO6  1       WING                   1        20        10
AIRFOIL 1       WING                   30       70                 40       1.0       CAIRI
+AIRI   10.0    0.0        0.0         20.
AIRFOIL 1       WING                   30       70                 40       1.0       +A45201
+A45201 10.0    60.0       0.0         20.
$
$    SPANWISE CUTS OF PANEL
$
AEFACT  10      0.0      15.0     30.      45.0     60.0
$
$    CHORDWISE CUTS OF PANEL
$
AEFACT  20      0.0     20.       80.0     100.
$
$     AIRFOIL PERCENT CHORD POINT FOR PROPERTY DEFINITIONS
$
AEFACT  30      0.0     10.       25.0      50.0     75.0   100.00
$
$     AIRFOIL CAMBER
$
AEFACT  40      0.0     -0.01745 -0.0436 -0.0872 -.1308  -.1745
$
$     AIRFOIL THICKNESS
$
AEFACT  70      0.0        1.0      1.0      1.0      1.0      0.0
```

Figure 38. Data Set RECTA.DAT - Aerodynamic Bulk Data for the Rectangular Wing

```
$
$
$   CANARD DATA
$
CAERO6  2       CANARD          1       20      50
AIRFOIL 2       CANARD          30      70                              1.0     CAIRC
+AIRC   90.     20.     0.0     10.0
AIRFOIL 2       CANARD          30      70                              1.0     CAIRC
+AIRC   85.0    0.0     0.0     15.
$
$    SPANWISE CUTS OF CANARD PANEL
$
AEFACT   50     0.0     10.0    20.0
$
$    PITCH CONTROL SURFACE
$
AESURF  100     ELEV    2               4       7
TRIM    100     0.8      6.5    1        2        8.0   0.274    9864.
$
$    ROLL CONTROL SURFACE
$
AESURF  200     AILERON   1              9       12
TRIM    200     0.8       6.5    -1     0         0.0   0.0      9864.
$
$     CONNECTIVITY OF AERO AND STRUCTURAL MODEL
$
ATTACH          10      2       2       7       20
SPLINE1          3              1       1       12      10
SET1            10      1       3       5        9      11      13      15  CSET
+SET            17      20
```

Figure 38. Data Set RECTA.DAT - Aerodynamic Bulk Data for the Rectangular Wing (Concluded)

```
ASSIGN DATABASE RECT KIMBERLY NEW DELETE
SOLUTION
TITLE = SIMPLIFIED WING STRUCTURE DESIGN
  OPTIMIZE STRATEGY = 57
  SUBTITLE = OPTIMIZATION FOR DISPLACEMENT AND STRENGTH CONSTRAINTS
     BOUNDARY MPC=200,SPC=10, SUPPORT=100
        SAERO (TRIM = 100, DCON = 100)
        PRINT DCON, TRIM
  END
  ANALYZE
  SUBTITLE = ANALYZE FOR THE ROLL EFFECTIVENESS
     BOUNDARY MPC=400,SPC=20, SUPPORT=101
         SAERO (TRIM = 200)
         PRINT TRIM
  END
BEGIN BULK
INCLUDE [EJ.APP]RECTS.DAT
INCLUDE [EJ.APP]RECTA.DAT
ENDDATA
```

(a) Case A Input Data Packet

```
ASSIGN DATABASE RECT KIMBERLY NEW DELETE
SOLUTION
TITLE = SIMPLIFIED WING STRUCTURE DESIGN
  OPTIMIZE STRATEGY = 57
  SUBTITLE = OPTIMIZATION FOR LIFT EFFECTIVENESS AND STRENGTH CONSTRAINTS
     BOUNDARY MPC=200,SPC=10, SUPPORT=100
        SAERO (TRIM = 100, DCON = 100)
        PRINT DCON, TRIM
  END
  ANALYZE
  SUBTITLE = ANALYZE FOR THE ROLL EFFECTIVENESS
     BOUNDARY MPC=400,SPC=20, SUPPORT=101
         SAERO (TRIM = 200)
         PRINT TRIM
  END
BEGIN BULK
INCLUDE [EJ.APP]DCONC.DAT
INCLUDE [EJ.APP]RECTS.DAT
INCLUDE [EJ.APP]RECTA.DAT
ENDDATA
```

(b) Case B Input

Figure 39. Input Data Streams for the Rectangular Wing Cases

```
ASSIGN DATABASE RECT KIMBERLY NEW DELETE
SOLUTION
TITLE = SIMPLIFIED WING STRUCTURE DESIGN
OPTIMIZE STRATEGY = 57
  BOUNDARY MPC=400,SPC=20, SUPPORT=101
  SUBTITLE = OPTIMIZE FOR AILERON EFFECTIVENESS ONLY
      SAERO (TRIM = 200, DCON = 200)
      PRINT DCON, TRIM
  END
  ANALYZE
  SUBTITLE = ANALYZE FOR LONGITUDINAL TRIM
     BOUNDARY MPC=200,SPC=10, SUPPORT=100
     SAERO (TRIM = 100)
     PRINT TRIM, DISP = ALL
END
BEGIN BULK
INCLUDE [EJ.APP]RECTS.DAT
INCLUDE [EJ.APP]RECTA.DAT
ENDDATA
```

(c) Case C Input Data Packet

```
ASSIGN DATABASE RECT KIMBERLY NEW DELETE
SOLUTION
TITLE = SIMPLIFIED WING STRUCTURE DESIGN
  OPTIMIZE STRATEGY = 57
  SUBTITLE = OPTIMIZE FOR SYMMETRIC AND ANTISYMMETRIC CONDITIONS SIMULTANEOUSLY
  PRINT DCON, DESIGN
  BOUNDARY MPC=200,SPC=10, SUPPORT=100
     LABEL = OPTIMIZATION FOR LIFT EFFECTIVENESS AND STRENGTH CONSTRAINTS
     SAERO (TRIM = 100, DCON = 100)
  BOUNDARY MPC=400,SPC=20, SUPPORT=101
     LABEL = OPTIMIZE FOR AILERON EFFECTIVENESS
     SAERO (TRIM = 200, DCON = 200)
  END
  ANALYZE
  SUBTITLE = PERFORM A FINAL ANALYSIS IN ORDER TO GET MORE COMPLETE PRINTS
  BOUNDARY MPC=200,SPC=10, SUPPORT=100
     LABEL = SYMMETRIC ANALYSES
     SAERO (TRIM = 100, DCON = 100)
     PRINT DCON, TRIM, DISP=ALL
  BOUNDARY MPC=400,SPC=20, SUPPORT=101
     LABEL = ANTISYMMETRIC ANALYSES
     SAERO (TRIM = 200, DCON = 200)
     PRINT DCON, TRIM
  END
BEGIN BULK
INCLUDE [EJ.APP]DCONC.DAT
INCLUDE [EJ.APP]RECTS.DAT
INCLUDE [EJ.APP]RECTA.DAT
ENDDATA
```

(d) Case D Input Data Packet

Figure 39. Input Data Streams for the Rectangular Wing Cases (Concluded)

The grid and connectivity data of **Figure** 37 are straightforward. The MAT1 entries specify separate materials for the substructure and the cover skins. The elastic properties of the two materials are identical, but the stress allowables in the substructure are 100 times greater than the allowables in the skins. Clearly, the substructure allowables should never be exceeded, but the example serves to show the capability of using different sets of allowables and the ability to impose strength constraints on finite elements that are not designed.

Two boundary conditions are included in the input packet of **Figure** 37. The first defines a symmetric condition with the grids in the y = 0.0 plane restrained from moving in the lateral direction. GRID 20 is the point at which the SUPORT degrees of freedom are specified and is at y = z = 0.0 and an x station that is at the 50 percent chord of the wing root. The 3 and 5 components of this grid are supported, allowing rigid body pitch and plunge modes. GRID 20 is not connected directly to the structure; instead, MPCs are used to constrain the vertical motion of the grid points directly above and below (GRIDs 7 and 8, respectively) to move in concert with the vertical motion of GRID 20 while the fore and aft motions of GRIDs 7 and 8 are rigidly restrained by MPC relations to move in concert with the pitch rotation of GRID 20.

For the second, antisymmetric boundary condition, the grids in the y=0.0 plane are restrained from moving in the lateral direction. GRID 20, which is again the SUPORT point, is restrained in pitch and yaw as well. The MPC conditions specify that the lateral translations of the grid points directly above and below the support point are constrained by the roll degree of freedom at the support point while the remaining lateral translations at the grid are determined based on the roll and yaw of the control point. Since the yaw motion of the support point is constrained to zero, the lateral motion of the root section is completely determined by the SUPORT roll degree of freedom.

The final set of data in **Figure** 37 are those required to define the design model. Four design variables control the thicknesses of the eight finite elements that make up the cover skins. As mentioned, the substructure is not designed for this case. The finite elements are linked so that fore and aft elements vary together while top and bottom and inboard and outboard

elements are free to vary independently. The linking is accomplished by reference to the property entries, which motivates the presence of four PQDMEM1 entries that differ only by their property ID. The PLIST entry provides the link that connects the DESVAR entries with the PQDMEM1 entries.

The displacement constraint given on the DCONDSP specifies that the elastic twist of the wing should not exceed one degree. Note that this is done by differencing two vertical displacements and dividing by the distance between them. For this example, it was also necessary to subtract out the rotation of the SUPORT grid because this represents a rigid body rotation that is present in each transverse displacement and must be suppressed. This subtraction should be done by the ASTROS code since this rigid body motion in the static displacement has no physical significance. This error will be removed in subsequent releases of ASTROS.

The DCONSTR entries apply stress constraints to the longitudinal responses. The actual stress limits are given on the MAT1 entries and have been discussed previously. Finally, the DCONALE entry specifies that the roll performance effectiveness cannot be less than 0.30.

The aerodynamic data for this example are very simple, as **Figure 38** indicates. The AEROS entry defines reference areas and lengths and designates GRID 20 as the point about which pitching stability derivatives are calculated. AIRFOIL data define the root and tip chord of the wing. AEFACT entries define the chordwise division points and the upper surface thickness and the camber at each of these divisions. In this example, the camber actually is used to model a built in twist of one tenth of a degree. The airfoil thickness is not realistic in that the two percent thick airfoil does not enclose the structural box, which has a depth of one inch. The CAERO6 entry for the wing indicates that the paneling chordwise divisions are the same as those given for the AIRFOIL divisions while the five spanwise cuts are given on a separate AEFACT entry. The canard is defined in a similar fashion with AIRFOIL entries defining the root and tip chords and a CAERO6 entry providing the paneling information.

The control surface and trim condition for the longitudinal response are defined next in the data packet of **Figure 38**. The elevator surface is modeled using the two trailing edge aerodynamic boxes of the canard surface. The TRIM entry specifies a Mach number of 0.8, a dynamic pressure of 6.5 psi

and a load factor of 8 g's. The pitch rate of 0.274 radians/second and the velocity of 9864.0 ft/sec are consistent with the previous input. There is a redundancy of input here with the burden on the user to make these data consistent. (cf. p. 129)

The control surface and "trim" data for the antisymmetric response are given next. The roll control surface is modeled using trailing edge boxes on the wing that extend from the midspan to the tip. The Mach number of 0.8 and the dynamic pressure of 6.5 psi are repeated for this antisymmetric analysis.

The data packets of **Figure 39** invoke the various design cases through a combination of boundary condition and INCLUDE commands. The flexibility to select bulk data information that is to be used in the OPTIMIZE and ANALYZE portions of the computer run is considered a strong feature of the ASTROS procedure.

4.4.3 Results

A summary of the results from performing the four design tasks is given in **Table 5** while **Figures 40 through 43** contain abridged output listings. For all the cases, the design was driven completely by stiffness

TABLE 5. DESIGN RESULTS FOR THE RECTANGULAR WING CASES

PARAMETER	CASE			
	A	B	C	D
Inboard Thickness (Inches)	0.136	0.174	0.113	0.174
Outboard Thickness (Inches)	0.081	0.057	0.073	0.057
Tip Rotation (Degrees)	1.000	1.000	1.123	1.000
Lift Effectiveness	1.835	1.600	2.067	1.600
Roll Effectiveness	0.311	0.313	0.300	0.313
Weight (Pounds)	26.001	27.681	22.295	27.681
Trimmed Angle of Attack (Degrees)	1.055	1.262	0.903	1.262
Trimmed Elevator Setting (Degrees)	-1.265	-1.559	-1.111	-1.559

SUMMARY OF ACTIVE CONSTRAINTS
12 CONSTRAINTS RETAINED OF 30 APPLIED

COUNT	CONSTRAINT VALUE	CONSTRAINT TYPE	TYPE COUNT	BOUNDARY ID	SUBCASE	ELEMENT TYPE	EID
1	-3.07281E-01	DISPLACEMENT	1	1	1		0
2	-5.65466E-01	VON MISES STRESS	1	1	1	QDMEM1	13
3	-9.29169E-01	VON MISES STRESS	2	1	1	QDMEM1	14
4	-9.31820E-01	VON MISES STRESS	3	1	1	QDMEM1	16
5	-6.71565E-01	VON MISES STRESS	4	1	1	QDMEM1	17
6	-5.78793E-01	VON MISES STRESS	5	1	1	QDMEM1	20
7	-9.20799E-01	VON MISES STRESS	6	1	1	QDMEM1	21
8	-9.34978E-01	VON MISES STRESS	7	1	1	QDMEM1	23
9	-6.82420E-01	VON MISES STRESS	8	1	1	QDMEM1	26
10	-9.83815E-01	VON MISES STRESS	10	1	1	ROD	2
11	-9.86741E-01	VON MISES STRESS	13	1	1	ROD	5
12	-9.86929E-01	VON MISES STRESS	28	1	1	SHEAR	29

```
****              ASTROS APPROXIMATE OPTIMIZATION                 ****
***                    SUMMARY - ITERATION  1                      ***
**                  METHOD = MATH PROGRAMMING                       **
*   CURRENT       PREVIOUS      OBJECTIVE     PERCENT   CONVERGENCE  *
*  OBJECTIVE      OBJECTIVE       CHANGE       CHANGE      FLAG      *
*  2.58835E+01   4.80000E+01  -2.21165E+01   -46.076  NOT CONVERGED  *
```

SIMPLIFIED WING STRUCTURE DESIGN — ASTROS VERSION 1.00 8/11/88 P. 17
OPTIMIZATION FOR DISPLACEMENT AND STRENGTH CONSTRAINTS — ASTROS ITERATION 5

NONDIMENSIONAL LONGITUDINAL STABILITY DERIVATIVES

MACH = 8.0000E-01 QDP = 6.5000E+00 REFERENCE GRID = 20

REFERENCE AREA = 2.4000E+03 REFERENCE CHORD = 2.0000E+01

PARAMETER	LIFT RIGID (DIRECT)	LIFT RIGID (SPLINED)	LIFT FLEXIBLE	PITCHING MOMENT RIGID (DIRECT)	PITCHING MOMENT RIGID (SPLINED)	PITCHING MOMENT FLEXIBLE
THICKNESS AND CAMBER	0.0099	0.0099	0.0196	0.0057	0.0057	0.0101
ALPHA(DEGS)	0.1173	0.1173	0.2153	-0.0062	-0.0062	0.0385
ALPHA(RADS)	6.7225	6.7224	12.3336	-0.3551	-0.3551	2.2047
ELEVATOR(DEGS)	0.0118	0.0118	0.0121	-0.0431	-0.0431	-0.0435
ELEVATOR(RADS)	0.6779	0.6779	0.6943	-2.4701	-2.4701	-2.4934
PITCH RATE(DEGS/SEC)	0.0923	0.0923	0.0996	-0.2033	-0.2033	-0.2012
PITCH RATE(RADS/SEC)	5.2904	5.2904	5.7041	-11.6503	-11.6503	-11.5274

TRIM RESULTS

ALPHA = 1.0555E+00 (DEGS) ELEVATOR = -1.2653E+00 (DEGS)

Figure 40. Abridged Results for Rectangular Wing Case A

S U M M A R Y   O F   A C T I V E   C O N S T R A I N T S
12 CONSTRAINTS RETAINED OF 30 APPLIED

COUNT	CONSTRAINT VALUE	CONSTRAINT TYPE	TYPE COUNT	BOUNDARY ID	SUBCASE	ELEMENT TYPE	EID
1	-1.56144E-04	DISPLACEMENT	1	1	1		0
2	-3.14137E-01	VON MISES STRESS	1	1	1	QDMEM1	13
3	-8.12386E-01	VON MISES STRESS	2	1	1	QDMEM1	14
4	-8.33888E-01	VON MISES STRESS	3	1	1	QDMEM1	16
5	-4.82639E-01	VON MISES STRESS	4	1	1	QDMEM1	17
6	-3.41126E-01	VON MISES STRESS	5	1	1	QDMEM1	20
7	-7.95897E-01	VON MISES STRESS	6	1	1	QDMEM1	21
8	-8.36996E-01	VON MISES STRESS	7	1	1	QDMEM1	23
9	-5.03517E-01	VON MISES STRESS	8	1	1	QDMEM1	26
10	-9.85110E-01	VON MISES STRESS	10	1	1	ROD	2
11	-9.87828E-01	VON MISES STRESS	13	1	1	ROD	5
12	-9.87711E-01	VON MISES STRESS	28	1	1	SHEAR	29

A S T R O S   D E S I G N   I T E R A T I O N   H I S T O R Y

ITERATION NUMBER	OBJECTIVE FUNCTION VALUE	NUMBER FUNCTION EVAL	NUMBER GRADIENT EVAL	NUMBER RETAINED CONSTRAINTS	NUMBER ACTIVE CONSTRAINTS	NUMBER VIOLATED CONSTRAINTS	NUMBER LOWER BOUNDS	NUMBER UPPER BOUNDS	APPROXIMATE PROBLEM CONVERGENCE
1	4.80000E+01	0	0	0	0	0	0	0	NOT CONVERGED
2	2.58835E+01	15	3	12	1	0	0	2	NOT CONVERGED
3	2.62437E+01	9	3	12	1	0	0	0	NOT CONVERGED
4	2.60331E+01	7	3	12	1	0	0	0	NOT CONVERGED
5	2.60096E+01	18	1	12	1	0	0	0	CONVERGED

THE FINAL OBJECTIVE FUNCTION VALUE IS:

FIXED =	2.01209E+02
+ DESIGNED =	2.60096E+01
TOTAL =	2.27219E+02

A S T R O S   D E S I G N   V A R I A B L E   V A L U E S

DESIGN VARIABLE ID	DESIGN VARIABLE VALUE	MINIMUM VALUE	MAXIMUM VALUE	OBJECTIVE SENSITIVITY	LINKING OPTION	USER LABEL
1	6.78795E-01	1.00000E-02	1.00000E+03	1.20000D+01	LINKED PHYSICAL	INBDSK
2	4.04900E-01	1.00000E-02	1.00000E+03	1.20000D+01	LINKED PHYSICAL	OTBDSK
3	6.78825E-01	1.00000E-02	1.00000E+03	1.20000D+01	LINKED PHYSICAL	INBDSK
4	4.04949E-01	1.00000E-02	1.00000E+03	1.20000D+01	LINKED PHYSICAL	OTBDSK

S U M M A R Y   O F   L O C A L   D E S I G N   V A R I A B L E S — F I N A L   R E S U L T S
Q D M E M 1   E L E M E N T S

EID	LAYER	LINKING OPTION	THICKNESS	T/TMIN	MINIMUM	MAXIMUM
13	0	LINKED PHYSICAL	1.35759071E-01	6.788E+01	2.000E-03	2.000E+02
14	0	LINKED PHYSICAL	8.09799656E-02	4.049E+01	2.000E-03	2.000E+02
16	0	LINKED PHYSICAL	8.09898600E-02	4.049E+01	2.000E-03	2.000E+02
17	0	LINKED PHYSICAL	1.35764971E-01	6.788E+01	2.000E-03	2.000E+02
20	0	LINKED PHYSICAL	1.35759071E-01	6.788E+01	2.000E-03	2.000E+02
21	0	LINKED PHYSICAL	8.09799656E-02	4.049E+01	2.000E-03	2.000E+02
23	0	LINKED PHYSICAL	8.09898600E-02	4.049E+01	2.000E-03	2.000E+02
26	0	LINKED PHYSICAL	1.35764971E-01	6.788E+01	2.000E-03	2.000E+02

Figure 40. Abridged Results for Rectangular Wing Case A (Concluded)

S U M M A R Y   O F   A C T I V E   C O N S T R A I N T S
12 CONSTRAINTS RETAINED OF 31 APPLIED

COUNT	CONSTRAINT VALUE	CONSTRAINT TYPE	TYPE COUNT	BOUNDARY ID	SUBCASE	ELEMENT TYPE	EID
1	-7.19965E-03	UPPER BND LIFT EFFECT	1	1	2		0
2	-3.07281E-01	DISPLACEMENT	1	1	1		0
3	-5.65466E-01	VON MISES STRESS	1	1	1	QDMEM1	13
4	-9.29169E-01	VON MISES STRESS	2	1	1	QDMEM1	14
5	-9.31820E-01	VON MISES STRESS	3	1	1	QDMEM1	16
6	-6.71565E-01	VON MISES STRESS	4	1	1	QDMEM1	17
7	-5.78793E-01	VON MISES STRESS	5	1	1	QDMEM1	20
8	-9.20799E-01	VON MISES STRESS	6	1	1	QDMEM1	21
9	-9.34978E-01	VON MISES STRESS	7	1	1	QDMEM1	23
10	-6.82420E-01	VON MISES STRESS	8	1	1	QDMEM1	26
11	-9.83815E-01	VON MISES STRESS	10	1	1	ROD	2
12	-9.86741E-01	VON MISES STRESS	13	1	1	ROD	5

```
****                ASTROS APPROXIMATE OPTIMIZATION                  ****
***                     SUMMARY - ITERATION  1                        ***
**                   METHOD = MATH PROGRAMMING                         **
*    CURRENT       PREVIOUS      OBJECTIVE      PERCENT    CONVERGENCE  *
*   OBJECTIVE     OBJECTIVE       CHANGE        CHANGE        FLAG      *
*  3.38150E+01   4.80000E+01   -1.41850E+01   -29.552    NOT CONVERGED  *
```

SIMPLIFIED WING STRUCTURE DESIGN — ASTROS VERSION 1.00 — 8/11/88 — P. 17
OPTIMIZATION FOR LIFT EFFECTIVENESS AND STRENGTH CONSTRAINTS — ASTROS ITERATION 5

NONDIMENSIONAL LONGITUDINAL STABILITY DERIVATIVES

MACH = 8.0000E-01   QDP = 6.5000E+00   REFERENCE GRID = 20

REFERENCE AREA = 2.4000E+03   REFERENCE CHORD = 2.0000E+01

PARAMETER	LIFT RIGID (DIRECT)	LIFT RIGID (SPLINED)	LIFT FLEXIBLE	PITCHING MOMENT RIGID (DIRECT)	PITCHING MOMENT RIGID (SPLINED)	PITCHING MOMENT FLEXIBLE
THICKNESS AND CAMBER	0.0099	0.0099	0.0167	0.0057	0.0057	0.0086
ALPHA(DEGS)	0.1173	0.1173	0.1878	-0.0062	-0.0062	0.0240
ALPHA(RADS)	6.7225	6.7224	10.7574	-0.3551	-0.3551	1.3769
ELEVATOR(DEGS)	0.0118	0.0118	0.0132	-0.0431	-0.0431	-0.0429
ELEVATOR(RADS)	0.6779	0.6779	0.7537	-2.4701	-2.4701	-2.4556
PITCH RATE(DEGS/SEC)	0.0923	0.0923	0.1006	-0.2033	-0.2033	-0.2002
PITCH RATE(RADS/SEC)	5.2904	5.2904	5.7653	-11.6503	-11.6503	-11.4679

TRIM RESULTS

ALPHA = 1.2616E+00 (DEGS)   ELEVATOR = -1.5590E+00 (DEGS)

Figure 41. Abridged Results for Rectangular Wing Case B

S U M M A R Y   O F   A C T I V E   C O N S T R A I N T S
12 CONSTRAINTS RETAINED OF 31 APPLIED

COUNT	CONSTRAINT VALUE	CONSTRAINT TYPE	TYPE COUNT	BOUNDARY ID	SUBCASE	ELEMENT TYPE	EID
1	1.34945E-04	UPPER BND LIFT EFFECT	1	1	2		0
2	-1.59796E-04	DISPLACEMENT	1	1	1		0
3	-4.46310E-01	VON MISES STRESS	1	1	1	QDMEM1	13
4	-7.25300E-01	VON MISES STRESS	2	1	1	QDMEM1	14
5	-7.73173E-01	VON MISES STRESS	3	1	1	QDMEM1	16
6	-5.82099E-01	VON MISES STRESS	4	1	1	QDMEM1	17
7	-4.68650E-01	VON MISES STRESS	5	1	1	QDMEM1	20
8	-7.23717E-01	VON MISES STRESS	6	1	1	QDMEM1	21
9	-7.83869E-01	VON MISES STRESS	7	1	1	QDMEM1	23
10	-5.99094E-01	VON MISES STRESS	8	1	1	QDMEM1	26
11	-9.85071E-01	VON MISES STRESS	10	1	1	ROD	2
12	-9.87761E-01	VON MISES STRESS	13	1	1	ROD	5

A S T R O S   D E S I G N   I T E R A T I O N   H I S T O R Y

ITERATION NUMBER	OBJECTIVE FUNCTION VALUE	NUMBER FUNCTION EVAL	NUMBER GRADIENT EVAL	NUMBER RETAINED CONSTRAINTS	NUMBER ACTIVE CONSTRAINTS	NUMBER VIOLATED CONSTRAINTS	NUMBER LOWER BOUNDS	NUMBER UPPER BOUNDS	APPROXIMATE PROBLEM CONVERGENCE
1	4.80000E+01	0	0	0	0	0	0	0	NOT CONVERGED
2	3.38150E+01	12	3	12	1	0	0	2	NOT CONVERGED
3	2.73448E+01	6	2	12	2	0	0	0	NOT CONVERGED
4	2.76811E+01	6	3	12	2	0	0	0	NOT CONVERGED
5	2.76811E+01	2	1	12	2	0	0	0	CONVERGED

THE FINAL OBJECTIVE FUNCTION VALUE IS:

FIXED = 2.01209E+02
+ DESIGNED = 2.76811E+01
TOTAL = 2.28890E+02

A S T R O S   D E S I G N   V A R I A B L E   V A L U E S

DESIGN VARIABLE ID	DESIGN VARIABLE VALUE	MINIMUM VALUE	MAXIMUM VALUE	OBJECTIVE SENSITIVITY	LINKING OPTION	USER LABEL
1	8.69247E-01	1.00000E-02	1.00000E+03	1.20000D+01	LINKED PHYSICAL	INBDSK
2	2.84174E-01	1.00000E-02	1.00000E+03	1.20000D+01	LINKED PHYSICAL	OTBDSK
3	8.69118E-01	1.00000E-02	1.00000E+03	1.20000D+01	LINKED PHYSICAL	INBDSK
4	2.84218E-01	1.00000E-02	1.00000E+03	1.20000D+01	LINKED PHYSICAL	OTBDSK

S U M M A R Y   O F   L O C A L   D E S I G N   V A R I A B L E S — F I N A L   R E S U L T S
Q D M E M 1   E L E M E N T S

EID	LAYER	LINKING OPTION	THICKNESS	T/TMIN	MINIMUM	MAXIMUM
13	0	LINKED PHYSICAL	1.73849449E-01	8.692E+01	2.000E-03	2.000E+02
14	0	LINKED PHYSICAL	5.68347946E-02	2.842E+01	2.000E-03	2.000E+02
16	0	LINKED PHYSICAL	5.68436570E-02	2.842E+01	2.000E-03	2.000E+02
17	0	LINKED PHYSICAL	1.73823684E-01	8.691E+01	2.000E-03	2.000E+02
20	0	LINKED PHYSICAL	1.73849449E-01	8.692E+01	2.000E-03	2.000E+02
21	0	LINKED PHYSICAL	5.68347946E-02	2.842E+01	2.000E-03	2.000E+02
23	0	LINKED PHYSICAL	5.68436570E-02	2.842E+01	2.000E-03	2.000E+02
26	0	LINKED PHYSICAL	1.73823684E-01	8.691E+01	2.000E-03	2.000E+02

Figure 41. Abridged Results for Rectangular Wing Case B (Concluded)

S U M M A R Y   O F   A C T I V E   C O N S T R A I N T S

1 CONSTRAINTS RETAINED OF 1 APPLIED

COUNT	CONSTRAINT VALUE	CONSTRAINT TYPE	TYPE COUNT	BOUNDARY ID	SUBCASE	ELEMENT TYPE	EID
1	-1.41297E-01	LOWER BND AILR EFFECT	1	1	1		0

```
****                 ASTROS APPROXIMATE OPTIMIZATION                  ****
***                     SUMMARY - ITERATION  1                         ***
**                  METHOD = MATH PROGRAMMING                           **
*    CURRENT      PREVIOUS      OBJECTIVE     PERCENT   CONVERGENCE    *
*   OBJECTIVE    OBJECTIVE       CHANGE        CHANGE       FLAG        *
*  2.40000E+01  4.80000E+01  -2.40000E+01   -50.000   NOT CONVERGED   *
```

SIMPLIFIED WING STRUCTURE DESIGN
OPTIMIZE FOR AILERON EFFECTIVENESS ONLY

ASTROS VERSION 1.00   8/11/88   P.   17
ASTROS ITERATION 5

NONDIMENSIONAL LATERAL ROLLING MOMENT STABILITY DERIVATIVES

MACH = 8.0000E-01   QDP = 6.5000E+00   REFERENCE GRID = 20

REFERENCE AREA = 2.4000E+03   REFERENCE SPAN = 2.0000E+01

PARAMETER	ROLLING MOMENT		
	RIGID (DIRECT)	RIGID (SPLINED)	FLEXIBLE
AILERON(DEGS)	0.0166	0.0166	0.0159
AILERON(RADS)	0.9508	0.9508	0.9129
ROLL RATE(DEGS/SEC)	-0.0418	-0.0418	-0.0531
ROLL RATE(RADS/SEC)	-2.3954	-2.3954	-3.0422

S U M M A R Y   O F   A C T I V E   C O N S T R A I N T S

1 CONSTRAINTS RETAINED OF 1 APPLIED

COUNT	CONSTRAINT VALUE	CONSTRAINT TYPE	TYPE COUNT	BOUNDARY ID	SUBCASE	ELEMENT TYPE	EID
1	-2.30312E-04	LOWER BND AILR EFFECT	1	1	1		0

A S T R O S   D E S I G N   I T E R A T I O N   H I S T O R Y

ITERATION NUMBER	OBJECTIVE FUNCTION VALUE	NUMBER FUNCTION EVAL	NUMBER GRADIENT EVAL	NUMBER RETAINED CONSTRAINTS	NUMBER ACTIVE CONSTRAINTS	NUMBER VIOLATED CONSTRAINTS	NUMBER LOWER BOUNDS	NUMBER UPPER BOUNDS	APPROXIMATE PROBLEM CONVERGENCE
1	4.80000E+01	0	0	0	0	0	0	0	NOT CONVERGED
2	2.40000E+01	6	2	1	0	0	0	4	NOT CONVERGED
3	2.26551E+01	7	3	1	1	0	0	0	NOT CONVERGED
4	2.23898E+01	7	3	1	1	0	0	0	NOT CONVERGED
5	2.22954E+01	14	3	1	1	0	0	0	CONVERGED

THE FINAL OBJECTIVE FUNCTION VALUE IS:

```
            FIXED =   2.01209E+02
       + DESIGNED =   2.22954E+01
                     ------------
            TOTAL =   2.23504E+02
```

Figure 42. Abridged Results for Rectangular Wing Case C

A S T R O S   D E S I G N   V A R I A B L E   V A L U E S

DESIGN VARIABLE ID	DESIGN VARIABLE VALUE	MINIMUM VALUE	MAXIMUM VALUE	OBJECTIVE SENSITIVITY	LINKING OPTION	USER LABEL
1	5.66106E-01	1.00000E-02	1.00000E+03	1.20000D+01	LINKED PHYSICAL	INBDSK
2	3.62869E-01	1.00000E-02	1.00000E+03	1.20000D+01	LINKED PHYSICAL	OTBDSK
3	5.66106E-01	1.00000E-02	1.00000E+03	1.20000D+01	LINKED PHYSICAL	INBDSK
4	3.62869E-01	1.00000E-02	1.00000E+03	1.20000D+01	LINKED PHYSICAL	OTBDSK

S U M M A R Y   O F   L O C A L   D E S I G N   V A R I A B L E S — F I N A L   R E S U L T S

Q D M E M 1   E L E M E N T S

EID	LAYER	LINKING OPTION	THICKNESS	T/TMIN	MINIMUM	MAXIMUM
13	0	LINKED PHYSICAL	1.13221288E-01	5.661E+01	2.000E-03	2.000E+02
14	0	LINKED PHYSICAL	7.25737065E-02	3.629E+01	2.000E-03	2.000E+02
16	0	LINKED PHYSICAL	7.25737065E-02	3.629E+01	2.000E-03	2.000E+02
17	0	LINKED PHYSICAL	1.13221288E-01	5.661E+01	2.000E-03	2.000E+02
20	0	LINKED PHYSICAL	1.13221288E-01	5.661E+01	2.000E-03	2.000E+02
21	0	LINKED PHYSICAL	7.25737065E-02	3.629E+01	2.000E-03	2.000E+02
23	0	LINKED PHYSICAL	7.25737065E-02	3.629E+01	2.000E-03	2.000E+02
26	0	LINKED PHYSICAL	1.13221288E-01	5.661E+01	2.000E-03	2.000E+02

Figure 42. Abridged Results for Rectangular Wing Case C (Concluded)

S U M M A R Y   O F   A C T I V E   C O N S T R A I N T S

12 CONSTRAINTS RETAINED OF 32 APPLIED

COUNT	CONSTRAINT VALUE	CONSTRAINT TYPE	TYPE COUNT	BOUNDARY ID	SUBCASE	ELEMENT TYPE	EID
1	-7.19965E-03	UPPER BND LIFT EFFECT	1	1	2		0
2	-3.07281E-01	DISPLACEMENT	1	1	1		0
3	-5.65466E-01	VON MISES STRESS	1	1	1	QDMEM1	13
4	-9.29169E-01	VON MISES STRESS	2	1	1	QDMEM1	14
5	-9.31820E-01	VON MISES STRESS	3	1	1	QDMEM1	16
6	-6.71565E-01	VON MISES STRESS	4	1	1	QDMEM1	17
7	-5.78793E-01	VON MISES STRESS	5	1	1	QDMEM1	20
8	-9.20799E-01	VON MISES STRESS	6	1	1	QDMEM1	21
9	-9.34978E-01	VON MISES STRESS	7	1	1	QDMEM1	23
10	-6.82420E-01	VON MISES STRESS	8	1	1	QDMEM1	26
11	-9.83815E-01	VON MISES STRESS	10	1	1	ROD	2
12	-1.41297E-01	LOWER BND AILR EFFECT	1	2	1		0

```
****              ASTROS APPROXIMATE OPTIMIZATION               ****
***                    SUMMARY - ITERATION  1                    ***
**                    METHOD = MATH PROGRAMMING                   **
*    CURRENT       PREVIOUS      OBJECTIVE     PERCENT  CONVERGENCE  *
*   OBJECTIVE     OBJECTIVE       CHANGE       CHANGE       FLAG     *
*  3.38150E+01   4.80000E+01   -1.41850E+01   -29.552  NOT CONVERGED *
```

Figure 43. Abridged Results for Rectangular Wing Case D

S U M M A R Y O F A C T I V E C O N S T R A I N T S
12 CONSTRAINTS RETAINED OF 32 APPLIED

COUNT	CONSTRAINT VALUE	CONSTRAINT TYPE	TYPE COUNT	BOUNDARY ID	SUBCASE	ELEMENT TYPE	EID
1	1.34945E-04	UPPER BND LIFT EFFECT	1	1	2		0
2	-1.59796E-04	DISPLACEMENT	1	1	1		0
3	-4.46310E-01	VON MISES STRESS	1	1	1	QDMEM1	13
4	-7.25300E-01	VON MISES STRESS	2	1	1	QDMEM1	14
5	-7.73173E-01	VON MISES STRESS	3	1	1	QDMEM1	16
6	-5.82099E-01	VON MISES STRESS	4	1	1	QDMEM1	17
7	-4.68650E-01	VON MISES STRESS	5	1	1	QDMEM1	20
8	-7.23717E-01	VON MISES STRESS	6	1	1	QDMEM1	21
9	-7.83869E-01	VON MISES STRESS	7	1	1	QDMEM1	23
10	-5.99094E-01	VON MISES STRESS	8	1	1	QDMEM1	26
11	-9.85071E-01	VON MISES STRESS	10	1	1	ROD	2
12	-4.53230E-02	LOWER BND AILR EFFECT	1	2	1		0

A S T R O S D E S I G N I T E R A T I O N H I S T O R Y

ITERATION NUMBER	OBJECTIVE FUNCTION VALUE	NUMBER FUNCTION EVAL	NUMBER GRADIENT EVAL	NUMBER RETAINED CONSTRAINTS	NUMBER ACTIVE CONSTRAINTS	NUMBER VIOLATED CONSTRAINTS	NUMBER LOWER BOUNDS	NUMBER UPPER BOUNDS	APPROXIMATE PROBLEM CONVERGENCE
1	4.80000E+01	0	0	0	0	0	0	0	NOT CONVERGED
2	3.38150E+01	12	3	12	1	0	0	2	NOT CONVERGED
3	2.73448E+01	6	2	12	2	0	0	0	NOT CONVERGED
4	2.76811E+01	6	3	12	2	0	0	0	NOT CONVERGED
5	2.76811E+01	2	1	12	2	0	0	0	CONVERGED

THE FINAL OBJECTIVE FUNCTION VALUE IS:
FIXED = 2.01209E+02
+ DESIGNED = 2.76811E+01

TOTAL = 2.28890E+02

A S T R O S D E S I G N V A R I A B L E V A L U E S

DESIGN VARIABLE ID	DESIGN VARIABLE VALUE	MINIMUM VALUE	MAXIMUM VALUE	OBJECTIVE SENSITIVITY	LINKING OPTION	USER LABEL
1	8.69247E-01	1.00000E-02	1.00000E+03	1.20000D+01	LINKED PHYSICAL	INBDSK
2	2.84174E-01	1.00000E-02	1.00000E+03	1.20000D+01	LINKED PHYSICAL	OTBDSK
3	8.69118E-01	1.00000E-02	1.00000E+03	1.20000D+01	LINKED PHYSICAL	INBDSK
4	2.84218E-01	1.00000E-02	1.00000E+03	1.20000D+01	LINKED PHYSICAL	OTBDSK

S U M M A R Y O F L O C A L D E S I G N V A R I A B L E S — F I N A L R E S U L T S
Q D M E M 1 E L E M E N T S

EID	LAYER	LINKING OPTION	THICKNESS	T/TMIN	MINIMUM	MAXIMUM
13	0	LINKED PHYSICAL	1.73849449E-01	8.692E+01	2.000E-03	2.000E+02
14	0	LINKED PHYSICAL	5.68347946E-02	2.842E+01	2.000E-03	2.000E+02
16	0	LINKED PHYSICAL	5.68436570E-02	2.842E+01	2.000E-03	2.000E+02
17	0	LINKED PHYSICAL	1.73823684E-01	8.691E+01	2.000E-03	2.000E+02
20	0	LINKED PHYSICAL	1.73849449E-01	8.692E+01	2.000E-03	2.000E+02
21	0	LINKED PHYSICAL	5.68347946E-02	2.842E+01	2.000E-03	2.000E+02
23	0	LINKED PHYSICAL	5.68436570E-02	2.842E+01	2.000E-03	2.000E+02
26	0	LINKED PHYSICAL	1.73823684E-01	8.691E+01	2.000E-03	2.000E+02

Figure 43. Abridged Results for Rectangular Wing Case D (Concluded)

requirements with no contribution from the strength constraints. For this reason, the top and bottom skins are driven to the same design so that it is possible to characterize the final design by two numbers which give the thickness of the inboard and the outboard panels. Addressing each of the cases in turn, Case A results in a final weight of 26.0 pounds with the tip rotation the only active constraint for the final design. An analysis of the other conditions that are considered in this subsection indicate that the final design for Case A does not satisfy the lift requirement of Case B, but that it does satisfy the roll effectiveness requirement of Case C.

For Case B, the final design weighs 27.7 pounds and the tip rotation and the lift effectiveness requirements are exactly at their limits. Case C has a weight of 22.3 pounds and it is perhaps of interest that the roll performance requirement tends to drive the design to one that is more uniform in the spanwise direction than was true in the first two cases. Finally, since the Case B design satisfied all the constraints imposed in Case D, it is not surprising to see that the Case D design is identical to that of Case B.

The output shown in Figures 40 through 43 is presented primarily to give a flavor of the available ASTROS outputs. In all the figures, a summary of the active constraints is first given for the initial design. In all cases, the starting design satisfied all the imposed constraints, although this is not a requirement of the procedure. The results of the first pass through the optimizer are given in terms of the weight modification which was made in this iteration. This is then followed by representative results for the final design. For example, the second summary of active constraints given in Figure 40 indicates that only the displacement constraint is active; i.e., near zero. The design iteration history is of interest in that it indicates the rapidity with which the design reached the optimum. In all cases, the final design was achieved in five iterations, including the initial design. The listing of the global and local design variables indicate that there is a factor of 0.2 difference in the two. This factor is from the PQDMEM1 bulk data entry. In all the figures, the final outputs were obtained from the analysis boundary conditions that followed the optimize boundary conditions.

4.5 BODY AERODYNAMICS

The simple wing planform of the previous subsection was augmented by a fuselage in order to validate the implementation of USSAEROs body capability. This model should assist the user in preparing bulk data entries when fuselage of pod aerodynamic elements are to be analyzed.

4.5.1 Problem Description

As discussed in Subsection 8.1 of the Theoretical Manual, the USSAERO procedure makes a distinction between body elements and lifting surfaces. Both surface types are discretized by a large number of boxes with a source singularity used to quantify the aerodynamic flow for the bodies and a vortex singularity used for the lifting surface boxes. A simple fuselage was added to the rectangular wing planform of the previous subsection in order to test this capability. **Figure 44** is a side view of the fuselage which was modeled by three separate segments. In the first segment, a small amount of fuselage camber is present while the second section is a circular, uncambered tube and the third segment is a cone.

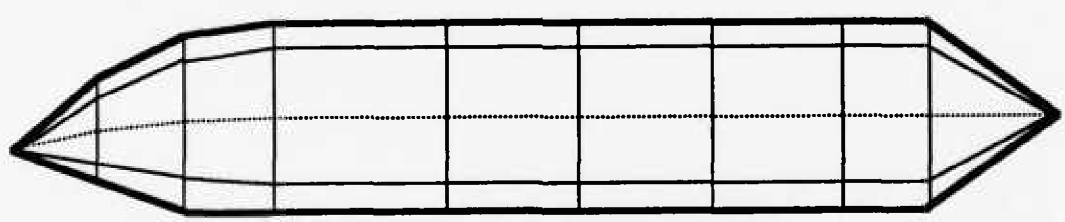

Figure 44. The Fuselage Planform

4.5.2 Input

Figure 45 shows the input for this case. The first item to note in this figure is that the MAPOL sequence has been edited to replace one line. This edit allows for intermediate print of the USSAERO results so that a quick check of the input data can be made (cf. Subsection 7.3.2 of the User's Manual). In particular, it is useful to scan the geometry data for obvious errors. Only an analysis is being performed for this test case so that the solution control packet is brief. The structural and lifting surface data for this test case were identical to that of the previous subsection. For this reason, the input packet given in **Figure 45** includes the RECTS.DAT file that

```
ASSIGN DATABASE WBDDES KIMBERLY NEW DELETE
EDIT NOLIST
REPLACE 221
       [GTKG], [GSTKG], [UGTKG], [AJJTL], [D1JK],[D2JK],[SKJ],3);
SOLUTION
TITLE = SIMPLIFIED WING PLUS BODY
LABEL = WING/BODY TEST CASE
ANALYZE
BOUNDARY MPC=200,SPC=10, SUPPORT=100
   SAERO (TRIM=100)
   PRINT DISP=ALL, TRIM
END
BEGIN BULK
$.
INCLUDE [EJ.APP]RECTS.DAT
$
$    AERODYNAMIC MODEL
$
AEROS                     20.0     60.0   2400.0   20
$
$    WING DATA
$
CAERO6  1       WING            1        20       10
AIRFOIL 1       WING            30       70                40       1.0      CAIRI
+AIRI   10.0    10.0    0.0     20.
AIRFOIL 1       WING            30       70                40       1.0      +A45201
+A45201 10.0    60.0    0.0     20.
$
$    SPANWISE CUTS OF PANEL
$
AEFACT  10      0.0     15.0     30.     45.0     60.0
$
$    CHORDWISE CUTS OF PANEL
$
AEFACT  20      0.0     20.     80.0     100.
$
$     AIRFOIL PERCENT CHORD POINT FOR PROPERTY DEFINITIONS
$
AEFACT  30      0.0     10.      25.0     50.0     75.0    100.00
$
$     AIRFOIL CAMBER
$
AEFACT  40      0.0     -0.01745 -0.0436 -0.0872 -.1308   -.1745
$
$     AIRFOIL THICKNESS
$
AEFACT  70      0.0       1.0      1.0      1.0      1.0      0.0
$
$
$   CANARD DATA
$
CAERO6  2       CANARD          1        20       50
AIRFOIL 2       CANARD          30       70                         1.0      CAIRC
```

Figure 45. Input Data Stream for the Rectangular Wing with Body Components

```
+AIRC   90.     20.     0.0     10.0
AIRFOIL 2       CANARD          30      70                      1.0     CAIRC
+AIRC   85.0    0.0     0.0     15.
$
$    SPANWISE CUTS OF CANARD PANEL
$
AEFACT  50      0.0     10.0    20.0
$
$    PITCH CONTROL SURFACE
$
AESURF  100     ELEV    2               4       7
TRIM    100     0.8     6.5     1       2               8.0     0.274   9864.
$
$    ROLL CONTROL SURFACE
$
AESURF  200     AILERON 1               9       12
TRIM    200     0.8     6.5     -1      0               0.0     0.0     9864.
$
$     CONNECTIVITY OF AERO AND STRUCTURAL MODEL
$
ATTACH        10       2       2       7      20
ATTACH        11      10      10      24      20
ATTACH        12      20      20      44      20
ATTACH        13      30      30      34      20
SPLINE1        3               1       1      12      10
SET1          10       1       3       5       9      11      13      15 CSET
+SET          17      20
$*************************************************
$    BODY DATA  -   MODELLED IN THREE SEGMENTS
$ ********   FIRST BODY SEGMENT   ***************
$
BODY      10      FUSEL
AXSTA     10      -20.0   -3.0            101     201
AXSTA     10      -10.0   -1.5            102     202
AXSTA     10        0.0   -0.5            103      203
AXSTA     10       10.0    0.0            104      204
AEFACT   101        0.0    0.0     0.0     0.0     0.0
AEFACT   201       -3.0   -3.0    -3.0    -3.0    -3.0
AEFACT   102        0.0  3.535     5.0   3.535    0.0
AEFACT   202       -6.5 -5.035    -1.5   2.035    3.5
AEFACT   103        0.0  6.364     9.0   6.364    0.0
AEFACT   203       -9.5 -5.864    -0.5   5.835    8.5
AEFACT   104        0.0  7.071    10.0   7.071    0.0
AEFACT   204      -10.0 -7.071     0.0   7.071   10.0
$ ********   SECOND BODY SEGMENT   ***************
BODY      20      FUSEL
AXSTA     20       10.0    0.0            104     204
 AXSTA    20       85.0    0.0            104     204
$ ********   THIRD BODY SEGMENT   ***************
BODY      30      FUSEL
AXSTA     30       85.0    0.0            104     204
AXSTA     30      100.0    0.0            101     101
PAERO6    10      FUSEL            1       6
```

Figure 45. Input Data Stream for the Rectangular Wing with Body Components (Continued)

```
PAERO6   20      FUSEL                 1       6               501
AEFACT  501       10.0    30.0    45.0     60.0     75.0    85.0
PAERO6   30      FUSEL                  1       6
ENDDATA
```

Figure 45. Input Data Stream for the Rectangular Wing with Body Components (Concluded)

has been given in **Figure 37**. Input data for the lifting surfaces are very similar to that given in **Figure 38** with the one difference being that the inboard airfoil has been moved out to accommodate the fuselage.

Configuration data for the fuselage are given by a combination of BODY and AXSTA entries with associated AEFACT entries. The circumferential cuts are given explicitly in this case, although the circular body option of the AXSTA entry could have been used for all the fuselage stations. All the data must be consistent in this respect in that it is impermissible to input some fuselage sections as circular and others as arbitrary. The paneling data for the fuselage are given by PAERO6 entries with six equal radial cuts used to divide the cross sections in all cases.

The ATTACH entries connect the aerodynamic panels on the fuselage to structural grid point 20 so that these forces are included in the stability derivative and the aeroelastic trim calculation.

4.5.3 Results

An abridged output listing for this case is given in **Figure 46**. The listing of body panel areas and inclination angles is one place to look for obvious errors in the data input. The delta incidence refers to the streamwise slope of the panel while the theta incidence refers to the circumferential slope. This theta slope is measured from a horizontal line emanating from the "top" of the panel back to the bottom of the panel.

The geometry output is followed by two sets of stability coefficients for the complete vehicle. These are USSAERO computed numbers with the first set corresponding to zero angle of attack so that any nonzero numbers can be attributed to the wing thickness and camber plus effects of the body. The second set of stability derivatives is for an angle of attack of one

degree. These USSAERO prints are followed by an ASTROS print of the same information. This ASTROS set of prints is discussed in Subsection 7.2.5 of the User's Manual. A difference between the USSAERO prints and the ASTROS print is that the ASTROS data represents coefficient derivatives while the USSAERO data are the coefficients. This is the reason why C_m at one degree angle of attack is -0.01392 in the USSAERO print while C_{m_α} is -0.0014 in the ASTROS print. If C_{m_α} and C_{m_0} are added together, they give the USSAERO C_m value. The remaining print in **Figure** 46 lists the trim requirements and the displacement vector that results for this trim condition.

4.6 THE MULTIDISCIPLINARY SWEPT WING MODEL

This example problem was developed for use in ASTROS to evaluate and demonstrate the treatment of multidisciplinary constraints by ASTROS. An early version of this sample problem was reported in "ASTROS - A Multidisciplinary Automated Structural Design Tool," by D. J. Neill, E. H. Johnson and R. A. Canfield at the 28th Structures, Structural Dynamics and Materials Conference. The structural, aerodynamic and design models are all very simplistic, but the sample problem is an ideal test bed for the majority of the ASTROS design constraints. In this particular sample case, the model is optimized subject to stress constraints for a static aeroelastic analysis, a frequency constraint for the normal modes discipline and a flutter constraint for an aeroelastic stability analysis. Three separate cases are presented in which each constraint type is added in turn, beginning with strength constraints alone and progressing to all three constraint types. This crude model with these particular constraints serve to illustrate many of the subtleties in performing multidisciplinary optimization.

4.6.1 Problem Description

This example problem is the first that exercises the multidisciplinary features of ASTROS. The manner in which ASTROS treats multidisciplinary constraints represents one of its principal advantages over earlier optimization codes. The Theoretical Manual, therefore, presents these features in some detail, principally in Section II. Of equal importance is the form of the flutter constraint in ASTROS. The constraint formulation places a requirement on the damping value at each velocity rather than explicitly specifying the required flutter speed. This approach does not require the computationally expensive determination of the flutter speed at each design iteration

BODY PANEL AREAS AND INCLINATION ANGLES

PANEL	AREA	DELTA RAD	THETA RAD	DELTA DEG	THETA DEG
1	16.08639	0.31272	-2.74871	17.91775	-157.48958
2	15.36985	0.34925	-2.15208	20.01072	-123.30494
3	15.45622	0.41568	-1.57080	23.81666	-90.00000
4	16.33759	0.48651	-0.98952	27.87484	-56.69505
5	17.85367	0.54077	-0.39288	30.98382	-22.51044
6	42.89130	0.23803	-2.66875	13.63817	-152.90808
7	41.21931	0.24756	-2.21654	14.18434	-126.99841
8	41.12995	0.33207	-1.58687	19.02637	-90.92092
9	43.69869	0.39004	-0.98751	22.34759	-56.57990
10	47.15047	0.43174	-0.39525	24.73660	-22.64643
11	57.13997	0.08066	-2.69031	4.62151	-154.14354
12	54.67947	0.10418	-2.19938	5.96928	-126.01526
13	53.26097	0.09404	-1.58258	5.38823	-90.67529
14	55.24080	0.11761	-0.98809	6.73872	-56.61311
15	58.69598	0.13870	-0.39454	7.94691	-22.60547
16	122.45812	0.00000	-2.74888	0.00000	-157.49934
17	115.53786	0.00000	-2.15198	0.00000	-123.29945
18	113.13602	0.00000	-1.57080	0.00000	-90.00000
19	115.53790	0.00000	-0.98961	0.00000	-56.70055
20	122.45811	0.00000	-0.39271	0.00000	-22.50066
21	91.84361	0.00000	-2.74888	0.00000	-157.49934
22	86.65341	0.00000	-2.15198	0.00000	-123.29945
23	84.85203	0.00000	-1.57080	0.00000	-90.00000
24	86.65341	0.00000	-0.98961	0.00000	-56.70055
25	91.84358	0.00000	-0.39271	0.00000	-22.50066
26	91.84361	0.00000	-2.74888	0.00000	-157.49934
27	86.65341	0.00000	-2.15198	0.00000	-123.29945
28	84.85203	0.00000	-1.57080	0.00000	-90.00000
29	86.65341	0.00000	-0.98961	0.00000	-56.70055
30	91.84358	0.00000	-0.39271	0.00000	-22.50066
31	91.84361	0.00000	-2.74888	0.00000	-157.49934
32	86.65341	0.00000	-2.15198	0.00000	-123.29945
33	84.85203	0.00000	-1.57080	0.00000	-90.00000
34	86.65341	0.00000	-0.98961	0.00000	-56.70055
35	91.84358	0.00000	-0.39271	0.00000	-22.50066
36	61.22906	0.00000	-2.74888	0.00000	-157.49934
37	57.76893	0.00000	-2.15198	0.00000	-123.29945
38	56.56801	0.00000	-1.57080	0.00000	-90.00000
39	57.76893	0.00000	-0.98961	0.00000	-56.70055
40	61.22906	0.00000	-0.39271	0.00000	-22.50066
41	53.93327	-0.55204	-2.74888	-31.62961	-157.49934
42	50.42600	-0.53707	-2.15198	-30.77160	-123.29945
43	49.22885	-0.53197	-1.57080	-30.47936	-90.00000
44	50.42599	-0.53707	-0.98961	-30.77160	-56.70055
45	53.93325	-0.55204	-0.39271	-31.62961	-22.50066

Figure 46. Abridged Results for the Rectangular Wing with Body Components

TOTAL COEFFICIENTS

ON THE COMPLETE CONFIGURATION

```
REFA=    2400.0000   REFB=      60.0000   REFC=      20.0000

REFX=      20.0000   REFZ=       0.0000

       MACH=     0.80000
      ALPHA=     0.00000
       BETA=     0.00000
  ROLL RATE=     0.00000
 PITCH RATE=     0.00000
   YAW RATE=     0.00000
         CX=    -0.00263
         CY=     0.00000
         CZ=     0.00007
        CMX=     0.00000
        CMY=    -0.01248
        CMZ=     0.00000
         CL=     0.00007
         CD=    -0.00263
         CS=     0.00000
        XCP=   171.62415
```

TOTAL COEFFICIENTS

ON THE COMPLETE CONFIGURATION

```
REFA=    2400.0000   REFB=      60.0000   REFC=      20.0000

REFX=      20.0000   REFZ=       0.0000

       MACH=     0.80000
      ALPHA=     1.00000
       BETA=     0.00000
  ROLL RATE=     0.00000
 PITCH RATE=     0.00000
   YAW RATE=     0.00000
         CX=    -0.00230
         CY=     0.00000
         CZ=     0.14653
        CMX=     0.00000
        CMY=    -0.01392
        CMZ=     0.00000
         CL=     0.14655
         CD=     0.00026
         CS=     0.00000
        XCP=     1.09498
```

Figure 46. Abridged Results for the Rectangular Wing with Body Components (Continued)

NONDIMENSIONAL LONGITUDINAL STABILITY DERIVATIVES

MACH = 8.0000E-01 QDP = 6.5000E+00 REFERENCE GRID = 20

REFERENCE AREA = 2.4000E+03 REFERENCE CHORD = 2.0000E+01

PARAMETER	LIFT RIGID (DIRECT)	LIFT RIGID (SPLINED)	LIFT FLEXIBLE	PITCHING MOMENT RIGID (DIRECT)	PITCHING MOMENT RIGID (SPLINED)	PITCHING MOMENT FLEXIBLE
THICKNESS AND CAMBER	0.0001	0.0050	0.0088	-0.0125	-0.0045	-0.0030
ALPHA(DEGS)	0.1465	0.1450	0.2081	-0.0014	0.0000	0.0258
ALPHA(RADS)	8.3923	8.3061	11.9259	-0.0822	0.0025	1.4790
ELEVATOR(DEGS)	0.0143	0.0134	0.0102	-0.0503	-0.0476	-0.0496
ELEVATOR(RADS)	0.8189	0.7670	0.5865	-2.8842	-2.7299	-2.8435
PITCH RATE(DEGS/SEC)	0.1048	0.0973	0.0941	-0.2434	-0.2157	-0.2194
PITCH RATE(RADS/SEC)	6.0068	5.5764	5.3936	-13.9455	-12.3600	-12.5687

TRIM RESULTS

ALPHA = 1.2559E+00 (DEGS) ELEVATOR = -1.5473E+00 (DEGS)

D I S P L A C E M E N T V E C T O R

POINT ID.	TYPE	T1	T2	T3	R1	R2	R3
1	G	4.71072E-03	0.00000E+00	-9.01536E-02	0.00000E+00	0.00000E+00	0.00000E+00
2	G	-4.71072E-03	0.00000E+00	-9.11172E-02	0.00000E+00	0.00000E+00	0.00000E+00
3	G	7.52866E-03	-1.87269E-02	5.59136E-01	0.00000E+00	0.00000E+00	0.00000E+00
4	G	-7.52866E-03	1.87269E-02	5.56122E-01	0.00000E+00	0.00000E+00	0.00000E+00
5	G	1.03463E-02	-2.01596E-02	1.74041E+00	0.00000E+00	0.00000E+00	0.00000E+00
6	G	-1.03463E-02	2.01596E-02	1.73966E+00	0.00000E+00	0.00000E+00	0.00000E+00
7	G	4.73227E-03	0.00000E+00	-2.22616E-01	0.00000E+00	0.00000E+00	0.00000E+00
8	G	-4.73227E-03	0.00000E+00	-2.22616E-01	0.00000E+00	0.00000E+00	0.00000E+00
9	G	9.04083E-03	-1.75258E-02	3.87943E-01	0.00000E+00	0.00000E+00	0.00000E+00
10	G	-9.04083E-03	1.75258E-02	3.85476E-01	0.00000E+00	0.00000E+00	0.00000E+00
11	G	1.00694E-02	-2.03904E-02	1.53502E+00	0.00000E+00	0.00000E+00	0.00000E+00
12	G	-1.00694E-02	2.03904E-02	1.53410E+00	0.00000E+00	0.00000E+00	0.00000E+00
13	G	6.97152E-03	0.00000E+00	-3.36153E-01	0.00000E+00	0.00000E+00	0.00000E+00
14	G	-6.97152E-03	0.00000E+00	-3.35993E-01	0.00000E+00	0.00000E+00	0.00000E+00
15	G	9.91442E-03	-1.70742E-02	1.96027E-01	0.00000E+00	0.00000E+00	0.00000E+00
16	G	-9.91442E-03	1.70742E-02	1.95479E-01	0.00000E+00	0.00000E+00	0.00000E+00
17	G	1.02443E-02	-2.04163E-02	1.32640E+00	0.00000E+00	0.00000E+00	0.00000E+00
18	G	-1.02443E-02	2.04163E-02	1.32656E+00	0.00000E+00	0.00000E+00	0.00000E+00
20	G	0.00000E+00	0.00000E+00	-2.22616E-01	0.00000E+00	9.46654E-03	0.00000E+00

Figure 46. Abridged Results for the Rectangular Wing with Body Components (Concluded)

and avoids the complexity of tracking multiple flutter branches. These topics are further discussed in Section X of the Theoretical Manual.

The swept wing structural and aerodynamic models are illustrated in Figure 47. The structural model divides the structural box into six equally spaced spanwise bays and two equal chordwise segments. The skins on both the upper and lower surface are modeled as isoparametric quadrilateral membrane elements. The ribs and spars are modeled as shear panels with rod elements for spar caps. Rod elements are also used as posts to connect all upper and lower surface nodes. This results in 57 rod elements, 24 quadrilateral membrane elements and 32 shear panels. The posts are fixed at 0.30 in^2 while the remaining elements make up the set of local design variables.

The sample problem includes both steady and unsteady aerodynamics models. In each case, the wing is represented as a flat plate with 50 boxes per surface. The steady aerodynamics model has a horizontal stabilizer to enable trim for both lift and pitching moment. The last two boxes in each chordwise strip on the tail are used to represent an elevator. There is no structure associated with the tail panel or with the fuselage.

The full multidisciplinary design problem minimizes the weight subject to constraints from three engineering disciplines and two boundary conditions. The first boundary condition cantilevers the wing root and uses the lowest five normal modes to represent the structure in a flutter analysis. The modal frequency of the first bending mode is constrained to be above 1.5 Hz, and the flutter damping ratio is constrained to be negative for a flight condition of 0.80 Mach number at sea level (530 KEAS). The second boundary condition "supports" the wing at the center root of the structural box, allowing for rigid pitch and plunge modes about this point. The stresses in the wing skins are constrained by

$$\sigma_t \leq 60 \text{ ksi}$$

$$\sigma_c \leq 50 \text{ ksi}$$

$$\tau_{xy} \leq 30 \text{ ksi}$$

during a trimmed symmetric aeroelastic 4g pullup at Mach 1.25 at 25,000 feet.

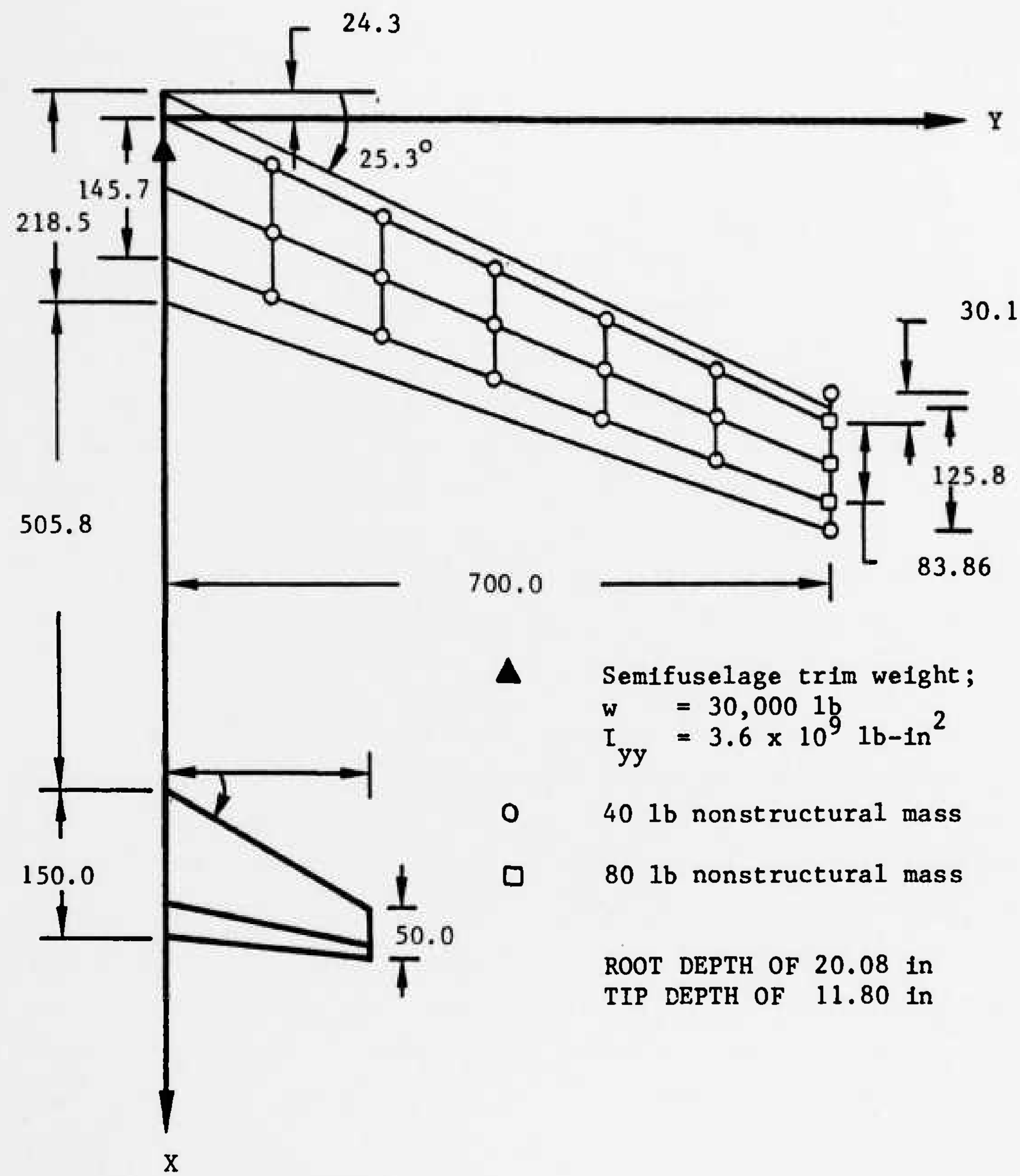

Figure 47. Aerodynamic and Structural Models of the Multidisciplinary Wing

The design variables for this model link elements in each of three spanwise segments, resulting in a total of 12 structural design variables. In each segment, the quadrilateral membrane elements on the upper and lower surfaces constitute one design variable with the spar elements, rib elements and spar cap elements in each segment making up the remainder of the design variables in each segment. In addition to the structural variables, the leading edge tip mass was allowed to vary as a 13th design variable representing a balance mass.

4.6.2 Input Description

Figure 48 shows the input for the full multidisciplinary test case. It includes the structural model, both boundary condition definitions, the eigenvalue extraction information, both the steady and unsteady aerodynamic models, the steady aerodynamic flight condition, the flutter flight condition and all the data related to the design variables and constraint definitions. For the other two cases, all that is required is that the Solution Control packet be modified to omit the flutter case and/or the modal analysis. Also, the frequency/stress constraint model includes a MAPOL packet to modify the standard sequence. It increases the maximum number of iterations from 15 (the default) to 50 (see Subsection 4.6.3).

The Solution Control packet includes two BOUNDARY commands. The first is the cantilever condition for the modal and flutter analyses while the second models the unrestrained vehicle for the steady aeroelastic analysis. Both boundary conditions use multipoint constraints (MPC), single point constraints (SPC) and Guyan reduction (REDUCE) to reduce the size of the solution set. The MPCs in the first boundary condition (set identification 101) are used to rigidly link the two tip masses (**Figure 47**) to the structural box and to attach a number of extra grid points to obtain improved spline interpolation for the aerodynamic forces. These extra grid points (200 to 214) increase the number of chordwise spline points, which tends to improve the results for the surface spline. In the second boundary condition, an MPCADD bulk data entry is used to combine the first boundary condition's MPC set with some additional equations to rigidly connect the root of the structural box to the support point degrees of freedom. This enables the structure to pitch and plunge about the support point for the steady aeroelastic analysis.

```
ASSIGN DATABASE SDM8 SHAZAM NEW DELETE
SOLUTION
   TITLE = SDM CONFERENCE EXAMPLE PROBLEM
   SUBTIT = USES TWO SPLINES
   OPTIMIZE STRATEGY = 57
      PRINT DCON, ROOTS=ALL, TRIM
      BOUNDARY MPC = 101, SPC=10, REDUCE=100, METHOD=99
         LABEL = FLUTTER ANALYSIS
         FLUTTER ( FLCOND = 99, DCON = 1099 )
         LABEL = MODAL ANALYSIS, 1.5 HZ LOWER BOUND CONSTRAINT
         MODES   ( DCON = 2099 )
      BOUNDARY MPC =2101, SPC=110, REDUCE=1100, SUPPORT=1
         LABEL = STATIC AERO BOUNDARY CONDITION SUPERSONIC
         SAERO ( TRIM = 1100 )
END
BEGIN BULK
$
$        SWEPT WING MODEL FROM
$        "A ROOT LOCUS BASED FLUTTER SYNTHESIS PROCEDURE" BY
$        P. HAJELA   STANFORD U.
$        WITH A FLUTTER CONSTRAINT AT SEA LEVEL FOR M=0.80
$        STRESS CONSTRAINTS UNDER A 4 G STATIC AIR LOAD AT
$        25000 FT. (M = 1.25) AND A 1.5 HZ LOW. BOUND FREQ. CONSTRNT.
$
GRID            1             0.0     0.0  10.039
GRID            2             0.0     0.0 -10.039
GRID            3         72.8345     0.0  10.039
GRID            4         72.8345     0.0 -10.039
GRID            5        145.6690     0.0  10.039
GRID            6        145.6690     0.0 -10.039
GRID            7         53.4758 116.667  9.3502
GRID            8         53.4758 116.667 -9.3502
GRID            9        121.1590 116.667  9.3502
GRID           10        121.1590 116.667 -9.3502
GRID           11        188.8430 116.667  9.3502
GRID           12        188.8430 116.667 -9.3502
GRID           13        106.9520 233.333  8.6613
GRID           14        106.9520 233.333 -8.6613
GRID           15        169.4840 233.333  8.6613
GRID           16        169.4840 233.333 -8.6613
GRID           17        232.0170 233.333  8.6613
GRID           18        232.0170 233.333 -8.6613
GRID           19        160.4280 350.0    7.9724
GRID           20        160.4280 350.0   -7.9724
GRID           21        217.8090 350.0    7.9724
GRID           22        217.8090 350.0   -7.9724
GRID           23        275.1910 350.0    7.9724
GRID           24        275.1910 350.0   -7.9724
GRID           25        213.9030 466.667  7.2834
GRID           26        213.9030 466.667 -7.2834
GRID           27        266.1340 466.667  7.2834
GRID           28        266.1340 466.667 -7.2834
GRID           29        318.3650 466.667  7.2834
```

Figure 48. Input Data Stream for the Multidisciplinary Wing

```
GRID          30        318.3650 466.667 -7.2834
GRID          31        267.3780 583.333  6.5945
GRID          32        267.3780 583.333 -6.5945
GRID          33        314.4590 583.333  6.5945
GRID          34        314.4590 583.333 -6.5945
GRID          35        361.5390 583.333  6.5945
GRID          36        361.5390 583.333 -6.5945
GRID          37        320.8550 700.0    5.9055
GRID          38        320.8550 700.0   -5.9055
GRID          39        362.7840 700.0    5.9055
GRID          40        362.7840 700.0   -5.9055
GRID          41        404.7130 700.0    5.9055
GRID          42        404.7130 700.0   -5.9055
GRID          43        290.7840 700.0       0.0
GRID          44        434.7830 700.0       0.0
GRID          45        72.8345  0.0         0.0
GRID         201        -24.267  0.0         0.0
GRID         202        194.233  0.0         0.0
GRID         203        30.915   116.667     0.0
GRID         204        233.965  116.667     0.0
GRID         205        85.688   233.333     0.0
GRID         206        273.825  233.333     0.0
GRID         207        141.301  350.0       0.0
GRID         208        313.445  350.0       0.0
GRID         209        196.493  466.667     0.0
GRID         210        353.186  466.667     0.0
GRID         211        251.685  583.333     0.0
GRID         212        392.926  583.333     0.0
GRID         213        306.874  700.0       0.0
GRID         214        432.674  700.0       0.0
$
$       BOUNDARY CONDITION 1
$
MPC,    101,    43,   1,   -4.0,  37,   1,  1.0, , MPC4311
+PC4311,  ,     38,   1,    1.0,  39,   1,  1.0, , MPC4312
+PC4312,  ,     40,   1,    1.0
MPC,    101,    44,   1,   -4.0,  39,   1,  1.0, , MPC4411
+PC4411,  ,     40,   1,    1.0,  41,   1,  1.0, , MPC4412
+PC4412,  ,     42,   1,    1.0
MPC,    101,    43,   2,   -4.0,  37,   2,  1.0, , MPC4321
+PC4321,  ,     38,   2,    1.0,  39,   2,  1.0, , MPC4322
+PC4322,  ,     40,   2,    1.0
MPC,    101,    44,   2,   -4.0,  39,   2,  1.0, , MPC4421
+PC4421,  ,     40,   2,    1.0,  41,   2,  1.0, , MPC4422
+PC4422,  ,     42,   2,    1.0
MPC,    101,    43,   3,       -1.0,  37,    3, 0.85859, , MPC4331
+PC4331,  ,     38,   3,   0.85859,  39,    3,-0.35859, , MPC4332
+PC4332,  ,     40,   3,  -0.35859
MPC,    101,    44,   3,       -1.0,  39,    3,-0.35859, , MPC4431
+PC4431,  ,     40,   3,  -0.35859,  41,    3, 0.85859, , MPC4432
+PC4432,  ,     42,   3,   0.85859
MPC,    101,   201,   3,       -1.0,  45,    3,     1.0, ,MPC20131
+PC20131, ,     45,   5,      97.1
```

Figure 48. Input Data Stream for the Multidisciplinary Wing (Continued)

```
MPC,    101,    202,    3,      -1.0,  45,    3,      1.0, ,MPC20231
+PC20231, ,      45,    5,    -121.4
MPC,    101,    203,    3,      -1.0,   7,    3,  0.6667, ,MPC20331
+PC20331, ,       8,    3,    0.6667,   9,    3, -0.1667, ,MPC20332
+PC20332, ,      10,    3,   -0.1667
MPC,    101,    204,    3,      -1.0,   9,    3, -0.3333, ,MPC20431
+PC20431, ,      10,    3,   -0.3333,  11,    3,  0.8333, ,MPC20432
+PC20432, ,      12,    3,    0.8333
MPC,    101,    205,    3,      -1.0,  13,    3,  0.6667, ,MPC20531
+PC20531, ,      14,    3,    0.6667,  15,    3, -0.1667, ,MPC20532
+PC20532, ,      16,    3,   -0.1667
MPC,    101,    206,    3,      -1.0,  15,    3, -0.3333, ,MPC20631
+PC20631, ,      16,    3,   -0.3333,  17,    3,  0.8333, ,MPC20632
+PC20632, ,      18,    3,    0.8333
MPC,    101,    207,    3,      -1.0,  19,    3,  0.6667, ,MPC20731
+PC20731, ,      20,    3,    0.6667,  21,    3, -0.1667, ,MPC20732
+PC20732, ,      22,    3,   -0.1667
MPC,    101,    208,    3,      -1.0,  21,    3, -0.3333, ,MPC20831
+PC20831, ,      22,    3,   -0.3333,  23,    3,  0.8333, ,MPC20832
+PC20832, ,      24,    3,    0.8333
MPC,    101,    209,    3,      -1.0,  25,    3,  0.6667, ,MPC20931
+PC20931, ,      26,    3,    0.6667,  27,    3, -0.1667, ,MPC20932
+PC20932, ,      28,    3,   -0.1667
MPC,    101,    210,    3,      -1.0,  27,    3, -0.3333, ,MPC21031
+PC21031, ,      28,    3,   -0.3333,  29,    3,  0.8333, ,MPC21032
+PC21032, ,      30,    3,    0.8333
MPC,    101,    211,    3,      -1.0,  31,    3,  0.6667, ,MPC21131
+PC21131, ,      32,    3,    0.6667,  33,    3, -0.1667, ,MPC21132
+PC21132, ,      34,    3,   -0.1667
MPC,    101,    212,    3,      -1.0,  33,    3, -0.3333, ,MPC21231
+PC21231, ,      34,    3,   -0.3333,  35,    3,  0.8333, ,MPC21232
+PC21232, ,      36,    3,    0.8333
MPC,    101,    213,    3,      -1.0,  37,    3,  0.6667, ,MPC21331
+PC21331, ,      38,    3,    0.6667,  39,    3, -0.1667, ,MPC21332
+PC21332, ,      40,    3,   -0.1667
MPC,    101,    214,    3,      -1.0,  39,    3, -0.3333, ,MPC21431
+PC21431, ,      40,    3,   -0.3333,  41,    3,  0.8333, ,MPC21432
+PC21432, ,      42,    3,    0.8333
$
SPC1,       10,  123456,    1,   THRU,    6,   45
SPC1,       10,     456,    7,   THRU,   44
SPC1,       10,   12456,  201,   THRU,  214
$
ASET1,  100,  3,  7,  9, 11, 13, 15, 17, ASETA
+SETA,   19, 21, 23, 25, 27, 29, 31, 33, ASETB
+SETB,   35, 37, 39, 41
$
$       BOUNDARY CONDITION 2
$
MPCADD,   2101,    101,    201
MPC,    201,     3,   1,      1.0,  45,    5,  -10.04
MPC,    201,     3,   3,      1.0,  45,    3,  -1.0
MPC,    201,     4,   1,      1.0,  45,    5,  10.04
```

Figure 48. Input Data Stream for the Multidisciplinary Wing (Continued)

```
MPC,    201,    4,   3,      1.0,  45,   3,  -1.0
$
SPC1,  110,    1246,     45
SPC1,  110,    2456,      1,    THRU,       6
SPC1,  110,     456,      7,    THRU,      44
SPC1,  110,   12456,    201,    THRU,     214
$
ASET1,  1100,  3,  7,  9, 11, 13, 15, 17, ASETA
+SETA,   19, 21, 23, 25, 27, 29, 31, 33, ASETB
+SETB,   35, 37, 39, 41, 45, 1, 5
ASET1, 1100, 5, 45
$
SUPORT,  1,      45,    35
$
$       UPPER AND LOWER SKINS 100 - UPPER, 200 - LOWER
$
CQDMEM1      101    1004       1       7       9       3
CQDMEM1      201    1004       2       8      10       4
CQDMEM1      102    1004       3       9      11       5
CQDMEM1      202    1004       4      10      12       6
CQDMEM1      103    1004       7      13      15       9
CQDMEM1      203    1004       8      14      16      10
CQDMEM1      104    1004       9      15      17      11
CQDMEM1      204    1004      10      16      18      12
CQDMEM1      105    1005      13      19      21      15
CQDMEM1      205    1005      14      20      22      16
CQDMEM1      106    1005      15      21      23      17
CQDMEM1      206    1005      16      22      24      18
CQDMEM1      107    1005      19      25      27      21
CQDMEM1      207    1005      20      26      28      22
CQDMEM1      108    1005      21      27      29      23
CQDMEM1      208    1005      22      28      30      24
CQDMEM1      109    1006      25      31      33      27
CQDMEM1      209    1006      26      32      34      28
CQDMEM1      110    1006      27      33      35      29
CQDMEM1      210    1006      28      34      36      30
CQDMEM1      111    1006      31      37      39      33
CQDMEM1      211    1006      32      38      40      34
CQDMEM1      112    1006      33      39      41      35
CQDMEM1      212    1006      34      40      42      36
$
$       MODEL SUB STRUCTURE
$       SHEAR PANELS:  300 - LE,   350 - MID, 400 - TE, 500 - CHORDWISE
$       AXIAL RODS:  600 - INBOARD  2 BAYS
$                    700 - MID SPAN 2 BAYS
$                    800 - OUTBOARD 2 BAYS
$
CSHEAR       301    2007       1       2       8       7
CSHEAR       351    2007       3       4      10       9
CSHEAR       401    2007       5       6      12      11
CSHEAR       302    2007       7       8      14      13
CSHEAR       352    2007       9      10      16      15
CSHEAR       402    2007      11      12      18      17
```

Figure 48. Input Data Stream for the Multidisciplinary Wing (Continued)

CSHEAR	303	2008	13	14	20	19
CSHEAR	353	2008	15	16	22	21
CSHEAR	403	2008	17	18	24	23
CSHEAR	304	2008	19	20	26	25
CSHEAR	354	2008	21	22	28	27
CSHEAR	404	2008	23	24	30	29
CSHEAR	305	2009	25	26	32	31
CSHEAR	355	2009	27	28	34	33
CSHEAR	405	2009	29	30	36	35
CSHEAR	306	2009	31	32	38	37
CSHEAR	356	2009	33	34	40	39
CSHEAR	406	2009	35	36	42	41
CSHEAR	501	2010	7	8	10	9
CSHEAR	502	2010	9	10	12	11
CSHEAR	503	2010	13	14	16	15
CSHEAR	504	2010	15	16	18	17
CSHEAR	505	2011	19	20	22	21
CSHEAR	506	2011	21	22	24	23
CSHEAR	507	2011	25	26	28	27
CSHEAR	508	2011	27	28	30	29
CSHEAR	509	2012	31	32	34	33
CSHEAR	510	2012	33	34	36	35
CSHEAR	511	2012	37	38	40	39
CSHEAR	512	2012	39	40	42	41
CSHEAR	513	2010	1	2	4	3
CSHEAR	514	2010	3	4	6	5
$						
CONROD	1201	1	2	90	0.3	
CONROD	1202	3	4	90	0.3	
CONROD	1203	5	6	90	0.3	
CONROD	1301	7	8	90	0.3	
CONROD	1302	13	14	90	0.3	
CONROD	1303	19	20	90	0.3	
CONROD	1304	25	26	90	0.3	
CONROD	1305	31	32	90	0.3	
CONROD	1306	37	38	90	0.3	
CONROD	1401	9	10	90	0.3	
CONROD	1402	15	16	90	0.3	
CONROD	1403	21	22	90	0.3	
CONROD	1404	27	28	90	0.3	
CONROD	1405	33	34	90	0.3	
CONROD	1406	39	40	90	0.3	
CONROD	1501	11	12	90	0.3	
CONROD	1502	17	18	90	0.3	
CONROD	1503	23	24	90	0.3	
CONROD	1504	29	30	90	0.3	
CONROD	1505	35	36	90	0.3	
CONROD	1506	41	42	90	0.3	
$						
CROD	601	6001	1	7		
CROD	602	6001	2	8		
CROD	603	6001	3	9		
CROD	604	6001	4	10		

Figure 48. Input Data Stream for the Multidisciplinary Wing (Continued)

CROD	605	6001	5	11
CROD	606	6001	6	12
CROD	607	6001	7	13
CROD	608	6001	8	14
CROD	609	6001	9	15
CROD	610	6001	10	16
CROD	611	6001	11	17
CROD	612	6001	12	18
CROD	701	7002	13	19
CROD	702	7002	14	20
CROD	703	7002	15	21
CROD	704	7002	16	22
CROD	705	7002	17	23
CROD	706	7002	18	24
CROD	707	7002	19	25
CROD	708	7002	20	26
CROD	709	7002	21	27
CROD	710	7002	22	28
CROD	711	7002	23	29
CROD	712	7002	24	30
CROD	801	8003	25	31
CROD	802	8003	26	32
CROD	803	8003	27	33
CROD	804	8003	28	34
CROD	805	8003	29	35
CROD	806	8003	30	36
CROD	807	8003	31	37
CROD	808	8003	32	38
CROD	809	8003	33	39
CROD	810	8003	34	40
CROD	811	8003	35	41
CROD	812	8003	36	42
$				
CONM2	50001	7		20.0
CONM2	50002	8		20.0
CONM2	50003	9		20.0
CONM2	50004	10		20.0
CONM2	50005	11		20.0
CONM2	50006	12		20.0
CONM2	50007	13		20.0
CONM2	50008	14		20.0
CONM2	50009	15		20.0
CONM2	50010	16		20.0
CONM2	50011	17		20.0
CONM2	50012	18		20.0
CONM2	50013	19		20.0
CONM2	50014	20		20.0
CONM2	50015	21		20.0
CONM2	50016	22		20.0
CONM2	50017	23		20.0
CONM2	50018	24		20.0
CONM2	50019	25		20.0
CONM2	50020	26		20.0

Figure 48. Input Data Stream for the Multidisciplinary Wing (Continued)

```
CONM2       50021      27           20.0
CONM2       50022      28           20.0
CONM2       50023      29           20.0
CONM2       50024      30           20.0
CONM2       50025      31           20.0
CONM2       50026      32           20.0
CONM2       50027      33           20.0
CONM2       50028      34           20.0
CONM2       50029      35           20.0
CONM2       50030      36           20.0
CONM2       50031      37           40.0
CONM2       50032      38           40.0
CONM2       50033      39           40.0
CONM2       50034      40           40.0
CONM2       50035      41           40.0
CONM2       50036      42           40.0
CONM2       50037      43           40.0
CONM2       50038      44           40.0
$
$     TRIM WEIGHT AT ROOT 1/4 CHORD INCLUDING ROTATIONAL INERTIA
$
CONM2,     51001,     45, , 30000.0, -36.0, , , , +CM01
+CM01,          ,        , 3.6E9
$
PQDMEM1, 1004,   91,   0.02
PQDMEM1, 1005,   91,   0.02
PQDMEM1, 1006,   91,   0.02
$
PSHEAR,  2007,   90,   0.02
PSHEAR,  2008,   90,   0.02
PSHEAR,  2009,   90,   0.02
PSHEAR,  2010,   90,   0.02
PSHEAR,  2011,   90,   0.02
PSHEAR,  2012,   90,   0.02
$
PROD,    6001,   90,   1.0
PROD,    7002,   90,   1.0
PROD,    8003,   90,   1.0
$
MAT1,      90,     10.E6,   ,   0.3,    0.1
MAT1,      91,     10.E6,   ,   0.3,    0.1, , , , ABC
+BC,   60000.0,   50000.0, 30000.0
$
$     MASS CONVERSION FACTOR
$
CONVERT,  MASS,  2.588E-3
$
$   EIGENVALUE EXTRACTION DATA
$
EIGR,   99,    GIV,  0.0,  700.0,  5,  5,  , , ABC
+BC,  MAX
$
$   STEADY AERODYNAMIC MODEL
```

Figure 48. Input Data Stream for the Multidisciplinary Wing (Continued)

```
$
$   WING DATA
$
CAERO6, 5000, WING, , 1, 5001, 5002
AEFACT, 5001, 0.0, 9.55, 34.55, 65.45, 90.45, 100.0
AEFACT, 5002, 0.0, 70.0, 140.0, 210.0, 280.0, 350.0, 420.0, +AE5002
+AE5002, 490.0,  560.0, 630.0, 700.0
$
AIRFOIL, 5000, WING, , 5101, 5102, , , , +A5000
+A5000,  -24.277, 0.0, 0.0, 218.5
AIRFOIL, 5000, WING, , 5101, 5102, , , , +A5000
+A5000,  306.874, 700.0, 0.0, 125.8
$
$   TAIL DATA
$
CAERO6, 6000, CANARD, , 1, 6001, 6002
AEFACT, 6001, 0.0, 9.55, 34.55, 65.45, 90.45, 100.0
AEFACT, 6002, 0.0, 21.6, 43.2, 64.8, 86.4, 108.0, 129.6, +AE6002
+AE6002, 151.2, 172.8, 194.4, 216.0
$
AESURF,  6100, ELEV, 6000, , 6003, 6049
AIRFOIL, 6000, CANARD, , 5101, 5102, , , , +A5000
+A5000,  700.0, 0.0, 0.0, 150.0
AIRFOIL, 6000, CANARD, , 5101, 5102, , , , +A5000
+A5000,  824.7, 216.0, 0.0, 50.0
AEFACT, 5101, 0.0, 10.0, 25.0, 50.0, 75.0, 90.0, 100.0
AEFACT, 5102, 0.0, 0.0, 0.0, 0.0, 0.0, 0.0, 0.0
$
$   AERO/STRUCTURAL INTERCONNECTION
$
SPLINE1, 15000,  , 5000,  5000, 5024, 10
SET1,  10,   1,   3,   5,   7,   9,  11,  13,  DEF
+EF,   15,  17,  19,  21,  23,  25,  27,  29,  GHI
+HI,  201, 202, 203, 204, 205, 206, 207, 208,  JKL
+KL,  209, 210
$
SPLINE1, 15100,  , 5000,  5025, 5049, 20
SET1,  20,  13,  15,  17,  19,  21,  23,  25,  DEF
+EF,   27,  29,  31,  33,  35,  37,  39,  41,  GHI
+HI,  205, 206, 207, 208, 209, 210, 211, 212,  JKL
+KL,  213, 214
$
ATTACH,  16000, 6000. 6000, 6049, 45
$
$    REFERENCE STEADY AERODYNAMIC DATA
$
AEROS, , , 187.6, 1400.0, 241010., 45
$
$    TRIM CONDITION IS 4 G'S AT 25000 FT, M = 1.25
$
TRIM, 1100, 1.25, 5.959, 1, 2, 4.0, 0.0760, 15232.8
$
$   UNSTEADY AERODYNAMIC MODEL
```

Figure 48. Input Data Stream for the Multidisciplinary Wing (Continued)

```
$
$   WING DATA
$
CAERO1, 1, , , 10, 5, , , 1, ABC
+BC, -24.277, 0.0, 0.0, 218.5, 306.874, 700.0, 0.0, 125.8
$
$   AERO/STRUCTURAL INTERCONNECTION USING SAME SET1 AS STEADY AERO
$
SPLINE1,  3,  , 1,  1, 25, 10
SPLINE1,  4,  , 1, 26, 50, 20
$                                     3
$       REFERENCE DENSITY IS (SLUGS/IN  )/12 AT SEA LEVEL
$
AERO, ,  187.6, 1.147E-7
MKAERO1, 1, 0, 0.80, , , , , , 0.05, 0.10, 0.5, 1.2, 2.0, 3.0
FLUTTER, 99, PK, 97, 96, 98, , , , ABC
+BC, 1, 0
FLFACT, 96, 0.80
FLFACT, 97, 1.0
FLFACT, 98, 8000.0, 8600.0, 9200.0, 9700.0, 10300.0, 10713.5, 11000.0
$
$    DESIGN INFORMATION
$
DCONFLT, 1099, , 0.0, 0.0, 1.E6, 0.0
DCONFRQ, 2099,      1,    LOWER, 1.5
DCONSTR,   91, VMISES
DESVAR,    1,  0.333333,    ,     8.0
DESVAR,    2,  0.333333,    ,     8.0
DESVAR,    3,  0.333333,    ,     8.0
DESVAR,    4,  1.667E-1,    ,     8.0
DESVAR,    5,  1.667E-1,    ,     8.0
DESVAR,    6,  1.667E-1,    ,     8.0
DESVAR,    7,  3.333E-1,    ,    16.0
DESVAR,    8,  3.333E-1,    ,    16.0
DESVAR,    9,  3.333E-1,    ,    16.0
DESVAR,   10,  1.667E-1,    ,     8.0
DESVAR,   11,  1.667E-1,    ,     8.0
DESVAR,   12,  1.667E-1,    ,     8.0
DESELM,   13,  50037, CONM2,    ,    ,    1.0
PLIST,     1,    PROD, 6001
PLIST,     2,    PROD, 7002
PLIST,     3,    PROD, 8003
PLIST,     4, PQDMEM1, 1004
PLIST,     5, PQDMEM1, 1005
PLIST,     6, PQDMEM1, 1006
PLIST,     7, PSHEAR, 2007
PLIST,     8, PSHEAR, 2008
PLIST,     9, PSHEAR, 2009
PLIST,    10, PSHEAR, 2010
PLIST,    11, PSHEAR, 2011
PLIST,    12, PSHEAR, 2012
ENDDATA
```

Figure 48. Input Data Stream for the Multidisciplinary Wing (Concluded)

The SPC entries for the first boundary condition cantilever the structural box at the root (GRID points 1 to 6) and constrain all rotational degrees of freedom at the remaining structural nodes. In addition, all the degrees of freedom for the spline points are constrained except for the out-of-plane translations that are needed for the spline. The second boundary condition has a very similar set of single point constraints except that the root degrees of freedom are left free to translate in the x-z plane so that they may be used in the multipoint constraint relationships defining the structural pitch and plunge modes about GRID 45. Also, GRID 45 is left unrestrained in the rotation about the y-axis and for translations in the z-direction so that these two degrees of freedom may be supported by the SUPORT bulk data entry. Note that the Solution Control refers to a SUPPORT condition which references the SUPORT bulk data entry. NASTRAN compatibility has dictated a retention of the shortened spelling for the bulk data entry, but this form was not used elsewhere in ASTROS.

The remainder of the boundary condition definitions are the ASET1 bulk data entries to define the Guyan reductions. For both boundary conditions, the out-of-plane translations at the free structural nodes are retained. For the second boundary condition, the out-of-plane translations for the leading and trailing edge root nodes are also retained in the analysis set as well as the support point degrees of freedom. In the first boundary condition, these degrees of freedom are restrained by SPC entries.

Following the boundary condition definitions, the structural model is defined. These input entries do not contain any special design dependent data and are, therefore, identical to their NASTRAN counterparts. The non-structural mass appears in this section of the input stream, with 20 pounds of mass associated with all the structural nodes except the chordwise strip at the tip. At this span station, 40 pounds are applied to each structural node and to the two extra nodes that are connected to the structural box via the multi-point constraint relations. Finally, CONM2 Element 51001 defines the mass and inertia of the fuselage and is connected to the support point with an offset to place it at approximately the quarter-chord of the wing root.

Two identical material properties are defined using the MAT1 entry. The first, MAT1/90, is used for the substructure elements and the second, MAT1/91, is used for the skin elements. Two material properties are used

because the stress constraints are only applied to the skins and not to the substructure. MAT1/91, therefore, contains the material stress allowables and is then referenced on a DCONSTR bulk data entry which selects that a von Mises stress criteria be applied to the elements connected to MAT1/91. Associated with the mass model is a CONVERT/MASS bulk data entry which converts the mass and material density values in the input stream (which are in pounds weight) to the proper mass units. The conversion is required for all the analysis disciplines since even the static aeroelastic analysis involves an unrestrained structure having inertial properties.

The eigenvalue extraction method selected in the definition of the first boundary condition is defined by EIGR entry 99. It selects that the eigenvectors for the first five normal modes be computed. The flutter analysis discipline always requires that the eigenvalue extraction method be specified in the boundary condition, since only a modal formulation of the flutter equation is supported. In this particular test case, however, the EIGR entry is also required by the MODES discipline. Note that the same eigenvalue extraction applies to both disciplines and that, should the normal modes analysis not be specified, the flutter discipline would automatically invoke it.

The next section of the Bulk Data packet is the definition of the steady aerodynamics model for the static aeroelastic analysis discipline. A steady lifting surface macroelement is defined by a combination of one or more AIRFOIL entries and a CAERO6 entry, all sharing the same element identification number. In this case, there are two macroelements: the wing with ID 5000 and the tail (CANARD) with ID 6000. The configuration of both macroelements is defined by two AIRFOIL entries each, both referring to AEFACT entries 5101 and 5102 to define the airfoil shapes via a set of chordwise cuts and thicknesses, respectively. Note that, since the "airfoil" is a flat plate, the thickness is zero at all points.

The CAERO6 entries for the two macroelements also refer to a pair of AEFACT entries. These entries define the paneling divisions rather than the geometry divisions defined in the AIRFOIL entries. The four AEFACT entries (5001 and 5002 for the WING and 6001 and 6002 for the CANARD) define the chordwise and spanwise cuts, respectively. One subtle point is that the chordwise cuts are given in percent chord while the spanwise division points are given as physical dimensions. Finally, the tail surface has an AESURF

entry associated with it which defines the elevator control surface. The control surface connection is made by the reference to the CAERO6 macroelement on the AESURF entry with the control surface defined by naming the inboard leading edge and the outboard trailing edge boxes that lie on the surface. Since the box numbering begins with the macroelement identification number and then increases along chordwise strips from leading to trailing edge, inboard to outboard, identifying two boxes is sufficient to define any rectangular set of boxes on the macroelement. In this case, the last two chordwise boxes (of five) in each strip are desired so Boxes 6003 and 6049 are used to define the elevator.

The aerodynamic forces are connected to the structural degrees of freedom through the use of two SPLINE1 surface splines. The spline identification number has no meaning in ASTROS and is used only for error messages. The connection of a surface spline to an aerodynamic macroelement is made just as for the AESURF entry previously described. The same is also true of the region within the macroelement to which a particular spline applies. Therefore, any number of splines may be defined for a single macroelement, each of which connects the aerodynamic boxes in that region to the set of structural points that are named on field seven of the SPLINE1 entry. In this case, one spline is used for the inboard half and one for the outboard half of the wing. Note that there is significant overlap in the set of structural nodes to which the two splines interpolate the aerodynamic forces. There are no restrictions as to how to name the associated grid points, although there can be problems in the spline computations if the grid points are coincident when projected onto the macroelement plane.

An ATTACH entry (ID 16000) is used to connect the tail forces to GRID 45 of the structure. Unlike the spline, the ATTACH is merely an equivalent force transfer rather than an interpolation. In this case, the forces are attached to the support point so no aeroelastic effects will be seen. The ATTACH is most useful when the aerodynamic element does not have any associated structure, although aeroelastic effects could be modeled if a flexible fuselage were available to which the tail forces could be attached.

The steady aerodynamics data are completed with the next two bulk data entries. The AEROS entry defines the reference aerodynamic data that are used to nondimensionalize the stability derivatives. The reference chord

length, wing span and wing area are given for the full configuration since ASTROS automatically adjusts the stability coefficients to account for the half model. Also, the reference span is not used or required for the symmetric analyses in this sample problem, but is included for completeness. The TRIM bulk data entry defines the trim condition to be used in the steady aeroelastic analysis and is referenced by the Solution Control for the SAERO discipline. It defines the Mach number, the dynamic pressure (in consistent units), the symmetry in the x-z plane and the trim type. In this case, the Mach number and dynamic pressure correspond to the required flight condition and the symmetry and trim types are such that a symmetric two degree of freedom trim is performed. In order to perform the two degree of freedom trim, the load factor (NZ), velocity and the pitch rate that corresponds to that load factor and velocity are also required inputs on the TRIM entry. These seemingly redundant inputs are needed because ASTROS does not make any assumptions about the value of the local gravitational acceleration.

The unsteady aerodynamics model follows the steady model in the Bulk Data packet. The geometry and paneling data for the single macroelement are defined on the CAERO1 bulk data entry. This particular problem uses equal chordwise and spanwise divisions to create the 50 boxes. Two splines are used for the aerodynamic/structural interconnection, using the same sets of structural nodes as for the steady model and an equivalent division of aerodynamic boxes between the splines. The AERO bulk data entry is the unsteady equivalent of the AEROS entry and gives the reference chord and the reference density. The density must be input in consistent mass units. Equally important is that the reduced frequency in ASTROS is defined to be nondimensionalized by the reference semi-chord (as is standard practice). This means that the reference chord on the AERO entry will be divided by two in the computation of the reduced frequency values. This becomes important in the selection of the "hard point" reduced frequencies at which the unsteady aerodynamic forces are computed. If the hard point reduced frequencies lie too far from the values required by the p-k flutter analysis, ASTROS may give warnings or even terminate due to a perceived lack of quality in the resultant interpolation/extrapolation of the aerodynamic terms. The MKAERO1 entry is used to select the set of Mach numbers, symmetries and reduced frequencies for which the unsteady aerodynamic influence coefficients are computed. In this case, a single symmetric case at Mach 0.80 is selected for a set of six reduced

frequencies ranging from 0.05 to 3.0. In general, a set of approximately 10 reduced frequencies is adequate. These reduced frequencies should be chosen such that they span the range of reduced frequencies resulting from using the maximum and minimum natural frequencies in combination with the maximum and minimum velocities at which the flutter analysis is to be performed.

The FLUTTER bulk data entry and its referenced FLFACT entries define the flutter analysis condition. The FLUTTER entry selects the symmetry option and the set of Mach numbers. These values must correspond to some set of the aerodynamic matrices computed as a result of the MKAERO inputs. In this case, a single set of matrices were computed and FLUTTER entry 99 selects the entire set. FLFACT entries 97 and 98, referenced by the FLUTTER entry, select the density ratios and velocities for the flutter analyses. In this case, the analyses are done at sea level for velocities that range from 8000 in/sec to 11,000 in/sec. The required flutter speed is included explicitly in this list as 10,713.5 in/sec, with the higher velocity included to provide a safety margin. In general, many flutter "subcases" may be performed as either a combination of multiple Mach numbers, density ratios and velocities on a single FLUTTER entry or as multiple conditions on multiple FLUTTER entries. This allows the user complete freedom in choosing the combinations of Mach number, density ratio and velocity to be analyzed in a single boundary condition from which a match point analysis can be performed.

The final set of bulk data inputs define the design model. The only new input for this sample case is the DCONFLT entry. This input entry defines a table of velocities and required damping values. ASTROS performs a linear interpolation/extrapolation on this table to determine the constraint value for the velocities actually used in the flutter analyses. Again, the velocities must be entered in the same units as on the FLFACT entries for the flutter analysis. One subtle input on the DCONFLT entry is the GFACT value in field three. This value defaults to 0.10 and is used to scale the constraint value. This value can become an important tool to modify the active constraint selection in that a small value tends to spread the flutter constraints along the real number line. This, in turn, can be helpful in avoiding the retention of a large number of negatively damped flutter roots that are numerically more "active" than some constraints from other disciplines (e.g., stress/strain constraints). In this particular sample case, the

default GFACT value is adequate and the required damping table is a simple two entries to place the required damping at zero for all velocities.

4.6.3 Results and Output Description

Figure 49 presents the design iteration histories for the strength alone, strength and frequency and the full multidisciplinary sample problem. As one would expect, the model with only static aeroelastic strength constraints of Figure 49(a) results in the lightest design with a final objective function value of 996.8 pounds. Equally unsurprising is the continued pattern of higher weight for each additional constraint type that is added. The objective function values are 1331.5 pounds after adding the frequency constraint (Figure 49(b)) and 2301.0 pounds after further adding the flutter constraint (Figure 49(c)).

These figures do not show, however, that the full optimization problem displays the characteristic that, at the final design, only the strength and frequency constraints are exactly satisfied. Only one flutter root is close to being active with a value of -0.093. Despite this fact, the full optimization problem converged to a weight almost 73 percent heavier than for the case without any flutter constraints. This result indicates the flutter constraints are driving the design despite the fact that no flutter constraints are critical at the final design.

The convergence behavior for this problem is particularly sensitive to the constraint values and to the optimization parameters. This may be due in part to the crudeness of the structural, aerodynamic and design models, but even this explanation appears inadequate. In this respect, it highlights the subtleties involved when multidisciplinary optimization is attempted. It often takes several passes before the proper set of optimization parameters are found which yield a solution to complex interdisciplinary optimization problems. ASTROS has a great deal of freedom to modify the internal MICRO-DOT and MAPOL parameters dealing with the optimization, but finding the correct set can be difficult. A case in point is the fact that the frequency constraint case shown in Figure 49(b) took 26 iterations to converge. It is likely that a smaller move limit following the third or fourth iteration would speed convergence considerably, although care must be taken to avoid premature convergence. Another possible modification to the full test case is to tighten the convergence criteria to determine if the problem is fully converged.

A S T R O S   D E S I G N   I T E R A T I O N   H I S T O R Y

ITERATION NUMBER	OBJECTIVE FUNCTION VALUE	NUMBER FUNCTION EVAL	NUMBER GRADIENT EVAL	NUMBER RETAINED CONSTRAINTS	NUMBER ACTIVE CONSTRAINTS	NUMBER VIOLATED CONSTRAINTS	NUMBER LOWER BOUNDS	NUMBER UPPER BOUNDS	APPROXIMATE PROBLEM CONVERGENCE
1	7.62098E+03	0	0	0	0	0	0	0	NOT CONVERGED
2	4.25121E+03	38	5	24	1	0	0	11	NOT CONVERGED
3	2.56909E+03	33	4	24	1	0	0	11	NOT CONVERGED
4	1.63787E+03	37	4	24	1	0	0	11	NOT CONVERGED
5	1.14031E+03	37	4	24	1	0	0	11	NOT CONVERGED
6	1.02267E+03	59	12	24	2	0	0	4	NOT CONVERGED
7	9.98570E+02	64	10	24	2	0	0	4	NOT CONVERGED
8	9.96773E+02	19	3	24	2	0	0	4	CONVERGED

THE FINAL OBJECTIVE FUNCTION VALUE IS:

FIXED = 3.08900E+04

\+ DESIGNED = 9.96773E+02

TOTAL = 3.18868E+04

(a) Static Aeroelastic Constraints Only

A S T R O S   D E S I G N   I T E R A T I O N   H I S T O R Y

ITERATION NUMBER	OBJECTIVE FUNCTION VALUE	NUMBER FUNCTION EVAL	NUMBER GRADIENT EVAL	NUMBER RETAINED CONSTRAINTS	NUMBER ACTIVE CONSTRAINTS	NUMBER VIOLATED CONSTRAINTS	NUMBER LOWER BOUNDS	NUMBER UPPER BOUNDS	APPROXIMATE PROBLEM CONVERGENCE
1	7.62098E+03	0	0	0	0	0	0	0	NOT CONVERGED
2	4.25621E+03	45	7	25	1	0	0	9	NOT CONVERGED
3	2.57152E+03	33	4	25	1	0	0	11	NOT CONVERGED
4	1.68193E+03	59	6	25	2	0	0	10	NOT CONVERGED
5	1.38892E+03	64	11	25	2	0	0	5	NOT CONVERGED
6	1.34069E+03	131	21	25	2	0	0	5	NOT CONVERGED
7	1.35093E+03	62	13	25	2	0	0	1	NOT CONVERGED
8	1.34300E+03	35	7	25	2	0	0	2	NOT CONVERGED
9	1.34752E+03	24	6	25	2	0	0	0	CONVERGED
10	1.33893E+03	27	5	25	2	0	0	1	NOT CONVERGED
11	1.34449E+03	20	4	25	2	0	0	0	CONVERGED
12	1.33561E+03	28	6	25	2	0	0	2	NOT CONVERGED
13	1.33756E+03	23	5	25	2	0	1	0	CONVERGED
14	1.33342E+03	22	5	25	2	0	0	1	CONVERGED
15	1.33345E+03	24	5	25	2	0	1	0	CONVERGED
16	1.32929E+03	22	5	25	2	0	0	2	CONVERGED
17	1.33056E+03	23	5	25	2	0	1	0	CONVERGED
18	1.32781E+03	17	5	25	3	0	0	1	CONVERGED
19	1.32967E+03	23	5	25	1	0	1	0	CONVERGED
20	1.32755E+03	22	5	25	2	0	0	1	CONVERGED
21	1.33055E+03	20	5	25	2	0	0	0	CONVERGED
22	1.32882E+03	20	5	25	2	0	0	1	CONVERGED
23	1.33051E+03	19	5	25	2	0	0	0	CONVERGED
24	1.32935E+03	22	4	25	2	0	0	1	CONVERGED
25	1.33034E+03	21	4	25	2	0	0	0	CONVERGED
26	1.33135E+03	7	2	25	2	0	0	0	CONVERGED

THE FINAL OBJECTIVE FUNCTION VALUE IS:

FIXED = 3.08900E+04

\+ DESIGNED = 1.33135E+03

TOTAL = 3.22214E+04

(b) Static Aeroelastic and Frequency Constraints

Figure 49. Design Iteration Histories for the Multidiscipinary Wing

ASTROS DESIGN ITERATION HISTORY

ITERATION NUMBER	OBJECTIVE FUNCTION VALUE	NUMBER FUNCTION EVAL	NUMBER GRADIENT EVAL	NUMBER RETAINED CONSTRAINTS	NUMBER ACTIVE CONSTRAINTS	NUMBER VIOLATED CONSTRAINTS	NUMBER LOWER BOUNDS	NUMBER UPPER BOUNDS	APPROXIMATE PROBLEM CONVERGENCE
1	7.62098E+03	0	0	0	0	0	0	0	NOT CONVERGED
2	5.32165E+03	72	6	39	2	0	0	7	NOT CONVERGED
3	3.10993E+03	33	4	39	1	0	0	11	NOT CONVERGED
4	3.20131E+03	85	9	39	2	0	2	2	NOT CONVERGED
5	2.95405E+03	45	9	39	2	0	0	2	NOT CONVERGED
6	2.72168E+03	29	7	39	2	0	0	1	NOT CONVERGED
7	2.59592E+03	27	6	39	2	0	0	2	NOT CONVERGED
8	2.48664E+03	26	7	39	3	0	0	2	NOT CONVERGED
9	2.37819E+03	22	6	39	3	0	0	2	NOT CONVERGED
10	2.30170E+03	24	6	39	3	0	0	2	NOT CONVERGED
11	2.30095E+03	6	2	39	2	0	0	2	CONVERGED

THE FINAL OBJECTIVE FUNCTION VALUE IS:

FIXED = 3.08900E+04
+ DESIGNED = 2.30095E+03

TOTAL = 3.31910E+04

(c) Static Aeroelastic, Frequency and Flutter Constraints

Figure 49. Design Iteration Histories for the Multidisciplinary Wing (Concluded)

This potentially attractive option yields the possibility that the problem will not be able to converge.

Despite, or maybe because of, its seeming simplicity, the multidisciplinary swept wing problem provides a great deal of insight into the treatment of multiple, multidisciplinary constraints in ASTROS. While the set of design constraints are completely arbitrary and the flight conditions are unrealistic, the test serves a useful function in demonstrating the features of ASTROS as well as the "art" of optimization.

4.7 THE INTERMEDIATE COMPLEXITY WING MODEL WITH STRENGTH CONSTRAINTS

This example problem, while performing optimization subject only to strength constraints, allows comparison with results obtained in FASTOP-3, another Air Force sponsored structural optimization code. The basic model is the same as that reported in AFFDL-TR-78-50, "FASTOP-3: A Strength, Deflection and Flutter Optimization Program for Metallic and Composite Structures," by J. Markowitz and G. Isakson. In addition, two other ASTROS cases based on this Intermediate Complexity Wing (ICW) model are presented to demonstrate the performance of the Fully Stressed Design (FSD) option in ASTROS and to compare alternative design variable linking schemes.

4.7.1 Problem Description

This example problem does not present any new constraint types, rather it represents a more realistic application of the strength constraints in ASTROS. It demonstrates, however, an additional feature of the ASTROS stress constraint in its application to composite elements. These constraints are more fully discussed in Subsection 5.3 of the Theoretical Manual.

The ICW structural model, shown in Figure 50, uses quadrilateral and triangular membrane elements to model the composite wing skins and shear panels to model the substructure. Rod elements are used as posts to complete the interconnection of the upper and lower surfaces. All the cases use a cantilevered boundary condition at the root and constrain all rotational degrees of freedom at each node. The substructure material is modeled as aluminum, while the wing skins are made of a graphite/epoxy composite. Table 6 shows the material properties, gauge limits and stress allowables for these two materials.

TABLE 6. MATERIAL PROPERTIES FOR THE INTERMEDIATE COMPLEXITY WING

ISOTROPIC MATERIAL		
$E = 10.5 \times 10^6$ psi		$\rho = 0.10$ lb/in^3
$\nu = 0.30$		$t_{min} = 0.02$ in
	$\sigma_T \leq 67$ ksi	
	$\sigma_c \leq 57$ ksi	
	$\tau_{xy} \leq 39$ ksi	
ORTHROTROPIC MATERIAL		
$E_1 = 18.5 \times 10^6$ psi		$\rho = 0.055$ lb/in^3
$E_2 = 1.6 \times 10^6$ psi		$t_{min} = 0.00525$
	$\nu_{12} = 0.25$	
	$G_{12} = 0.65 \times 10^6$ psi	
	$\lvert\sigma_x\rvert \leq 115$ ksi	
	$\lvert\sigma_y\rvert \leq 115$ ksi	

No. of Nodes	No. of Elements		No. of DOF's	
88	39	Rods	294	Constrained
	55	Shear Panels	234	Unconstrained
	62	Quadrilateral Membrane	528	Total
	2	Triangular Membrane		
	158	Total		

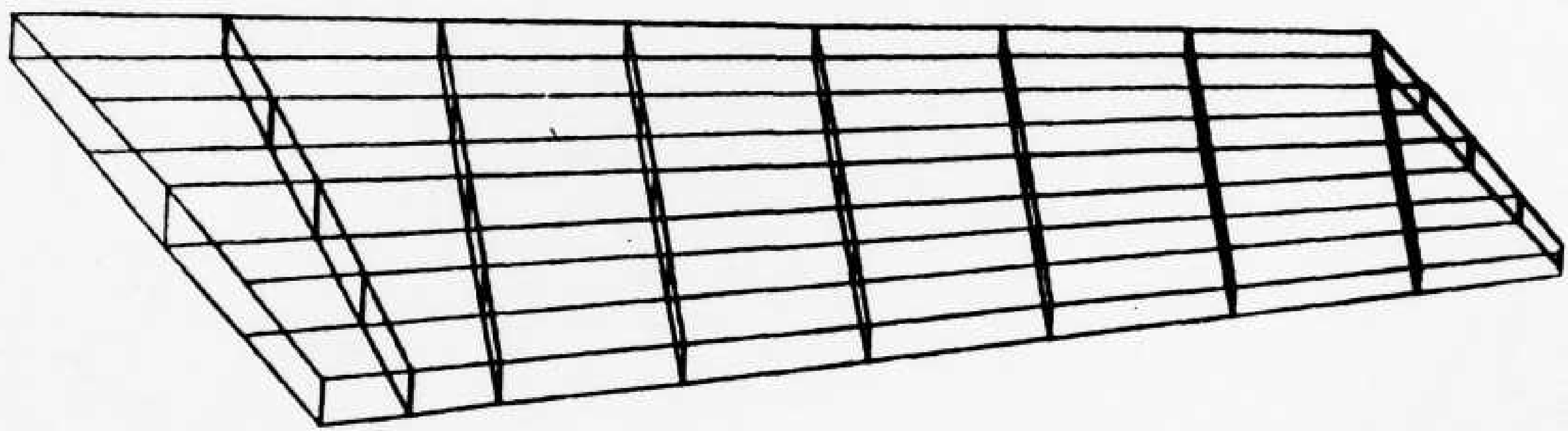

Figure 50. The Structural Model for the Intermediate Complexity Wing

The design problem minimizes the weight subject to the material stress allowables and gauge constraints under two static loads representing a subsonic and a supersonic air load. The load conditions in ASTROS are NASTRAN static loads equivalent to the original FASTOP loading conditions. The original design model was developed to emulate FASTOP with the recognition that the load cases were such that the optimum design would be symmetric about the mid-plane and that the FASTOP design resulted in minimum gauge thicknesses for all the rib shear elements. Consequently, the upper and lower skin surface layers of the same ply orientation for each quadrilateral or triangular membrane element are linked, resulting in 128 global design variables for the skins. The 23 shear panels representing the spars are each given a separate global design variable and the posts and the rib shear panels are each linked as two additional variables for a total of 153 global design variables. This design linking scheme is such that the ASTROS result and the FASTOP result can be directly compared.

In addition to the FASTOP comparison, two related cases are discussed in this subsection. The first utilizes the identical structural model and design model, but uses the ASTROS FSD option to perform a number of FSD resizing cycles prior to reverting to mathematical programming methods. The second additional case uses the same structural model and load cases, but utilizes a completely different design model in which the global design variables controlling the composite skin and spar shear panel thicknesses are shape functions. Shape functions were employed to produce a design that more nearly approximates manufacturing limits and to ease the design task by reducing the number of global variables. A total of 22 shape function design variables were used:

4 variables	-	A uniform thickness over the wing surface for each ply orientation
4 variables	-	A chordwise linear taper over the wing surface for each ply orientation
4 variables	-	A spanwise linear taper over the wing surface for each ply orientation
4 variables	-	A spanwise quadratic taper over the wing surface for each ply orientation

3 variables - A uniform thickness over the length of the leading edge, mid-chord and trailing edge spars, respectively

3 variables - A linear taper over the length of the leading edge, mid-chord and trailing edge spars, respectively

with the posts and ribs remaining physically linked to two additional global design variables, as in the original design model.

4.7.1 Input Description

Figure 51 shows the input for the "FASTOP" version of this example. In this sample problem, a MAPOL packet is included in the input stream to make minor modifications to the standard executive sequence. The packet is initiated with the EDIT NOLIST command line which informs the system that the remainder of the packet is a set of edit operations to be applied to the standard sequence and that the resultant executive sequence is not to be echoed to the output. The first edit is a REPLACE of the call to the Input File Processor (IFP) in order to suppress the output echo of the bulk data packet. The second edit operation is a REPLACE to redefine the NRFAC constraint retention parameter. This parameter is used by the ACTCON module to determine the number of constraints to retain for the sensitivity phase of the optimization loop. The default value of this parameter is 3.0, which causes a minimum of three times the number of global design variables constraints to be retained. Since this example has 153 design variables, an NRFAC value of three causes retention of more constraints that are necessary to adequately define the optimization problem at each iteration. Therefore, the NRFAC value is reduced to 1.0 so that a minimum of 153 constraints are retained at each iteration. This value results in a more efficient, yet, equally effective, sensitivity phase. Although there are no encoded restrictions in ASTROS and each design problem presents unique demands in tailoring the optimization parameters, experience with ASTROS indicates that 100 to 200 constraints are adequate in mathematical programming methods. When the number of design variables is 50 or less, the default value should be adequate.

The solution control packet contains only an optimization subpacket, starting with the OPTIMIZE command, which has a single boundary condition with two static analyses. No specific design constraints are selected by either

```
ASSIGN DATABASE ICWCU PASS NEW DELETE
EDIT NOLIST
REPLACE 191
  CALL IFP (GSIZE,,1);
REPLACE 758
  NRFAC := 1.0;
SOLUTION
TITLE = INTERMEDIATE COMPLEXITY WING
SUBTIT = QUAD4 ELEMENTS WITH 153 DESIGN VARIABLES
OPTIMIZE STRATEGY = 57
 PRINT DCON
   BOUNDARY SPC = 1
      STATICS ( MECH = 1  )
      STATICS ( MECH = 2  )
      LABEL = COMPOSITE STRUCTURE WITH FIBER ORIENTATIONS (0,90,+45,-45)
END
BEGIN BULK
MPPARM, DABOBJ, 0.01, DELOBJ, 0.0001, CTLMIN, 0.0001, STOL, 0.0001, +ADSPAR
+ADSPAR, ITRMOP, 6, ITMAX, 75
$
$ BULK DATA FOR INTERMEDIATE COMPLEXITY WING
$
GRID           1        63.5000 90.0000 1.1250
GRID           2        63.5000 90.0000 -1.1250
GRID           3        70.8330 90.0000 1.3130
GRID           4        70.8330 90.0000 -1.3130
GRID           5        78.1670 90.0000 1.5000
GRID           6        78.1670 90.0000 -1.5000
GRID           7        85.5000 90.0000 1.3130
GRID           8        85.5000 90.0000 -1.3130
GRID           9        92.8330 90.0000 1.1250
GRID          10        92.8330 90.0000 -1.1250
GRID          11        69.6860 87.4710 1.3490
GRID          12        69.6860 87.4710 -1.3490
GRID          13        76.0970 84.8510 1.5860
GRID          14        76.0970 84.8510 -1.5860
GRID          15        82.7460 82.1330 1.4270
GRID          16        82.7460 82.1330 -1.4270
GRID          17        89.6470 79.3120 1.2590
GRID          18        89.6470 79.3120 -1.2590
GRID          19        57.2660 77.6690 1.2790
GRID          20        57.2660 77.6690 -1.2790
GRID          21        63.9920 74.9200 1.5320
GRID          22        63.9920 74.9200 -1.5320
GRID          23        70.9620 72.0710 1.7990
GRID          24        70.9620 72.0710 -1.7990
GRID          25        78.1910 69.1160 1.6170
GRID          26        78.1910 69.1160 -1.6170
GRID          27        85.6920 66.0500 1.4240
GRID          28        85.6920 66.0500 -1.4240
GRID          29        51.0320 65.3390 1.4330
GRID          30        51.0320 65.3390 -1.4330
GRID          31        58.2970 62.3690 1.7150
GRID          32        58.2970 62.3690 -1.7150
GRID          33        65.8260 59.2910 2.0120
GRID          34        65.8260 59.2910 -2.0120
GRID          35        73.6350 56.1000 1.8070
GRID          36        73.6350 56.1000 -1.8070
GRID          37        81.7380 52.7870 1.5900
GRID          38        81.7380 52.7870 -1.5900
GRID          39        44.7990 53.0080 1.5870
GRID          40        44.7990 53.0080 -1.5870
GRID          41        52.6030 49.8180 1.8980
GRID          42        52.6030 49.8180 -1.8980
GRID          43        60.6910 46.5120 2.2250
GRID          44        60.6910 46.5120 -2.2250
GRID          45        69.0790 43.0830 1.9970
GRID          46        69.0790 43.0830 -1.9970
GRID          47        77.7840 39.5250 1.7560
GRID          48        77.7840 39.5250 -1.7560
GRID          49        38.5650 40.6780 1.742
GRID          50        38.5650 40.6780 -1.7420
GRID          51        46.9080 37.2670 2.0820
```

Figure 51. Input Data Stream for the Intermediate Complexity Wing

```
GRID        52       46.9080 37.2670 -2.0820
GRID        53       55.5550 33.7320 2.4380
GRID        54       55.5550 33.7320 -2.4380
GRID        55       64.5230 30.0670 2.1870
GRID        56       64.5230 30.0670 -2.1870
GRID        57       73.8300 26.2620 1.9220
GRID        58       73.8300 26.2620 -1.9220
GRID        59       32.3310 28.3470 1.8960
GRID        60       32.3310 28.3470 -1.8960
GRID        61       41.2140 24.7160 2.2650
GRID        62       41.2140 24.7160 -2.2650
GRID        63       50.4200 20.9530 2.6510
GRID        64       50.4200 20.9530 -2.6510
GRID        65       59.9670 17.0500 2.3760
GRID        66       59.9670 17.0500 -2.3760
GRID        67       69.8760 13.0000 2.0880
GRID        68       69.8760 13.0000 -2.0880
GRID        69       25.1660 14.1730 2.0730
GRID        70       25.1660 14.1730 -2.0730
GRID        71       35.5830 12.3040 2.4460
GRID        72       35.5830 12.3040 -2.4460
GRID        73       46.1810 10.4030 2.8270
GRID        74       46.1810 10.4030 -2.8270
GRID        75       56.9640 8.4690  2.5020
GRID        76       56.9640 8.4690  -2.5020
GRID        77       67.9380 6.5000  2.1690
GRID        78       67.9380 6.5000  -2.1690
GRID        79       18.0000 0.0000  2.2500
GRID        80       18.0000 0.0000  -2.2500
GRID        81       30.0000 0.0000  2.6250
GRID        82       30.0000 0.0000  -2.6250
GRID        83       42.0000 0.0000  3.0000
GRID        84       42.0000 0.0000  -3.0000
GRID        85       54.0000 0.0000  2.6250
GRID        86       54.0000 0.0000  -2.6250
GRID        87       66.0000 0.0000  2.2500
GRID        88       66.0000 0.0000  -2.2500
GRDSET                                                  456
SPC1, 1, 123, 79, THRU, 88
$
CROD       120  10001      1      2
CROD       121  10001      3      4
CROD       122  10001      5      6
CROD       123  10001      7      8
CROD       124  10001      9     10
CROD       125  10001     11     12
CROD       126  10001     13     14
CROD       127  10001     15     16
CROD       128  10001     17     18
CROD       129  10001     19     20
CROD       130  10001     21     22
CROD       131  10001     23     24
CROD       132  10001     25     26
CROD       133  10001     27     28
CROD       134  10001     29     30
CROD       135  10001     31     32
CROD       136  10001     33     34
CROD       137  10001     35     36
CROD       138  10001     37     38
CROD       139  10001     39     40
CROD       140  10001     41     42
CROD       141  10001     43     44
CROD       142  10001     45     46
CROD       143  10001     47     48
CROD       144  10001     49     50
CROD       145  10001     51     52
CROD       146  10001     53     54
CROD       147  10001     55     56
CROD       148  10001     57     58
CROD       149  10001     59     60
CROD       150  10001     61     62
CROD       151  10001     63     64
CROD       152  10001     65     66
```

Figure 51. Input Data Stream for the Intermediate Complexity Wing (Continued)

```
CROD        153  10001     67     68
CROD        154  10001     69     70
CROD        155  10001     71     72
CROD        156  10001     73     74
CROD        157  10001     75     76
CROD        158  10001     77     78
PROD      10001     10   1.00   0.00  0.000  0.000
$
CTRMEM        1  10001      1      3     11    101
CTRMEM        2  12001      2      4     12    101
CQUAD4        3  30001      3      5     13     11    101
CQUAD4        4  32001      4      6     14     12    101
CQUAD4        5  30002      5      7     15     13    101
CQUAD4        6  32002      6      8     16     14    101
CQUAD4        7  30003      7      9     17     15    101
CQUAD4        8  32003      8     10     18     16    101
CQUAD4        9  30004      1     11     21     19    101
CQUAD4       10  32004      2     12     22     20    101
CQUAD4       11  30005     11     13     23     21    101
CQUAD4       12  32005     12     14     24     22    101
CQUAD4       13  30006     13     15     25     23    101
CQUAD4       14  32006     14     16     26     24    101
CQUAD4       15  30007     15     17     27     25    101
CQUAD4       16  32007     16     18     28     26    101
CQUAD4       17  30008     19     21     31     29    101
CQUAD4       18  32008     20     22     32     30    101
CQUAD4       19  30009     21     23     33     31    101
CQUAD4       20  32009     22     24     34     32    101
CQUAD4       21  30010     23     25     35     33    101
CQUAD4       22  32010     24     26     36     34    101
CQUAD4       23  30011     25     27     37     35    101
CQUAD4       24  32011     26     28     38     36    101
CQUAD4       25  30012     29     31     41     39    101
CQUAD4       26  32012     30     32     42     40    101
CQUAD4       27  30013     31     33     43     41    101
CQUAD4       28  32013     32     34     44     42    101
CQUAD4       29  30014     33     35     45     43    101
CQUAD4       30  32014     34     36     46     44    101
CQUAD4       31  30015     35     37     47     45    101
CQUAD4       32  32015     36     38     48     46    101
CQUAD4       33  30016     39     41     51     49    101
CQUAD4       34  32016     40     42     52     50    101
CQUAD4       35  30017     41     43     53     51    101
CQUAD4       36  32017     42     44     54     52    101
CQUAD4       37  30018     43     45     55     53    101
CQUAD4       38  32018     44     46     56     54    101
CQUAD4       39  30019     45     47     57     55    101
CQUAD4       40  32019     46     48     58     56    101
CQUAD4       41  30020     49     51     61     59    101
CQUAD4       42  32020     50     52     62     60    101
CQUAD4       43  30021     51     53     63     61    101
CQUAD4       44  32021     52     54     64     62    101
CQUAD4       45  30022     53     55     65     63    101
CQUAD4       46  32022     54     56     66     64    101
CQUAD4       47  30023     55     57     67     65    101
CQUAD4       48  32023     56     58     68     66    101
CQUAD4       49  30024     59     61     71     69    101
CQUAD4       50  32024     60     62     72     70    101
CQUAD4       51  30025     61     63     73     71    101
CQUAD4       52  32025     62     64     74     72    101
CQUAD4       53  30026     63     65     75     73    101
CQUAD4       54  32026     64     66     76     74    101
CQUAD4       55  30027     65     67     77     75    101
CQUAD4       56  32027     66     68     78     76    101
CQUAD4       57  30028     69     71     81     79    101
CQUAD4       58  32028     70     72     82     80    101
CQUAD4       59  30029     71     73     83     81    101
CQUAD4       60  32029     72     74     84     82    101
CQUAD4       61  30030     73     75     85     83    101
CQUAD4       62  32030     74     76     86     84    101
CQUAD4       63  30031     75     77     87     85    101
CQUAD4       64  32031     76     78     88     86    101
PCOMP     10001 -.0105    0.0 0.65E6   TSAI .00525            MEM    +CMD1
```

Figure 51. Input Data Stream for the Intermediate Complexity Wing (Continued)

```
+CMD1        70 1.000   0.0    YES     70    1.000    90.    YES   +CMDA1
+CMDA1       70 1.000   45.    YES     70    1.000    -45.    YES
PCOMP     12001 -.0105  0.0    0.65E6  TSAI  .00525          MEM   +CMD1
+CMD1        72 1.000   0.0    YES     72    1.000    90.    YES   +CMDA1
+CMDA1       72 1.000   45.    YES     72    1.000    -45.    YES
PCOMP     30001 -.0105  0.0    0.65E6  TSAI  .00525          MEM   +CM01
+CM01        70 1.000   0.0    YES     70    1.000    90.    YES   +CMA1
+CMA1        70 1.000   45.    YES     70    1.000    -45.    YES
PCOMP     32001 -.0105  0.0    0.65E6  TSAI  .00525          MEM   +CM02
+CM02        72 1.000   0.0    YES     72    1.000    90.    YES   +CMA2
+CMA2        72 1.000   45.    YES     72    1.000    -45.    YES
PCOMP     30002 -.0105  0.0    0.65E6  TSAI  .00525          MEM   +CM03
+CM03        70 1.000   0.0    YES     70    1.000    90.    YES   +CMA3
+CMA3        70 1.000   45.    YES     70    1.000    -45.    YES
PCOMP     32002 -.0105  0.0    0.65E6  TSAI  .00525          MEM   +CM04
+CM04        72 1.000   0.0    YES     72    1.000    90.    YES   +CMA4
+CMA4        72 1.000   45.    YES     72    1.000    -45.    YES
PCOMP     30003 -.0105  0.0    0.65E6  TSAI  .00525          MEM   +CM05
+CM05        70 1.000   0.0    YES     70    1.000    90.    YES   +CMA5
+CMA5        70 1.000   45.    YES     70    1.000    -45.    YES
PCOMP     32003 -.0105  0.0    0.65E6  TSAI  .00525          MEM   +CM06
+CM06        72 1.000   0.0    YES     72    1.000    90.    YES   +CMA6
+CMA6        72 1.000   45.    YES     72    1.000    -45.    YES
PCOMP     30004 -.0105  0.0    0.65E6  TSAI  .00525          MEM   +CM07
+CM07        70 1.000   0.0    YES     70    1.000    90.    YES   +CMA7
+CMA7        70 1.000   45.    YES     70    1.000    -45.    YES
PCOMP     32004 -.0105  0.0    0.65E6  TSAI  .00525          MEM   +CM08
+CM08        72 1.000   0.0    YES     72    1.000    90.    YES   +CMA8
+CMA8        72 1.000   45.    YES     72    1.000    -45.    YES
PCOMP     30005 -.0105  0.0    0.65E6  TSAI  .00525          MEM   +CM09
+CM09        70 1.000   0.0    YES     70    1.000    90.    YES   +CMA9
+CMA9        70 1.000   45.    YES     70    1.000    -45.    YES
PCOMP     32005 -.0105  0.0    0.65E6  TSAI  .00525          MEM   +CM10
+CM10        72 1.000   0.0    YES     72    1.000    90.    YES   +CMA10
+CMA10       72 1.000   45.    YES     72    1.000    -45.    YES
PCOMP     30006 -.0105  0.0    0.65E6  TSAI  .00525          MEM   +CM11
+CM11        70 1.000   0.0    YES     70    1.000    90.    YES   +CMA11
+CMA11       70 1.000   45.    YES     70    1.000    -45.    YES
PCOMP     32006 -.0105  0.0    0.65E6  TSAI  .00525          MEM   +CM12
+CM12        72 1.000   0.0    YES     72    1.000    90.    YES   +CMA12
+CMA12       72 1.000   45.    YES     72    1.000    -45.    YES
PCOMP     30007 -.0105  0.0    0.65E6  TSAI  .00525          MEM   +CM13
+CM13        70 1.000   0.0    YES     70    1.000    90.    YES   +CMA13
+CMA13       70 1.000   45.    YES     70    1.000    -45.    YES
PCOMP     32007 -.0105  0.0    0.65E6  TSAI  .00525          MEM   +CM14
+CM14        72 1.000   0.0    YES     72    1.000    90.    YES   +CMA14
+CMA14       72 1.000   45.    YES     72    1.000    -45.    YES
PCOMP     30008 -.0105  0.0    0.65E6  TSAI  .00525          MEM   +CM15
+CM15        70 1.000   0.0    YES     70    1.000    90.    YES   +CMA15
+CMA15       70 1.000   45.    YES     70    1.000    -45.    YES
PCOMP     32008 -.0105  0.0    0.65E6  TSAI  .00525          MEM   +CM16
+CM16        72 1.000   0.0    YES     72    1.000    90.    YES   +CMA16
+CMA16       72 1.000   45.    YES     72    1.000    -45.    YES
PCOMP     30009 -.0105  0.0    0.65E6  TSAI  .00525          MEM   +CM17
+CM17        70 1.000   0.0    YES     70    1.000    90.    YES   +CMA17
+CMA17       70 1.000   45.    YES     70    1.000    -45.    YES
PCOMP     32009 -.0105  0.0    0.65E6  TSAI  .00525          MEM   +CM18
+CM18        72 1.000   0.0    YES     72    1.000    90.    YES   +CMA18
+CMA18       72 1.000   45.    YES     72    1.000    -45.    YES
PCOMP     30010 -.0105  0.0    0.65E6  TSAI  .00525          MEM   +CM19
+CM19        70 1.000   0.0    YES     70    1.000    90.    YES   +CMA19
+CMA19       70 1.000   45.    YES     70    1.000    -45.    YES
PCOMP     32010 -.0105  0.0    0.65E6  TSAI  .00525          MEM   +CM20
+CM20        72 1.000   0.0    YES     72    1.000    90.    YES   +CMA20
+CMA20       72 1.000   45.    YES     72    1.000    -45.    YES
PCOMP     30011 -.0105  0.0    0.65E6  TSAI  .00525          MEM   +CM21
+CM21        70 1.000   0.0    YES     70    1.000    90.    YES   +CMA21
+CMA21       70 1.000   45.    YES     70    1.000    -45.    YES
PCOMP     32011 -.0105  0.0    0.65E6  TSAI  .00525          MEM   +CM22
+CM22        72 1.000   0.0    YES     72    1.000    90.    YES   +CMA22
+CMA22       72 1.000   45.    YES     72    1.000    -45.    YES
PCOMP     30012 -.0105  0.0    0.65E6  TSAI  .00525          MEM   +CM23
+CM23        70 1.000   0.0    YES     70    1.000    90.    YES   +CMA23
```

Figure 51. Input Data Stream for the Intermediate Complexity Wing (Continued)

```
+CMA23      70 1.000   45.    YES    70    1.000    -45.    YES
PCOMP    32012 -.0105  0.0   0.65E6  TSAI  .00525           MEM    +CM24
+CM24       72 1.000   0.0    YES    72    1.000    90.     YES    +CMA24
+CMA24      72 1.000   45.    YES    72    1.000    -45.    YES
PCOMP    30013 -.0105  0.0   0.65E6  TSAI  .00525           MEM    +CM25
+CM25       70 1.000   0.0    YES    70    1.000    90.     YES    +CMA25
+CMA25      70 1.000   45.    YES    70    1.000    -45.    YES
PCOMP    32013 -.0105  0.0   0.65E6  TSAI  .00525           MEM    +CM27
+CM27       72 1.000   0.0    YES    72    1.000    90.     YES    +CMA27
+CMA27      72 1.000   45.    YES    72    1.000    -45.    YES
PCOMP    30014 -.0105  0.0   0.65E6  TSAI  .00525           MEM    +CM28
+CM28       70 1.000   0.0    YES    70    1.000    90.     YES    +CMA28
+CMA28      70 1.000   45.    YES    70    1.000    -45.    YES
PCOMP    32014 -.0105  0.0   0.65E6  TSAI  .00525           MEM    +CM29
+CM29       72 1.000   0.0    YES    72    1.000    90.     YES    +CMA29
+CMA29      72 1.000   45.    YES    72    1.000    -45.    YES
PCOMP    30015 -.0105  0.0   0.65E6  TSAI  .00525           MEM    +CM30
+CM30       70 1.000   0.0    YES    70    1.000    90.     YES    +CMA30
+CMA30      70 1.000   45.    YES    70    1.000    -45.    YES
PCOMP    32015 -.0105  0.0   0.65E6  TSAI  .00525           MEM    +CM31
+CM31       72 1.000   0.0    YES    72    1.000    90.     YES    +CMA31
+CMA31      72 1.000   45.    YES    72    1.000    -45.    YES
PCOMP    30016 -.0105  0.0   0.65E6  TSAI  .00525           MEM    +CM32
+CM32       70 1.000   0.0    YES    70    1.000    90.     YES    +CMA32
+CMA32      70 1.000   45.    YES    70    1.000    -45.    YES
PCOMP    32016 -.0105  0.0   0.65E6  TSAI  .00525           MEM    +CM33
+CM33       72 1.000   0.0    YES    72    1.000    90.     YES    +CMA33
+CMA33      72 1.000   45.    YES    72    1.000    -45.    YES
PCOMP    30017 -.0105  0.0   0.65E6  TSAI  .00525           MEM    +CM34
+CM34       70 1.000   0.0    YES    70    1.000    90.     YES    +CMA34
+CMA34      70 1.000   45.    YES    70    1.000    -45.    YES
PCOMP    32017 -.0105  0.0   0.65E6  TSAI  .00525           MEM    +CM35
+CM35       72 1.000   0.0    YES    72    1.000    90.     YES    +CMA35
+CMA35      72 1.000   45.    YES    72    1.000    -45.    YES
PCOMP    30018 -.0105  0.0   0.65E6  TSAI  .00525           MEM    +CM36
+CM36       70 1.000   0.0    YES    70    1.000    90.     YES    +CMA36
+CMA36      70 1.000   45.    YES    70    1.000    -45.    YES
PCOMP    32018 -.0105  0.0   0.65E6  TSAI  .00525           MEM    +CM37
+CM37       72 1.000   0.0    YES    72    1.000    90.     YES    +CMA37
+CMA37      72 1.000   45.    YES    72    1.000    -45.    YES
PCOMP    30019 -.0105  0.0   0.65E6  TSAI  .00525           MEM    +CMF36
+CMF36      70 1.000   0.0    YES    70    1.000    90.     YES    +CMFA36
+CMFA36     70 1.000   45.    YES    70    1.000    -45.    YES
PCOMP    32019 -.0105  0.0   0.65E6  TSAI  .00525           MEM    +CMF37
+CMF37      72 1.000   0.0    YES    72    1.000    90.     YES    +CMFA37
+CMFA37     72 1.000   45.    YES    72    1.000    -45.    YES
PCOMP    30020 -.0105  0.0   0.65E6  TSAI  .00525           MEM    +CM38
+CM38       70 1.000   0.0    YES    70    1.000    90.     YES    +CMA38
+CMA38      70 1.000   45.    YES    70    1.000    -45.    YES
PCOMP    32020 -.0105  0.0   0.65E6  TSAI  .00525           MEM    +CM39
+CM39       72 1.000   0.0    YES    72    1.000    90.     YES    +CMA39
+CMA39      72 1.000   45.    YES    72    1.000    -45.    YES
PCOMP    30021 -.0105  0.0   0.65E6  TSAI  .00525           MEM    +CM40
+CM40       70 1.000   0.0    YES    70    1.000    90.     YES    +CMA40
+CMA40      70 1.000   45.    YES    70    1.000    -45.    YES
PCOMP    32021 -.0105  0.0   0.65E6  TSAI  .00525           MEM    +CM41
+CM41       72 1.000   0.0    YES    72    1.000    90.     YES    +CMA41
+CMA41      72 1.000   45.    YES    72    1.000    -45.    YES
PCOMP    30022 -.0105  0.0   0.65E6  TSAI  .00525           MEM    +CM42
+CM42       70 1.000   0.0    YES    70    1.000    90.     YES    +CMA42
+CMA42      70 1.000   45.    YES    70    1.000    -45.    YES
PCOMP    32022 -.0105  0.0   0.65E6  TSAI  .00525           MEM    +CM43
+CM43       72 1.000   0.0    YES    72    1.000    90.     YES    +CMA43
+CMA43      72 1.000   45.    YES    72    1.000    -45.    YES
PCOMP    30023 -.0105  0.0   0.65E6  TSAI  .00525           MEM    +CM44
+CM44       70 1.000   0.0    YES    70    1.000    90.     YES    +CMA44
+CMA44      70 1.000   45.    YES    70    1.000    -45.    YES
PCOMP    32023 -.0105  0.0   0.65E6  TSAI  .00525           MEM    +CM45
+CM45       72 1.000   0.0    YES    72    1.000    90.     YES    +CMA45
+CMA45      72 1.000   45.    YES    72    1.000    -45.    YES
PCOMP    30024 -.0105  0.0   0.65E6  TSAI  .00525           MEM    +CM46
+CM46       70 1.000   0.0    YES    70    1.000    90.     YES    +CMA46
+CMA46      70 1.000   45.    YES    70    1.000    -45.    YES
```

Figure 51. Input Data Stream for the Intermediate Complexity Wing (Continued)

```
PCOMP     32024 -.0105  0.0   0.65E6   TSAI  .00525         MEM   +CM47
+CM47        72 1.000   0.0    YES     72     1.000   90.   YES   +CMA47
+CMA47       72 1.000   45.    YES     72     1.000  -45.   YES
PCOMP     30025 -.0105  0.0   0.65E6   TSAI  .00525         MEM   +CM48
+CM48        70 1.000   0.0    YES     70     1.000   90.   YES   +CMA48
+CMA48       70 1.000   45.    YES     70     1.000  -45.   YES
PCOMP     32025 -.0105  0.0   0.65E6   TSAI  .00525         MEM   +CM49
+CM49        72 1.000   0.0    YES     72     1.000   90.   YES   +CMA49
+CMA49       72 1.000   45.    YES     72     1.000  -45.   YES
PCOMP     30026 -.0105  0.0   0.65E6   TSAI  .00525         MEM   +CM50
+CM50        70 1.000   0.0    YES     70     1.000   90.   YES   +CMA50
+CMA50       70 1.000   45.    YES     70     1.000  -45.   YES
PCOMP     32026 -.0105  0.0   0.65E6   TSAI  .00525         MEM   +CM51
+CM51        72 1.000   0.0    YES     72     1.000   90.   YES   +CMA51
+CMA51       72 1.000   45.    YES     72     1.000  -45.   YES
PCOMP     30027 -.0105  0.0   0.65E6   TSAI  .00525         MEM   +CM52
+CM52        70 1.000   0.0    YES     70     1.000   90.   YES   +CMA52
+CMA52       70 1.000   45.    YES     70     1.000  -45.   YES
PCOMP     32027 -.0105  0.0   0.65E6   TSAI  .00525         MEM   +CM53
+CM53        72 1.000   0.0    YES     72     1.000   90.   YES   +CMA53
+CMA53       72 1.000   45.    YES     72     1.000  -45.   YES
PCOMP     30028 -.0105  0.0   0.65E6   TSAI  .00525         MEM   +CM54
+CM54        70 1.000   0.0    YES     70     1.000   90.   YES   +CMA54
+CMA54       70 1.000   45.    YES     70     1.000  -45.   YES
PCOMP     32028 -.0105  0.0   0.65E6   TSAI  .00525         MEM   +CM55
+CM55        72 1.000   0.0    YES     72     1.000   90.   YES   +CMA55
+CMA55       72 1.000   45.    YES     72     1.000  -45.   YES
PCOMP     30029 -.0105  0.0   0.65E6   TSAI  .00525         MEM   +CM56
+CM56        70 1.000   0.0    YES     70     1.000   90.   YES   +CMA56
+CMA56       70 1.000   45.    YES     70     1.000  -45.   YES
PCOMP     32029 -.0105  0.0   0.65E6   TSAI  .00525         MEM   +CM57
+CM57        72 1.000   0.0    YES     72     1.000   90.   YES   +CMA57
+CMA57       72 1.000   45.    YES     72     1.000  -45.   YES
PCOMP     30030 -.0105  0.0   0.65E6   TSAI  .00525         MEM   +CM58
+CM58        70 1.000   0.0    YES     70     1.000   90.   YES   +CMA58
+CMA58       70 1.000   45.    YES     70     1.000  -45.   YES
PCOMP     32030 -.0105  0.0   0.65E6   TSAI  .00525         MEM   +CM59
+CM59        72 1.000   0.0    YES     72     1.000   90.   YES   +CMA59
+CMA59       72 1.000   45.    YES     72     1.000  -45.   YES
PCOMP     30031 -.0105  0.0   0.65E6   TSAI  .00525         MEM   +CM60
+CM60        70 1.000   0.0    YES     70     1.000   90.   YES   +CMA60
+CMA60       70 1.000   45.    YES     70     1.000  -45.   YES
PCOMP     32031 -.0105  0.0   0.65E6   TSAI  .00525         MEM   +CM61
+CM61        72 1.000   0.0    YES     72     1.000   90.   YES   +CMA61
+CMA61       72 1.000   45.    YES     72     1.000  -45.   YES
$
CSHEAR       65   40001       1       2       4       3
CSHEAR       66   40001       3       4       6       5
CSHEAR       67   40001       5       6       8       7
CSHEAR       68   40001       7       8      10       9
CSHEAR       69   40001       1       2      12      11
CSHEAR       70   40001      11      12      14      13
CSHEAR       71   40001      13      14      16      15
CSHEAR       72   40001      15      16      18      17
CSHEAR       73   40001      19      20      22      21
CSHEAR       74   40001      21      22      24      23
CSHEAR       75   40001      23      24      26      25
CSHEAR       76   40001      25      26      28      27
CSHEAR       77   40001      29      30      32      31
CSHEAR       78   40001      31      32      34      33
CSHEAR       79   40001      33      34      36      35
CSHEAR       80   40001      35      36      38      37
CSHEAR       81   40001      39      40      42      41
CSHEAR       82   40001      41      42      44      43
CSHEAR       83   40001      43      44      46      45
CSHEAR       84   40001      45      46      48      47
CSHEAR       85   40001      49      50      52      51
CSHEAR       86   40001      51      52      54      53
CSHEAR       87   40001      53      54      56      55
CSHEAR       88   40001      55      56      58      57
CSHEAR       89   40001      59      60      62      61
CSHEAR       90   40001      61      62      64      63
CSHEAR       91   40001      63      64      66      65
```

Figure 51. Input Data Stream for the Intermediate Complexity Wing (Continued)

```
CSHEAR        92   40001      65      66      68      67
CSHEAR        93   40001      69      70      72      71
CSHEAR        94   40001      71      72      74      73
CSHEAR        95   40001      73      74      76      75
CSHEAR        96   40001      75      76      78      77
CSHEAR        97   40002       1       2      20      19
CSHEAR        98   40003      19      20      30      29
CSHEAR        99   40004      29      30      40      39
CSHEAR       100   40005      39      40      50      49
CSHEAR       101   40006      49      50      60      59
CSHEAR       102   40007      59      60      70      69
CSHEAR       103   40008      69      70      80      79
CSHEAR       104   40009       5       6      14      13
CSHEAR       105   40010      13      14      24      23
CSHEAR       106   40011      23      24      34      33
CSHEAR       107   40012      33      34      44      43
CSHEAR       108   40013      43      44      54      53
CSHEAR       109   40014      53      54      64      63
CSHEAR       110   40015      63      64      74      73
CSHEAR       111   40016      73      74      84      83
CSHEAR       112   40017       9      10      18      17
CSHEAR       113   40018      17      18      28      27
CSHEAR       114   40019      27      28      38      37
CSHEAR       115   40020      37      38      48      47
CSHEAR       116   40021      47      48      58      57
CSHEAR       117   40022      57      58      68      67
CSHEAR       118   40023      67      68      78      77
CSHEAR       119   40024      77      78      88      87
PSHEAR     40001      10 1.0
PSHEAR     40002      10 1.0                    0.02
PSHEAR     40003      10 1.0                    0.02
PSHEAR     40004      10 1.0                    0.02
PSHEAR     40005      10 1.0                    0.02
PSHEAR     40006      10 1.0                    0.02
PSHEAR     40007      10 1.0                    0.02
PSHEAR     40008      10 1.0                    0.02
PSHEAR     40009      10 1.0                    0.02
PSHEAR     40010      10 1.0                    0.02
PSHEAR     40011      10 1.0                    0.02
PSHEAR     40012      10 1.0                    0.02
PSHEAR     40013      10 1.0                    0.02
PSHEAR     40014      10 1.0                    0.02
PSHEAR     40015      10 1.0                    0.02
PSHEAR     40016      10 1.0                    0.02
PSHEAR     40017      10 1.0                    0.02
PSHEAR     40018      10 1.0                    0.02
PSHEAR     40019      10 1.0                    0.02
PSHEAR     40020      10 1.0                    0.02
PSHEAR     40021      10 1.0                    0.02
PSHEAR     40022      10 1.0                    0.02
PSHEAR     40023      10 1.0                    0.02
PSHEAR     40024      10 1.0                    0.02
$
CORD1R       101      84      83       6
MAT1          10 1.05E+[illegible] 4.04E+6 0.30000 0.10000 0.00000 0.00000 0.00000+MT3
+MT3     6.70E+4 5.70E+4 3.90E+4
MAT8          70 1.85E+7 1.60E+6 0.25000 0.65E6                           0.05500+MT5
+MT5     0.0     0.0     100.    1.15E+5 1.15E+5 1.15E+5 1.15E+5 1.0E+15
MAT8          72 1.85E+7 1.60E+6 0.25000 0.65E6                           0.05500+MT6
+MT6     0.0     0.0     100.    4500.0  3200.0
$
FORCE          1       1       0     1.0   205.0 -7380.0   926.0
FORCE          1       2       0     1.0  -205.0  7380.0   926.0
FORCE          1       3       0     1.0     0.0     0.0    29.0
FORCE          1       4       0     1.0     0.0     0.0    29.0
FORCE          1       5       0     1.0 -2800.0 -6960.0  1130.0
FORCE          1       6       0     1.0  2800.0  6960.0  1130.0
FORCE          1       7       0     1.0     0.0     0.0    90.9
FORCE          1       8       0     1.0     0.0     0.0    90.9
FORCE          1       9       0     1.0 -9870.0 -9780.0  1130.0
FORCE          1      10       0     1.0  9870.0  9780.0  1130.0
FORCE          1      11       0     1.0     0.0     0.0   178.0
FORCE          1      12       0     1.0     0.0     0.0   178.0
```

Figure 51. Input Data Stream for the Intermediate Complexity Wing (Continued)

FORCE	1	13	0	1.0	0.0	0.0	214.0
FORCE	1	14	0	1.0	0.0	0.0	214.0
FORCE	1	15	0	1.0	0.0	0.0	253.0
FORCE	1	16	0	1.0	0.0	0.0	253.0
FORCE	1	17	0	1.0	-5680.0	2320.0	1020.0
FORCE	1	18	0	1.0	5680.0	-2320.0	1020.0
FORCE	1	19	0	1.0	2310.0	-946.0	723.0
FORCE	1	20	0	1.0	-2310.0	946.0	723.0
FORCE	1	21	0	1.0	0.0	0.0	314.0
FORCE	1	22	0	1.0	0.0	0.0	314.0
FORCE	1	23	0	1.0	0.0	0.0	326.0
FORCE	1	24	0	1.0	0.0	0.0	326.0
FORCE	1	25	0	1.0	0.0	0.0	338.0
FORCE	1	26	0	1.0	0.0	0.0	338.0
FORCE	1	27	0	1.0	-4070.0	1660.0	902.0
FORCE	1	28	0	1.0	4070.0	-1660.0	902.0
FORCE	1	29	0	1.0	1740.0	-713.0	646.0
FORCE	1	30	0	1.0	-1740.0	713.0	646.0
FORCE	1	31	0	1.0	0.0	0.0	340.0
FORCE	1	32	0	1.0	0.0	0.0	340.0
FORCE	1	33	0	1.0	0.0	0.0	352.0
FORCE	1	34	0	1.0	0.0	0.0	352.0
FORCE	1	35	0	1.0	0.0	0.0	365.0
FORCE	1	36	0	1.0	0.0	0.0	365.0
FORCE	1	37	0	1.0	-4250.0	1740.0	974.0
FORCE	1	38	0	1.0	4250.0	-1740.0	974.0
FORCE	1	39	0	1.0	1820.0	-743.0	694.0
FORCE	1	40	0	1.0	-1820.0	743.0	694.0
FORCE	1	41	0	1.0	0.0	0.0	365.0
FORCE	1	42	0	1.0	0.0	0.0	365.0
FORCE	1	43	0	1.0	0.0	0.0	378.0
FORCE	1	44	0	1.0	0.0	0.0	378.0
FORCE	1	45	0	1.0	0.0	0.0	392.0
FORCE	1	46	0	1.0	0.0	0.0	392.0
FORCE	1	47	0	1.0	-4440.0	1820.0	1050.0
FORCE	1	48	0	1.0	4440.0	-1820.0	1050.0
FORCE	1	49	0	1.0	1890.0	-773.0	742.0
FORCE	1	50	0	1.0	-1890.0	773.0	742.0
FORCE	1	51	0	1.0	0.0	0.0	390.0
FORCE	1	52	0	1.0	0.0	0.0	390.0
FORCE	1	53	0	1.0	0.0	0.0	404.0
FORCE	1	54	0	1.0	0.0	0.0	404.0
FORCE	1	55	0	1.0	0.0	0.0	420.0
FORCE	1	56	0	1.0	0.0	0.0	420.0
FORCE	1	57	0	1.0	-4640.0	1900.0	1120.0
FORCE	1	58	0	1.0	4640.0	-1900.0	1120.0
FORCE	1	59	0	1.0	2290.0	-937.0	883.0
FORCE	1	60	0	1.0	-2290.0	937.0	883.0
FORCE	1	61	0	1.0	0.0	0.0	413.0
FORCE	1	62	0	1.0	0.0	0.0	413.0
FORCE	1	63	0	1.0	0.0	0.0	391.0
FORCE	1	64	0	1.0	0.0	0.0	391.0
FORCE	1	65	0	1.0	0.0	0.0	368.0
FORCE	1	66	0	1.0	0.0	0.0	368.0
FORCE	1	67	0	1.0	-3030.0	1240.0	804.0
FORCE	1	68	0	1.0	3030.0	-1240.0	804.0
FORCE	1	69	0	1.0	3070.0	-520.0	1040.0
FORCE	1	70	0	1.0	-3070.0	520.0	1040.0
FORCE	1	71	0	1.0	0.0	0.0	433.0
FORCE	1	72	0	1.0	0.0	0.0	433.0
FORCE	1	73	0	1.0	0.0	0.0	370.0
FORCE	1	74	0	1.0	0.0	0.0	370.0
FORCE	1	75	0	1.0	0.0	0.0	304.0
FORCE	1	76	0	1.0	0.0	0.0	304.0
FORCE	1	77	0	1.0	-1370.0	262.0	446.0
FORCE	1	78	0	1.0	1370.0	-262.0	446.0
FORCE	2	1	0	1.0	351.0	-12600.0	1530.0
FORCE	2	2	0	1.0	-351.0	12600.0	1530.0
FORCE	2	3	0	1.0	0.0	0.0	29.5
FORCE	2	4	0	1.0	0.0	0.0	29.5
FORCE	2	5	0	1.0	-2420.0	-6020.0	979.0
FORCE	2	6	0	1.0	2420.0	6020.0	979.0
FORCE	2	7	0	1.0	0.0	0.0	55.9

Figure 51. Input Data Stream for the Intermediate Complexity Wing (Continued)

```
FORCE         2       8       0     1.0     0.0     0.0    55.9
FORCE         2       9       0     1.0 -4020.0 -3980.0   474.0
FORCE         2      10       0     1.0  4020.0  3980.0   474.0
FORCE         2      11       0     1.0     0.0     0.0   194.0
FORCE         2      12       0     1.0     0.0     0.0   194.0
FORCE         2      13       0     1.0     0.0     0.0   175.0
FORCE         2      14       0     1.0     0.0     0.0   175.0
FORCE         2      15       0     1.0     0.0     0.0   157.0
FORCE         2      16       0     1.0     0.0     0.0   157.0
FORCE         2      17       0     1.0 -1600.0   653.0   325.0
FORCE         2      18       0     1.0  1600.0  -653.0   325.0
FORCE         2      19       0     1.0  5510.0 -2250.0  1550.0
FORCE         2      20       0     1.0 -5510.0  2250.0  1550.0
FORCE         2      21       0     1.0     0.0     0.0   347.0
FORCE         2      22       0     1.0     0.0     0.0   347.0
FORCE         2      23       0     1.0     0.0     0.0   270.0
FORCE         2      24       0     1.0     0.0     0.0   270.0
FORCE         2      25       0     1.0     0.0     0.0   213.0
FORCE         2      26       0     1.0     0.0     0.0   213.0
FORCE         2      27       0     1.0 -1210.0   496.0   311.0
FORCE         2      28       0     1.0  1210.0  -496.0   311.0
FORCE         2      29       0     1.0  3990.0 -1630.0  1310.0
FORCE         2      30       0     1.0 -3990.0  1630.0  1310.0
FORCE         2      31       0     1.0     0.0     0.0   375.0
FORCE         2      32       0     1.0     0.0     0.0   375.0
FORCE         2      33       0     1.0     0.0     0.0   291.0
FORCE         2      34       0     1.0     0.0     0.0   291.0
FORCE         2      35       0     1.0     0.0     0.0   230.0
FORCE         2      36       0     1.0     0.0     0.0   230.0
FORCE         2      37       0     1.0 -1270.0   518.0   336.0
FORCE         2      38       0     1.0  1270.0  -518.0   336.0
FORCE         2      39       0     1.0  4160.0 -1700.0  1410.0
FORCE         2      40       0     1.0 -4160.0  1700.0  1410.0
FORCE         2      41       0     1.0     0.0     0.0   402.0
FORCE         2      42       0     1.0     0.0     0.0   402.0
FORCE         2      43       0     1.0     0.0     0.0   313.0
FORCE         2      44       0     1.0     0.0     0.0   313.0
FORCE         2      45       0     1.0     0.0     0.0   247.0
FORCE         2      46       0     1.0     0.0     0.0   247.0
FORCE         2      47       0     1.0 -1320.0   541.0   361.0
FORCE         2      48       0     1.0  1320.0  -541.0   361.0
FORCE         2      49       0     1.0  4330.0 -1770.0  1500.0
FORCE         2      50       0     1.0 -4330.0  1770.0  1500.0
FORCE         2      51       0     1.0     0.0     0.0   430.0
FORCE         2      52       0     1.0     0.0     0.0   430.0
FORCE         2      53       0     1.0     0.0     0.0   334.0
FORCE         2      54       0     1.0     0.0     0.0   334.0
FORCE         2      55       0     1.0     0.0     0.0   264.0
FORCE         2      56       0     1.0     0.0     0.0   264.0
FORCE         2      57       0     1.0 -1380.0   565.0   386.0
FORCE         2      58       0     1.0  1380.0  -565.0   386.0
FORCE         2      59       0     1.0  5300.0 -2170.0  1820.0
FORCE         2      60       0     1.0 -5300.0  2170.0  1820.0
FORCE         2      61       0     1.0     0.0     0.0   458.0
FORCE         2      62       0     1.0     0.0     0.0   458.0
FORCE         2      63       0     1.0     0.0     0.0   326.0
FORCE         2      64       0     1.0     0.0     0.0   326.0
FORCE         2      65       0     1.0     0.0     0.0   233.0
FORCE         2      66       0     1.0     0.0     0.0   233.0
FORCE         2      67       0     1.0  -922.0   377.0   287.0
FORCE         2      68       0     1.0   922.0  -377.0   287.0
FORCE         2      69       0     1.0  7160.0 -1210.0  2180.0
FORCE         2      70       0     1.0 -7160.0  1210.0  2180.0
FORCE         2      71       0     1.0     0.0     0.0   484.0
FORCE         2      72       0     1.0     0.0     0.0   484.0
FORCE         2      73       0     1.0     0.0     0.0   310.0
FORCE         2      74       0     1.0     0.0     0.0   310.0
FORCE         2      75       0     1.0     0.0     0.0   194.0
FORCE         2      76       0     1.0     0.0     0.0   194.0
FORCE         2      77       0     1.0  -451.0    86.0   175.0
FORCE         2      78       0     1.0   451.0   -86.0   175.0
$
$ DESIGN CARDS
```

Figure 51. Input Data Stream for the Intermediate Complexity Wing (Continued)

```
$
DESVAR  33    0.02        0.10          RIBS
DESVAR  34    0.02        0.10          SHEAR1
DESVAR  35    0.02        0.10          SHEAR2
DESVAR  36    0.02        0.10          SHEAR3
DESVAR  37    0.02        0.10          SHEAR4
DESVAR  38    0.02        0.10          SHEAR5
DESVAR  39    0.02        0.10          SHEAR6
DESVAR  40    0.02        0.10          SHEAR7
DESVAR  41    0.02        0.10          SHEAR8
DESVAR  42    0.02        0.10          SHEAR9
DESVAR  43    0.02        0.10          SHEAR10
DESVAR  44    0.02        0.10          SHEAR11
DESVAR  45    0.02        0.10          SHEAR12
DESVAR  46    0.02        0.10          SHEAR13
DESVAR  47    0.02        0.10          SHEAR14
DESVAR  48    0.02        0.10          SHEAR15
DESVAR  49    0.02        0.10          SHEAR16
DESVAR  50    0.02        0.10          SHEAR17
DESVAR  51    0.02        0.10          SHEAR18
DESVAR  52    0.02        0.10          SHEAR19
DESVAR  53    0.02        0.10          SHEAR20
DESVAR  54    0.02        0.10          SHEAR21
DESVAR  55    0.02        0.10          SHEAR22
DESVAR  56    0.02        0.10          SHEAR23
DESVAR  57    0.02        0.10          POSTS
DESVAR  1101  0.00525     0.10    1     1TRMEM1
DESVAR  1102  0.00525     0.10    1     1CQUAD1
DESVAR  1103  0.00525     0.10    1     1CQUAD1
DESVAR  1104  0.00525     0.10    1     1CQUAD4
DESVAR  1105  0.00525     0.10    1     1CQUAD5
DESVAR  1106  0.00525     0.10    1     1CQUAD6
DESVAR  1107  0.00525     0.10    1     1CQUAD7
DESVAR  1108  0.00525     0.10    1     1CQUAD8
DESVAR  1109  0.00525     0.10    1     1CQUAD9
DESVAR  1110  0.00525     0.10    1     1CQUAD10
DESVAR  1111  0.00525     0.10    1     1CQUAD11
DESVAR  1112  0.00525     0.10    1     1CQUAD12
DESVAR  1113  0.00525     0.10    1     1CQUAD13
DESVAR  1114  0.00525     0.10    1     1CQUAD14
DESVAR  1115  0.00525     0.10    1     1CQUAD15
DESVAR  1116  0.00525     0.10    1     1CQUAD16
DESVAR  1117  0.00525     0.10    1     1CQUAD17
DESVAR  1118  0.00525     0.10    1     1CQUAD18
DESVAR  1119  0.00525     0.10    1     1CQUAD19
DESVAR  1120  0.00525     0.10    1     1CQUAD20
DESVAR  1121  0.00525     0.10    1     1CQUAD21
DESVAR  1122  0.00525     0.10    1     1CQUAD22
DESVAR  1123  0.00525     0.10    1     1CQUAD23
DESVAR  1124  0.00525     0.10    1     1CQUAD24
DESVAR  1125  0.00525     0.10    1     1CQUAD25
DESVAR  1126  0.00525     0.10    1     1CQUAD26
DESVAR  1127  0.00525     0.10    1     1CQUAD27
DESVAR  1128  0.00525     0.10    1     1CQUAD28
DESVAR  1129  0.00525     0.10    1     1CQUAD29
DESVAR  1130  0.00525     0.10    1     1CQUAD30
DESVAR  1131  0.00525     0.10    1     1CQUAD31
DESVAR  1132  0.00525     0.10    1     1CQUAD32
DESVAR  1201  0.00525     0.10    2     2TRMEM1
DESVAR  1202  0.00525     0.10    2     2CQUAD1
DESVAR  1203  0.00525     0.10    2     2CQUAD1
DESVAR  1204  0.00525     0.10    2     2CQUAD4
DESVAR  1205  0.00525     0.10    2     2CQUAD5
DESVAR  1206  0.00525     0.10    2     2CQUAD6
DESVAR  1207  0.00525     0.10    2     2CQUAD7
DESVAR  1208  0.00525     0.10    2     2CQUAD8
DESVAR  1209  0.00525     0.10    2     2CQUAD9
DESVAR  1210  0.00525     0.10    2     2CQUAD10
DESVAR  1211  0.00525     0.10    2     2CQUAD11
DESVAR  1212  0.00525     0.10    2     2CQUAD12
DESVAR  1213  0.00525     0.10    2     2CQUAD13
DESVAR  1214  0.00525     0.10    2     2CQUAD14
DESVAR  1215  0.00525     0.10    2     2CQUAD15
```

Figure 51. Input Data Stream for the Intermediate Complexity Wing (Continued)

DESVAR	1216	0.00525	0.10	2	2CQUAD16
DESVAR	1217	0.00525	0.10	2	2CQUAD17
DESVAR	1218	0.00525	0.10	2	2CQUAD18
DESVAR	1219	0.00525	0.10	2	2CQUAD19
DESVAR	1220	0.00525	0.10	2	2CQUAD20
DESVAR	1221	0.00525	0.10	2	2CQUAD21
DESVAR	1222	0.00525	0.10	2	2CQUAD22
DESVAR	1223	0.00525	0.10	2	2CQUAD23
DESVAR	1224	0.00525	0.10	2	2CQUAD24
DESVAR	1225	0.00525	0.10	2	2CQUAD25
DESVAR	1226	0.00525	0.10	2	2CQUAD26
DESVAR	1227	0.00525	0.10	2	2CQUAD27
DESVAR	1228	0.00525	0.10	2	2CQUAD28
DESVAR	1229	0.00525	0.10	2	2CQUAD29
DESVAR	1230	0.00525	0.10	2	2CQUAD30
DESVAR	1231	0.00525	0.10	2	2CQUAD31
DESVAR	1232	0.00525	0.10	2	2CQUAD32
DESVAR	1301	0.00525	0.10	3	3TRMEM1
DESVAR	1302	0.00525	0.10	3	3CQUAD1
DESVAR	1303	0.00525	0.10	3	3CQUAD1
DESVAR	1304	0.00525	0.10	3	3CQUAD4
DESVAR	1305	0.00525	0.10	3	3CQUAD5
DESVAR	1306	0.00525	0.10	3	3CQUAD6
DESVAR	1307	0.00525	0.10	3	3CQUAD7
DESVAR	1308	0.00525	0.10	3	3CQUAD8
DESVAR	1309	0.00525	0.10	3	3CQUAD9
DESVAR	1310	0.00525	0.10	3	3CQUAD10
DESVAR	1311	0.00525	0.10	3	3CQUAD11
DESVAR	1312	0.00525	0.10	3	3CQUAD12
DESVAR	1313	0.00525	0.10	3	3CQUAD13
DESVAR	1314	0.00525	0.10	3	3CQUAD14
DESVAR	1315	0.00525	0.10	3	3CQUAD15
DESVAR	1316	0.00525	0.10	3	3CQUAD16
DESVAR	1317	0.00525	0.10	3	3CQUAD17
DESVAR	1318	0.00525	0.10	3	3CQUAD18
DESVAR	1319	0.00525	0.10	3	3CQUAD19
DESVAR	1320	0.00525	0.10	3	3CQUAD20
DESVAR	1321	0.00525	0.10	3	3CQUAD21
DESVAR	1322	0.00525	0.10	3	3CQUAD22
DESVAR	1323	0.00525	0.10	3	3CQUAD23
DESVAR	1324	0.00525	0.10	3	3CQUAD24
DESVAR	1325	0.00525	0.10	3	3CQUAD25
DESVAR	1326	0.00525	0.10	3	3CQUAD26
DESVAR	1327	0.00525	0.10	3	3CQUAD27
DESVAR	1328	0.00525	0.10	3	3CQUAD28
DESVAR	1329	0.00525	0.10	3	3CQUAD29
DESVAR	1330	0.00525	0.10	3	3CQUAD30
DESVAR	1331	0.00525	0.10	3	3CQUAD31
DESVAR	1332	0.00525	0.10	3	3CQUAD32
DESVAR	1401	0.00525	0.10	4	4TRMEM1
DESVAR	1402	0.00525	0.10	4	4CQUAD1
DESVAR	1403	0.00525	0.10	4	4CQUAD1
DESVAR	1404	0.00525	0.10	4	4CQUAD4
DESVAR	1405	0.00525	0.10	4	4CQUAD5
DESVAR	1406	0.00525	0.10	4	4CQUAD6
DESVAR	1407	0.00525	0.10	4	4CQUAD7
DESVAR	1408	0.00525	0.10	4	4CQUAD8
DESVAR	1409	0.00525	0.10	4	4CQUAD9
DESVAR	1410	0.00525	0.10	4	4CQUAD10
DESVAR	1411	0.00525	0.10	4	4CQUAD11
DESVAR	1412	0.00525	0.10	4	4CQUAD12
DESVAR	1413	0.00525	0.10	4	4CQUAD13
DESVAR	1414	0.00525	0.10	4	4CQUAD14
DESVAR	1415	0.00525	0.10	4	4CQUAD15
DESVAR	1416	0.00525	0.10	4	4CQUAD16
DESVAR	1417	0.00525	0.10	4	4CQUAD17
DESVAR	1418	0.00525	0.10	4	4CQUAD18
DESVAR	1419	0.00525	0.10	4	4CQUAD19
DESVAR	1420	0.00525	0.10	4	4CQUAD20
DESVAR	1421	0.00525	0.10	4	4CQUAD21
DESVAR	1422	0.00525	0.10	4	4CQUAD22
DESVAR	1423	0.00525	0.10	4	4CQUAD23
DESVAR	1424	0.00525	0.10	4	4CQUAD24

Figure 51. Input Data Stream for the Intermediate Complexity Wing (Continued)

```
DESVAR  1425    0.00525         0.10    4       4CQUAD25
DESVAR  1426    0.00525         0.10    4       4CQUAD26
DESVAR  1427    0.00525         0.10    4       4CQUAD27
DESVAR  1428    0.00525         0.10    4       4CQUAD28
DESVAR  1429    0.00525         0.10    4       4CQUAD29
DESVAR  1430    0.00525         0.10    4       4CQUAD30
DESVAR  1431    0.00525         0.10    4       4CQUAD31
DESVAR  1432    0.00525         0.10    4       4CQUAD32
PLIST   33      PSHEAR  40001
PLIST   34      PSHEAR  40002
PLIST   35      PSHEAR  40003
PLIST   36      PSHEAR  40004
PLIST   37      PSHEAR  40005
PLIST   38      PSHEAR  40006
PLIST   39      PSHEAR  40007
PLIST   40      PSHEAR  40008
PLIST   41      PSHEAR  40009
PLIST   42      PSHEAR  40010
PLIST   43      PSHEAR  40011
PLIST   44      PSHEAR  40012
PLIST   45      PSHEAR  40013
PLIST   46      PSHEAR  40014
PLIST   47      PSHEAR  40015
PLIST   48      PSHEAR  40016
PLIST   49      PSHEAR  40017
PLIST   50      PSHEAR  40018
PLIST   51      PSHEAR  40019
PLIST   52      PSHEAR  40020
PLIST   53      PSHEAR  40021
PLIST   54      PSHEAR  40022
PLIST   55      PSHEAR  40023
PLIST   56      PSHEAR  40024
PLIST   57      PROD    10001
PLIST   1101    PCOMP   10001   12001
PLIST   1102    PCOMP   30001   32001
PLIST   1103    PCOMP   30002   32002
PLIST   1104    PCOMP   30003   32003
PLIST   1105    PCOMP   30004   32004
PLIST   1106    PCOMP   30005   32005
PLIST   1107    PCOMP   30006   32006
PLIST   1108    PCOMP   30007   32007
PLIST   1109    PCOMP   30008   32008
PLIST   1110    PCOMP   30009   32009
PLIST   1111    PCOMP   30010   32010
PLIST   1112    PCOMP   30011   32011
PLIST   1113    PCOMP   30012   32012
PLIST   1114    PCOMP   30013   32013
PLIST   1115    PCOMP   30014   32014
PLIST   1116    PCOMP   30015   32015
PLIST   1117    PCOMP   30016   32016
PLIST   1118    PCOMP   30017   32017
PLIST   1119    PCOMP   30018   32018
PLIST   1120    PCOMP   30019   32019
PLIST   1121    PCOMP   30020   32020
PLIST   1122    PCOMP   30021   32021
PLIST   1123    PCOMP   30022   32022
PLIST   1124    PCOMP   30023   32023
PLIST   1125    PCOMP   30024   32024
PLIST   1126    PCOMP   30025   32025
PLIST   1127    PCOMP   30026   32026
PLIST   1128    PCOMP   30027   32027
PLIST   1129    PCOMP   30028   32028
PLIST   1130    PCOMP   30029   32029
PLIST   1131    PCOMP   30030   32030
PLIST   1132    PCOMP   30031   32031
PLIST   1201    PCOMP   10001   12001
PLIST   1202    PCOMP   30001   32001
PLIST   1203    PCOMP   30002   32002
PLIST   1204    PCOMP   30003   32003
PLIST   1205    PCOMP   30004   32004
PLIST   1206    PCOMP   30005   32005
PLIST   1207    PCOMP   30006   32006
PLIST   1208    PCOMP   30007   32007
```

Figure 51. Input Data Stream for the Intermediate Complexity Wing (Continued)

PLIST	1209	PCOMP	30008	32008
PLIST	1210	PCOMP	30009	32009
PLIST	1211	PCOMP	30010	32010
PLIST	1212	PCOMP	30011	32011
PLIST	1213	PCOMP	30012	32012
PLIST	1214	PCOMP	30013	32013
PLIST	1215	PCOMP	30014	32014
PLIST	1216	PCOMP	30015	32015
PLIST	1217	PCOMP	30016	32016
PLIST	1218	PCOMP	30017	32017
PLIST	1219	PCOMP	30018	32018
PLIST	1220	PCOMP	30019	32019
PLIST	1221	PCOMP	30020	32020
PLIST	1222	PCOMP	30021	32021
PLIST	1223	PCOMP	30022	32022
PLIST	1224	PCOMP	30023	32023
PLIST	1225	PCOMP	30024	32024
PLIST	1226	PCOMP	30025	32025
PLIST	1227	PCOMP	30026	32026
PLIST	1228	PCOMP	30027	32027
PLIST	1229	PCOMP	30028	32028
PLIST	1230	PCOMP	30029	32029
PLIST	1231	PCOMP	30030	32030
PLIST	1232	PCOMP	30031	32031
PLIST	1301	PCOMP	10001	12001
PLIST	1302	PCOMP	30001	32001
PLIST	1303	PCOMP	30002	32002
PLIST	1304	PCOMP	30003	32003
PLIST	1305	PCOMP	30004	32004
PLIST	1306	PCOMP	30005	32005
PLIST	1307	PCOMP	30006	32006
PLIST	1308	PCOMP	30007	32007
PLIST	1309	PCOMP	30008	32008
PLIST	1310	PCOMP	30009	32009
PLIST	1311	PCOMP	30010	32010
PLIST	1312	PCOMP	30011	32011
PLIST	1313	PCOMP	30012	32012
PLIST	1314	PCOMP	30013	32013
PLIST	1315	PCOMP	30014	32014
PLIST	1316	PCOMP	30015	32015
PLIST	1317	PCOMP	30016	32016
PLIST	1318	PCOMP	30017	32017
PLIST	1319	PCOMP	30018	32018
PLIST	1320	PCOMP	30019	32019
PLIST	1321	PCOMP	30020	32020
PLIST	1322	PCOMP	30021	32021
PLIST	1323	PCOMP	30022	32022
PLIST	1324	PCOMP	30023	32023
PLIST	1325	PCOMP	30024	32024
PLIST	1326	PCOMP	30025	32025
PLIST	1327	PCOMP	30026	32026
PLIST	1328	PCOMP	30027	32027
PLIST	1329	PCOMP	30028	32028
PLIST	1330	PCOMP	30029	32029
PLIST	1331	PCOMP	30030	32030
PLIST	1332	PCOMP	30031	32031
PLIST	1401	PCOMP	10001	12001
PLIST	1402	PCOMP	30001	32001
PLIST	1403	PCOMP	30002	32002
PLIST	1404	PCOMP	30003	32003
PLIST	1405	PCOMP	30004	32004
PLIST	1406	PCOMP	30005	32005
PLIST	1407	PCOMP	30006	32006
PLIST	1408	PCOMP	30007	32007
PLIST	1409	PCOMP	30008	32008
PLIST	1410	PCOMP	30009	32009
PLIST	1411	PCOMP	30010	32010
PLIST	1412	PCOMP	30011	32011
PLIST	1413	PCOMP	30012	32012
PLIST	1414	PCOMP	30013	32013
PLIST	1415	PCOMP	30014	32014
PLIST	1416	PCOMP	30015	32015
PLIST	1417	PCOMP	30016	32016

Figure 51. Input Data Stream for the Intermediate Complexity Wing (Continued)

```
PLIST   1418   PCOMP   30017   32017
PLIST   1419   PCOMP   30018   32018
PLIST   1420   PCOMP   30019   32019
PLIST   1421   PCOMP   30020   32020
PLIST   1422   PCOMP   30021   32021
PLIST   1423   PCOMP   30022   32022
PLIST   1424   PCOMP   30023   32023
PLIST   1425   PCOMP   30024   32024
PLIST   1426   PCOMP   30025   32025
PLIST   1427   PCOMP   30026   32026
PLIST   1428   PCOMP   30027   32027
PLIST   1429   PCOMP   30028   32028
PLIST   1430   PCOMP   30029   32029
PLIST   1431   PCOMP   30030   32030
PLIST   1432   PCOMP   30031   32031
$
$    STRESS CONSTRAINTS
$
DCONSTR,  70,   TSAIWU
DCONSTR,  10,   VMISES
ENDDATA
```

Figure 51. Input Data Stream for the Intermediate Complexity Wing (Concluded)

statics discipline since the only constraints are the stress limits and gauge constraints, both of which are implicitly defined in the bulk data packet. The stress constraints are imposed through the appearance of two DCONSTR bulk data entries which declare that MATi entries 70 and 10 have associated Tsai-Wu and von Mises stress criteria, respectively. The MATi entries, in this case, are a MAT8 and a MAT1, with the tension and compression stress limits given in the stress allowable fields. Note that the input stream has been set up such that, if desired, a principal strain constraint may be imposed instead of the Tsai-Wu criteria by applying a DCONSTR/STRAIN constraint on the MAT8 with identification number 72 and removing the DCONSTR/TSAIWU. The strain allowables for tension and compression are then given in the stress allowable fields of the corresponding MATi entry as can be seen on MAT8/72.

The basic structural model contains composite materials. A complication arises due to the definition of the material coordinate system. In order to maintain compatibility with NASTRAN, ASTROS assumes that the material axis and the element axis coincide unless an angular offset or a coordinate system identification number is given on the element connectivity entry. In this problem, an element coordinate system has been defined using a CORD1R entry with identification 101. The x-axis of this coordinate system defines

the zero degree fiber orientation of the material referred to by any connectivity entry with "101" appearing in the "THETA" field. In this case, the zero direction is defined to be parallel to the mid-chord spar and every quadrilateral and triangular membrane element uses this coordinate system for its material orientation "angle."

The skin elements refer to PCOMP entries that define the layup of the composite skins. Separate, identical, PCOMP entries are shown in **Figure** 51 for each skin element. This is done to facilitate the subsequent design variable linking, both for this case and for other linking schemes that were tested using this basic ICW input stream. Each PCOMP entry defines the four composite plies by specifying their fiber orientation and a ply thickness. The fiber orientations defined on the PCOMP entries are then applied to the zero angle defined by the external "material" coordinate system. In the bulk data packet for this example the ply thicknesses are set to unity to make the definition of the initial design easy, since it is now fully specified by the initial global variable values for both physical and shape function linking. Unit values are also used for the initial PSHEAR and PROD local variable values for the same reason. Also, the "TMIN" fields on the PCOMP entries and on the PSHEAR entries associated with the spars have been specified. These values are not used in the FASTOP design model, but are defined in anticipation of the shape function linking in which the TMIN fields must be defined to provide the gauge constraints on the local design variables.

The design variable definition consists of the 153 DESVAR entries and their associated PLIST entries. The two digit design variable identification numbers (33 to 57) are associated with the substructure and the four digit ID's with the composite skins. In this sample problem, the four digit design variable number, xyzz, has been structured for user convenience to have the following meaning:

x The surface number, 1 or 2, denoting upper or lower surface, respectively. In this case the lower surface is linked to the upper so no 2yzz design variables appear.

y The layer number associated with the design variable. For design linking, the layers are numbered in the order of their definition on the PCOMPi entries. In this case, 0, 90, +45, -45 are layers 1, 2, 3, and 4, respectively.

zz Skin element identification number, either triangular or quadrilateral membrane.

Note that design variables 34 through 56 are uniquely linked to one finite element and could, therefore, have been defined with DESELM entries. There is no functional difference in using the DESVAR/PLIST combination, however, and it allows the user to modify the design variable linking with less effort. All the other variables specify physical linking of multiple finite elements. Since the basic model uses only physical linking, the physical gauge constraints are imposed through the specification of minima and maxima on the DESVAR global design variable definition entry. The upper bounds are not specified in this case and default to be 1000.0. The initial global variable values are all set to 0.10, which means that each substructure element has an initial thickness or cross-sectional area of 0.10 and each ply of each composite element has a thickness of 0.10.

The FSD test case input differs from the FASTOP input stream only in the Solution Control packet. In order to select the FSD option, the Solution Control:

OPTIMIZE STRATEGY = 57

in the original input stream must be modified to:

OPTIMIZE STRATEGY = 1057

Any strategy greater than 999 will invoke the FSD option. The number of leading FSD cycles and the move limit for FSD are set in the MAPOL sequence by the integer variable MAXFSD and the real variable ALPHA, respectively. The case presented here makes use of the default FSD parameters, which select three leading FSD cycles with an exponential move limit of 0.90.

The shape function design variable linking case differs from the FASTOP case in two respects: (1) the default value of NRFAC is used since there are only 24 global variables and (2) the DESVAR/PLIST entries in the original test case of **Figure 51** are replaced with the bulk data entries shown in **Figure 52**. The first pair of DESVAR/PLIST entries in **Figure 52** define the physically linked posts and ribs that are identical to the FASTOP test case. The remainder of the DESVAR entries define the shape function design variables. Again, the global design variable identification number was chosen to

```
$
$    PHYSICALLY LINKED RIBS AND POSTS
$
DESVAR  33      0.02            0.10            RIBS
DESVAR  57      0.02            0.10            POSTS
PLIST   33      PSHEAR  40001
PLIST   57      PROD    10001
$
$    SHAPE FUNCTION LINKED COMPOSITE SKINS
$
DESVAR,  11, 0.04, 1000.0, 0.10,1, UNIFORM
DESVAR,  12, -.04, 1000.0, 0.00,1, LINEARX
DESVAR,  14, -.04, 1000.0, 0.00,1, LINEARY
DESVAR,  17, -.04, 1000.0, 0.00,1, QUADY
DESVAR,  21, 0.04, 1000.0, 0.10,2, UNIFORM
DESVAR,  22, -.04, 1000.0, 0.00,2, LINEARX
DESVAR,  24, -.04, 1000.0, 0.00,2, LINEARY
DESVAR,  27, -.04, 1000.0, 0.00,2, QUADY
DESVAR,  31, 0.04, 1000.0, 0.10,3, UNIFORM
DESVAR,  32, -.04, 1000.0, 0.00,3, LINEARX
DESVAR,  34, -.04, 1000.0, 0.00,3, LINEARY
DESVAR,  37, -.04, 1000.0, 0.00,3, QUADY
DESVAR,  41, 0.04, 1000.0, 0.10,4, UNIFORM
DESVAR,  42, -.04, 1000.0, 0.00,4, LINEARX
DESVAR,  44, -.04, 1000.0, 0.00,4, LINEARY
DESVAR,  47, -.04, 1000.0, 0.00,4, QUADY
DESVAR, 111, 0.04, 1000.0, 0.10,, SPRFUNI
DESVAR, 114, -.04, 1000.0, 0.00,, SPRFLINY
DESVAR, 121, 0.04, 1000.0, 0.10,, SPRMUNI
DESVAR, 124, -.04, 1000.0, 0.00,, SPRMLINY
DESVAR, 131, 0.04, 1000.0, 0.10,, SPRAUNI
DESVAR, 134, -.04, 1000.0, 0.00,, SPRALINY
 ELIST         11 CTRMEM        1  1.0000      2  1.0000
 ELIST         12 CTRMEM        1 0.69354      2 0.69354
 ELIST         14 CTRMEM        1 1.01222      2 1.01222
 ELIST         11 CQUAD4        3 1.00000      4 1.00000      5 1.00000+A
+A              6 1.00000       7 1.00000      8 1.00000      9 1.00000+A2
+A2            10 1.00000      11 1.00000     12 1.00000     13 1.00000+A3
+A3            14 1.00000      15 1.00000     16 1.00000     17 1.00000+A4
+A4            18 1.00000      19 1.00000     20 1.00000     21 1.00000+A5
+A5            22 1.00000      23 1.00000     24 1.00000     25 1.00000+A6
+A6            26 1.00000      27 1.00000     28 1.00000     29 1.00000+A7
+A7            30 1.00000      31 1.00000     32 1.00000     33 1.00000+A8
+A8            34 1.00000      35 1.00000     36 1.00000     37 1.00000+A9
+A9            38 1.00000      39 1.00000     40 1.00000     41 1.00000+A10
+A10           42 1.00000      43 1.00000     44 1.00000     45 1.00000+A11
+A11           46 1.00000      47 1.00000     48 1.00000     49 1.00000+A12
+A12           50 1.00000      51 1.00000     52 1.00000     53 1.00000+A13
+A13           54 1.00000      55 1.00000     56 1.00000     57 1.00000+A14
+A14           58 1.00000      59 1.00000     60 1.00000     61 1.00000+A15
+A15           62 1.00000      63 1.00000     64 1.00000
 ELIST         12 CQUAD4        3 0.79929      4 0.79929      5 0.89877+B
+B              6 0.89877       7 1.00000      8 1.00000      9 0.65456+B2
```

Figure 52. DESVAR/ELIST Bulk Data Entries for Shape Function Linking for the Intermediate Complexity Wing

```
+B2        10 0.65456   11 0.74889   12 0.74889   13 0.84669+B3
+B3        14 0.84669   15 0.94815   16 0.94815   17 0.56897+B4
+B4        18 0.56897   19 0.67118   20 0.67118   21 0.77716+B5
+B5        22 0.77716   23 0.88709   24 0.88709   25 0.48338+B6
+B6        26 0.48338   27 0.59347   28 0.59347   29 0.70761+B7
+B7        30 0.70761   31 0.82602   32 0.82602   33 0.39779+B8
+B8        34 0.39779   35 0.51576   36 0.51576   37 0.63807+B9
+B9        38 0.63807   39 0.76496   40 0.76496   41 0.31220+B10
+B10       42 0.31220   43 0.43805   44 0.43805   45 0.56853+B11
+B11       46 0.56853   47 0.70390   48 0.70390   49 0.22350+B12
+B12       50 0.22350   51 0.36380   52 0.36380   53 0.50778+B13
+B13       54 0.50778   55 0.65564   56 0.65564   57 0.13184+B14
+B14       58 0.13184   59 0.29335   60 0.29335   61 0.45616+B15
+B15       62 0.45616   63 0.62033   64 0.62033
 ELIST     14 CQUAD4     3 1.00000    4 1.00000    5 0.98484+D
+D          6 0.98484    7 0.96912    8 0.96912    9 0.93681+D2
+D2        10 0.93681   11 0.90630   12 0.90630   13 0.87468+D3
+D3        14 0.87468   15 0.84187   16 0.84187   17 0.79556+D4
+D4        18 0.79556   19 0.76251   20 0.76251   21 0.72825+D5
+D5        22 0.72825   23 0.69269   24 0.69269   25 0.65432+D6
+D6        26 0.65432   27 0.61871   28 0.61871   29 0.58182+D7
+D7        30 0.58182   31 0.54352   32 0.54352   33 0.51308+D8
+D8        34 0.51308   35 0.47493   36 0.47493   37 0.43537+D9
+D9        38 0.43537   39 0.39434   40 0.39434   41 0.37184+D10
+D10       42 0.37184   43 0.33114   44 0.33114   45 0.28895+D11
+D11       46 0.28895   47 0.24517   48 0.24517   49 0.22576+D12
+D12       50 0.22576   51 0.19407   52 0.19407   53 0.16143+D13
+D13       54 0.16143   55 0.12778   56 0.12778   57 0.07515+D14
+D14       58 0.07515   59 0.06445   60 0.06445   61 0.05356+D15
+D15       62 0.05356   63 0.04248   64 0.04248
 ELIST     17 CTRMEM     1 1.024575   2 1.024575
 ELIST     17 CQUAD4     3 1.00000    4 1.00000    5 0.96992+G
+G          6 0.96992    7 0.93919    8 0.93919    9 0.87761+G2
+G2        10 0.87761   11 0.82138   12 0.82138   13 0.76507+G3
+G3        14 0.76507   15 0.70875   16 0.70875   17 0.63292+G4
+G4        18 0.63292   19 0.58143   20 0.58143   21 0.53035+G5
+G5        22 0.53035   23 0.47982   24 0.47982   25 0.42813+G6
+G6        26 0.42813   27 0.38281   28 0.38281   29 0.33851+G7
+G7        30 0.33851   31 0.29542   32 0.29542   33 0.26326+G8
+G8        34 0.26326   35 0.22556   36 0.22556   37 0.18955+G9
+G9        38 0.18955   39 0.15551   40 0.15551   41 0.13826+G10
+G10       42 0.13826   43 0.10965   44 0.10965   45 0.08349+G11
+G11       46 0.08349   47 0.06011   48 0.06011   49 0.05097+G12
+G12       50 0.05097   51 0.03766   52 0.03766   53 0.02606+G13
+G13       54 0.02606   55 0.01633   56 0.01633   57 0.00565+G14
+G14       58 0.00565   59 0.00415   60 0.00415   61 0.00287+G15
+G15       62 0.00287   63 0.00180   64 0.00180
 ELIST     21 CTRMEM     1  1.0000    2  1.0000
 ELIST     22 CTRMEM     1 0.69354    2 0.69354
 ELIST     24 CTRMEM     1 1.01222    2 1.01222
 ELIST     21 CQUAD4     3 1.00000    4 1.00000    5 1.00000+A
+A          6 1.00000    7 1.00000    8 1.00000    9 1.00000+A2
+A2        10 1.00000   11 1.00000   12 1.00000   13 1.00000+A3
```

Figure 52. DESVAR/ELIST Bulk Data Entries for Shape Function Linking for the Intermediate Complexity Wing (Continued)

+A3	14	1.00000	15	1.00000	16	1.00000	17	1.00000+A4
+A4	18	1.00000	19	1.00000	20	1.00000	21	1.00000+A5
+A5	22	1.00000	23	1.00000	24	1.00000	25	1.00000+A6
+A6	26	1.00000	27	1.00000	28	1.00000	29	1.00000+A7
+A7	30	1.00000	31	1.00000	32	1.00000	33	1.00000+A8
+A8	34	1.00000	35	1.00000	36	1.00000	37	1.00000+A9
+A9	38	1.00000	39	1.00000	40	1.00000	41	1.00000+A10
+A10	42	1.00000	43	1.00000	44	1.00000	45	1.00000+A11
+A11	46	1.00000	47	1.00000	48	1.00000	49	1.00000+A12
+A12	50	1.00000	51	1.00000	52	1.00000	53	1.00000+A13
+A13	54	1.00000	55	1.00000	56	1.00000	57	1.00000+A14
+A14	58	1.00000	59	1.00000	60	1.00000	61	1.00000+A15
+A15	62	1.00000	63	1.00000	64	1.00000		
ELIST	22	CQUAD4	3	0.79929	4	0.79929	5	0.89877+B
+B	6	0.89877	7	1.00000	8	1.00000	9	0.65456+B2
+B2	10	0.65456	11	0.74889	12	0.74889	13	0.84669+B3
+B3	14	0.84669	15	0.94815	16	0.94815	17	0.56897+B4
+B4	18	0.56897	19	0.67118	20	0.67118	21	0.77716+B5
+B5	22	0.77716	23	0.88709	24	0.88709	25	0.48338+B6
+B6	26	0.48338	27	0.59347	28	0.59347	29	0.70761+B7
+B7	30	0.70761	31	0.82602	32	0.82602	33	0.39779+B8
+B8	34	0.39779	35	0.51576	36	0.51576	37	0.63807+B9
+B9	38	0.63807	39	0.76496	40	0.76496	41	0.31220+B10
+B10	42	0.31220	43	0.43805	44	0.43805	45	0.56853+B11
+B11	46	0.56853	47	0.70390	48	0.70390	49	0.22350+B12
+B12	50	0.22350	51	0.36380	52	0.36380	53	0.50778+B13
+B13	54	0.50778	55	0.65564	56	0.65564	57	0.13184+B14
+B14	58	0.13184	59	0.29335	60	0.29335	61	0.45616+B15
+B15	62	0.45616	63	0.62033	64	0.62033		
ELIST	24	CQUAD4	3	1.00000	4	1.00000	5	0.98484+D
+D	6	0.98484	7	0.96912	8	0.96912	9	0.93681+D2
+D2	10	0.93681	11	0.90630	12	0.90630	13	0.87468+D3
+D3	14	0.87468	15	0.84187	16	0.84187	17	0.79556+D4
+D4	18	0.79556	19	0.76251	20	0.76251	21	0.72825+D5
+D5	22	0.72825	23	0.69269	24	0.69269	25	0.65432+D6
+D6	26	0.65432	27	0.61871	28	0.61871	29	0.58182+D7
+D7	30	0.58182	31	0.54352	32	0.54352	33	0.51308+D8
+D8	34	0.51308	35	0.47493	36	0.47493	37	0.43537+D9
+D9	38	0.43537	39	0.39434	40	0.39434	41	0.37184+D10
+D10	42	0.37184	43	0.33114	44	0.33114	45	0.28895+D11
+D11	46	0.28895	47	0.24517	48	0.24517	49	0.22576+D12
+D12	50	0.22576	51	0.19407	52	0.19407	53	0.16143+D13
+D13	54	0.16143	55	0.12778	56	0.12778	57	0.07515+D14
+D14	58	0.07515	59	0.06445	60	0.06445	61	0.05356+D15
+D15	62	0.05356	63	0.04248	64	0.04248		
ELIST	27	CTRMEM	1	1.024575	2	1.024575		
ELIST	27	CQUAD4	3	1.00000	4	1.00000	5	0.96992+G
+G	6	0.96992	7	0.93919	8	0.93919	9	0.87761+G2
+G2	10	0.87761	11	0.82138	12	0.82138	13	0.76507+G3
+G3	14	0.76507	15	0.70875	16	0.70875	17	0.63292+G4
+G4	18	0.63292	19	0.58143	20	0.58143	21	0.53035+G5
+G5	22	0.53035	23	0.47982	24	0.47982	25	0.42813+G6
+G6	26	0.42813	27	0.38281	28	0.38281	29	0.33851+G7

Figure 52. DESVAR/ELIST Bulk Data Entries for Shape Function Linking for the Intermediate Complexity Wing (Continued)

+G7	30 0.33851	31 0.29542	32 0.29542	33 0.26326+G8
+G8	34 0.26326	35 0.22556	36 0.22556	37 0.18955+G9
+G9	38 0.18955	39 0.15551	40 0.15551	41 0.13826+G10
+G10	42 0.13826	43 0.10965	44 0.10965	45 0.08349+G11
+G11	46 0.08349	47 0.06011	48 0.06011	49 0.05097+G12
+G12	50 0.05097	51 0.03766	52 0.03766	53 0.02606+G13
+G13	54 0.02606	55 0.01633	56 0.01633	57 0.00565+G14
+G14	58 0.00565	59 0.00415	60 0.00415	61 0.00287+G15
+G15	62 0.00287	63 0.00180	64 0.00180	
ELIST	31 CTRMEM	1 1.0000	2 1.0000	
ELIST	32 CTRMEM	1 0.69354	2 0.69354	
ELIST	34 CTRMEM	1 1.01222	2 1.01222	
ELIST	31 CQUAD4	3 1.00000	4 1.00000	5 1.00000+A
+A	6 1.00000	7 1.00000	8 1.00000	9 1.00000+A2
+A2	10 1.00000	11 1.00000	12 1.00000	13 1.00000+A3
+A3	14 1.00000	15 1.00000	16 1.00000	17 1.00000+A4
+A4	18 1.00000	19 1.00000	20 1.00000	21 1.00000+A5
+A5	22 1.00000	23 1.00000	24 1.00000	25 1.00000+A6
+A6	26 1.00000	27 1.00000	28 1.00000	29 1.00000+A7
+A7	30 1.00000	31 1.00000	32 1.00000	33 1.00000+A8
+A8	34 1.00000	35 1.00000	36 1.00000	37 1.00000+A9
+A9	38 1.00000	39 1.00000	40 1.00000	41 1.00000+A10
+A10	42 1.00000	43 1.00000	44 1.00000	45 1.00000+A11
+A11	46 1.00000	47 1.00000	48 1.00000	49 1.00000+A12
+A12	50 1.00000	51 1.00000	52 1.00000	53 1.00000+A13
+A13	54 1.00000	55 1.00000	56 1.00000	57 1.00000+A14
+A14	58 1.00000	59 1.00000	60 1.00000	61 1.00000+A15
+A15	62 1.00000	63 1.00000	64 1.00000	
ELIST	32 CQUAD4	3 0.79929	4 0.79929	5 0.89877+B
+B	6 0.89877	7 1.00000	8 1.00000	9 0.65456+B2
+B2	10 0.65456	11 0.74889	12 0.74889	13 0.84669+B3
+B3	14 0.84669	15 0.94815	16 0.94815	17 0.56897+B4
+B4	18 0.56897	19 0.67118	20 0.67118	21 0.77716+B5
+B5	22 0.77716	23 0.88709	24 0.88709	25 0.48338+B6
+B6	26 0.48338	27 0.59347	28 0.59347	29 0.70761+B7
+B7	30 0.70761	31 0.82602	32 0.82602	33 0.39779+B8
+B8	34 0.39779	35 0.51576	36 0.51576	37 0.63807+B9
+B9	38 0.63807	39 0.76496	40 0.76496	41 0.31220+B10
+B10	42 0.31220	43 0.43805	44 0.43805	45 0.56853+B11
+B11	46 0.56853	47 0.70390	48 0.70390	49 0.22350+B12
+B12	50 0.22350	51 0.36380	52 0.36380	53 0.50778+B13
+B13	54 0.50778	55 0.65564	56 0.65564	57 0.13184+B14
+B14	58 0.13184	59 0.29335	60 0.29335	61 0.45616+B15
+B15	62 0.45616	63 0.62033	64 0.62033	
ELIST	34 CQUAD4	3 1.00000	4 1.00000	5 0.98484+D
+D	6 0.98484	7 0.96912	8 0.96912	9 0.93681+D2
+D2	10 0.93681	11 0.90630	12 0.90630	13 0.87468+D3
+D3	14 0.87468	15 0.84187	16 0.84187	17 0.79556+D4
+D4	18 0.79556	19 0.76251	20 0.76251	21 0.72825+D5
+D5	22 0.72825	23 0.69269	24 0.69269	25 0.65432+D6
+D6	26 0.65432	27 0.61871	28 0.61871	29 0.58182+D7
+D7	30 0.58182	31 0.54352	32 0.54352	33 0.51308+D8
+D8	34 0.51308	35 0.47493	36 0.47493	37 0.43537+D9

Figure 52. DESVAR/ELIST Bulk Data Entries for Shape Function Linking for the Intermediate Complexity Wing (Continued)

```
+D9        38 0.43537    39 0.39434    40 0.39434    41 0.37184+D10
+D10       42 0.37184    43 0.33114    44 0.33114    45 0.28895+D11
+D11       46 0.28895    47 0.24517    48 0.24517    49 0.22576+D12
+D12       50 0.22576    51 0.19407    52 0.19407    53 0.16143+D13
+D13       54 0.16143    55 0.12778    56 0.12778    57 0.07515+D14
+D14       58 0.07515    59 0.06445    60 0.06445    61 0.05356+D15
+D15       62 0.05356    63 0.04248    64 0.04248
 ELIST     37 CTRMEM     1 1.024575    2 1.024575
 ELIST     37 CQUAD4      3 1.00000     4 1.00000     5 0.96992+G
+G          6 0.96992     7 0.93919     8 0.93919     9 0.87761+G2
+G2        10 0.87761    11 0.82138    12 0.82138    13 0.76507+G3
+G3        14 0.76507    15 0.70875    16 0.70875    17 0.63292+G4
+G4        18 0.63292    19 0.58143    20 0.58143    21 0.53035+G5
+G5        22 0.53035    23 0.47982    24 0.47982    25 0.42813+G6
+G6        26 0.42813    27 0.38281    28 0.38281    29 0.33851+G7
+G7        30 0.33851    31 0.29542    32 0.29542    33 0.26326+G8
+G8        34 0.26326    35 0.22556    36 0.22556    37 0.18955+G9
+G9        38 0.18955    39 0.15551    40 0.15551    41 0.13826+G10
+G10       42 0.13826    43 0.10965    44 0.10965    45 0.08349+G11
+G11       46 0.08349    47 0.06011    48 0.06011    49 0.05097+G12
+G12       50 0.05097    51 0.03766    52 0.03766    53 0.02606+G13
+G13       54 0.02606    55 0.01633    56 0.01633    57 0.00565+G14
+G14       58 0.00565    59 0.00415    60 0.00415    61 0.00287+G15
+G15       62 0.00287    63 0.00180    64 0.00180
 ELIST     41 CTRMEM      1  1.0000     2  1.0000
 ELIST     42 CTRMEM      1 0.69354     2 0.69354
 ELIST     44 CTRMEM      1 1.01222     2 1.01222
 ELIST     41 CQUAD4      3 1.00000     4 1.00000     5 1.00000+A
+A          6 1.00000     7 1.00000     8 1.00000     9 1.00000+A2
+A2        10 1.00000    11 1.00000    12 1.00000    13 1.00000+A3
+A3        14 1.00000    15 1.00000    16 1.00000    17 1.00000+A4
+A4        18 1.00000    19 1.00000    20 1.00000    21 1.00000+A5
+A5        22 1.00000    23 1.00000    24 1.00000    25 1.00000+A6
+A6        26 1.00000    27 1.00000    28 1.00000    29 1.00000+A7
+A7        30 1.00000    31 1.00000    32 1.00000    33 1.00000+A8
+A8        34 1.00000    35 1.00000    36 1.00000    37 1.00000+A9
+A9        38 1.00000    39 1.00000    40 1.00000    41 1.00000+A10
+A10       42 1.00000    43 1.00000    44 1.00000    45 1.00000+A11
+A11       46 1.00000    47 1.00000    48 1.00000    49 1.00000+A12
+A12       50 1.00000    51 1.00000    52 1.00000    53 1.00000+A13
+A13       54 1.00000    55 1.00000    56 1.00000    57 1.00000+A14
+A14       58 1.00000    59 1.00000    60 1.00000    61 1.00000+A15
+A15       62 1.00000    63 1.00000    64 1.00000
 ELIST     42 CQUAD4      3 0.79929     4 0.79929     5 0.89877+B
+B          6 0.89877     7 1.00000     8 1.00000     9 0.65456+B2
+B2        10 0.65456    11 0.74889    12 0.74889    13 0.84669+B3
+B3        14 0.84669    15 0.94815    16 0.94815    17 0.56897+B4
+B4        18 0.56897    19 0.67118    20 0.67118    21 0.77716+B5
+B5        22 0.77716    23 0.88709    24 0.88709    25 0.48338+B6
+B6        26 0.48338    27 0.59347    28 0.59347    29 0.70761+B7
+B7        30 0.70761    31 0.82602    32 0.82602    33 0.39779+B8
+B8        34 0.39779    35 0.51576    36 0.51576    37 0.63807+B9
+B9        38 0.63807    39 0.76496    40 0.76496    41 0.31220+B10
```

Figure 52. DESVAR/ELIST Bulk Data Entries for Shape Function Linking for the Intermediate Complexity Wing (Continued)

```
+B10        42 0.31220     43 0.43805     44 0.43805     45 0.56853+B11
+B11        46 0.56853     47 0.70390     48 0.70390     49 0.22350+B12
+B12        50 0.22350     51 0.36380     52 0.36380     53 0.50778+B13
+B13        54 0.50778     55 0.65564     56 0.65564     57 0.13184+B14
+B14        58 0.13184     59 0.29335     60 0.29335     61 0.45616+B15
+B15        62 0.45616     63 0.62033     64 0.62033
 ELIST      44 CQUAD4       3 1.00000      4 1.00000      5 0.98484+D
+D           6 0.98484      7 0.96912      8 0.96912      9 0.93681+D2
+D2         10 0.93681     11 0.90630     12 0.90630     13 0.87468+D3
+D3         14 0.87468     15 0.84187     16 0.84187     17 0.79556+D4
+D4         18 0.79556     19 0.76251     20 0.76251     21 0.72825+D5
+D5         22 0.72825     23 0.69269     24 0.69269     25 0.65432+D6
+D6         26 0.65432     27 0.61871     28 0.61871     29 0.58182+D7
+D7         30 0.58182     31 0.54352     32 0.54352     33 0.51308+D8
+D8         34 0.51308     35 0.47493     36 0.47493     37 0.43537+D9
+D9         38 0.43537     39 0.39434     40 0.39434     41 0.37184+D10
+D10        42 0.37184     43 0.33114     44 0.33114     45 0.28895+D11
+D11        46 0.28895     47 0.24517     48 0.24517     49 0.22576+D12
+D12        50 0.22576     51 0.19407     52 0.19407     53 0.16143+D13
+D13        54 0.16143     55 0.12778     56 0.12778     57 0.07515+D14
+D14        58 0.07515     59 0.06445     60 0.06445     61 0.05356+D15
+D15        62 0.05356     63 0.04248     64 0.04248
 ELIST      47 CTRMEM      1  1.024575    2  1.024575
 ELIST      47 CQUAD4       3 1.00000      4 1.00000      5 0.96992+G
+G           6 0.96992      7 0.93919      8 0.93919      9 0.87761+G2
+G2         10 0.87761     11 0.82138     12 0.82138     13 0.76507+G3
+G3         14 0.76507     15 0.70875     16 0.70875     17 0.63292+G4
+G4         18 0.63292     19 0.58143     20 0.58143     21 0.53035+G5
+G5         22 0.53035     23 0.47982     24 0.47982     25 0.42813+G6
+G6         26 0.42813     27 0.38281     28 0.38281     29 0.33851+G7
+G7         30 0.33851     31 0.29542     32 0.29542     33 0.26326+G8
+G8         34 0.26326     35 0.22556     36 0.22556     37 0.18955+G9
+G9         38 0.18955     39 0.15551     40 0.15551     41 0.13826+G10
+G10        42 0.13826     43 0.10965     44 0.10965     45 0.08349+G11
+G11        46 0.08349     47 0.06011     48 0.06011     49 0.05097+G12
+G12        50 0.05097     51 0.03766     52 0.03766     53 0.02606+G13
+G13        54 0.02606     55 0.01633     56 0.01633     57 0.00565+G14
+G14        58 0.00565     59 0.00415     60 0.00415     61 0.00287+G15
+G15        62 0.00287     63 0.00180     64 0.00180
 ELIST     111 CSHEAR      97 1.00000     98 1.00000     99 1.00000+A
+A         100 1.00000    101 1.00000    102 1.00000    103 1.00000
 ELIST     114 CSHEAR      97 1.00000     98 0.85291     99 0.70584+D
+D         100 0.55875    101 0.41168    102 0.25359    103 0.08454
 ELIST     121 CSHEAR     104 1.00000    105 1.00000    106 1.00000+A
+A         107 1.00000    108 1.00000    109 1.00000    110 1.00000+A2
+A2        111 1.00000
 ELIST     124 CSHEAR     104 1.00000    105 0.89746    106 0.75128+D
+D         107 0.60509    108 0.45893    109 0.31276    110 0.17933+D2
+D2        111 0.05949
 ELIST     131 CSHEAR     112 1.00000    113 1.00000    114 1.00000+A
+A         115 1.00000    116 1.00000    117 1.00000    118 1.00000+A2
+A2        119 1.00000
 ELIST     134 CSHEAR     112 1.00000    113 0.85855    114 0.70189+D
```

Figure 52. DESVAR/ELIST Bulk Data Entries for Shape Function Linking for the Intermediate Complexity Wing (Continued)

```
+D          115 0.54522    116 0.38856    117 0.23189    118 0.11517+D2
+D2         119 0.03839
$
$   THICKNESS CONSTRAINTS
$
DCONTHK   QUAD4      7      63      57      25      31      41      47
DCONTHK   TRMEM      1
DCONTHK   SHEAR     97     103     104     111     112     119
$
```

Figure 52. DESVAR/ELIST Bulk Data Entries for Shape Function Linking for the Intermediate Complexity Wing (Concluded)

have meaning to ease the interpretation of results. In this case the design variable identification numbers, xyz, can be interpreted as:

x   Skin or spar variable flag: x = 0 for skins, x = 1 for spars.

y   The layer number associated with the design variable for skins or the spar location for spar variables. The spars are numbered from leading edge to trailing edge.

z   The shape associated with the design variable. These shapes are given the following identifiers denoting the shape.

y / x	1	x	x^2
1	1	2	3
y	4	5	6
y^2	7	8	9

The generation of the ELIST entries by hand requires a substantial amount of effort and automated techniques can be developed. This was done for this sample problem as discussed in the Appendix. The result is a set of coefficients (PREF values) and finite element identification numbers that define the shape. For example, the uniform shape function of design variable 11 is a vector of unit values associated with every finite element or layer that is to be controlled by the corresponding global design variable. Note that more than one ELIST entry can be used for a given design variable. This feature allows multiple finite element types to be linked to the same shape function. In this case, QUAD4 elements and TRMEM elements are linked in each of the skin thickness shape functions. In an identical manner, the chordwise linear taper of design variable 12 is defined by a series of coefficients representing a

linear variation in the x-coordinate of the linked finite elements. In the sample case shown, the PREF values were generated automatically from the element centroidal coordinates and normalized such that the largest component was unity. This normalization is not necessary, but provides improved behavior in the optimizer since large PREF coefficients result in very large objective function and constraint sensitivities, which may "desensitize" the optimization algorithm.

A final requirement in defining shape function design variables is the specification of DCONTHK thickness constraints. In general, since shape function global variables may represent any shape, no side constraints can be applied to these variables. In ASTROS, very large positive and negative values automatically override the user defined VMAX and VMIN values on the DESVAR entry when linked with ELIST entries. Thus, the local gauge constraints play two important roles in shape function optimization: the first is to supply the minimum gauges for the local design variables and the second is to constrain the optimizer from selecting physically meaningless designs (e.g., negative thicknesses) or from moving too far in a single iteration. Since mathematical programming methods become slower as the number of retained constraints increases, and since there is a potential for many thousands of pseudo-side constraints, the user must select a subset of elements linked to shape functions that are then always retained in the optimization phase. This set of elements should be selected such that all designed elements will be adequately constrained by the application of the thickness constraints to the specified subset of elements. As a safety measure, all thickness constraints are computed by ASTROS to ensure "reasonableness," but only those named on DCONTHK entries are considered "active" unless the constraint is violated. If a negative local variable value is encountered at any point in the optimization, the ASTROS system terminates immediately.

4.7.3 Results and Output Description

Figure 53(a) shows the design iteration histories for the FASTOP comparison case, **Figure 53(b)** the case with FASTOP-like linking, but using leading FSD cycles and **Figure 53(c)** the case using shape function linking. The FSD case produces results that are nearly identical to the baseline 153 design variable case (as expected), while the shape function linked design weighs 8.5 percent more than the first two cases due to the reduced freedom

A S T R O S   D E S I G N   I T E R A T I O N   H I S T O R Y

ITERATION NUMBER	OBJECTIVE FUNCTION VALUE	NUMBER FUNCTION EVAL	NUMBER GRADIENT EVAL	NUMBER RETAINED CONSTRAINTS	NUMBER ACTIVE CONSTRAINTS	NUMBER VIOLATED CONSTRAINTS	NUMBER LOWER BOUNDS	NUMBER UPPER BOUNDS	APPROXIMATE PROBLEM CONVERGENCE
1	1.76326E+02	0	0	0	0	0	0	0	NOT CONVERGED
2	8.96786E+01	225	37	153	10	0	0	140	NOT CONVERGED
3	5.67327E+01	297	63	153	26	0	0	89	NOT CONVERGED
4	4.21956E+01	224	55	153	37	0	0	71	NOT CONVERGED
5	3.55030E+01	129	29	153	41	0	0	6	NOT CONVERGED
6	3.28255E+01	190	39	153	47	0	0	54	NOT CONVERGED
7	3.22768E+01	117	29	153	49	0	0	69	NOT CONVERGED
8	3.21595E+01	26	11	153	40	0	0	69	CONVERGED

THE FINAL OBJECTIVE FUNCTION VALUE IS:

FIXED = 0.00000E+00
\+ DESIGNED = 3.21595E+01

TOTAL = 3.21595E+01

(a) Mathematical Programming Only

A S T R O S   D E S I G N   I T E R A T I O N   H I S T O R Y

ITERATION NUMBER	OBJECTIVE FUNCTION VALUE	NUMBER FUNCTION EVAL	NUMBER GRADIENT EVAL	NUMBER RETAINED CONSTRAINTS	NUMBER ACTIVE CONSTRAINTS	NUMBER VIOLATED CONSTRAINTS	NUMBER LOWER BOUNDS	NUMBER UPPER BOUNDS	APPROXIMATE PROBLEM CONVERGENCE
1	1.76326E+02	0	0	0	0	0	0	0	NOT CONVERGED
2	3.62432E+01	0	0	444	0	0	213	0	NOT CONVERGED
3	3.14308E+01	0	0	444	0	0	253	0	NOT CONVERGED
4	3.15597E+01	0	0	444	0	0	273	0	CONVERGED
5	3.26219E+01	104	43	153	46	0	0	77	NOT CONVERGED
6	3.23658E+01	21	16	153	33	0	0	77	NOT CONVERGED
7	3.22104E+01	50	16	153	48	0	0	82	CONVERGED
8	3.21255E+01	16	9	153	36	0	0	82	CONVERGED

THE FINAL OBJECTIVE FUNCTION VALUE IS:

FIXED = 0.00000E+00
\+ DESIGNED = 3.21255E+01

TOTAL = 3.21255E+01

(b) Fully-Stressed Design Plus Mathematical Programming

Figure 53. Design Iteration Histories for the Intermediate Complexity Wing

A S T R O S   D E S I G N   I T E R A T I O N   H I S T O R Y

ITERATION NUMBER	OBJECTIVE FUNCTION VALUE	NUMBER FUNCTION EVAL	NUMBER GRADIENT EVAL	NUMBER RETAINED CONSTRAINTS	NUMBER ACTIVE CONSTRAINTS	NUMBER VIOLATED CONSTRAINTS	NUMBER LOWER BOUNDS	NUMBER UPPER BOUNDS	APPROXIMATE PROBLEM CONVERGENCE
1	1.76326E+02	0	0	0	0	0	0	0	NOT CONVERGED
2	8.59776E+01	59	27	110	34	0	2	0	NOT CONVERGED
3	5.46782E+01	50	27	110	34	0	2	0	NOT CONVERGED
4	4.21012E+01	49	26	108	31	0	2	0	NOT CONVERGED
5	3.56519E+01	51	30	108	34	0	2	0	NOT CONVERGED
6	3.48312E+01	58	25	109	28	0	2	0	NOT CONVERGED
7	3.48692E+01	80	18	88	26	0	2	0	CONVERGED
8	3.48413E+01	22	7	89	27	0	2	0	CONVERGED

THE FINAL OBJECTIVE FUNCTION VALUE IS:

FIXED =	0.00000E+00
+ DESIGNED =	3.48413E+01
TOTAL =	3.48413E+01

(c) Shape Function Linking

Figure 53. Design Iteration Histories for the Intermediate Complexity Wing (Concluded)

granted the optimizer through limiting the number and nature of the design variables. The FASTOP result to which these designs are compared weighed 37.3 pounds. This number is significantly higher than the 32.16 pounds obtained by the equivalent ASTROS model.

Figures 54 and 55 show the local element thicknesses and ply counts from FASTOP and from each ASTROS ICW test case for the substructure and the composite wing skins, respectively. The results indicate that the ASTROS result and the FASTOP result for the equivalent design variable linking schemes are very similar, despite the difference in final objective function. There are several possible explanations for the discrepancy in weight. One difference is that ASTROS treats the design variables as continuous, whereas FASTOP rounds to whole ply counts at each redesign cycle. The ASTROS ply counts indicated in the figure, therefore, do not represent a design that weighs exactly the value given as the final objective function. Also, the accumulated effects of rounding to whole plies at each iteration could lead to a slightly different final design, irrespective of any other considerations. Finally, and most importantly, the finite elements, stress computations and stress constraint formulations are not identical between FASTOP and ASTROS.

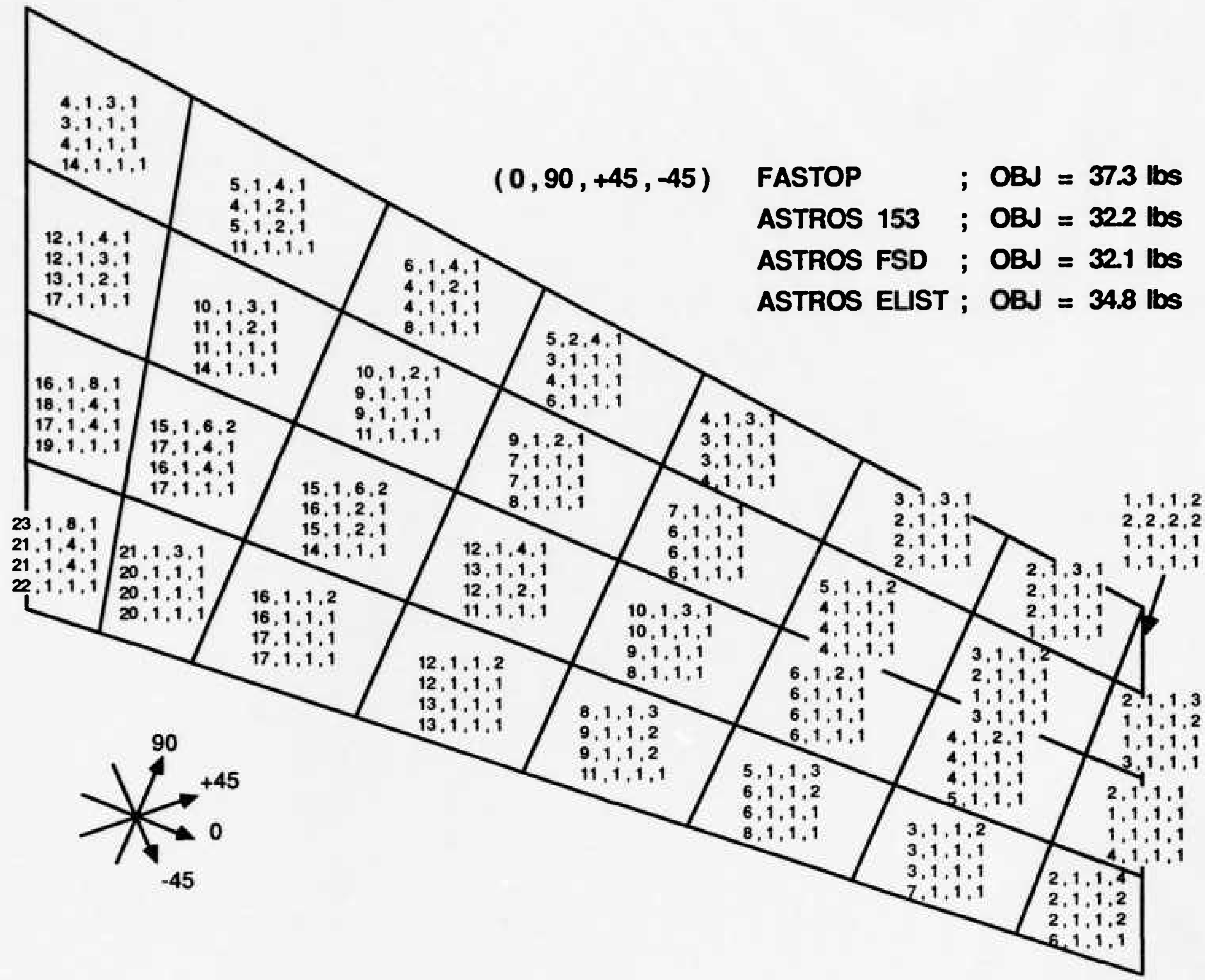

Figure 54. Final Ply Counts for the ICW Cover Skins

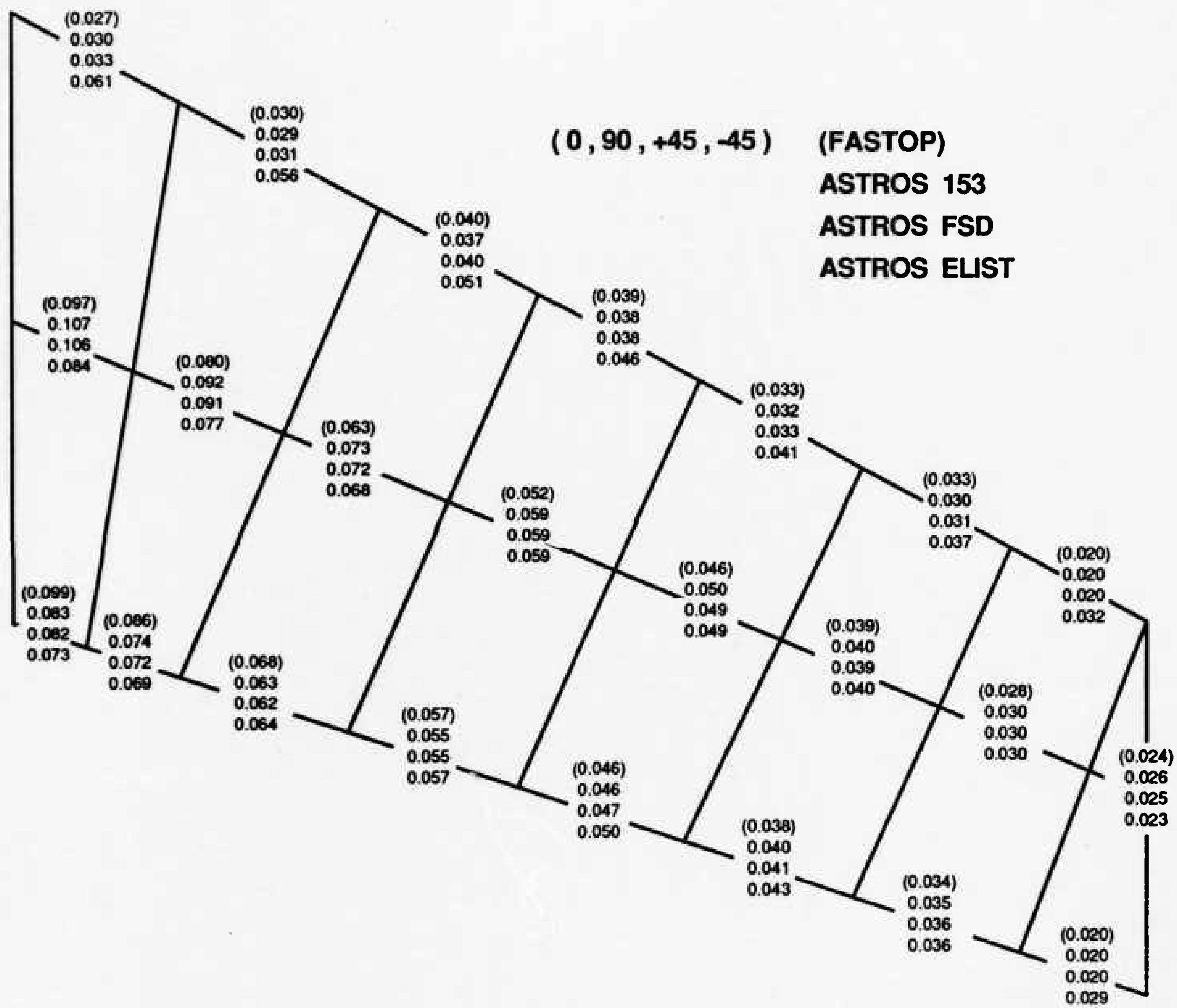

Figure 55. Final Thicknesses of Elements for the ICW Substructure

In general, however, the comparison gives confidence that the ASTROS system is functioning properly and that the final designs obtained can, in certain circumstances, be reproduced using other optimization tools.

The ASTROS result using shape function design variable linking is interesting, despite the fact that comparison data are not given. In this case, the limitations imposed by using shape functions as design variables results in the optimizer's selection of all zero degree fibers to satisfy the stress constraints. Other fiber orientations are taken to minimum gauge. This result, while still weighing more than the uniquely linked result of the first two test cases, illustrates an "optimal" solution given external constraints like manufacturing limits, limits in the rate of ply drop-off or other factors not explicitly treated by the ASTROS engineering disciplines. Further, it is obvious that the two final designs represent radically different methods of addressing the same set of physical (stress) constraints.

4.8 *THE ICW MODEL WITH STRENGTH AND FLUTTER CONSTRAINTS*

This example problem is a variation on the previous example and also allows comparison with results obtained in FASTOP-3. As before, the design problem minimizes the weight subject to the material stress allowables and gauge constraints under two static loads, but an additional requirement of a minimum flutter speed of 925 KEAS at Mach 0.80 is imposed.

4.8.1 Problem Description

This example problem introduces the flutter constraint as it is formulated in the ASTROS system. This formulation is somewhat novel in several aspects, which are fully discussed in Section X of the Theoretical Manual. In addition, the unsteady aerodynamic analyses, in terms of the selection and use of the reduced frequencies to be used in the unsteady aerodynamic influence coefficient computations and their role in the subsequent flutter analyses, is also new to this example. The reader is referred to Sections VIII and X of the Theoretical Manual for a more complete discussion of these aspects of the flutter analysis and constraint definition.

The structural model is identical to the previous example except that the structural masses are augmented by a mass model for the nonstructural mass components to properly model the flutter behavior. In addition, an unsteady aerodynamics model is defined to represent the lifting surface of the

wing and the interconnection between the aerodynamics model and the structural model is defined. The same two design models developed for the strength case alone are used in this example problem and the FSD option is applied as before to the FASTOP-like design model as an additional case.

4.8.2 Input Description

Figure 56 shows the input that is added or modified relative to the "FASTOP" version of this previous example to form the "FASTOP" version of this example. The MAPOL packet is unchanged relative to the previous problem. The solution control packet is augmented by a more complex boundary condition definition for the dynamic nature of this problem and includes multipoint constraints, a Guyan reduction set and an eigenvalue extraction method. The latter two are innovations relative to NASTRAN in that the Guyan reduction has a set identification and that the eigenvalue extraction method appears at the boundary condition level. The solution control is further modified by the appearance of a FLUTTER discipline selection which selects the corresponding FLUTTER bulk data entry with the flutter constraint applied via the DCON discipline option referring to the DCONFLT bulk data entry. The static load conditions and the associated stress constraints are identical to those in the strength design.

The bulk data additions and modifications are more pronounced and begin with additional grid points required for the dynamics portion of this model. Grid points 102 through 105 are used to define two additional rectangular coordinate systems, 2 and 3, via a CORD1R bulk data entry. Several of the CONM2 concentrated mass elements are then defined in these coordinate systems. Note that a CORD2R could have been used instead and would not have required the additional grid points. The coordinate systems are defined such that System 2 has its x-axis aligned parallel to the leading edge of the structural box while the x-axis of System 3 is parallel to the trailing edge. Additional grids 201 through 217 are used for the concentrated mass elements representing the nonstructural mass of the ICW while grid points 301 through 308 are used to give additional chordwise nodes for splining the aerodynamic forces to the structural degrees of freedom.

The boundary condition definition is more complex for this dynamic model relative to the static version of the previous example. Instead of

```
SOLUTION
TITLE = INTERMEDIATE COMPLEXITY WING
SUBTIT = QUAD4 ELEMENTS WITH 153 DESIGN VARIABLES
OPTIMIZE STRATEGY = 57
   BOUNDARY SPC = 1, MPC = 200, REDUCE= 30, METHOD = 10
      STATICS ( MECH = 1 )
      STATICS ( MECH = 2 )
      LABEL = FLUTTER SOLUTION
      FLUTTER (FLCOND=20, DCON = 1099)
END
$
$    ADDITIONAL GRID POINTS FOR COORDINATE SYSTEM DEFINITION
$
GRID          102          42.0     -12.1333 0.0             123456
GRID          103          78.0     -3.57736 0.0             123456
GRID          104          18.0     0.0      0.0             123456
GRID          105          66.0     0.0      0.0             123456
CORD1R          2      104       79      102        3     105       87      103
$
$    ADDITIONAL GRID POINTS FOR THE MASS MODEL
$
GRID       207      2      0.0      15.881   0.0      2
GRID       206      2      0.0      31.764   0.0      2
GRID       205      2      0.0      45.581   0.0      2
GRID       204      2      0.0      59.397   0.0      2
GRID       203      2      0.0      73.214   0.0      2
GRID       202      2      0.0      87.030   0.0      2
GRID       201      2      0.0      100.848  0.0      2
GRID       215      3      0.0      6.783    0.0      3
GRID       214      3      0.0      13.565   0.0      3
GRID       213      3      0.0      27.404   0.0      3
GRID       212      3      0.0      41.244   0.0      3
GRID       211      3      0.0      55.083   0.0      3
GRID       210      3      0.0      68.923   0.0      3
GRID       209      3      0.0      82.762   0.0      3
GRID       208      3      0.0      93.915   0.0      3
GRID       216             70.833   90.000   0.0
GRID       217             85.5     90.000   0.0
$
$    ADDITIONAL GRID POINTS AERODYNAMIC/STRUCTURAL SPLINING
$
GRID       301      2      0.0      121.018  0.0      2
GRID       302      3      0.0      112.698  0.0      3
GRID       303             52.5     90.0     0.0
GRID       304             107.5    90.0     0.0
GRID       305             40.264   69.740   0.0
GRID       306             98.897   45.772   0.0
GRID       307             26.364   45.663   0.0
GRID       308             93.538   18.206   0.0
$
$    SPC'S TO REPLACE THE GRDSET AND SPC'S OF THE STRENGTH MODEL
$
SPC1,     1, 123456,     79,    THRU,    88
```

Figure 56. Additions and Modifications to the Input Data Stream of Figure 51 to Include Flutter Constraints in the Design of the ICW

```
SPC1,    1,    456,     1,   THRU,    78
$
$    MODIFIED BOUNDARY CONDITIONS TO ACCOMODATE ADDITIONAL GRIDS
$
SPC1,    1,  12456,   301,   THRU,   308
SPC1,    1,      6,   201,   THRU,   217
$
$     GUYAN REDUCTION FOR MODAL ANALYSIS
$
ASET1           30       3      71      61      51      41      31     35+BC
+BC             21      11      73      63      53      43      33     25+DE
+DE             23      13       5      75      65      55      45     15
ASET1,  30,     35,    201,   THRU,   215
ASET1,  30,    345,    216,   THRU,   217
OMIT1,  30,     12,    201,   THRU,   217
$
$     MULTIPOINT CONSTRAINTS TO ATTACH MASS GRIDS AND SPLINE GRIDS
$
MPC      200      69       3      1.0     207     3       -1.0
MPC      200      70       3      1.0     207     3       -1.0
MPC      200      59       3      1.0     206     3       -1.0
MPC      200      60       3      1.0     206     3       -1.0
MPC      200      49       3      1.0     205     3       -1.0
MPC      200      50       3      1.0     205     3       -1.0
MPC      200      39       3      1.0     204     3       -1.0
MPC      200      40       3      1.0     204     3       -1.0
MPC      200      29       3      1.0     203     3       -1.0
MPC      200      30       3      1.0     203     3       -1.0
MPC      200      19       3      1.0     202     3       -1.0
MPC      200      20       3      1.0     202     3       -1.0
MPC      200       1       3      1.0     201     3       -1.0
MPC      200       2       3      1.0     201     3       -1.0
MPC      200      77       3      1.0     215     3       -1.0
MPC      200      78       3      1.0     215     3       -1.0
MPC      200      67       3      1.0     214     3       -1.0
MPC      200      68       3      1.0     214     3       -1.0
MPC      200      57       3      1.0     213     3       -1.0
MPC      200      58       3      1.0     213     3       -1.0
MPC      200      47       3      1.0     212     3       -1.0
MPC      200      48       3      1.0     212     3       -1.0
MPC      200      37       3      1.0     211     3       -1.0
MPC      200      38       3      1.0     211     3       -1.0
MPC      200      27       3      1.0     210     3       -1.0
MPC      200      28       3      1.0     210     3       -1.0
MPC      200      17       3      1.0     209     3       -1.0
MPC      200      18       3      1.0     209     3       -1.0
MPC      200       9       3      1.0     208     3       -1.0
MPC      200      10       3      1.0     208     3       -1.0
MPC      200       3       3      1.0     216     3       -1.0
MPC      200       4       3      1.0     216     3       -1.0
MPC      200       7       3      1.0     217     3       -1.0
MPC      200       8       3      1.0     217     3       -1.0
MPC      200      69      1       1.0     207     1       -.8924          +1
```

Figure 56. Additions and Modifications to the Input Data Stream of Figure 51 to Include Flutter Constraints in the Design of the ICW (Continued)

+1		207	5	-1.8500	207	2	-.4512	+2
+2		207	4	.9353				
MPC	200	70	1	1.0	207	1	-.8924	+1
+1		207	5	1.8500	207	2	-.4512	+2
+2		207	4	-.9353				
MPC	200	59	1	1.0	206	1	-.8924	+1
+1		206	5	-1.6921	206	2	-.4512	+2
+2		206	4	.8554				
MPC	200	60	1	1.0	206	1	-.8924	+1
+1		206	5	1.6921	206	2	-.4512	+2
+2		206	4	-.8554				
MPC	200	49	1	1.0	205	1	-.8924	+1
+1		205	5	-1.5546	205	2	-.4512	+2
+2		205	4	.7859				
MPC	200	50	1	1.0	205	1	-.8924	+1
+1		205	5	1.5546	205	2	-.4512	+2
+2		205	4	-.7859				
MPC	200	39	1	1.0	204	1	-.8924	+1
+1		204	5	-1.4163	204	2	-.4512	+2
+2		204	4	.7160				
MPC	200	40	1	1.0	204	1	-.8924	+1
+1		204	5	1.4163	204	2	-.4512	+2
+2		204	4	-.7160				
MPC	200	29	1	1.0	203	1	-.8924	+1
+1		203	5	-1.2789	203	2	-.4512	+2
+2		203	4	.6465				
MPC	200	30	1	1.0	203	1	-.8924	+1
+1		203	5	1.2789	203	2	-.4512	+2
+2		203	4	-.6465				
MPC	200	19	1	1.0	202	1	-.8924	+1
+1		202	5	-1.1414	202	2	-.4512	+2
+2		202	4	.5771				
MPC	200	20	1	1.0	202	1	-.8924	+1
+1		202	5	1.1414	202	2	-.4512	+2
+2		202	4	-.5771				
MPC	200	1	1	1.0	201	1	-.8924	+1
+1		201	5	-1.0040	201	2	-.4512	+2
+2		201	4	.5076				
MPC	200	2	1	1.0	201	1	-.8924	+1
+1		201	5	1.0040	201	2	-.4512	+2
+2		201	4	-.5076				
MPC	200	77	1	1.0	215	1	-.9583	+1
+1		215	5	-2.0786	215	2	-.2857	+2
+2		215	4	.6197				
MPC	200	78	1	1.0	215	1	-.9583	+1
+1		215	5	2.0786	215	2	-.2857	+2
+2		215	4	-.6197				
MPC	200	67	1	1.0	214	1	-.9583	+1
+1		214	5	-2.0010	214	2	-.2857	+2
+2		214	4	.5966				
MPC	200	68	1	1.0	214	1	-.9583	+1
+1		214	5	2.0010	214	2	-.2857	+2
+2		214	4	-.5966				

Figure 56. Additions and Modifications to the Input Data Stream of Figure 51 to Include Flutter Constraints in the Design of the ICW (Continued)

MPC	200	57	1	1.0	213	1	-.9583	+1
+1		213	5	-1.8419	213	2	-.2857	+2
+2		213	4	.5491				
MPC	200	58	1	1.0	213	1	-.9583	+1
+1		213	5	1.8419	213	2	-.2857	+2
+2		213	4	-.5491				
MPC	200	47	1	1.0	212	1	-.9583	+1
+1		212	5	-1.6828	212	2	-.2857	+2
+2		212	4	.5017				
MPC	200	48	1	1.0	212	1	-.9583	+1
+1		212	5	1.6828	212	2	-.2857	+2
+2		212	4	-.5017				
MPC	200	37	1	1.0	211	1	-.9583	+1
+1		211	5	-1.5237	211	2	-.2857	+2
+2		211	4	.4543				
MPC	200	38	1	1.0	211	1	-.9583	+1
+1		211	5	1.5237	211	2	-.2857	+2
+2		211	4	-.4543				
MPC	200	27	1	1.0	210	1	-.9583	+1
+1		210	5	-1.3646	210	2	-.2857	+2
+2		210	4	.4069				
MPC	200	28	1	1.0	210	1	-.9583	+1
+1		210	5	1.3646	210	2	-.2857	+2
+2		210	4	-.4069				
MPC	200	17	1	1.0	209	1	-.9583	+1
+1		209	5	-1.2065	209	2	-.2857	+2
+2		209	4	.3597				
MPC	200	18	1	1.0	209	1	-.9583	+1
+1		209	5	1.2065	209	2	-.2857	+2
+2		209	4	-.3597				
MPC	200	9	1	1.0	208	1	-.9583	+1
+1		208	5	-1.0781	208	2	-.2857	+2
+2		208	4	.3214				
MPC	200	10	1	1.0	208	1	-.9583	+1
+1		208	5	1.0781	208	2	-.2857	+2
+2		208	4	-.3214				
MPC	200	3	1	1.0	216	1	-1.0	+1
+1		216	5	-1.313				
MPC	200	4	1	1.0	216	1	-1.0	+1
+1		216	5	1.313				
MPC	200	7	1	1.0	217	1	-1.0	+1
+1		217	5	-1.313				
MPC	200	8	1	1.0	217	1	-1.0	+1
+1		217	5	1.313				
MPC	200	69	2	1.0	207	2	-.8924	+1
+1		207	1	.4512	207	5	.9353	+2
+2		207	4	1.8500				
MPC	200	70	2	1.0	207	2	-.8924	+1
+1		207	1	.4512	207	5	-.9353	+2
+2		207	4	-1.8500				
MPC	200	59	2	1.0	206	2	-.8924	+1
+1		206	1	.4512	206	5	.8554	+2
+2		206	4	1.6921				

Figure 56. Additions and Modifications to the Input Data Stream of Figure 51 to Include Flutter Constraints in the Design of the ICW (Continued)

MPC	200	60	2	1.0	206	2	-.8924	+1
+1		206	1	.4512	206	5	-.8554	+2
+2		206	4	-1.6921				
MPC	200	49	2	1.0	205	2	-.8924	+1
+1		205	1	.4512	205	5	.7859	+2
+2		205	4	1.5546				
MPC	200	50	2	1.0	205	2	-.8924	+1
+1		205	1	.4512	205	5	-.7859	+2
+2		205	4	-1.5546				
MPC	200	39	2	1.0	204	2	-.8924	+1
+1		204	1	.4512	204	5	.7160	+2
+2		204	4	1.4163				
MPC	200	40	2	1.0	204	2	-.8924	+1
+1		204	1	.4512	204	5	-.7160	+2
+2		204	4	-1.4163				
MPC	200	29	2	1.0	203	2	-.8924	+1
+1		203	1	.4512	203	5	.6465	+2
+2		203	4	1.2789				
MPC	200	30	2	1.0	203	2	-.8924	+1
+1		203	1	.4512	203	5	-.6465	+2
+2		203	4	-1.2789				
MPC	200	19	2	1.0	202	2	-.8924	+1
+1		202	1	.4512	202	5	.5771	+2
+2		202	4	1.1414				
MPC	200	20	2	1.0	202	2	-.8924	+1
+1		202	1	.4512	202	5	-.5771	+2
+2		202	4	-1.1414				
MPC	200	1	2	1.0	201	2	-.8924	+1
+1		201	1	.4512	201	5	.5076	+2
+2		201	4	1.0040				
MPC	200	2	2	1.0	201	2	-.8924	+1
+1		201	1	.4512	201	5	-.5076	+2
+2		201	4	-1.0040				
MPC	200	77	2	1.0	215	2	-.9583	+1
+1		215	1	.2857	215	5	.6197	+2
+2		215	4	2.0786				
MPC	200	78	2	1.0	215	2	-.9583	+1
+1		215	1	.2857	215	5	-.6197	+2
+2		215	4	-2.0786				
MPC	200	67	2	1.0	214	2	-.9583	+1
+1		214	1	.2857	214	5	.5966	+2
+2		214	4	2.0010				
MPC	200	68	2	1.0	214	2	-.9583	+1
+1		214	1	.2857	214	5	-.5966	+2
+2		214	4	-2.0010				
MPC	200	57	2	1.0	213	2	-.9583	+1
+1		213	1	.2857	213	5	.5491	+2
+2		213	4	1.8419				
MPC	200	58	2	1.0	213	2	-.9583	+1
+1		213	1	.2857	213	5	-.5491	+2
+2		213	4	-1.8419				
MPC	200	47	2	1.0	212	2	-.9583	+1
+1		212	1	.2857	212	5	.5017	+2

Figure 56. Additions and Modifications to the Input Data Stream of Figure 51 to Include Flutter Constraints in the Design of the ICW (Continued)

+2		212	4	1.6828				
MPC	200	48	2	1.0	212	2	-.9583	+1
+1		212	1	.2857	212	5	-.5017	+2
+2		212	4	-1.6828				
MPC	200	37	2	1.0	211	2	-.9583	+1
+1		211	1	.2857	211	5	.4543	+2
+2		211	4	1.5237				
MPC	200	38	2	1.0	211	2	-.9583	+1
+1		211	1	.2857	211	5	-.4543	+2
+2		211	4	-1.5237				
MPC	200	27	2	1.0	210	2	-.9583	+1
+1		210	1	.2857	210	5	.4069	+2
+2		210	4	1.3646				
MPC	200	28	2	1.0	210	2	-.9583	+1
+1		210	1	.2857	210	5	-.4069	+2
+2		210	4	-1.3646				
MPC	200	17	2	1.0	209	2	-.9583	+1
+1		209	1	.2857	209	5	.3597	+2
+2		209	4	1.2065				
MPC	200	18	2	1.0	209	2	-.9583	+1
+1		209	1	.2857	209	5	-.3597	+2
+2		209	4	-1.2065				
MPC	200	9	2	1.0	208	2	-.9583	+1
+1		208	1	.2857	208	5	.3214	+2
+2		208	4	1.0781				
MPC	200	10	2	1.0	208	2	-.9583	+1
+1		208	1	.2857	208	5	-.3214	+2
+2		208	4	-1.0781				
MPC	200	3	2	1.0	216	2	-1.0	+1
+1		216	4	1.3130				
MPC	200	4	2	1.0	216	2	-1.0	+1
+1		216	4	-1.3130				
MPC	200	7	2	1.0	217	2	-1.0	+1
+1		217	4	1.3130				
MPC	200	8	2	1.0	217	2	-1.0	+1
+1		217	4	-1.3130				
MPC	200	301	3	1.0	201	3	-1.0	+1
+1		201	4	-20.170				
MPC	200	302	3	1.0	208	3	-1.0	+1
+1		208	4	-18.783				
MPC	200	303	3	1.0	201	3	-1.0	+1
+1		201	4	4.963	201	5	-9.817	
MPC	200	304	3	1.0	208	3	-1.0	+1
+1		208	4	-4.191	208	5	13.089	
MPC	200	305	3	1.0	203	3	-1.0	+1
+1		203	4	.861	203	5	-10.734	
MPC	200	306	3	1.0	211	3	-1.0	+1
+1		211	4	1.684	211	5	17.076	
MPC	200	307	3	1.0	205	3	-1.0	+1
+1		205	4	1.054	205	5	-13.139	
MPC	200	308	3	1.0	213	3	-1.0	+1
+1		213	4	1.934	213	5	19.613	
$								

Figure 56. Additions and Modifications to the Input Data Stream of Figure 51 to Include Flutter Constraints in the Design of the ICW (Continued)

```
$
$    MASS MODEL AND EIGENVALUE EXTRACTION METHOD DEFINITION
$
EIGR    10      GIV                                     6
CONVERT MASS     .00259
CONM2           1       207       2 20.50  -1.904                        +1
+1                              224.
CONM2           2       206       2 9.729  -1.646                        +1
+1                              83.
CONM2           3       205       2 7.481  -1.5                          +1
+1                              32.
CONM2           4       204       2 7.573  -1.5                          +1
+1                              27.
CONM2           5       203       2 3.657  -1.25                         +1
+1                              19.
CONM2           6       202       2 3.729  -1.25                         +1
+1                              19.
CONM2           7       201       2 4.479                                +1
+1                              20.
CONM2           8        71         3.69
CONM2           9        61         3.049
CONM2          10        51         2.619
CONM2          11        41         2.278
CONM2          12        31         2.432
CONM2          13        21         1.565
CONM2          14        11         0.46
CONM2          15       216         1.911   2.975   3.5                  +1
+1      33.                     36.
CONM2          16        73         5.323
CONM2          17        63         4.178
CONM2          18        53         3.067
CONM2          19        43         2.795
CONM2          20        33         3.097
CONM2          21        23         2.915
CONM2          22        13         0.65
CONM2          23         5         1.871
CONM2          24        75         5.116
CONM2          25        65         4.065
CONM2          26        55         2.5
CONM2          27        45         2.342
CONM2          28        35         2.155
CONM2          29        25         1.965
CONM2          30        15         0.098
CONM2          31       217         1.869   2.465   4.0                  +1
+1      15.                     35.
CONM2          32       215       3 6.86    3.718                        +1
+1                              26.
CONM2          33       214       3 6.455   3.425                        +1
+1                              44.
CONM2          34       213       3 6.188   3.425                        +1
+1                              14.
CONM2          35       212       3 6.083   3.0                          +1
+1                              27.
```

Figure 56. Additions and Modifications to the Input Data Stream of Figure 51 to Include Flutter Constraints in the Design of the ICW (Continued)

```
CONM2           36      211             3 5.341  3.0                              +1
+1                               26.
CONM2           37      210             3 4.542  2.0                              +1
+1                               50.
CONM2           38      209             3 2.717  3.3333                           +1
+1                               37.
CONM2           39      208             3 2.889  5.0                              +1
+1                               5.
$
$
$    UNSTEADY AERO MODEL
$
AERO            48.0    1.147E-7
CAERO1  10                                      100     200     1       +CA1
+CA1    0.0     0.0     0.0     90.0    63.0    108.0   0.0     48.0
AEFACT  100     0.0     0.150   0.300   0.400   0.500   0.600   0.700   +AE1
+AE1    0.800   0.900   1.000
AEFACT  200     0.0     0.095   0.190   0.286   0.429   0.572   0.715   +AE2
+AE2    0.858   1.0
$
$     AERO-STRUCTURAL INTERCONNECTION
$
SPLINE1 30              10      10      49      40      10.0
SPLINE1 40              10      50      81      60      10.0
SET1    60      1       3       5       7       9       11      13      +ST1
+ST1    15      17      19      21      23      25      27      29      +ST2
+ST2    31      33      35      37      301     302     303     304     +ST3
+ST3    305     306
SET1    40      19      21      23      25      27      29      31      +S41
+S41    33      35      37      39      41      43      45      47      +S42
+S42    49      51      53      55      57      59      61      63      +S43
+S43    65      67      69      71      73      75      77      79      +S44
+S44    81      83      85      87      305     306     307     308
$
$      M-K PAIR DEFINITIONS
$
MKAERO1 1               0.80                                            +MK1
+MK1    0.0001  0.13333 0.1818  .3000   0.40    1.00    2.00
$
$     FLUTTER FLIGHT CONDITION
$
FLUTTER 20      PK      20      30      40                              +FL1
+FL1     1
$
$     DENSITY RATIOS
$
FLFACT  20      1.0
$
$     MACH NUMBERS
$
FLFACT  30      0.8
$
$     VELOCITIES (IN KNOTS, CONVERTED TO CONSISTENT UNITS)
```

Figure 56. Additions and Modifications to the Input Data Stream of Figure 51 to Include Flutter Constraints in the Design of the ICW (Continued)

```
$
FLFACT  40      500.0   750.0   850.0   900.0   925.0
CONVERT VELOCITY 20.23
$
$    FLUTTER CONSTRAINT
$
DCONFLT 1099            0.0     0.0     1.0E7   0.0
```

Figure 56. Additions and Modifications to the Input Data Stream of Figure 51 to Include Flutter Constraints in the Design of the ICW (Concluded)

using a GRDSET bulk data entry to restrain all the rotational degrees of freedom, the GRDSET and SPC1 entries that defined the cantilever condition are now replaced with SPC1 entries alone. This modification is made because the rotational properties of the mass elements are necessary for the flutter model and, therefore, the rotational degrees of freedom for the additional mass element grid points must be left unrestrained. Additional SPC entries are then used to restrain all but the out-of-plane displacements for the splining points and the in-plane rotations for the mass element points. The real eigenanalysis for the modal flutter analysis requires a selection of an "analysis set." A reduction is required since the ASTROS implementation of the Givens Method of eigenvalue extraction requires that the mass matrix be positive definite. The analysis set is defined by ASET1 and OMIT1 entries with set identification 30. All the out-of-plane displacements on the structural box and the mass grid points are retained as well as the rotations about the x and y axis of the local coordinate system (either 2 or 3) for the mass points. The x and y displacements are explicitly omitted for the mass points. Since the analysis set is defined by a combination of ASET and OMIT bulk data entries, any degree of freedom not explicitly appearing on a reduction bulk data entry will be omitted. In this case, then, the OMIT1 entry is redundant.

The last additional input for the boundary condition definition is the multipoint constraint set definition. These bulk data entries rigidly attach the mass points and the out-of-plane displacements at the spline points (i.e., GRIDs 301 through 308) to the nearby structural box nodes. Note that the additional grid points are not used as the dependent degrees of freedom

since the out-of-plane deflections of these nodes are important in the solution. Instead, one of the nearby structural degrees of freedom is selected to be the dependent degree of freedom in each multipoint constraint relation.

The modified boundary condition definition is followed by the mass model and eigenvalue extraction data. The EIGR bulk data entry defines the extraction parameters referred to by the Solution Control "BOUNDARY METHOD=n" option. It selects that six eigenvectors be computed to be used in the flutter analysis. In ASTROS the flutter analysis discipline requires the EIGR specification in both the Solution Control and the Bulk Data since a modal flutter analysis will be performed. The absence of either specification will cause termination. Following the EIGR input are the CONM2 bulk data entries defining the nonstructural masses. A CONVERT bulk data entry specifies the conversion between the input "mass" units and the true mass units. In this case, the masses are input in pounds (weight) and the conversion factor converts these inputs to consistent mass units (0.00259 = 1.0 / (32.2 * 12.0)).

The remainder of the bulk data additions define the unsteady aerodynamics model, the aerostructural connectivity and the flutter analysis and constraint definition. The aerodynamic geometry is very simple in this problem with a single CAERO1 aerodynamic macroelement (or panel) defining the lifting surface. The macroelement is subdivided into boxes using AEFACT entry 100 for the spanwise cuts (in fractions of the macroelement span) and entry 200 for the chordwise cuts (in fractions of the macroelement chord). The AERO entry defines the reference chord length and the reference air density in consistent units. Note that the air density is not subject to the CONVERT/ MASS parameter and must, therefore, be input in consistent mass units. In this case, the reference air density is that of the sea level standard atmosphere.

The aerostructural interconnection is defined through the use of two surface splines defined by SPLINE1 bulk data entries. The inboard aerodynamic boxes (10 through 49) comprise one spline and the output boxes (50 through 81) comprise the second. The box numbering for the unsteady aerodynamic boxes is such that the root leading edge of the macroelement is given the macroelement identification number and the subsequent boxes are numbered sequentially in chordwise strips from leading to trailing edge, root to tip. In this case, the 72 boxes are numbered 10 to 81 since the CAERO1 entry is given identification number 10. The structural points to which these two splines are attached

are listed on the SET1 bulk data entries 40 and 60, respectively. Both splines are attached to a subset of the 300 series of added splining nodes.

The MKAERO1 bulk data entry defines the set of reduced frequencies, Mach numbers and symmetry options for which the unsteady aerodynamic influence coefficients will be computed in the aerodynamics preface (design independent) modules. In this simple case, a single symmetric boundary condition with the 0.80 Mach number is selected with a range of reduced frequencies sufficient to cover the range of expected frequencies. As a general rule, the lowest reduced frequency should be lower than that resulting from the combination of the lowest natural frequency and the highest selected flutter velocity and the highest reduced frequency should be higher than the combination of highest natural frequency and the lowest flutter velocity.

The remaining input entries define the flutter analysis. Most input fields on the FLUTTER bulk data entry refer to FLFACT bulk data entries defining the density ratio(s) relative to the reference density on the AERO entry, the Mach number(s) and the velocities. In this case, there is only one Mach number, one density and five flutter velocities. The highest velocity is that of the required flutter speed to ensure that the flutter requirement of 925 KEAS is just satisfied. Since the velocities are entered in knots, a CONVERT/VELOCITY factor is used to convert to consistent velocity units (inches/sec). Finally, the DCONFLT bulk data entry referenced by Solution Control defines the required damping values for the range of velocities. In this case, the requirement states that the damping be less than or equal to zero for all velocities. The actual maximum required velocity is an indirect input in that it appears as a velocity at which a p-k flutter analysis will be performed, whereas the constraint applies to all the computed flutter roots in a generic fashion.

4.8.3 Results and Output Description

Figure 57(a) shows the design iteration history for the FASTOP comparison case, Figure 57(b) the case with FASTOP-like linking, but using leading FSD cycles and Figure 57(c) the case using shape function linking. The FSD case produces results that are nearly identical to the baseline 153 design variable case (as expected), while the shape function linked design weighs significantly more than the first two cases (15.4 percent) due to the reduced freedom granted the optimizer through limiting the number and nature

A S T R O S   D E S I G N   I T E R A T I O N   H I S T O R Y

ITERATION NUMBER	OBJECTIVE FUNCTION VALUE	NUMBER FUNCTION EVAL	NUMBER GRADIENT EVAL	NUMBER RETAINED CONSTRAINTS	NUMBER ACTIVE CONSTRAINTS	NUMBER VIOLATED CONSTRAINTS	NUMBER LOWER BOUNDS	NUMBER UPPER BOUNDS	APPROXIMATE PROBLEM CONVERGENCE
1	1.76326E+02	0	0	0	0	0	0	0	NOT CONVERGED
2	8.96750E+01	252	45	153	10	0	0	140	NOT CONVERGED
3	5.67406E+01	335	67	153	26	0	0	89	NOT CONVERGED
4	4.22059E+01	229	49	153	36	0	0	71	NOT CONVERGED
5	3.74484E+01	74	48	153	35	0	0	12	NOT CONVERGED
6	3.48906E+01	176	53	153	44	0	0	41	NOT CONVERGED
7	3.38777E+01	83	44	153	47	0	0	51	NOT CONVERGED
8	3.33712E+01	91	36	153	50	0	0	59	NOT CONVERGED
9	3.32507E+01	23	11	153	34	0	0	59	CONVERGED

THE FINAL OBJECTIVE FUNCTION VALUE IS:

FIXED = 1.60233E+02

\+ DESIGNED = 3.32507E+01

TOTAL = 1.93484E+02

(a) Mathematical Programming Only

A S T R O S   D E S I G N   I T E R A T I O N   H I S T O R Y

ITERATION NUMBER	OBJECTIVE FUNCTION VALUE	NUMBER FUNCTION EVAL	NUMBER GRADIENT EVAL	NUMBER RETAINED CONSTRAINTS	NUMBER ACTIVE CONSTRAINTS	NUMBER VIOLATED CONSTRAINTS	NUMBER LOWER BOUNDS	NUMBER UPPER BOUNDS	APPROXIMATE PROBLEM CONVERGENCE
1	1.76326E+02	0	0	0	0	0	0	0	NOT CONVERGED
2	3.62432E+01	0	0	444	0	0	213	0	NOT CONVERGED
3	3.14308E+01	0	0	444	0	0	253	0	NOT CONVERGED
4	3.15597E+01	0	0	444	0	0	273	0	CONVERGED
5	3.48873E+01	128	47	153	38	0	2	58	NOT CONVERGED
6	3.38443E+01	117	22	153	38	0	0	62	NOT CONVERGED
7	3.33433E+01	95	25	153	44	0	0	64	NOT CONVERGED
8	3.31684E+01	25	13	153	33	0	0	66	NOT CONVERGED
9	3.31531E+01	14	5	153	40	0	0	67	CONVERGED

THE FINAL OBJECTIVE FUNCTION VALUE IS:

FIXED = 1.60233E+02

\+ DESIGNED = 3.31531E+01

TOTAL = 1.93386E+02

(b) Fully-Stressed Design Plus Mathematical Programming

Figure 57. Design Iteration Histories for the ICW with Flutter Constraints

A S T R O S   D E S I G N   I T E R A T I O N   H I S T O R Y

ITERATION NUMBER	OBJECTIVE FUNCTION VALUE	NUMBER FUNCTION EVAL	NUMBER GRADIENT EVAL	NUMBER RETAINED CONSTRAINTS	NUMBER ACTIVE CONSTRAINTS	NUMBER VIOLATED CONSTRAINTS	NUMBER LOWER BOUNDS	NUMBER UPPER BOUNDS	APPROXIMATE PROBLEM CONVERGENCE
1	1.76326E+02	0	0	0	0	0	0	0	NOT CONVERGED
2	8.96807E+01	49	24	114	42	0	2	0	NOT CONVERGED
3	5.56570E+01	60	31	114	35	0	2	0	NOT CONVERGED
4	4.22251E+01	58	26	112	36	0	2	0	NOT CONVERGED
5	3.87491E+01	126	22	112	30	0	2	0	NOT CONVERGED
6	4.09510E+01	80	18	111	22	0	2	0	NOT CONVERGED
7	3.98051E+01	58	31	95	22	0	2	0	NOT CONVERGED
8	3.93650E+01	69	31	99	27	0	2	0	NOT CONVERGED
9	3.87216E+01	88	22	99	22	0	2	0	NOT CONVERGED
10	3.82339E+01	54	15	98	22	0	2	0	NOT CONVERGED
11	3.81411E+01	118	28	98	25	0	2	0	CONVERGED
12	3.80071E+01	84	23	97	26	0	2	0	CONVERGED
13	3.84140E+01	39	10	97	16	0	2	0	NOT CONVERGED
14	3.83813E+01	39	16	98	21	0	2	0	CONVERGED

THE FINAL OBJECTIVE FUNCTION VALUE IS:

FIXED =	1.60233E+02
+ DESIGNED =	3.83813E+01
TOTAL =	1.98614E+02

(c) Shape Function Linking

Figure 57. Design Iteration Histories for the ICW with Flutter Constraints (Concluded)

of the design variables. The FASTOP result to which these designs are compared weighed 44.0 pounds. This number is significantly higher than the 33.25 pounds obtained by the equivalent ASTROS model.

Figure 58 shows the local element ply counts from FASTOP and from each ASTROS ICW test case for the composite wing skins. The substructure results are not available for the FASTOP results with the flutter requirement and so the ASTROS results are not shown. Unlike the previous sample problem with strength constraints alone, the ply counts in **Figure 58** show little agreement between ASTROS and FASTOP. The ASTROS result is significantly lighter, even when the restrictive shape function variables are used. There are several possible explanations for the differences. First, and most important, is that ASTROS treats the strength and flutter constraints simultaneously at each iteration whereas the FASTOP algorithm treats each constraint type sequentially and applies ad-hoc move limits on "flutter critical" and

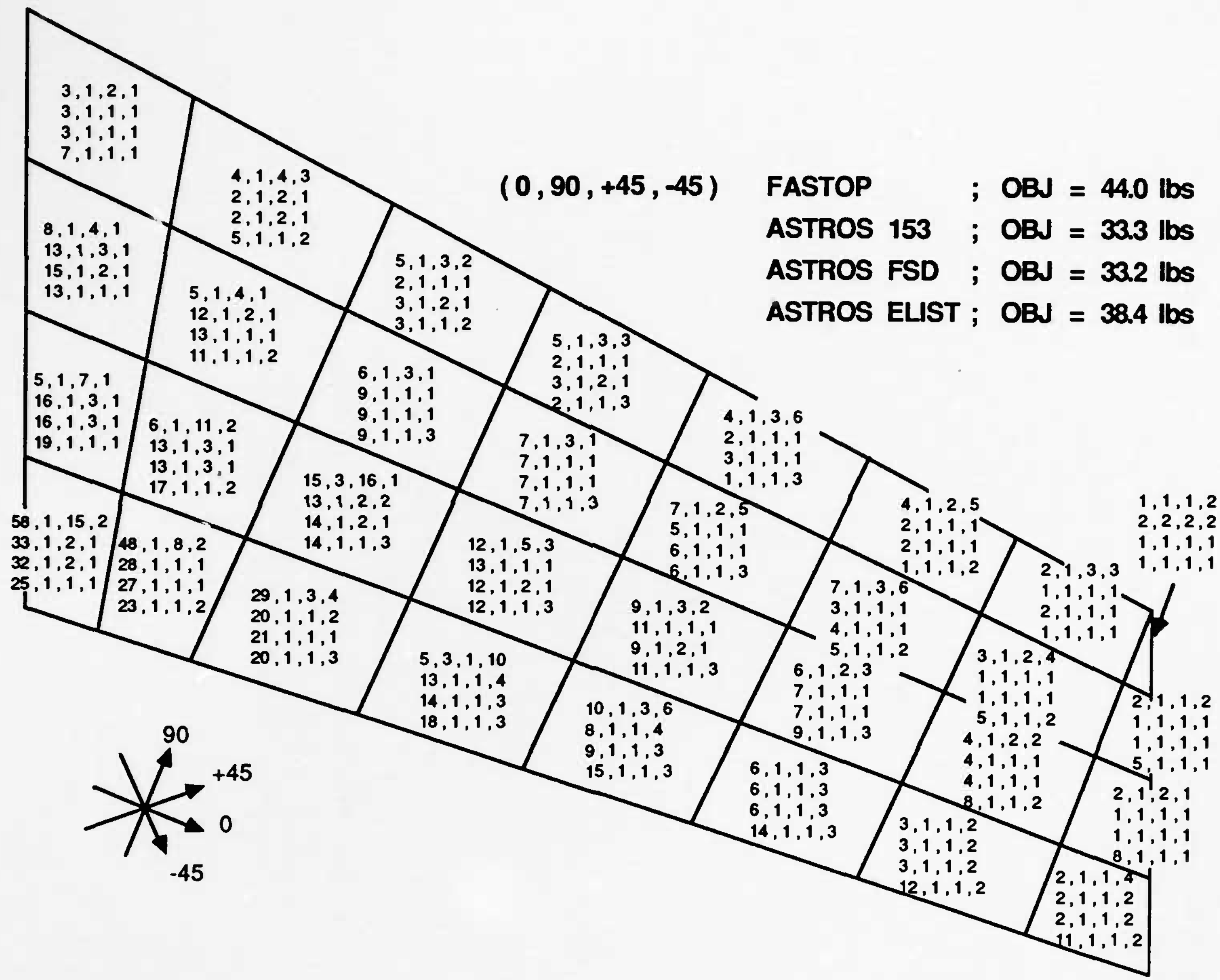

Figure 58. Final Ply Counts for the ICW Cover Skins when Flutter Constraints are Included

"strength critical" elements in between each cycle. Such an algorithm does not necessarily lead to an optimal solution. A second important factor is that the two systems use different methods to couple the aerodynamic and structural deflections and may, therefore, produce different flutter results for the same model.

The ASTROS result using shape function design variable linking is interesting, despite the lack of comparison data. In this case, the limitations imposed by using shape functions as design variables results in the smearing of the zero degree fibers over a greater area around the aft inboard root section, which is obviously important in controlling the flutter behavior. As a result, there are fewer zero degree plies along the inboard trailing edge in the shape function linked model, but more plies ahead of the trailing edge and extending further out the span. This result, as in the previous example, illustrates an alternative "optimal" solution. In this case, however, it is not clear that the resultant final design represents a different mechanism for controlling the same set of constraints. It appears, instead, to be the optimal application of the same mechanism (increasing aft inboard zero degree plies) under the restrictions imposed by the available shapes.

4.9 AGARD TEST CASE

This test case exercises several of the more advanced features of ASTROS, including direct matrix input and a significantly modified MAPOL sequence, to perform a flutter analysis of simple wind tunnel model. A similar test case was performed by the Air Force and is extensively documented in:

> French, M. and Canfield, R.A., "Flutter Analysis with ASTROS Using Measured Modal Data," AFWAL-TM-173-FIBR, April 1988.

4.9.1 Problem Description

The AGARD Structures and Materials Panel is in the process of establishing standard test cases that can be used to evaluate existing codes for aeroelastic analysis. The first candidate structure has been defined and is documented in:

> Yates, E. Carson, Jr., "AGARD Standard Configurations for Dynamic Response, Candidate Configuration I - Wing 445.6," NASA TM-100492, August 1987.

Figure 59 is taken from the appendix to this NASA report and indicates the geometry of the wind tunnel model used for this test case. A large amount of test data from several wind tunnel tests are available on this model, making it an ideal test case. The structural data for this model are given in terms of modal frequencies and mode shapes. This is contrary to the standard ASTROS practice of determining these data based on the physical properties of the structure. However, it is possible to readily accommodate this type of data in ASTROS and the key feature of this example is to indicate how this is done.

4.9.2 Input

The input packet for this test case is given in **Figure 60**. The standard MAPOL sequence is extensively modified for this case and could easily have been replaced completely. The shell of the sequence was of use, however, and was retained. The first modification declares two matrix entities. MODES defines the measured structural modes while KFLUT is the user defined generalized stiffness matrix. The deletion of MAPOL lines 196 through 215 removes all the preface operations that define the structural mass and stiffness properties in the standard sequence. The calculations for the aerodynamic entities are retained from the standard MAPOL sequence, but all ensuing calculations are replaced by the four MAPOL statements that are required to complete the flutter analysis. The call to NREDUCE partitions the unsteady spline matrix from the g-set to the f-set required by the input structural modes. The call to REIG is solely for the purpose of filling the LAMBDA relation with eigenvalue data that are required by the flutter analysis. The REIG module normally performs the modal analysis, but in this case, the modal data are contained in the bulk data packet. The call to QHHLGEN produces the generalized aerodynamic forces while the FLUTTRAN call performs the flutter analysis.

The solution control input is very simple for this case in that there is a single analysis boundary condition and two disciplines (modes and flutter) within that boundary condition.

The MODES discipline is included in order to obtain a print of the input model shapes. The bulk data begins with the input of grid data on an 11 by 11 mesh. Permanent SPCs restrain all but the out-of-plane displacement. The DMI bulk data entry is used to input the five normal mode vectors that are given in the referenced NASA report. Each mode has 121 degrees of freedom corresponding to the 121 grid points. This is followed by a standard EIGR

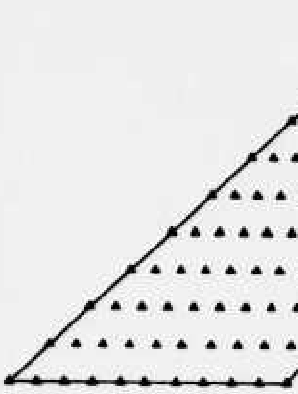

(a) Joint locations

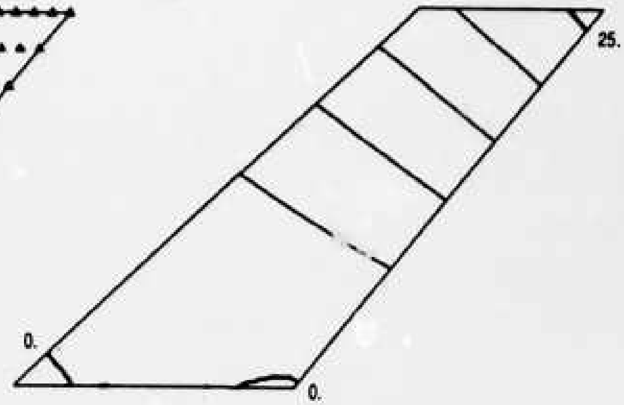

(b) Mode 1, f_1 = 14.1201 Hz

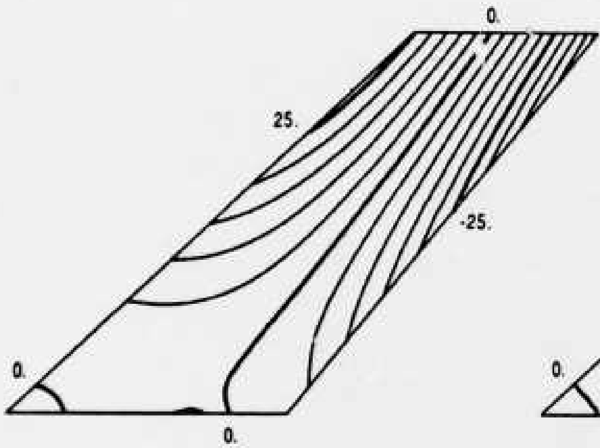

(c) Mode 2, f_2 = 50.9125 Hz

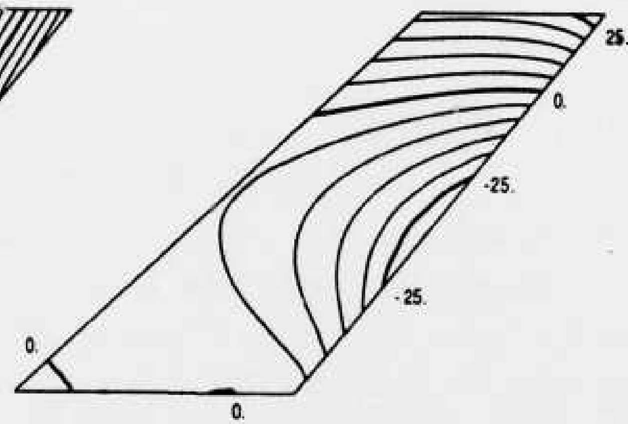

(d) Mode 3, f_3 = 68.9416 Hz

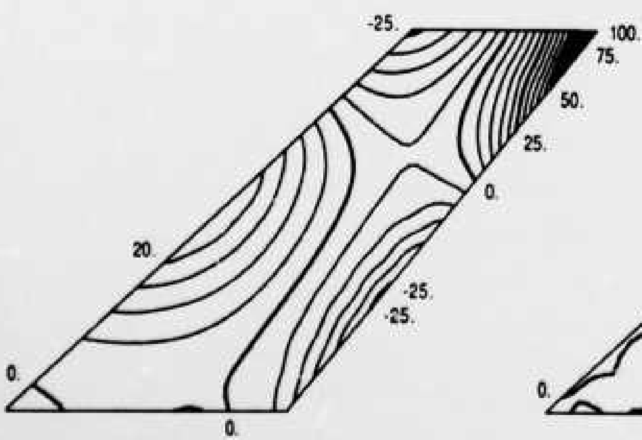

(e) Mode 4, f_4 = 122.2556 Hz

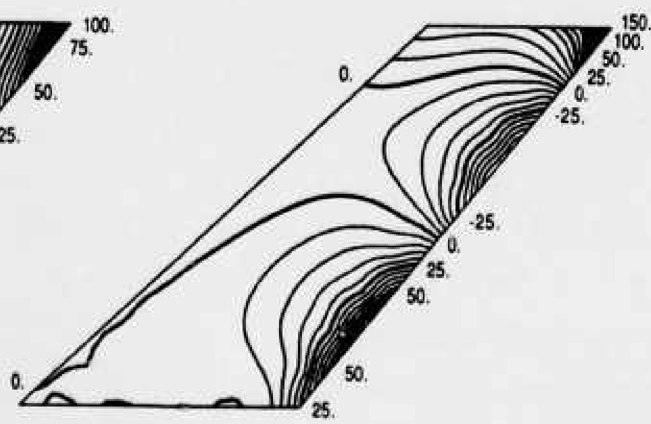

(f) Mode 5, f_5 = 160.5292 Hz

Figure 59. Planform of the AGARD Standard Configuration for Aeroelastic Analysis

```
ASSIGN DATABASE WEAK KIMBERLY NEW DELETE
EDIT NOLIST
INSERT 7
MATRIX [MODES], [KFLUT];
DELETE 196, 215
REPLACE 224, 1528
CALL NREDUCE ( , [UGTKG], [PNSF(1)], , , , , [UGTKA] );
CALL REIG ( 1, [KAA], [MAA], , , LAMBDA, [PHIA], [MII], HSIZE );
CALL QHHLGEN (1,[QKKL],[QKJL],[UGTKA],[MODES],[PHIKH],[QHHL(1)],[QHJL] );
CALL FLUTTRAN ( 1, [QHHL(1)], LAMBDA, HSIZE, [MAA], [KFLUT], 1);
SOLUTION
TITLE = AGARD TEST CASE
ANALYZE
   PRINT ROOT = ALL, MODE ALL
   BOUNDARY METHOD =10
     MODES
     LABEL = WEAK MODES
     FLUTTER (FLCOND = 1)
END
BEGIN BULK
$
GRID     1            0.0     0.0     0.0             12456
GRID     2            2.196   0.0     0.0             12456
GRID     3            4.392   0.0     0.0             12456
GRID     4            6.588   0.0     0.0             12456
GRID     5            8.784   0.0     0.0             12456
GRID     6            10.75   0.0     0.0             12456
GRID     7            13.17   0.0     0.0             12456
GRID     8            15.37   0.0     0.0             12456
GRID     9            17.56   0.0     0.0             12456
GRID     10           19.76   0.0     0.0             12456
GRID     11           21.96   0.0     0.0             12456
$
GRID     12           3.1866  3.0     0.0             12456
GRID     13           5.3079  3.0     0.0             12456
GRID     14           7.4293  3.0     0.0             12456
GRID     15           9.5506  3.0     0.0             12456
GRID     16           11.672  3.0     0.0             12456
GRID     17           13.650  3.0     0.0             12456
GRID     18           15.914  3.0     0.0             12456
GRID     19           18.036  3.0     0.0             12456
GRID     20           20.157  3.0     0.0             12456
GRID     21           22.278  3.0     0.0             12456
GRID     22           24.400  3.0     0.0             12456
$
GRID     23           6.3732  6.0     0.0             12456
GRID     24           8.4199  6.0     0.0             12456
GRID     25           10.466  6.0     0.0             12456
GRID     26           12.513  6.0     0.0             12456
GRID     27           14.560  6.0     0.0             12456
GRID     28           16.600  6.0     0.0             12456
GRID     29           18.653  6.0     0.0             12456
GRID     30           20.700  6.0     0.0             12456
```

Figure 60. Input Data Stream for the Standard AGARD Configuration

```
GRID    31          22.744  6.0     0.0             12456
GRID    32          24.793  6.0     0.0             12456
GRID    33          26.840  6.0     0.0             12456
$
GRID    34          9.5598  9.0     0.0             12456
GRID    35          11.531  9.0     0.0             12456
GRID    36          13.504  9.0     0.0             12456
GRID    37          15.476  9.0     0.0             12456
GRID    38          17.448  9.0     0.0             12456
GRID    39          19.500  9.0     0.0             12456
GRID    40          21.392  9.0     0.0             12456
GRID    41          23.364  9.0     0.0             12456
GRID    42          25.336  9.0     0.0             12456
GRID    43          27.308  9.0     0.0             12456
GRID    44          29.280  9.0     0.0             12456
$
GRID    45          12.746  12.0    0.0             12456
GRID    46          14.643  12.0    0.0             12456
GRID    47          16.541  12.0    0.0             12456
GRID    48          18.438  12.0    0.0             12456
GRID    49          20.336  12.0    0.0             12456
GRID    50          22.300  12.0    0.0             12456
GRID    51          24.131  12.0    0.0             12456
GRID    52          26.028  12.0    0.0             12456
GRID    53          27.925  12.0    0.0             12456
GRID    54          29.823  12.0    0.0             12456
GRID    55          31.720  12.0    0.0             12456
$
GRID    56          15.933  15.0    0.0             12456
GRID    57          17.755  15.0    0.0             12456
GRID    58          19.578  15.0    0.0             12456
GRID    59          21.401  15.0    0.0             12456
GRID    60          23.224  15.0    0.0             12456
GRID    61          25.200  15.0    0.0             12456
GRID    62          26.869  15.0    0.0             12456
GRID    63          28.692  15.0    0.0             12456
GRID    64          30.515  15.0    0.0             12456
GRID    65          32.338  15.0    0.0             12456
GRID    66          34.161  15.0    0.0             12456
$
GRID    67          19.119  18.0    0.0             12456
GRID    68          20.867  18.0    0.0             12456
GRID    69          22.615  18.0    0.0             12456
GRID    70          24.364  18.0    0.0             12456
GRID    71          26.112  18.0    0.0             12456
GRID    72          28.100  18.0    0.0             12456
GRID    73          29.609  18.0    0.0             12456
GRID    74          31.356  18.0    0.0             12456
GRID    75          33.105  18.0    0.0             12456
GRID    76          34.853  18.0    0.0             12456
GRID    77          36.601  18.0    0.0             12456
$
GRID    78          22.306  21.0    0.0             12456
```

Figure 60. Input Data Stream for the Standard AGARD Configuration (Continued)

```
GRID    79              23.979  21.0    0.0             12456
GRID    80              25.653  21.0    0.0             12456
GRID    81              27.327  21.0    0.0             12456
GRID    82              29.000  21.0    0.0             12456
GRID    83              30.900  21.0    0.0             12456
GRID    84              32.347  21.0    0.0             12456
GRID    85              34.021  21.0    0.0             12456
GRID    86              35.694  21.0    0.0             12456
GRID    87              37.368  21.0    0.0             12456
GRID    88              39.041  21.0    0.0             12456
$
GRID    89              25.493  24.0    0.0             12456
GRID    90              27.092  24.0    0.0             12456
GRID    91              28.691  24.0    0.0             12456
GRID    92              30.290  24.0    0.0             12456
GRID    93              31.888  24.0    0.0             12456
GRID    94              33.700  24.0    0.0             12456
GRID    95              35.086  24.0    0.0             12456
GRID    96              36.685  24.0    0.0             12456
GRID    97              38.284  24.0    0.0             12456
GRID    98              39.883  24.0    0.0             12456
GRID    99              41.482  24.0    0.0             12456
$
GRID    100             28.679  27.0    0.0             12456
GRID    101             30.204  27.0    0.0             12456
GRID    102             31.728  27.0    0.0             12456
GRID    103             33.252  27.0    0.0             12456
GRID    104             34.776  27.0    0.0             12456
GRID    105             36.700  27.0    0.0             12456
GRID    106             37.825  27.0    0.0             12456
GRID    107             39.349  27.0    0.0             12456
GRID    108             40.873  27.0    0.0             12456
GRID    109             42.398  27.0    0.0             12456
GRID    110             43.922  27.0    0.0             12456
$
GRID    111             31.866  30.0    0.0             12456
GRID    112             33.316  30.0    0.0             12456
GRID    113             34.765  30.0    0.0             12456
GRID    114             36.215  30.0    0.0             12456
GRID    115             37.664  30.0    0.0             12456
GRID    116             39.500  30.0    0.0             12456
GRID    117             40.564  30.0    0.0             12456
GRID    118             42.013  30.0    0.0             12456
GRID    119             43.463  30.0    0.0             12456
GRID    120             44.912  30.0    0.0             12456
GRID    121             46.362  30.0    0.0             12456
$
$           INPUT MODE SHAPES
$
DMI     MODES   RDP     REC     121     5                               ABC
+BC     1       1       -.0405  -.0153  0.0     0.0     0.0     0.0     M1T6
+1T6    0.0     0.0     0.0     -0.0524 -0.104  0.00638 0.0352  0.0691  M1T14
+1T14   0.113   0.166   0.225   0.306   0.402   0.538   0.697   0.914   M1T22
```

Figure 60. Input Data Stream for the Standard AGARD Configuration (Continued)

+1T22	0.195	0.317	0.462	0.628	0.816	1.03	1.27	1.56	M1T30
+1T30	1.88	2.25	2.68	0.815	1.08	1.38	1.70	2.05	M1T38
+1T38	2.45	2.86	3.32	3.84	4.41	5.03	2.01	2.42	M1T46
+1T46	2.87	3.35	3.86	4.43	5.00	5.63	6.30	7.03	M1T54
+1T54	7.80	3.80	4.36	4.95	5.57	6.22	6.97	7.63	M1T62
+1T62	8.39	9.19	10.0	10.9	6.16	6.85	7.56	8.29	M1T70
+1T70	9.06	9.96	10.7	11.5	12.4	13.3	14.3	9.05	M1T78
+1T78	9.82	10.6	11.4	12.3	13.3	14.0	14.9	15.9	M1T86
+1T86	16.9	17.9	12.4	13.2	14.0	14.9	15.8	16.8	M1T94
+1T94	17.6	18.5	19.5	20.5	21.5	16.0	16.8	17.7	M1T102
+1T102	18.6	19.5	20.6	21.3	22.2	23.2	24.2	25.1	M1T110
+1T110	19.8	20.6	21.5	22.4	23.2	24.4	25.0	26.0	M1T118
+1T118	26.9	27.8	28.8	2	1	-0.351	-0.128	0.00	M2T3
+2T3	0.0	0.0	0.0	0.0	0.0	0.0	-0.686	-2.28	M2T11
+2T11	0.137	0.335	0.514	0.668	0.767	0.778	0.636	0.238	M2T19
+2T19	-0.719	-2.35	-4.79	1.62	2.16	2.59	2.83	2.83	M2T27
+2T27	2.50	1.74	0.444	-1.50	-4.11	-7.53	5.22	5.84	M2T35
+2T35	6.13	6.03	5.48	4.35	2.76	0.476	-2.47	-6.10	M2T43
+2T43	-10.6	10.5	10.7	10.4	9.51	8.05	5.90	3.28	M2T51
+2T51	-0.074	-4.09	-8.80	-14.4	16.5	15.8	14.4	12.5	M2T59
+2T59	9.91	6.41	2.86	-1.61	-6.72	-12.5	-19.2	22.0	M2T67
+2T67	20.0	17.4	14.3	10.5	5.47	11.6	-4.39	-10.5	M2T75
+2T75	-17.3	-24.9	25.9	22.6	18.70	14.3	9.40	3.17	M2T83
+2T83	-2.01	-8.48	-15.5	-23.0	-31.30	27.40	22.90	17.9	M2T91
+2T91	12.40	6.52	-0.653	-6.50	-13.60	-21.2	-29.2	-37.9	M2T99
+2T99	26.30	20.70	14.80	8.64	2.11	-6.59	-11.9	-19.4	M2T107
+2T107	-27.3	-35.6	-44.50	22.6	16.50	10.2	3.58	-3.28	M2T115
+2T115	-12.4	-17.8	-25.6	-33.7	-42.3	-52.6	3	1	M3T0
+3T0	0.083	0.028	0.0	0.0	0.0	0.0	0.0	0.0	M3T8
+3T8	0.0	-0.566	-2.30	0.004	-0.034	-0.092	-0.196	-0.371	M3T16
+3T16	-0.631	-1.12	-1.95	-3.60	-6.19	-10.3	-1.62	-0.366	M3T24
+3T24	-0.694	-1.20	-1.95	-3.06	-4.68	-6.99	-10.2	-14.30	M3T32
+3T32	-20.0	-1.714	-1.25	-2.02	-3.13	-4.64	-6.76	-9.32	M3T40
+3T40	-12.7	-16.80	-21.90	-28.4	-1.45	-2.36	-3.62	-5.29	M3T48
+3T48	-7.44	-10.20	-13.4	-17.2	-21.7	-26.90	-33.20	-1.70	M3T56
+3T56	-2.93	-4.55	-6.59	-9.06	-12.2	-15.3	-19.1	-23.3	M3T64
+3T64	-27.9	-33.4	-0.549	-1.96	-3.72	-5.83	-8.27	-11.4	M3T72
+3T72	-14.1	-17.4	-20.8	-24.5	-28.7	2.87	1.46	-0.219	M3T80
+3T80	-2.15	-4.31	-6.98	-9.13	-11.7	-14.3	-16.8	-19.6	M3T88
+3T88	9.08	7.77	6.27	4.61	2.83	0.748	-0.857	-2.67	M3T96
+3T96	-4.39	-5.96	-7.42	17.9	16.6	15.3	13.9	12.4	M3T104
+3T104	10.7	9.73	8.52	7.48	6.67	6.20	28.2	26.9	M3T112
+3T112	25.7	24.5	23.4	22.1	21.4	20.7	20.3	20.2	M3T120
+3T120	21.0	4	1	-1.08	-0.416	0.0	0.0	0.0	M4T5
+4T5	0.0	0.0	0.0	0.0	-1.42	-5.22	0.482	1.01	M4T13
+4T13	1.43	1.73	1.85	1.77	1.34	-0.436	-1.56	-4.92	M4T21
+4T21	-10.7	4.61	5.67	6.33	6.46	6.01	4.90	3.04	M4T29
+4T29	0.289	-3.49	-8.37	-15.5	12.80	13.2	12.9	11.7	M4T37
+4T37	9.63	6.71	3.29	-0.953	-5.84	-11.4	-18.8	21.7	M4T45
+4T45	20.1	17.6	14.4	10.5	5.98	1.43	-3.46	-8.44	M4T53
+4T53	-13.4	-19.6	26.5	22.3	17.6	12.6	7.55	2.16	M4T61
+4T61	-2.14	-6.40	-10.1	-13.0	-16.0	23.7	17.6	11.8	M4T69
+4T69	6.36	1.49	-3.13	-5.83	-7.94	-8.79	-8.18	-6.13	M4T77

Figure 60. Input Data Stream for the Standard AGARD Configuration (Continued)

```
+4T77   13.0    6.90    1.72    -2.42   -5.38   -7.16   -7.28   -5.93   M4T85
+4T85   -2.81   2.36    10.5    -2.49   -6.48   -9.10   -10.3   -9.97   M4T93
+4T93   -7.71   -4.51   0.890    8.34    18.2    32.5   -17.3   -17.6   M4T101
+4T101  -16.5   -14.10  -10.1   -2.75   2.83    12.1    23.7    38.2    M4T109
+4T109  58.3    -26.2   -22.9   -18.6   -13.0   -5.87   5.57    13.6    M4T117
+4T117  26.7    42.8    63.6    104.0   5       1       -0.053  -0.03   M5T2
+5T2    0.0     0.0     0.0     0.0     0.0     0.0     0.0     -2.72   M5T10
+5T10   -12.1   0.087   0.130   0.118   -0.006  -0.302  -0.821  -1.92   M5T18
+5T18   -4.00   -8.76   -17.0   -35.0   0.674   0.589   0.213   -0.596  M5T26
+5T26   -2.0    -4.24   -7.70   -12.9   -20.4   -30.7   -50.1   1.88    M5T34
+5T34   1.26    0.099   -1.75   -4.41   -8.14   -12.6   -18.2   -24.7   M5T42
+5T42   -32.1   -44.6   3.88    2.49    0.521   -2.04   -5.10   -8.63   M5T50
+5T50   -12.0   -15.2   -17.6   -18.7   -19.1   6.74    4.64    2.28    M5T58
+5T58   -0.164  -2.42   -4.27   -4.97   -4.35   -1.70   3.76    14.5    M5T66
+5T66   9.50    7.07    4.97    3.43     2.75   3.43    5.25    9.13    M5T74
+5T74   15.3    24.3    40.1    10.0     7.77   6.38    6.00    6.79    M5T82
+5T82   9.30    12.4    17.4    23.9     32.1   45.4    5.49    3.89    M5T90
+5T90   3.33    3.82    5.31    8.10     10.9   14.6    18.5    22.5    M5T98
+5T98   27.8    -5.57   -6.15   -5.98   -5.15   -3.85   -1.94   -0.901  M5T106
+5T106  0.032   -0.069  -1.91   -6.70   -21.1   -20.7   -20.2   -19.5   M5T114
+5T114  -18.9   -19.0   -19.7   -22.3   -27.4   -37.5   -70.9
$
EIGR    10      GIV     5.      200.            5                       +EI
+EI     MASS
$
$       DIRECT INPUT OF THE GENERALIZED MASS MATRIX FOR THE
$       NORMAL MODES ANALYSIS
$
DMI     MAA     RDP     DIAG    5       5                               +D3
+D3     1       1       1.      2       2       1.      3       3       +D4
+D4     1.      4       4       1.      5       5       1.
$
$       DIRECT INPUT OF THE GENERALIZED STIFFNESS MATRIX FOR THE
$       NORMAL MODES ANALYSIS
$
DMI     KAA     RDP     DIAG    5       5                               +D1
+D1     1       1       3637.72 2       2       57502.973       3       +D2
+D2     92282.714       4       330846.95       5       550752.7
$
$      DATA FOR UNSTEADY AERODYNAMICS GENERATION
$
AERO            21.96   1.145E-7
MKAERO1  1              0.901                                           +MK1
+MK1    0.0001  0.13333 0.1818  .3000   0.40    1.00
CAERO1  1000                    8       8                       1       +CA1
+CA1    0.0     0.0     0.0     21.96   31.866  30.     0.0     14.496
SPLINE1 40              1000    1000    1063    60
SET1    60      1       THRU    121
$
$      DATA FOR THE FLUTTER ANALYSIS
$
FLUTTER 1       PK      301     201     40                              +FL5
+FL5    1
```

Figure 60. Input Data Stream for the Standard AGARD Configuration (Continued)

```
FLFACT  201      .901
FLFACT  301      .08116
FLFACT  40       400.     550.     700.     900.
CONVERT VELOCITY 20.23
$
$        DIRECT INPUT OF THE GENERALIZED STIFFNESS MATRIX FOR THE
$        FLUTTER ANALYSIS
$
DMI     KFLUT    CDP      DIAG     5        5                          +D5
+D5     1        1        3637.72 0.        2        2        57502.970.     +D6
+D6     3        3        92282.710.        4        4        330846.90.     +D7
+D7     5        5        550752.70.
ENDDATA
```

Figure 60. Input Data Stream for the Standard AGARD Configuration (Concluded)

entry and then by the direct matrix input of the mass and stiffness matrices required by the eigenvalue analysis. The mass matrix is a 5 x 5 identity matrix while the stiffness matrix is a diagonal matrix whose nonzero values are the required eigenvalues. As mentioned, the purpose of providing this information is to load the LAMBDA relation with the correct frequency information for the flutter analysis.

The unsteady aerodynamic data are given next in the input deck with an AERO entry first defining the reference chord and density. The air density is input in units of slugs/in^3 divided by twelve in order to get this variable into consistent units. The MKAERO1 entry specifies that the aerodynamics are to be calculated at M=0.901 and at a range of reduced frequencies. The CAERO1 entry defines the aerodynamic planform and specifies that it is to be divided into 64 boxes with equal spanwise and chordwise cuts. The SPLINE1 entry connects all 64 boxes to all 121 grid points.

Flutter analysis inputs, the final set of data, specify that the analysis is to be carried out at M=0.901 and a density ratio of 0.06528. Four initial velocities are selected for the p-k flutter analysis and the CONVERT entry changes these velocities from the input units of knots to the consistent units of inches/sec. A complex generalized stiffness matrix is input for the flutter analysis. This matrix is identical to the matrix used for the eigenanalysis except that the imaginary terms equal to zero are speci-fied. It is necessary to make this additional input since the FLUTTRAN module assumes that the generalized stiffness matrix is complex.

4.9.3 Results

The abridged output listings of **Figure 61** list the predicted flutter speed and present a summary of the p-k flutter analysis. The indicated flutter speed is 976.3 ft/sec and the frequency is 105.4 Hz. This compares with wind tunnel results, as reported in the referenced NASA report, of 973.4 ft/sec and 101.1 Hz. This unusually good level of agreement can perhaps be attributed to the simplicity of the model. The fact that the wing has a relatively low thickness ratio may explain why the results are so good at the high subsonic Mach number of 0.901.

The modal participation factors printed in the output represent the eigenvector of the generalized coordinates at the flutter speed and they indicate that the first mode dominates the vector in this case. A summary of the flutter analysis for the first two modes is then presented showing the complex eigenvalues and the corresponding damping and frequencies for each of the modes at each of the velocities at which the analysis is performed. The input requested flutter analyses at only 4 velocities, but the output has results for 17. This is because the flutter algorithm refines the velocity increments whenever it has difficulty in tracking the flutter behavior. Also, the print at the last two velocities has the print reversed in the first two modes. The ASTROS procedure prints results in increasing frequency order, but this is not appropriate when two frequencies cross. A more sophisticated algorithm could provide improved mode tracking, but this introduces complexity and possible errors and was not attempted.

4.10 TRANSIENT RESPONSE WITH A CONTROL SYSTEM

A simple example was constructed in order to test a variety of transient response features, including initial conditions, transfer functions, extra points and solution print requests. The example should also be helpful to the user in defining loading conditions for a transient analysis.

4.10.1 Problem Description

Section XI of the Theoretical Manual describes the dynamic analysis capabilities of ASTROS. This writeup includes a description of the assembly of the structural matrices required for dynamic loads analysis, the dynamic loads generation and the solution algorithms. The structure that is analyzed

MODAL PARTICIPATION FACTORS FOR CRITICAL FLUTTER SPEED OF:

MACH	=	0.9010
V(TRUE)	=	11716.9639
V(EQ)	=	3337.9983
DENSITY RATIO	=	0.081160
FREQUENCY	=	16.771383 HZ, 105.377708 RAD/S

INDEX	REAL	IMAG	INDEX	REAL	IMAG	INDEX	REAL	IMAG
1	9.8757E-01	0.0000E+00	2	-1.5278E-01	3.3036E-02	3	1.6333E-02	1.0773E-03
4	-7.3569E-04	2.0458E-03	5	1.1140E-03	-3.2672E-04			

S U M M A R Y O F P - K F L U T T E R E V A L U A T I O N

MODE = 1   MACH NUMBER = 0.9010   DENSITY RATIO = 8.1160E-02

NO	VELOCITY EQUIVALENT	VELOCITY TRUE	DAMPING RATIO	FREQUENCY CYC/SEC	FREQUENCY RAD/SEC	COMPLEX EIGENVALUE REAL	COMPLEX EIGENVALUE IMAGINARY
1	2.305297E+03	8.092000E+03	-6.816896E-02	1.218832E+01	7.658147E+01	-3.541822E-03	1.039130E-01
2	2.478194E+03	8.698900E+03	-6.777072E-02	1.269548E+01	7.976806E+01	-3.411765E-03	1.006855E-01
3	2.651092E+03	9.305801E+03	-6.517854E-02	1.328009E+01	8.344129E+01	-3.208516E-03	9.845315E-02
4	2.823989E+03	9.912701E+03	-5.945402E-02	1.395794E+01	8.770033E+01	-2.887771E-03	9.714301E-02
5	2.996886E+03	1.051960E+04	-4.900233E-02	1.475074E+01	9.268163E+01	-2.370191E-03	9.673791E-02
6	3.169784E+03	1.112650E+04	-3.083361E-02	1.568822E+01	9.857197E+01	-1.499655E-03	9.727408E-02
7	3.337998E+03	1.171696E+04	-3.006993E-06	1.677138E+01	1.053777E+02	-1.484699E-07	9.874975E-02
8	3.342681E+03	1.173340E+04	1.130455E-03	1.680410E+01	1.055833E+02	5.584661E-05	9.880378E-02
9	3.515578E+03	1.234030E+04	5.936432E-02	1.809685E+01	1.137059E+02	3.002998E-03	1.011718E-01
10	3.688476E+03	1.294720E+04	1.580587E-01	1.936399E+01	1.216676E+02	8.154358E-03	1.031814E-01
11	3.861373E+03	1.355410E+04	2.811834E-01	2.025397E+01	1.272595E+02	1.449377E-02	1.030912E-01
12	4.034270E+03	1.416100E+04	3.996954E-01	2.078544E+01	1.305988E+02	2.023702E-02	1.012622E-01
13	4.264800E+03	1.497020E+04	5.395566E-01	2.121670E+01	1.333085E+02	2.637785E-02	9.777604E-02
14	4.495330E+03	1.577940E+04	6.624696E-01	2.150925E+01	1.351466E+02	3.114963E-02	9.404093E-02
15	4.725859E+03	1.658860E+04	7.730645E-01	2.174282E+01	1.366142E+02	3.495216E-02	9.042495E-02
16	4.956390E+03	1.739780E+04	-1.675235E+00	2.177198E+01	1.367974E+02	-7.231553E-02	8.633476E-02
17	5.186919E+03	1.820700E+04	-1.874893E+00	2.124621E+01	1.334939E+02	-7.546955E-02	8.050544E-02

Figure 61. Selected Results for the Standard AGARD Test Case

MODE = 2 MACH NUMBER = 0.9010 DENSITY RATIO = 8.1160E-02

NO	VELOCITY EQUIVALENT	VELOCITY TRUE	DAMPING RATIO	FREQUENCY CYC/SEC	FREQUENCY RAD/SEC	COMPLEX EIGENVALUE REAL	COMPLEX EIGENVALUE IMAGINARY
1	2.305297E+03	8.092000E+03	-1.257132E-01	3.529620E+01	2.217726E+02	-1.891496E-02	3.009222E-01
2	2.478194E+03	8.698900E+03	-1.447213E-01	3.470110E+01	2.180334E+02	-1.991422E-02	2.752080E-01
3	2.651092E+03	9.305801E+03	-1.662827E-01	3.400995E+01	2.136908E+02	-2.096290E-02	2.521358E-01
4	2.823989E+03	9.912701E+03	-1.911038E-01	3.320674E+01	2.086441E+02	-2.208288E-02	2.311088E-01
5	2.996886E+03	1.051960E+04	-2.205168E-01	3.226712E+01	2.027403E+02	-2.333216E-02	2.116134E-01
6	3.169784E+03	1.112650E+04	-2.571362E-01	3.115422E+01	1.957478E+02	-2.483555E-02	1.931704E-01
7	3.337998E+03	1.171696E+04	-3.051389E-01	2.985010E+01	1.875537E+02	-2.681517E-02	1.757571E-01
8	3.342681E+03	1.173340E+04	-3.067434E-01	2.981005E+01	1.873020E+02	-2.688229E-02	1.752754E-01
9	3.515578E+03	1.234030E+04	-3.836821E-01	2.817022E+01	1.769987E+02	-3.021260E-02	1.574877E-01
10	3.688476E+03	1.294720E+04	-5.163099E-01	2.637440E+01	1.657152E+02	-3.628017E-02	1.405364E-01
11	3.861373E+03	1.355410E+04	-6.943833E-01	2.503856E+01	1.573219E+02	-4.424762E-02	1.274444E-01
12	4.034270E+03	1.416100E+04	-8.687090E-01	2.421582E+01	1.521525E+02	-5.124268E-02	1.179743E-01
13	4.264800E+03	1.497020E+04	-1.082208E+00	2.345922E+01	1.473986E+02	-5.849905E-02	1.081106E-01
14	4.495330E+03	1.577940E+04	-1.283107E+00	2.285174E+01	1.435817E+02	-6.409789E-02	9.991045E-02
15	4.725859E+03	1.658860E+04	-1.479146E+00	2.230139E+01	1.401238E+02	-6.859389E-02	9.274796E-02
16	4.956390E+03	1.739780E+04	8.743891E-01	2.195227E+01	1.379302E+02	3.805764E-02	8.704968E-02
17	5.186919E+03	1.820700E+04	9.683117E-01	2.215511E+01	1.392047E+02	4.064460E-02	8.394942E-02

MODE = 3 MACH NUMBER = 0.9010 DENSITY RATIO = 8.1160E-02

NO	VELOCITY EQUIVALENT	VELOCITY TRUE	DAMPING RATIO	FREQUENCY CYC/SEC	FREQUENCY RAD/SEC	COMPLEX EIGENVALUE REAL	COMPLEX EIGENVALUE IMAGINARY
1	2.305297E+03	8.092000E+03	-2.856112E-02	4.928448E+01	3.096635E+02	-6.000420E-03	4.201811E-01
2	2.478194E+03	8.698900E+03	-3.081586E-02	4.941796E+01	3.105022E+02	-6.038748E-03	3.919247E-01
3	2.651092E+03	9.305801E+03	-3.305160E-02	4.955614E+01	3.113704E+02	-6.071394E-03	3.673888E-01
4	2.823989E+03	9.912701E+03	-3.525920E-02	4.969866E+01	3.122659E+02	-6.097859E-03	3.458875E-01
5	2.996886E+03	1.051960E+04	-3.742582E-02	4.984527E+01	3.131871E+02	-6.117137E-03	3.268940E-01
6	3.169784E+03	1.112650E+04	-3.953956E-02	4.999574E+01	3.141325E+02	-6.128559E-03	3.099963E-01
7	3.337998E+03	1.171696E+04	-4.153949E-02	5.014593E+01	3.150762E+02	-6.132449E-03	2.952588E-01
8	3.342681E+03	1.173340E+04	-4.159195E-02	5.015007E+01	3.151022E+02	-6.132099E-03	2.948695E-01
9	3.515578E+03	1.234030E+04	-4.357758E-02	5.030840E+01	3.160970E+02	-6.128159E-03	2.812529E-01
10	3.688476E+03	1.294720E+04	-4.548882E-02	5.047076E+01	3.171172E+02	-6.116752E-03	2.689343E-01
11	3.861373E+03	1.355410E+04	-4.732415E-02	5.063734E+01	3.181638E+02	-6.098671E-03	2.577403E-01
12	4.034270E+03	1.416100E+04	-4.908273E-02	5.080828E+01	3.192379E+02	-6.074652E-03	2.475271E-01
13	4.264800E+03	1.497020E+04	-5.131134E-02	5.104327E+01	3.207144E+02	-6.034989E-03	2.352302E-01
14	4.495330E+03	1.577940E+04	-5.341175E-02	5.128667E+01	3.222437E+02	-5.988292E-03	2.242313E-01
15	4.725859E+03	1.658860E+04	-5.539142E-02	5.153879E+01	3.238278E+02	-5.936346E-03	2.143417E-01
16	4.956390E+03	1.739780E+04	-5.725852E-02	5.179995E+01	3.254687E+02	-5.880676E-03	2.054079E-01
17	5.186919E+03	1.820700E+04	-5.902286E-02	5.207050E+01	3.271686E+02	-5.822717E-03	1.973038E-01

Figure 61. Selected Results for the Standard AGARD Test Case (Concluded)

in this case is a cantilevered beam that has an imposed initial deformation that corresponds to the beam being loaded at the tip by a force sufficient to achieve a 10.0 inch tip displacement. The beam is released from this initial condition and the ensuing displacement pattern is computed in the time and spatial domains. A prototype "control system" is also present in this model that affects the response of the structure. The control system is such that a force is applied to the tip that is proportional to the velocity of the displacement at the tip. The form of the control law is:

$$\frac{F_{TIP}}{w_{TIP}} = \frac{ks}{s^2 + 100s + 10{,}000.0}$$

where s is the Laplace operator and k is a control system gain. A negative value of k essentially adds damping to the system while a positive value tends to destabilize the system.

4.10.2 Input

Figure 62 shows the input data packet for this example and indicates that four different cases are run with one job submittal. The cases differ in their gain setting, which is specified in the transfer function that is called out as part of the boundary condition. The first boundary condition is open loop and therefore requires no TFL specification. The control laws also require an extra point, which is referred to by the ESET parameter in the boundary condition. The TRANSIENT discipline options indicate that the direct method is to be used (this is required by the initial conditions) and that initial conditions are present. The DLOAD option is required, but is a dummy input in this case and generates null applied load vectors. The single PRINT command in the solution control packet specifies that results are to be printed at the times specified on a TIMELIST bulk data entry and at locations specified on a GRIDLIST entry.

The structural model for this case is simply three bar elements with freedom to deflect and bend in the x-z plane. As mentioned, the DLOAD entry has the net effect of producing null load vectors, but it does so in an indirect way. It has a nonzero spatial load vector, but the magnitude of the time variation, as given on the TABLED1 entry, is always zero. The IC bulk data entries specify the initial deformation (with no initial velocities) while a small amount of structural damping is specified using the VSDAMP data entry.

```
ASSIGN DATABASE TRANS1 KIMBERLY NEW DELETE
SOLUTION
ANALYZE
   PRINT TIME 5, DISP=5
   BOUNDARY DAMPING=6, REDUCE=1000
      TRANSIENT DIRECT (DLOAD=12, IC=10,TSTEP=20)
   BOUNDARY TFL = 30, ESET =20, DAMPING = 6, REDUCE=1000
      TRANSIENT DIRECT (DLOAD=12, IC=10,TSTEP=20)
   BOUNDARY TFL = 40, ESET =20, DAMPING=6, REDUCE=1000
      TRANSIENT DIRECT (DLOAD=12, IC=10,TSTEP=20)
   BOUNDARY TFL = 50, ESET =20, DAMPING=6, REDUCE=1000
      TRANSIENT DIRECT (DLOAD=12, IC=10,TSTEP=20)
END
BEGIN BULK
$
$    ASTROS SAMPLE PROBLEM 10
$
$    TRANSIENT RESPONSE OF A BAR FEATURING:
$       INITIAL CONDITIONS
$       BOUNDARY CONDITION DEPENDENT TRANSFER FUNCTION INPUT
$       OUTPUT REQUESTS AS A FUNCTION OF TIME
$       OUTPUT REQUESTS FOR SPECIFIED GRID POINTS
$
$    THE STRUCTURAL MODEL
$
GRID    1               0.0     0.0     0.0             123456
GRID    3               10.0    0.0     0.0             246
GRID    5               20.0     0.0     0.0             246
GRID    7               30.0     0.0     0.0             246
CBAR    101     100     1       3       0.0     1.0
CBAR    103     100     3       5       0.0     1.0
CBAR    105     100     5       7       0.0     1.0
MAT1    100     1.E+7           .3      0.1
PBAR    100     100     0.125   1.0     1.628E-4
CONVERT MASS    0.00259
$
$    REDUCE SET SPECIFICATIONS
$
OMIT1   1000    1       3       5       7
$
$    INITIAL CONDITIONS - CORRESPONDS TO THE STATIC DEFLECTION OF A
$                         UNIFORM BAR WITH A LOAD AT THE TIP
$
IC        10      7       3       10.0
IC        10      5       3        5.186
IC        10      3       3        1.478
IC        10      7       5       -0.500
IC        10      5       5       -0.444
IC        10      3       5       -0.278
$
$     DYNAMIC RESPONSE INPUTS
$
DLOAD   12      1.      1.0     30
```

Figure 62. Input Data Stream for the Transient Response Test Case

```
TLOAD1  30       20       34
DLAGS   20       35
FORCE   35       7                 1.       0.0      0.0      1.0
TSTEP    20       100      0.010    1
TABLED1 34                                                             +TT1
+TT1    -0.1     0.0      0.0      0.0      0.0      0.0      0.1      0.0      +TT2
+TT2     0.1     0.0      10.0     0.0
VSDAMP      6       0.01     5.0
$
$    BOUNDARY CONDITION DEPENDENT TRANSFER FUNCTIONS
$
EPOINT      20      101
TF          30      101              10000.0  100.0    1.0                  TF30
+F30         7        3      0.0      -20.0    0.0
TF          30        7        3        0.0    0.0      0.0                  TF30
+F30       101               1.0        0.0    0.0
TF          40      101              10000.0  100.0    1.0                  TF40
+F40         7        3      0.0     -100.0    0.0
TF          40        7        3        0.0    0.0      0.0                  TF40
+F40       101                          1.0    0.0      0.0
TF          50      101              10000.0   100.0   1.0                  TF50
+F50         7        3      0.0       20.0    0.0
TF          50        7        3        0.0    0.0      0.0                  TF50
+F50       101               1.0        0.0    0.0
$
$     OUTPUT REQUESTS
$
GRIDLIST    5       7       101
TIMELIST    5       0.0     0.01      0.1      0.2      0.3      0.4      0.5  TIME
+IME        0.6     0.7     0.8       0.9      1.0
ENDDATA
```

Figure 62. Input Data Stream for the Transient Response Test Case (Concluded)

The final input data relate to the transfer functions that define the control systems. Each set of transfer functions is made up of two entries. The first entry of each set specifies the relation between the extra point and the tip deflection using the transfer function given in the problem description of Subsection 4.10.1. The second entry applies this extra point as a force on the tip of the beam. Gains of -20.0, -100.0 and 20.0 are specified for the closed loop systems of the last three boundary conditions.

4.10.3 Results

A composite plot of the results from all four boundary conditions, given in **Figure 63**, shows that the open loop (k=0) response is lightly damped and that the system stability is enhanced by increasingly negative values of k. The positive k value is shown to make the system very unstable. **Figure 64** shows some of the printed output. **Figure 64(a)** gives the open loop response at the tip at t=0.0, 0.5 and 1.0 while **Figure 64(b)** shows the closed loop response of the tip and the extra point at the same time for k=-20.0.

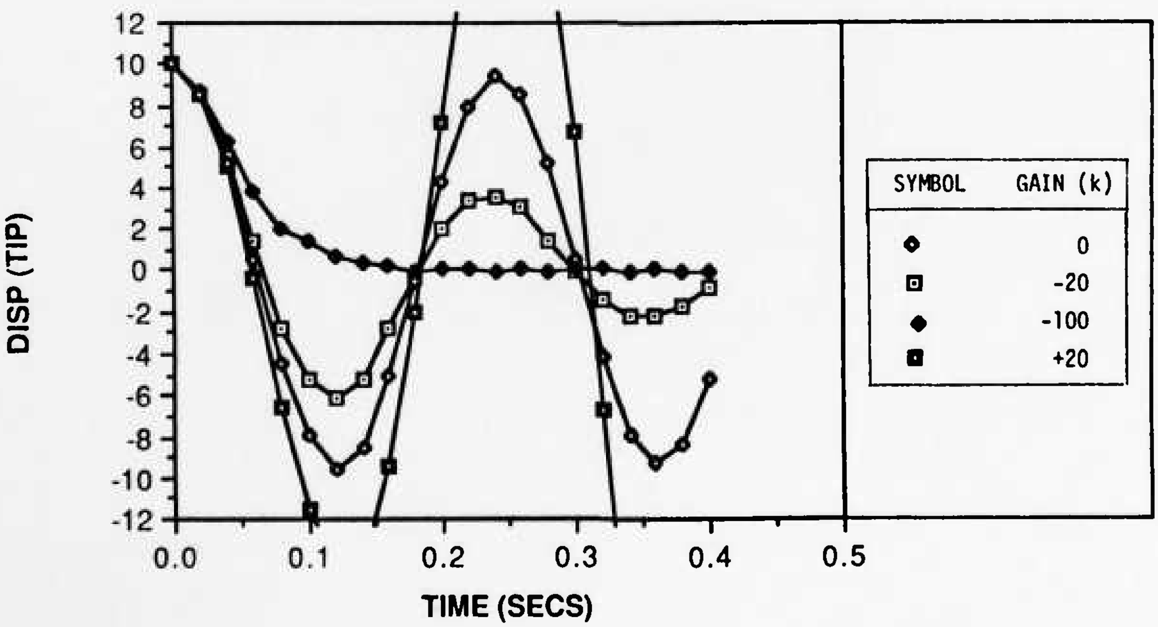

Figure 63. Transient Response of a Cantilevered Beam as a Function of Gain Setting

TRANSIENT ANALYSIS: BOUNDARY 1, TIME = 0.0000000E+00

D I S P L A C E M E N T   V E C T O R

POINT ID.	TYPE	T1	T2	T3	R1	R2	R3
7	G	0.00000E+00	0.00000E+00	1.00000E+01	0.00000E+00	-5.00000E-01	0.00000E+00

TRANSIENT ANALYSIS: BOUNDARY 1, TIME = 4.9999982E-01

D I S P L A C E M E N T   V E C T O R

POINT ID.	TYPE	T1	T2	T3	R1	R2	R3
7	G	0.00000E+00	0.00000E+00	8.23595E+00	0.00000E+00	-3.80589E-01	0.00000E+00

TRANSIENT ANALYSIS: BOUNDARY 1, TIME = 9.9999934E-01

D I S P L A C E M E N T   V E C T O R

POINT ID.	TYPE	T1	T2	T3	R1	R2	R3
7	G	0.00000E+00	0.00000E+00	5.05730E+00	0.00000E+00	-2.40933E-01	0.00000E+00

(a) k = 0.0

TRANSIENT ANALYSIS: BOUNDARY 2, TIME = 0.0000000E+00

D I S P L A C E M E N T   V E C T O R

POINT ID.	TYPE	T1	T2	T3	R1	R2	R3
7	G	0.00000E+00	0.00000E+00	1.00000E+01	0.00000E+00	-5.00000E-01	0.00000E+00
101	E	0.00000E+00					

TRANSIENT ANALYSIS: BOUNDARY 2, TIME = 4.9999982E-01

D I S P L A C E M E N T   V E C T O R

POINT ID.	TYPE	T1	T2	T3	R1	R2	R3
7	G	0.00000E+00	0.00000E+00	9.04002E-01	0.00000E+00	-3.45846E-02	0.00000E+00
101	E	-5.12504E-02					

TRANSIENT ANALYSIS: BOUNDARY 2, TIME = 9.9999934E-01

D I S P L A C E M E N T   V E C T O R

POINT ID.	TYPE	T1	T2	T3	R1	R2	R3
7	G	0.00000E+00	0.00000E+00	7.69470E-03	0.00000E+00	-3.18056E-03	0.00000E+00
101	E	-5.46079E-03					

(b) k = -20.0

Figure 64. Selected Results for the Transient Response Test Case

4.11 FREQUENCY RESPONSE

This test case is a modification of the transient response test case of the previous subsection to perform a frequency response. Its primary use is for guidance in preparing frequency dependent loads. The same problem is solved using the direct and the modal approaches to frequency analysis.

4.11.1 Problem Description

Section XI of the Theoretical Manual describes the dynamic analysis capabilities of ASTROS. This writeup includes a description of the assembly of the structural matrices required for dynamic loads analysis, the dynamic loads generation and the solution algorithms. Both the direct approach, wherein the frequency equations are solved in physical coordinates of the system, and the modal approach, wherein the equations are solved in the modal coordinates, are used in this example. The structure that is analyzed in this case is a cantilevered beam that is loaded at the tip by a force of magnitude 1.0 at all the frequencies of interest.

4.11.2 Input

Figure 65 shows the input data packets for this example. A separate boundary condition is required for the two methods of solution with the MODAL approach requiring the METHOD specification as part of the boundary condition. The print request specifies that displacements at grids identified by bulk data entry GRIDLIST 7 are to be printed in polar format for all the frequencies at which the calculations are performed.

The structural model for this case is six bar elements with freedom to deflect and bend in the x-z plane. The rotational degrees of freedom are omitted from the solution with no loss in accuracy. The DLOAD entry defines overall scale factors and refers to the RLOAD1 entry, which in turn refers to the DLAGS entry to obtain the spatial component of the loads and to the TABLED1 entry to obtain the frequency component. The spatial load is defined by the single FORCE entry while the TABLED1 entry shows a flat input spectrum for the loads from 0.0 to 1000.0 Hz. The FREQ2 entry specifies that results are to be computed at 50 frequencies ranging from 3.0 to 100.0 Hz with logrithmic increments. The GRIDLIST entry requests that output is to be given at the tip.

```
ASSIGN DATABASE FREQ1 KIMBERLY NEW DELETE
SOLUTION
ANALYZE
   TITLE = FREQUENCY RESPONSE OF A CANTILEVERED BAR
   BOUNDARY  REDUCE = 20, DAMPING=6
      SUBTITLE = DIRECT METHOD OF SOLUTION
      PRINT DISP(POLA) = 7, FREQ ALL
      FREQUENCY DIRECT (DLOAD=12, FSTEP=20)
   BOUNDARY  REDUCE = 20, DAMPING=6, METHOD = 5
      SUBTITLE = MODAL METHOD OF SOLUTION
      PRINT ROOT = ALL
      MODES
      FREQUENCY MODAL(DLOAD=12, FSTEP=20)
      PRINT DISP(POLA) = 7, FREQ ALL
END
BEGIN BULK
$
$    ASTROS SAMPLE PROBLEM 11
$
$    FREQUENCY RESPONSE OF A BAR FEATURING:
$       DIRECT AND MODAL METHODS OF SOLUTION
$       OUTPUT REQUESTS AS A FUNCTION OF FREQUENCY IN POLAR FORMAT
$
$    THE STRUCTURAL MODEL
$
GRID    1               0.0     0.0     0.0             123456
GRID    2               5.0     0.0     0.0             246
GRID    3               10.0    0.0     0.0             246
GRID    4               15.0    0.0     0.0             246
GRID    5               20.0     0.0     0.0             246
GRID    6               25.0     0.0     0.0             246
GRID    7               30.0     0.0     0.0             246
OMIT1    20      5      2       THRU     7
$
CBAR    101     100     1       2       0.0     1.0
CBAR    102     100     2       3       0.0     1.0
CBAR    103     100     3       4       0.0     1.0
CBAR    104     100     4       5       0.0     1.0
CBAR    105     100     5       6       0.0     1.0
CBAR    106     100     6       7       0.0     1.0
PBAR    100     100     0.125   1.0     1.628E-4
MAT1    100     1.E+7           .3      0.1
CONVERT MASS    .00259
$
EIGR     5       GIV                            5                       EIGR
+IGR     MAX
$
$    FREQUENCY DEPENDENT LOADS GENERATON
$
DLOAD   12      1.      1.0     30
RLOAD1  30      20      34
DLAGS   20      35
FORCE   35       7              1.      0.0     0.0     1.0
```

Figure 65. Input Data Stream for the Frequency Response Test Case

```
TABLED1 34                                                          +TT1
+TT1    -0.1    0.0     0.0     1.0     10000.0     1.0
FREQ2   20      3.0     100.0   50
VSDAMP      6       .10
$
GRIDLIST 7          7
ENDDATA
```

Figure 65. Input Data Stream for the Frequency Response Test Case (Concluded)

4.11.3 Results

Figure 66 shows the frequency response that was computed using the direct approach for this case. Results for the modal approach are indistinguishable for this case and are not presented. The first three natural frequencies for the structure are at 4.35, 26.5, and 72.2 Hertz and these resonant frequencies are evident in **Figure 66**. **Figure 67** is a sampling of the output for the two boundary conditions and the printed results can be compared to see how closely the two methods agree. The direct approach consumed four times more computer resources (48 seconds vs 12 seconds on a MicroVAX II system) than the modal approach in the part of the solution where the algorithms differ.

4.12 SERVOELASTIC RESPONSE OF A FLEXIBLE MISSILE

This test case presents a more complex transient response problem than was given in Subsection 4.10. The model is of an air-to-air surface missile obtained from Subsection 6.2.10 of the <u>MSC/NASTRAN Handbook for Aeroelastic Analysis</u>. The servo system for this model is relatively complex, thereby aiding the user in the definition of real world control systems in ASTROS.

4.12.1 Theory

Figure 68, taken from the MSC Handbook, is a representation of the missile and the block diagram of the servo system. The input packet is sufficient to describe the structural model, but the servo system requires special comment. In the context of **Figure 68(b)**, the e_1 signal is the summation of the commanded value and a signal proportional the output of the rate gyro

$$e_1 = e_c - e_4$$

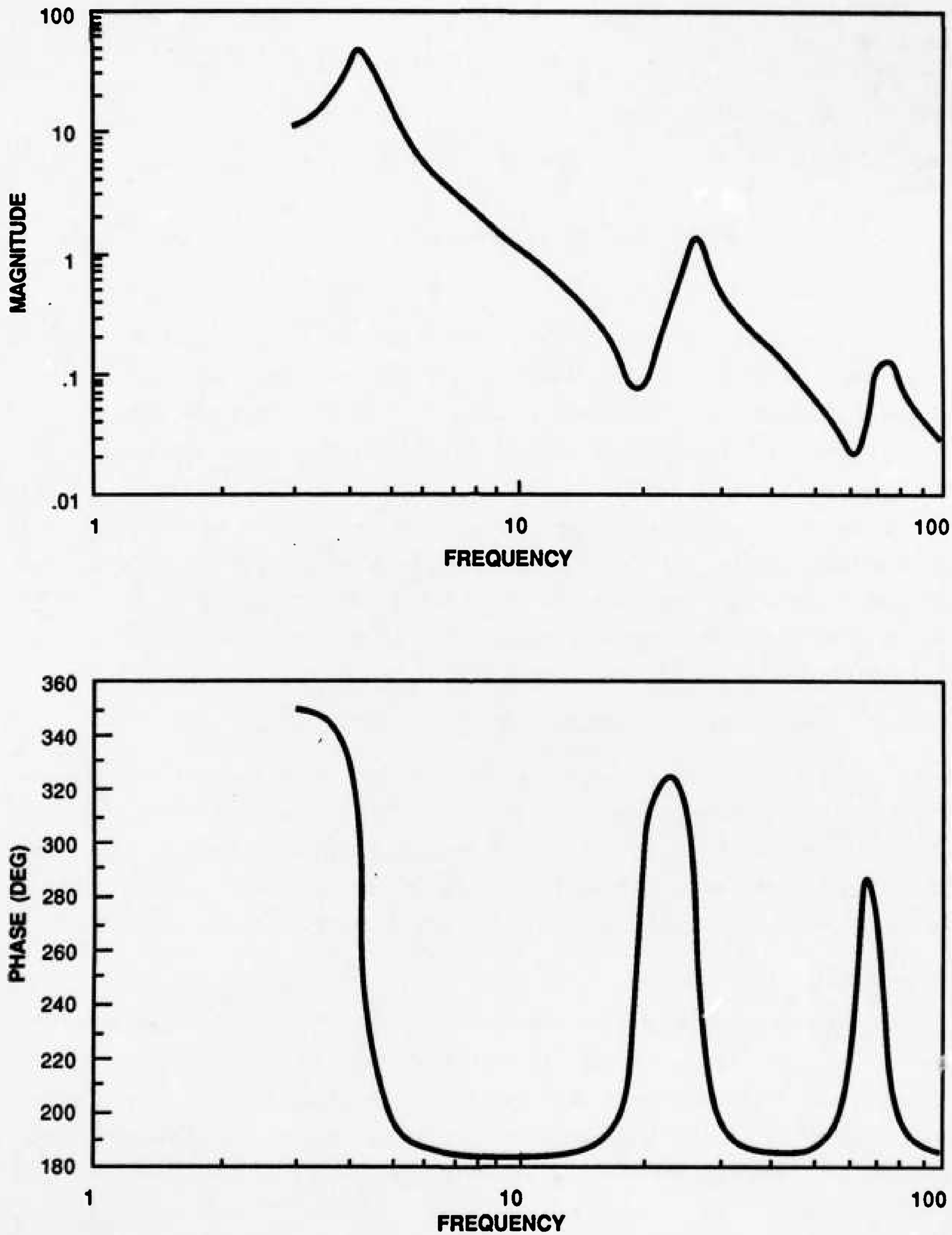

Figure 66. Frequency Response of a Cantilevered Beam

FREQUENCY ANALYSIS: BOUNDARY 1, FREQ = 3.0000000E+00

C O M P L E X D I S P L A C E M E N T V E C T O R
P O L A R F O R M

POINT ID.	TYPE	T1	T2	T3	R1	R2	R3
7	G	0.00000E+00	0.00000E+00	1.02177E+01	0.00000E+00	4.93234E-01	0.00000E+00
		0.00000E+00	0.00000E+00	3.49289E+02	0.00000E+00	1.69499E+02	0.00000E+00

FREQUENCY ANALYSIS: BOUNDARY 1, FREQ = 4.2599955E+00

C O M P L E X D I S P L A C E M E N T V E C T O R
P O L A R F O R M

POINT ID.	TYPE	T1	T2	T3	R1	R2	R3
7	G	0.00000E+00	0.00000E+00	4.96337E+01	0.00000E+00	2.30484E+00	0.00000E+00
		0.00000E+00	0.00000E+00	2.93195E+02	0.00000E+00	1.13656E+02	0.00000E+00

FREQUENCY ANALYSIS: BOUNDARY 1, FREQ = 4.5694795E+00

C O M P L E X D I S P L A C E M E N T V E C T O R
P O L A R F O R M

POINT ID.	TYPE	T1	T2	T3	R1	R2	R3
7	G	0.00000E+00	0.00000E+00	3.76878E+01	0.00000E+00	1.72883E+00	0.00000E+00
		0.00000E+00	0.00000E+00	2.24710E+02	0.00000E+00	4.52533E+01	0.00000E+00

FREQUENCY ANALYSIS: BOUNDARY 1, FREQ = 2.6381905E+01

C O M P L E X D I S P L A C E M E N T V E C T O R
P O L A R F O R M

POINT ID.	TYPE	T1	T2	T3	R1	R2	R3
7	G	0.00000E+00	0.00000E+00	1.26535E+00	0.00000E+00	2.18307E-01	0.00000E+00
		0.00000E+00	0.00000E+00	2.67776E+02	0.00000E+00	9.36280E+01	0.00000E+00

FREQUENCY ANALYSIS: BOUNDARY 1, FREQ = 2.8298519E+01

C O M P L E X D I S P L A C E M E N T V E C T O R
P O L A R F O R M

POINT ID.	TYPE	T1	T2	T3	R1	R2	R3
7	G	0.00000E+00	0.00000E+00	8.23582E-01	0.00000E+00	1.25286E-01	0.00000E+00
		0.00000E+00	0.00000E+00	2.10602E+02	0.00000E+00	3.53456E+01	0.00000E+00

FREQUENCY ANALYSIS: BOUNDARY 1, FREQ = 1.0000001E+02

C O M P L E X D I S P L A C E M E N T V E C T O R
P O L A R F O R M

POINT ID.	TYPE	T1	T2	T3	R1	R2	R3
7	G	0.00000E+00	0.00000E+00	2.90541E-02	0.00000E+00	4.03609E-03	0.00000E+00
		0.00000E+00	0.00000E+00	1.84920E+02	0.00000E+00	1.48350E+01	0.00000E+00

(a) Direct Method

Figure 67. Selected Output for the Frequency Response Test Case

FREQUENCY RESPONSE OF A CANTILEVERED BAR ASTROS VERSION 1.00 8/11/88 P. 57
MODAL METHOD OF SOLUTION

FREQUENCY ANALYSIS: BOUNDARY 2, FREQ = 3.0000000E+00

C O M P L E X   D I S P L A C E M E N T   V E C T O R
P O L A R   F O R M

POINT ID.	TYPE	T1	T2	T3	R1	R2	R3
7	G	0.00000E+00	0.00000E+00	1.02177E+01	0.00000E+00	4.93190E-01	0.00000E+00
		0.00000E+00	0.00000E+00	3.49289E+02	0.00000E+00	1.69498E+02	0.00000E+00

FREQUENCY ANALYSIS: BOUNDARY 2, FREQ = 4.2599955E+00

C O M P L E X   D I S P L A C E M E N T   V E C T O R
P O L A R   F O R M

POINT ID.	TYPE	T1	T2	T3	R1	R2	R3
7	G	0.00000E+00	0.00000E+00	4.96337E+01	0.00000E+00	2.30482E+00	0.00000E+00
		0.00000E+00	0.00000E+00	2.93195E+02	0.00000E+00	1.13655E+02	0.00000E+00

FREQUENCY ANALYSIS: BOUNDARY 2, FREQ = 4.5694795E+00

C O M P L E X   D I S P L A C E M E N T   V E C T O R
P O L A R   F O R M

POINT ID.	TYPE	T1	T2	T3	R1	R2	R3
7	G	0.00000E+00	0.00000E+00	3.76879E+01	0.00000E+00	1.72886E+00	0.00000E+00
		0.00000E+00	0.00000E+00	2.24710E+02	0.00000E+00	4.52522E+01	0.00000E+00

FREQUENCY ANALYSIS: BOUNDARY 2, FREQ = 2.6381905E+01

C O M P L E X   D I S P L A C E M E N T   V E C T O R
P O L A R   F O R M

POINT ID.	TYPE	T1	T2	T3	R1	R2	R3
7	G	0.00000E+00	0.00000E+00	1.26535E+00	0.00000E+00	2.18299E-01	0.00000E+00
		0.00000E+00	0.00000E+00	2.67774E+02	0.00000E+00	9.36166E+01	0.00000E+00

FREQUENCY ANALYSIS: BOUNDARY 2, FREQ = 2.8298519E+01

C O M P L E X   D I S P L A C E M E N T   V E C T O R
P O L A R   F O R M

POINT ID.	TYPE	T1	T2	T3	R1	R2	R3
7	G	0.00000E+00	0.00000E+00	8.23611E-01	0.00000E+00	1.25320E-01	0.00000E+00
		0.00000E+00	0.00000E+00	2.10600E+02	0.00000E+00	3.53323E+01	0.00000E+00

FREQUENCY ANALYSIS: BOUNDARY 2, FREQ = 1.0000001E+02

C O M P L E X   D I S P L A C E M E N T   V E C T O R
P O L A R   F O R M

POINT ID.	TYPE	T1	T2	T3	R1	R2	R3
7	G	0.00000E+00	0.00000E+00	2.90939E-02	0.00000E+00	4.08266E-03	0.00000E+00
		0.00000E+00	0.00000E+00	1.84904E+02	0.00000E+00	1.45799E+01	0.00000E+00

(b) Modal Method

Figure 67. Selected Output for the Frequency Response Test Case (Concluded)

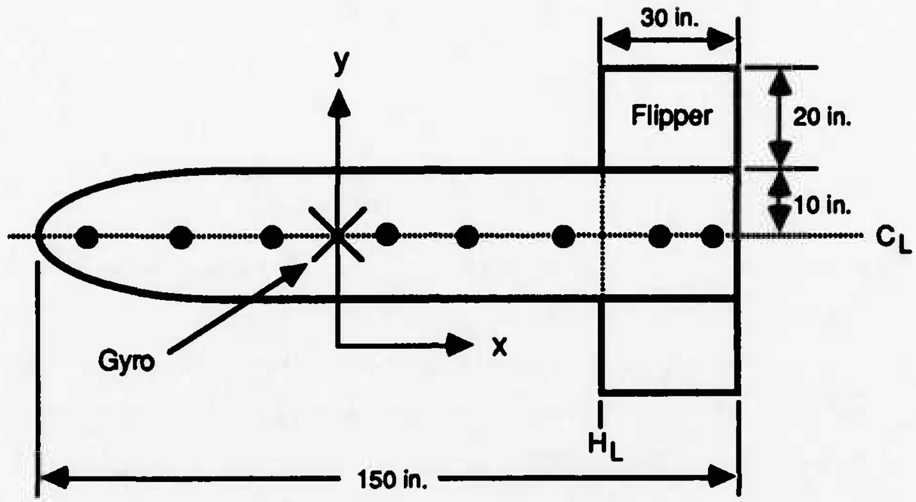

(a) Structural Model of the Missile - Flipper Combination

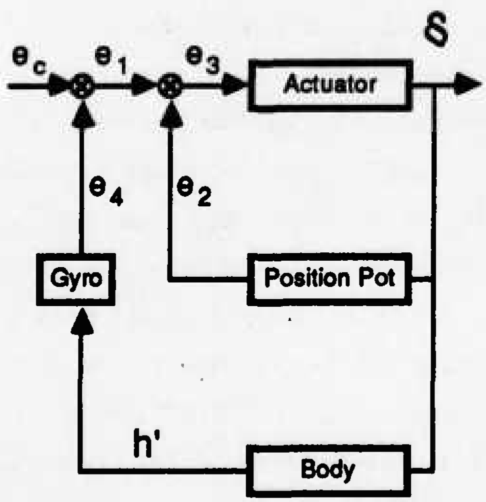

(b) Missile Servo Block Diagram

Figure 68. Air-to-Air Missile

The actuator transfer function is defined as

$$H_a = \frac{\delta}{e_3} = \frac{0.16667}{0.01p^2 + p}$$

while the gyroscope, which measures the rate of the bending slope of the missile, has a transfer function of the form

$$\frac{e_4}{h'} = \frac{0.3p}{7.036.0^{-6}p^2 + 3.7140.0^{-3}p + 1.0}$$

The position pot has a unity gain so that

$$e_2 = \delta$$

while h' is the structural rotation about the y-axis at Grid 45.

The MSC Handbook results are in terms of eigenvalues of the open and closed loop system. ASTROS does not currently have a capability to extract eigenvalues of the nonsymmetric matrices that result from the control system. Therefore, the analysis was changed to predicting the transient response due to a unit step pulse to the controller.

4.12.2 Input

Figure 69 presents the input data packet for this case. There are two alters to the standard MAPOL sequence. The first deletes the optimization portion of the sequence, thereby expediting the compilation of the MAPOL sequence, while the second prints the matrices used in the transient analysis. This is done so as to compare the matrices with NASTRAN quantities and thereby corroborate the ASTROS results. The BOUNDARY specification is lengthy in this case since extra points, transfer functions, direct matrix input and damping are all requested in addition to the more standard requests for the eigen-analysis and the Guyan reduction. The METHOD specification is necessary because the transient analysis is to be performed using the modal method. The presence of transfer function data requires that the transient analysis be performed using coupled equations. The PRINT solution control command specifies that displacements and accelerations for the points specified by the GRIDLIST 2 bulk data entry are to be printed for all the times for which there are data.

```
ASSIGN DATABASE TRANS1 KIMBERLY NEW DELETE
EDIT NOLIST
DELETE 229, 1033
INSERT 1320
CALL UTMPRT ( , [MHH(BC)], [BHH],[KHHT], [PDT] );
SOLUTION
ANALYZE
TITLE = SERVOELASTIC ANALYSIS OF AN AIR-TO-AIR MISSILE
   BOUNDARY  METHOD=14,ESET=20,DAMPING=1,TFL=1,M2PP=FLIPMASS,REDUCE=100
      TRANSIENT MODAL (DLOAD=12,TSTEP=20)
      PRINT DISP = 2, ACCEL = 2, TIME ALL
END
BEGIN BULK
$
GRID     1              -52.5   0.                      1246
GRID     2              -37.5   0.                      1246
GRID     3              -22.5   0.                      1246
GRID     4              -7.5    0.                      1246
GRID     5              7.5     0.                      1246
GRID     6              22.5    0.                      1246
GRID     7              37.5    0.                      1246
GRID     8              52.5    0.                      1246
GRID     9              67.5    0.                      1246
GRID     10             82.5    0.                      1246
GRID     45             0.0     0.                      1246
ASET1    100     3      1       THRU    10
$
CBAR     1       1       1       2      0.0     0.0     1.0
CBAR     2       1       2       3      0.0     0.0     1.0
CBAR     3       1       3       4      0.0     0.0     1.0
CBAR     4       1       4      45      0.0     0.0     1.0
CBAR     5       1       5       6      0.0     0.0     1.0
CBAR     6       1       6       7      0.0     0.0     1.0
CBAR     7       1       7       8      0.0     0.0     1.0
CBAR     8       1       8       9      0.0     0.0     1.0
CBAR     9       1       9      10      0.0     0.0     1.0
CBAR     45      1      45       5      0.0     0.0     1.0
PBAR     1       1      1.0+8   135.31  135.31  1.0+8
MAT1     1       1.0+7          0.33    0.0
$
CMASS2   1       100.   1       3
CMASS2   2       100.   2       3
CMASS2   3       100.   3       3
CMASS2   4       100.   4       3
CMASS2   5       100.   5       3
CMASS2   6       100.   6       3
CMASS2   7       100.   7       3
CMASS2   8       100.   8       3
CMASS2   9       100.   9       3
CMASS2   10      100.   10      3
CONVERT MASS     .00259
$
EIGR     14      GIV    0.0     300.0           5                       +INV
```

Figure 69. Input Data Stream for the Servoelastic Test Case

```
+INV    MAX
$
TSTEP    20      84        .002    2
DLOAD   12       1.       1.0      30
TLOAD1  30       20       34
TABLED1  34                                                               +T1
+T1      0.      1.0        10.0   1.0
DLAGS   20       35
DLONLY  35       20                1.
$
DMIG    FLIPMASSRDP        REC                                            +FLIP
+FLIP   21                 9       3       1.94301                        +FLP1
+FLP1   21                 10      3       5.82902
$
TABDMP1 1       G         45.      .03     125.4   .05     248.2   .08
EPOINT  20      20        21       51      52      53      54
TF      1       21                         1.0     .01                    +2153
+2153   53               -.166667
TF      1       51                 1.0                                    +511
+511    54                 1.0                                            +512
+512    20                -1.0
TF      1       52                 1.0                                    +521
+521    21                -1.0
TF      1       53                 1.0                                    +531
+531    51                -1.0                                            +532
+532    52                 1.0
TF      1       54                1.0      3.7136-37.0362-6               +5445
+5445   45      5                 -0.3
$
TF      1       20                 1.0
GRIDLIST, 2, 45,20,21,51,52,53,54
ENDDATA
```

Figure 69. Input Data Stream for the Servoelastic Test Case (Concluded)

For the structural model, the grids are along the fuselage of the missile with GRID 45 the location of the rate gyro. Bar elements connect all of the grids and concentrated masses represent the mass of the fuselage. The mass coupling caused by the flipper motion is determined by the static unbalance of the grid points on the flipper. For GRID 9, the unbalance about the hinge line is 1.943 $lb\text{-}sec^2$ and for GRID 10 it is 5.829 $lb\text{-}sec^2$. These are input in consistent units since the CONVERT entry for the mass does not apply to direct matrix input.

Extra points define the flipper rotation and the nodes in the control system. EPOINT 20 is the command to the actuator while EPOINT 21 is the flipper rotation. EPOINTs 51, 52, 53, and 54 correspond to signals e_1, e_2, e_3, and e_4 of **Figure 68**, respectively. The transient load specification starts with the DLOAD entry which defines scaling factors and references a TLOAD1 entry, which in turn references a TABLED1 and a DLAGS entry. The TABLED1 entry defines the step load while the DLAGS entry directs the construction of the spatial component of the applied load. In this case, this is a command to the flipper so that a DLONLY entry is required to apply a unit load to EPOINT 20.

The TSTEP entry specifies that 84 time steps are to be computed at two millisecond intervals and that data are to be saved for every other time step. It is to these latter times that the TIME ALL print request applies.

The transfer function bulk data define the control system as given in the Problem Description of this subsection. ASTROS does not have the NASTRAN requirement that all second order coefficients be nonzero so that this input differs from that given in the Handbook. The term "transfer function" is confusing in that the data specified by these entries are added to matrices in the positions indicated and do not necessarily represent an input/output relationship that is typically implied by the term transfer function. For example, the last TF bulk data entry of the packet places a 1.0 on the diagonal of the stiffness matrix corresponding to EPOINT 20. Clearly, this is not a transfer function, but instead allows the commanded signal associated with the DLONLY entry to excite the system.

The TABDMP1 entry provides frequency-dependent viscous damping to represent the structural damping effects. The data were selected with knowledge of the flexible mode frequencies and specify g=0.03 for the first mode,

0.05 for the second and 0.08 for the third. The GRIDLIST entry requests output at the gyro location and all the extra points.

4.12.3 Results

This example is contrived inasmuch as, due to limitations in ASTROS, it calculates the response of an unsupported missile with no air or gravity loads when the flipper undergoes a step pulse. The only loads on the structure are inertial due to the static unbalance of the flipper. **Figure 70** contains abridged output for this case and first shows the matrix print of the modal mass matrix. Terms in this matrix that are zero are suppressed for the most part. There are a number of off-diagonal terms that result from the direct matrix input and the transfer function input.

The remainder of **Figure 70** consists of prints of the requested output at several of the requested times. There is minimal response of the flipper and of the structure to the commanded signal. The algorithm that is used to initiate the Newmark-Beta process is known to produce "ringing" when the load is applied to massless degrees of freedom, as in the present case. This is manifested by the fact that the response of EPOINT 20 is not a unit step, but that it instead fluctuates about 1.0. The net result is that the response has little meaning in this case and is presented more for formatting and for procedure checkout.

4.13 GUST ANALYSIS

This example illustrates the performance of gust analysis in the frequency domain within ASTROS.

4.13.1 Problem Description

A description of the loads generation for gust analysis in the frequency domain is given in Subsection 11.2.3 of the Theoretical Manual while the response calculation is discussed in Subsection 11.4.2 of the same manual.

The structural model is the swept wing described in Subsection 4.6 (**Figure** 47). Only the wing is included in this example with the tail surface removed for simplification. The current ASTROS capability for gust response is to compute the frequency response to a one dimensional gust with a user defined frequency variation. Power spectral techniques, including RMS response values, are not implemented. These operations could be performed by a postprocessing operation on the available data.

```
PRINT OF DOUBLE PRECISION RECTANGULAR MATRIX MHH  000, 11 ROWS BY 11 COLUMNS

ROWS          1 THROUGH       1 OF COLUMN       1

 7.7420D-01

ROWS          2 THROUGH       2 OF COLUMN       2

 7.9752D-01

ROWS          3 THROUGH       3 OF COLUMN       3

 1.0565D+00

ROWS          4 THROUGH       4 OF COLUMN       4

 1.5584D+00

ROWS          5 THROUGH       5 OF COLUMN       5

 1.5390D+00

COLUMN        6 IS NULL

ROWS          1 THROUGH      11 OF COLUMN       7

-1.7277D+00  7.5147D+00  6.6280D+00  5.5359D+00 -3.4284D+00  0.0000D+00  1.0000D-02  0.0000D+00  0.0000D+00  0.0000D+00
 0.0000D+00

COLUMNS       8 THROUGH      10 ARE NULL

ROWS          1 THROUGH      11 OF COLUMN      11

 0.0000D+00  0.0000D+00  0.0000D+00  0.0000D+00  0.0000D+00  0.0000D+00  0.0000D+00  0.0000D+00  0.0000D+00  0.0000D+00
 7.0362D-06

FINISHED WITH MATRIX MHH  000
```

Figure 70. Abridged Output for the Servoelastic Test Case

SERVOELASTIC ANALYSIS OF AN AIR-TO-AIR MISSILE ASTROS VERSION 1.00 8/11/88 P. 12

TRANSIENT ANALYSIS: BOUNDARY 1, TIME = 0.0000000E+00

D I S P L A C E M E N T   V E C T O R

POINT ID.	TYPE	T1	T2	T3	R1	R2	R3
20	E	0.00000E+00					
21	E	0.00000E+00					
45	G	0.00000E+00	0.00000E+00	0.00000E+00	0.00000E+00	0.00000E+00	0.00000E+00
51	E	0.00000E+00					
52	E	0.00000E+00					
53	E	0.00000E+00					
54	E	0.00000E+00					

SERVOELASTIC ANALYSIS OF AN AIR-TO-AIR MISSILE ASTROS VERSION 1.00 8/11/88 P. 13

TRANSIENT ANALYSIS: BOUNDARY 1, TIME = 0.0000000E+00

A C C E L E R A T I O N   V E C T O R

POINT ID.	TYPE	T1	T2	T3	R1	R2	R3
20	E	3.75000E+05					
21	E	7.57569E+00					
45	G	0.00000E+00	0.00000E+00	4.88276E+00	0.00000E+00	-1.30685E-01	0.00000E+00
51	E	3.75003E+05					
52	E	7.57569E+00					
53	E	3.74996E+05					
54	E	-3.24465E+00					

SERVOELASTIC ANALYSIS OF AN AIR-TO-AIR MISSILE ASTROS VERSION 1.00 8/11/88 P. 14

TRANSIENT ANALYSIS: BOUNDARY 1, TIME = 4.0000002E-03

D I S P L A C E M E N T   V E C T O R

POINT ID.	TYPE	T1	T2	T3	R1	R2	R3
20	E	1.00000E+00					
21	E	1.05599E-04					
45	G	0.00000E+00	0.00000E+00	1.11592E-04	0.00000E+00	-5.70030E-07	0.00000E+00
51	E	1.00003E+00					
52	E	1.05599E-04					
53	E	9.99922E-01					
54	E	-2.78358E-05					

SERVOELASTIC ANALYSIS OF AN AIR-TO-AIR MISSILE ASTROS VERSION 1.00 8/11/88 P. 15

TRANSIENT ANALYSIS: BOUNDARY 1, TIME = 4.0000002E-03

A C C E L E R A T I O N   V E C T O R

POINT ID.	TYPE	T1	T2	T3	R1	R2	R3
20	E	0.00000E+00					
21	E	1.17269E+01					
45	G	0.00000E+00	0.00000E+00	1.72199E+01	0.00000E+00	1.24774E+00	0.00000E+00
51	E	-3.49787E+01					
52	E	1.17269E+01					
53	E	-4.67056E+01					
54	E	3.49787E+01					

Figure 70 Abridged Output for the Servoelastic Test Case (Continued)

```
SERVOELASTIC ANALYSIS OF AN AIR-TO-AIR MISSILE                      ASTROS VERSION 1.00   8/11/88   P.   22

                                                  TRANSIENT ANALYSIS: BOUNDARY 1, TIME = 2.0000001E-02

                                   D I S P L A C E M E N T   V E C T O R

   POINT ID.   TYPE        T1            T2            T3            R1            R2            R3
       20        E     1.50000E+00
       21        E     1.84124E-03
       45        G     0.00000E+00   0.00000E+00  -3.07978E-03   0.00000E+00   2.04676E-04   0.00000E+00
       51        E     1.49439E+00
       52        E     1.84124E-03
       53        E     1.49255E+00
       54        E     5.61117E-03
SERVOELASTIC ANALYSIS OF AN AIR-TO-AIR MISSILE                      ASTROS VERSION 1.00   8/11/88   P.   23

                                                  TRANSIENT ANALYSIS: BOUNDARY 1, TIME = 2.0000001E-02

                                   A C C E L E R A T I O N   V E C T O R

   POINT ID.   TYPE        T1            T2            T3            R1            R2            R3
       20        E    -3.75000E+05
       21        E     2.29173E+00
       45        G     0.00000E+00   0.00000E+00   2.71156E+01   0.00000E+00  -1.56393E+00   0.00000E+00
       51        E    -3.74865E+05
       52        E     2.29173E+00
       53        E    -3.74867E+05
       54        E    -1.34762E+02
SERVOELASTIC ANALYSIS OF AN AIR-TO-AIR MISSILE                      ASTROS VERSION 1.00   8/11/88   P.   32

                                                  TRANSIENT ANALYSIS: BOUNDARY 1, TIME = 4.0000003E-02

                                   D I S P L A C E M E N T   V E C T O R

   POINT ID.   TYPE        T1            T2            T3            R1            R2            R3
       20        E     1.00000E+00
       21        E     4.95319E-03
       45        G     0.00000E+00   0.00000E+00  -7.06870E-03   0.00000E+00   5.18944E-04   0.00000E+00
       51        E     9.94313E-01
       52        E     4.95319E-03
       53        E     9.89360E-01
       54        E     5.68708E-03
SERVOELASTIC ANALYSIS OF AN AIR-TO-AIR MISSILE                      ASTROS VERSION 1.00   8/11/88   P.   33

                                                  TRANSIENT ANALYSIS: BOUNDARY 1, TIME = 4.0000003E-02

                                   A C C E L E R A T I O N   V E C T O R

   POINT ID.   TYPE        T1            T2            T3            R1            R2            R3
       20        E     0.00000E+00
       21        E     2.70406E-01
       45        G     0.00000E+00   0.00000E+00  -3.14077E+00   0.00000E+00  -9.91934E-01   0.00000E+00
       51        E     6.71435E+01
       52        E     2.70406E-01
       53        E     6.68731E+01
       54        E    -6.71435E+01
```

Figure 70 Abridged Output for the Servoelastic Test Case (Continued)

SERVOELASTIC ANALYSIS OF AN AIR-TO-AIR MISSILE ASTROS VERSION 1.00 8/11/88 P. 62

TRANSIENT ANALYSIS: BOUNDARY 1, TIME = 1.0000001E-01

D I S P L A C E M E N T   V E C T O R

POINT ID.	TYPE	T1	T2	T3	R1	R2	R3
20	E	1.00000E+00					
21	E	1.47888E-02					
45	G	0.00000E+00	0.00000E+00	-2.05840E-02	0.00000E+00	1.53038E-03	0.00000E+00
51	E	9.95731E-01					
52	E	1.47888E-02					
53	E	9.80942E-01					
54	E	4.26872E-03					

SERVOELASTIC ANALYSIS OF AN AIR-TO-AIR MISSILE ASTROS VERSION 1.00 8/11/88 P. 63

TRANSIENT ANALYSIS: BOUNDARY 1, TIME = 1.0000001E-01

A C C E L E R A T I O N   V E C T O R

POINT ID.	TYPE	T1	T2	T3	R1	R2	R3
20	E	0.00000E+00					
21	E	-1.33052E-02					
45	G	0.00000E+00	0.00000E+00	-3.27249E+01	0.00000E+00	3.08332E-01	0.00000E+00
51	E	-5.59999E+01					
52	E	-1.33052E-02					
53	E	-5.59866E+01					
54	E	5.59999E+01					

Figure 70 Abridged Output for the Servoelastic Test Case (Concluded)

4.13.2 Input

Figure 71 shows the input data stream for this example. Much of this input has already been described in Subsection 4.9.2. The unique features of this model relate to the FREQUENCY discipline invoked in the solution control packet. The DLOAD bulk data entry is a dummy input in this case in that it is not required in the solution process and is there only because DLOAD is a required option for the frequency response. The FSTEP option of the solution control command invokes the FREQ2 bulk data which indicates that the response is to be calculated at forty frequencies that vary in a logrithmic fashion from 0.1 Hz to 10.0 Hz. The GUST solution control option invokes the GUST bulk data entry which defines the gust parameters:

w_g = 1.0×10^{-4} in/sec

x_o = -2.5 inches

V = 10,000 inches/sec

$\bar{q}$ = 0.5 psi

M = 0.5789

and specifies that a symmetric analysis is to be performed. Since the analysis is being performed in the frequency domain, the RLOAD1 bulk data entry is referenced by the GUST entry. The RLOAD1 entry indicates, in turn, that a shaping function specified by TABLED1 data be used to describe the frequency content of the gust input. In this case, a flat frequency input of 1.0 is specified for the range of 0.0 to 1000.0 Hz. The RLOAD1 entry also references a DLAGS entry which, like the DLOAD specification, is required for error checking purposes, but is unused in the gust analysis procedure. The same comment also applies to the FORCE entry with SID=20 that is referenced on the DLAGS entry.

4.13.3 Results

The PRINT solution control request of Figure 71 specifies that displacement results are to be printed in polar format at points given by GRIDLIST 7 for all frequencies. The GRIDLIST entry indicates that the displacements are to be printed at GRID 37. Figure 72 lists the results of the print request for f = 0.1, 1.0 and 10.0 Hertz. The polar form of the output

```
ASSIGN DATABASE GUST SHAZAM NEW DELETE
SOLUTION
ANALYZE
TITLE = MULTIDISCIPLINARY SAMPLE PROBLEM
SUBTITLE = ADAPTED FOR GUST ANALYSIS
BOUNDARY MPC = 101, SPC=10, REDUCE=100, METHOD=99
   PRINT DISP(POLA) = 7, FREQ ALL
   FREQUENCY MODAL (DLOAD=10, FSTEP = 30, GUST = 60)
END
BEGIN BULK
$
$        SWEPT WING MODEL FROM
$        "A ROOT LOCUS BASED FLUTTER SYNTHESIS PROCEDURE" BY
$        P. HAJELA        GUST ANALYSIS ONLY
$
GRIDLIST, 7,    37
FORCE, 20, 1, , 1.0, 0.0, 0.0, 0.0
GRID           1           0.0     0.0  10.039
GRID           2           0.0     0.0 -10.039
GRID           3       72.8345     0.0  10.039
GRID           4       72.8345     0.0 -10.039
GRID           5      145.6690     0.0  10.039
GRID           6      145.6690     0.0 -10.039
GRID           7       53.4758 116.667  9.3502
GRID           8       53.4758 116.667 -9.3502
GRID           9      121.1590 116.667  9.3502
GRID          10      121.1590 116.667 -9.3502
GRID          11      188.8430 116.667  9.3502
GRID          12      188.8430 116.667 -9.3502
GRID          13      106.5920 233.333  8.6613
GRID          14      106.5920 233.333 -8.6613
GRID          15      169.4840 233.333  8.6613
GRID          16      169.4840 233.333 -8.6613
GRID          17      232.0170 233.333  8.6613
GRID          18      232.0170 233.333 -8.6613
GRID          19      160.4280 350.0    7.9724
GRID          20      160.4280 350.0   -7.9724
GRID          21      217.8090 350.0    7.9724
GRID          22      217.8090 350.0   -7.9724
GRID          23      275.1910 350.0    7.9724
GRID          24      275.1910 350.0   -7.9724
GRID          25      213.9030 466.667  7.2834
GRID          26      213.9030 466.667 -7.2834
GRID          27      266.1340 466.667  7.2834
GRID          28      266.1340 466.667 -7.2834
GRID          29      318.3650 466.667  7.2834
GRID          30      318.3650 466.667 -7.2834
GRID          31      267.3780 583.333  6.5945
GRID          32      267.3780 583.333 -6.5945
GRID          33      314.4590 583.333  6.5945
GRID          34      314.4590 583.333 -6.5945
GRID          35      361.5390 583.333  6.5945
GRID          36      361.5390 583.333 -6.5945
```

Figure 71. Input Data Stream for the Gust Test Case

```
GRID          37         320.8550 700.0    5.9055
GRID          38         320.8550 700.0   -5.9055
GRID          39         362.7840 700.0    5.9055
GRID          40         362.7840 700.0   -5.9055
GRID          41         404.7130 700.0    5.9055
GRID          42         404.7130 700.0   -5.9055
GRID          43         290.7840 700.0       0.0
GRID          44         434.7830 700.0       0.0
ASET1,  100,  3,  7,  9, 11, 13, 15, 17, ASETA
+SETA,   19, 21, 23, 25, 27, 29, 31, 33, ASETB
+SETB,   35, 37, 39, 41
SPC1          10  123456       1     THRU       6
SPC1          10     456       7     THRU      44
MPC,   101,    43,   1,   -4.0,  37,   1,  1.0, , MPC4311
+PC4311,  ,    38,   1,    1.0,  39,   1,  1.0, , MPC4312
+PC4312,  ,    40,   1,    1.0
MPC,   101,    44,   1,   -4.0,  39,   1,  1.0, , MPC4411
+PC4411,  ,    40,   1,    1.0,  41,   1,  1.0, , MPC4412
+PC4412,  ,    42,   1,    1.0
MPC,   101,    43,   2,   -4.0,  37,   2,  1.0, , MPC4321
+PC4321,  ,    38,   2,    1.0,  39,   2,  1.0, , MPC4322
+PC4322,  ,    40,   2,    1.0
MPC,   101,    44,   2,   -4.0,  39,   2,  1.0, , MPC4421
+PC4421,  ,    40,   2,    1.0,  41,   2,  1.0, , MPC4422
+PC4422,  ,    42,   2,    1.0
MPC,   101,    43,   3,      -1.0,  37,   3, 0.85859, , MPC4331
+PC4331,  ,    38,   3,  0.85859,  39,   3,-0.35859, , MPC4332
+PC4332,  ,    40,   3, -0.35859
MPC,   101,    44,   3,      -1.0,  39,   3,-0.35859, , MPC4431
+PC4431,  ,    40,   3, -0.35859,  41,   3, 0.85859, , MPC4432
+PC4432,  ,    42,   3,  0.85859
$
$       UPPER AND LOWER SKINS 100 - UPPER, 200 - LOWER
$
CQDMEM1      101     1004        1        7        9        3
CQDMEM1      201     1004        2        8       10        4
CQDMEM1      102     1004        3        9       11        5
CQDMEM1      202     1004        4       10       12        6
CQDMEM1      103     1004        7       13       15        9
CQDMEM1      203     1004        8       14       16       10
CQDMEM1      104     1004        9       15       17       11
CQDMEM1      204     1004       10       16       18       12
CQDMEM1      105     1005       13       19       21       15
CQDMEM1      205     1005       14       20       22       16
CQDMEM1      106     1005       15       21       23       17
CQDMEM1      206     1005       16       22       24       18
CQDMEM1      107     1005       19       25       27       21
CQDMEM1      207     1005       20       26       28       22
CQDMEM1      108     1005       21       27       29       23
CQDMEM1      208     1005       22       28       30       24
CQDMEM1      109     1006       25       31       33       27
CQDMEM1      209     1006       26       32       34       28
CQDMEM1      110     1006       27       33       35       29
```

Figure 71. Input Data Stream for the Gust Test Case (Continued)

```
CQDMEM1      210    1006     28     34     36     30
CQDMEM1      111    1006     31     37     39     33
CQDMEM1      211    1006     32     38     40     34
CQDMEM1      112    1006     33     39     41     35
CQDMEM1      212    1006     34     40     42     36
$
$       MODEL SUB STRUCTURE
$       QUAD  MEMS:  300 - LE,   350 - MID, 400 - TE, 500 - CHORDWISE
$       AXIAL RODS:  600 - INBOARD, 700 - MID,  800 - OUTBOARD BAYS
$
CSHEAR       301    2007      1      2      8      7
CSHEAR       351    2007      3      4     10      9
CSHEAR       401    2007      5      6     12     11
CSHEAR       302    2007      7      8     14     13
CSHEAR       352    2007      9     10     16     15
CSHEAR       402    2007     11     12     18     17
CSHEAR       303    2008     13     14     20     19
CSHEAR       353    2008     15     16     22     21
CSHEAR       403    2008     17     18     24     23
CSHEAR       304    2008     19     20     26     25
CSHEAR       354    2008     21     22     28     27
CSHEAR       404    2008     23     24     30     29
CSHEAR       305    2009     25     26     32     31
CSHEAR       355    2009     27     28     34     33
CSHEAR       405    2009     29     30     36     35
CSHEAR       306    2009     31     32     38     37
CSHEAR       356    2009     33     34     40     39
CSHEAR       406    2009     35     36     42     41
CSHEAR       501    2010      7      8     10      9
CSHEAR       502    2010      9     10     12     11
CSHEAR       503    2010     13     14     16     15
CSHEAR       504    2010     15     16     18     17
CSHEAR       505    2011     19     20     22     21
CSHEAR       506    2011     21     22     24     23
CSHEAR       507    2011     25     26     28     27
CSHEAR       508    2011     27     28     30     29
CSHEAR       509    2012     31     32     34     33
CSHEAR       510    2012     33     34     36     35
CSHEAR       511    2012     37     38     40     39
CSHEAR       512    2012     39     40     42     41
$
CONROD      1301       7      8     90    0.3
CONROD      1302      13     14     90    0.3
CONROD      1303      19     20     90    0.3
CONROD      1304      25     26     90    0.3
CONROD      1305      31     32     90    0.3
CONROD      1306      37     38     90    0.3
CONROD      1401       9     10     90    0.3
CONROD      1402      15     16     90    0.3
CONROD      1403      21     22     90    0.3
CONROD      1404      27     28     90    0.3
CONROD      1405      33     34     90    0.3
CONROD      1406      39     40     90    0.3
```

Figure 71. Input Data Stream for the Gust Test Case (Continued)

```
CONROD      1501     11     12     90     0.3
CONROD      1502     17     18     90     0.3
CONROD      1503     23     24     90     0.3
CONROD      1504     29     30     90     0.3
CONROD      1505     35     36     90     0.3
CONROD      1506     41     42     90     0.3
$
CROD         601   6001      1      7
CROD         602   6001      2      8
CROD         603   6001      3      9
CROD         604   6001      4     10
CROD         605   6001      5     11
CROD         606   6001      6     12
CROD         607   6001      7     13
CROD         608   6001      8     14
CROD         609   6001      9     15
CROD         610   6001     10     16
CROD         611   6001     11     17
CROD         612   6001     12     18
CROD         701   7002     13     19
CROD         702   7002     14     20
CROD         703   7002     15     21
CROD         704   7002     16     22
CROD         705   7002     17     23
CROD         706   7002     18     24
CROD         707   7002     19     25
CROD         708   7002     20     26
CROD         709   7002     21     27
CROD         710   7002     22     28
CROD         711   7002     23     29
CROD         712   7002     24     30
CROD         801   8003     25     31
CROD         802   8003     26     32
CROD         803   8003     27     33
CROD         804   8003     28     34
CROD         805   8003     29     35
CROD         806   8003     30     36
CROD         807   8003     31     37
CROD         808   8003     32     38
CROD         809   8003     33     39
CROD         810   8003     34     40
CROD         811   8003     35     41
CROD         812   8003     36     42
$
CONM2      50001      7          20.0
CONM2      50002      8          20.0
CONM2      50003      9          20.0
CONM2      50004     10          20.0
CONM2      50005     11          20.0
CONM2      50006     12          20.0
CONM2      50007     13          20.0
CONM2      50008     14          20.0
CONM2      50009     15          20.0
```

Figure 71. Input Data Stream for the Gust Test Case (Continued)

```
CONM2       50010     16           20.0
CONM2       50011     17           20.0
CONM2       50012     18           20.0
CONM2       50013     19           20.0
CONM2       50014     20           20.0
CONM2       50015     21           20.0
CONM2       50016     22           20.0
CONM2       50017     23           20.0
CONM2       50018     24           20.0
CONM2       50019     25           20.0
CONM2       50020     26           20.0
CONM2       50021     27           20.0
CONM2       50022     28           20.0
CONM2       50023     29           20.0
CONM2       50024     30           20.0
CONM2       50025     31           20.0
CONM2       50026     32           20.0
CONM2       50027     33           20.0
CONM2       50028     34           20.0
CONM2       50029     35           20.0
CONM2       50030     36           20.0
CONM2       50031     37           40.0
CONM2       50032     38           40.0
CONM2       50033     39           40.0
CONM2       50034     40           40.0
CONM2       50035     41           40.0
CONM2       50036     42           40.0
CONM2       50037     43           40.0
CONM2       50038     44           40.0
$
PQDMEM1,  1004,   91,    0.02
PQDMEM1,  1005,   91,    0.02
PQDMEM1,  1006,   91,    0.02
$
PSHEAR,   2007,   90,    0.02
PSHEAR,   2008,   90,    0.02
PSHEAR,   2009,   90,    0.02
PSHEAR,   2010,   90,    0.02
PSHEAR,   2011,   90,    0.02
PSHEAR,   2012,   90,    0.02
$
PROD,     6001,   90,    1.0
PROD,     7002,   90,    1.0
PROD,     8003,   90,    1.0
$
MAT1,       90,     10.E6,   ,   0.3,    0.1
MAT1,       91,     10.E6,   ,   0.3,    0.1, , , , ABC
+BC,   30000.0,   25000.0, 15000.0
CONVERT,  MASS,  2.588E-3
$
$   AERODYNAMIC MODEL
$
CAERO1, 1, , , 10, 8, , , 1, ABC
```

Figure 71. Input Data Stream for the Gust Test Case (Continued)

```
+BC, -24.277, 0.0, 0.0, 218.5, 306.874, 700.0, 0.0, 125.8
SPLINE1, 3, , 1, 1, 80, 10
SET1, 10, 1, 3, 5, 7, 9, 11, 13, DEF
+EF, 15, 17, 19, 21, 23, 25, 27, 29, GHI
+HI, 31, 33, 35, 37, 39, 41
$
AERO, , 187.6, 8.464E-8
MKAERO1   1     0     0.5789                                  MKA
+KA       0.0589 0.2357
EIGR, 99, GIV, 0.0, 700.0, 2, 2, , , ABC
+BC, MAX
DLOAD, 10, 1.0, 1.0, 6
FREQ2, 30, 0.1, 10.0, 40
GUST, 60, 61, 1.0E-4, -2.5, 10000., 0.5, .5789, ,+GS1, +GS1, 1, 0
RLOAD1, 61, 65, 70
DLAGS, 65, 20
TABLED1   70                                                  +T1
+T1       0.0     1.0     1000.    1.0
ENDDATA
```

Figure 71. Input Data Stream for the Gust Test Case (Concluded)

```
                                         FREQUENCY ANALYSIS: BOUNDARY 1, FREQ = 1.0000000E-01

                     C O M P L E X   D I S P L A C E M E N T   V E C T O R
                                     P O L A R   F O R M

POINT ID.   TYPE        T1            T2            T3            R1            R2            R3
   37         G     1.50576E-04   1.11551E-03   1.00108E-01   0.00000E+00   0.00000E+00   0.00000E+00
                    1.75200E+02   1.76943E+02   3.57007E+02   0.00000E+00   0.00000E+00   0.00000E+00

                                         FREQUENCY ANALYSIS: BOUNDARY 1, FREQ = 1.0000000E+00

                     C O M P L E X   D I S P L A C E M E N T   V E C T O R
                                     P O L A R   F O R M

POINT ID.   TYPE        T1            T2            T3            R1            R2            R3
   37         G     7.36010E-04   1.97223E-03   1.65621E-01   0.00000E+00   0.00000E+00   0.00000E+00
                    1.35201E+02   1.40968E+02   3.21593E+02   0.00000E+00   0.00000E+00   0.00000E+00

                                         FREQUENCY ANALYSIS: BOUNDARY 1, FREQ = 1.0000001E+01

                     C O M P L E X   D I S P L A C E M E N T   V E C T O R
                                     P O L A R   F O R M

POINT ID.   TYPE        T1            T2            T3            R1            R2            R3
   37         G     1.54310E-04   3.43810E-05   6.03861E-04   0.00000E+00   0.00000E+00   0.00000E+00
                    1.59266E+02   1.62640E+02   1.41107E+02   0.00000E+00   0.00000E+00   0.00000E+00
```

Figure 72. Selected Output for the Gust Response Test Case

lists the magnitude on the first line and the corresponding phase (in degrees) on a second line. A plot of the frequency response data is given in Figure 73 and indicates that the response is dominated by the structural resonance at 1.5 Hertz.

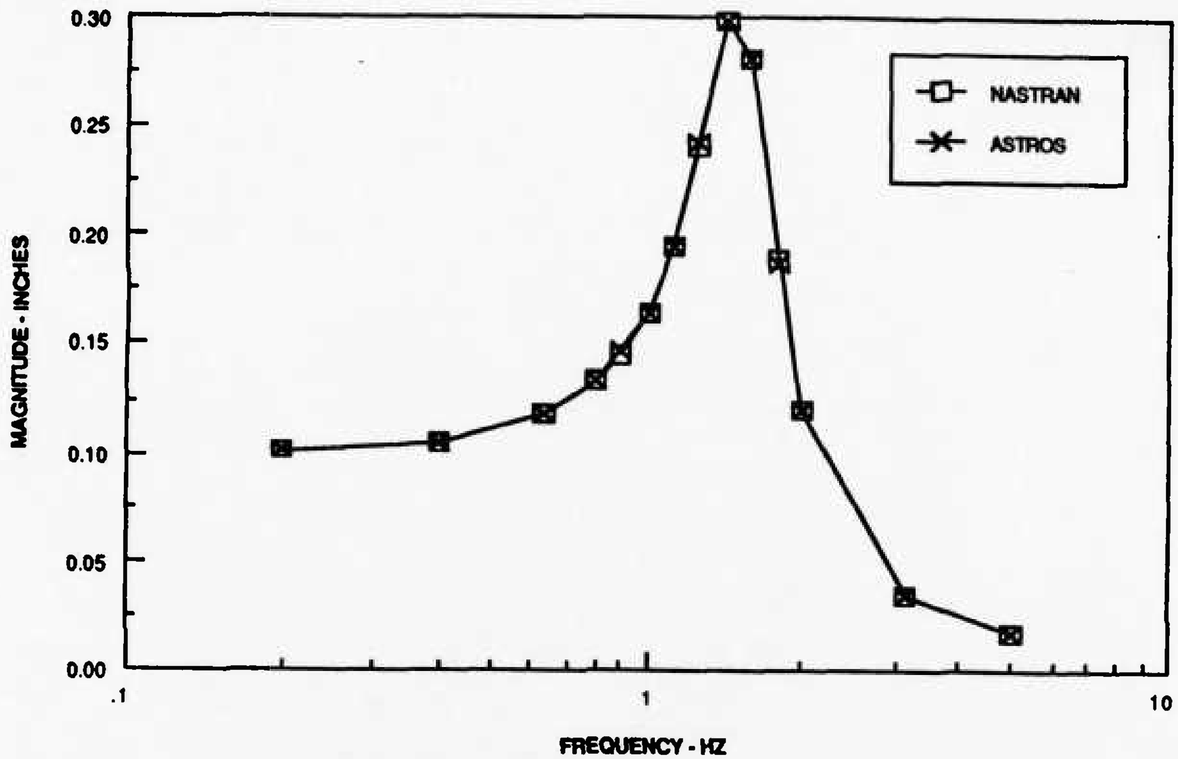

Figure 73. Response of the Multidisciplinary Wing of Subsection 4.6 to a Gust Input

4.14 BLAST RESPONSE

This final example exercises the blast response capability of ASTROS. This capability encompasses unsteady aerodynamics and transient response components so that much of the input duplicates previously presented information.

4.14.1 Problem Description

Section XI of the Theoretical Manual discusses the approach used in ASTROS to calculate the response of an aircraft to a nuclear blast. This response is calculated in the time domain while the underlying unsteady aerodynamics are calculated in the frequency domain. Appendix B of the Theoretical Manual discusses how the aerodynamics are transformed to the time domain.

The example presented here was developed primarily to check out the implementation of the blast response capability and to assess whether the results appear reasonable. No comparable test case was available to correlate the computed results so that the blast response capability must be considered immature until more rigorous test cases are performed.

The test case utilizes the same structural model that was applied in Subsections 4.4 and 4.5. The aircraft is assumed to be performing a 9g pullup when it is impacted by a nuclear blast that has a yield of 100 kilotons that was detonated 20,000.0 feet below and 1,000.0 feet ahead of the aircraft.

4.14.2 Input

Figure 74 shows the input data stream for this case. The RECTS.DAT data set of Figure 37 has been included so that the depicted bulk data are limited. The boundary condition specification includes a METHOD option since the blast analysis is performed in modal coordinates. A Guyan reduction is performed prior to the eigenanalysis. The PRINT command requests output at the designated grids for all the time steps at which data have been saved.

In the bulk data packet, the ASET1 entries retain all out-of-plane displacements for the structure as well as the rotation at the support point. The MKAERO1 entry specifies a symmetric aerodynamics analysis (the blast response is currently limited to symmetric responses) be performed at a single Mach number and a series of reduced frequencies. Unsteady aerodynamics are required for the blast analysis rather than the steady aerodynamics of Subsection 4.4. The planform data are therefore converted into the form suitable for the Doublet Lattice procedure. The BLAST entry specifies the parameters of the nuclear blast. Units for these inputs are in a foot/pound/seconds system. Default parameters were accepted for this entry, thereby removing the need for the second continuation entry. The TSTEP entry specifies that results are to be computed every 2 milliseconds and are to be written to the data base every fifth time step.

```
ASSIGN DATABASE BLAST SHAZAM NEW DELETE
SOLUTION
ANALYZE
BOUNDARY MPC=200,SPC=10, SUPPORT=100, REDUCE=100, METHOD=99
   PRINT DISP = 10, TIME ALL
   BLAST (BLCOND=10, TSTEP=10)
END
BEGIN BULK
INCLUDE RECTS.DAT
ASET1        100      3      1      2      3      4      5      6
ASET1        100      3      9     10     11     12
ASET1        100      3     13     14     15     16     17     18
ASET1        100     35     20
EIGR          99    GIV    0.0  700.0      2      4                EIG
+IG          MAX
$
MKAERO1        1      0  0.763                                      +MKA
+MKA    0.000081    0.1    0.2    0.5   0.75    1.0    1.5    2.0
$
$   WING DATA
$
AERO                40.0     1.
CAERO1         1                    5      5                  1 +CAE
+CAE        10.0    0.0    0.0   20.0   10.0   60.0    0.0   20.0
$
$   CANARD DATA
$
CAERO1         2                    2      3                  1 +CCA
+CCA        85.0    0.0    0.0   15.0   90.0   20.0    0.0   10.0
$
SPLINE1        3            1      1     25     10
SET1          10      1     3      5      9     11     13     15 +SET
+SET          17     20
AESURF        10   ELEV     2             4      7
ATTACH        10      2     2      7     20
$
BLAST         10   4.0E4  741.0  100.0  20000.  0.763  1000.    0.0 +ABC
+ABC           0   200.      1      0     10    9.0
TSTEP         10    100   .002      5
$
GRIDLIST      10      5     11     17     20
$
ENDDATA
```

Figure 74. Input Data Stream for the Blast Response Test Case

4.14.3 Results

Figure 75 presents abridged output for this example. The displacements are in an inertial coordinate system fixed to the surface of the earth so that the vertical displacements are approximately 40,000 feet. (Note: in the process of documenting this example it was realized that the structural dimensions and deformations are in terms of inches while the blast data is in feet. This inconsistency has not been removed, but it could be by adjusting the RECTS.DAT file of **Figure** 37.) Since there is no comparison data and since there are known errors in the input, these output data are being presented primarily as a baseline that allows further investigators to check the implementation of the current procedure before performing enhancements.

BLAST ANALYSIS: BOUNDARY 1, TIME = 0.0000000E+00

D I S P L A C E M E N T   V E C T O R

POINT ID.	TYPE	T1	T2	T3	R1	R2	R3
5	G	9.09497E-04	-2.20560E-03	4.00002E+04	0.00000E+00	0.00000E+00	0.00000E+00
11	G	9.22787E-04	-2.18666E-03	4.00002E+04	0.00000E+00	0.00000E+00	0.00000E+00
17	G	9.67411E-04	-2.19494E-03	4.00001E+04	0.00000E+00	0.00000E+00	0.00000E+00
20	G	0.00000E+00	0.00000E+00	4.00000E+04	0.00000E+00	9.06239E-04	0.00000E+00

BLAST ANALYSIS: BOUNDARY 1, TIME = 1.0000001E-02

D I S P L A C E M E N T   V E C T O R

POINT ID.	TYPE	T1	T2	T3	R1	R2	R3
5	G	2.64377E-03	-2.29536E-03	4.00001E+04	0.00000E+00	0.00000E+00	0.00000E+00
11	G	2.59169E-03	-2.25966E-03	4.00000E+04	0.00000E+00	0.00000E+00	0.00000E+00
17	G	2.67926E-03	-2.24247E-03	4.00000E+04	0.00000E+00	0.00000E+00	0.00000E+00
20	G	0.00000E+00	0.00000E+00	3.99998E+04	0.00000E+00	9.46677E-04	0.00000E+00

BLAST ANALYSIS: BOUNDARY 1, TIME = 2.0000001E-02

D I S P L A C E M E N T   V E C T O R

POINT ID.	TYPE	T1	T2	T3	R1	R2	R3
5	G	3.93032E-03	-6.66073E-03	4.00005E+04	0.00000E+00	0.00000E+00	0.00000E+00
11	G	3.94475E-03	-6.59729E-03	4.00004E+04	0.00000E+00	0.00000E+00	0.00000E+00
17	G	4.09555E-03	-6.61223E-03	4.00004E+04	0.00000E+00	0.00000E+00	0.00000E+00
20	G	0.00000E+00	0.00000E+00	3.99999E+04	0.00000E+00	3.78194E-03	0.00000E+00

BLAST ANALYSIS: BOUNDARY 1, TIME = 3.0000003E-02

D I S P L A C E M E N T   V E C T O R

POINT ID.	TYPE	T1	T2	T3	R1	R2	R3
5	G	5.24542E-03	-1.17985E-02	4.00012E+04	0.00000E+00	0.00000E+00	0.00000E+00
11	G	5.34979E-03	-1.17052E-02	4.00011E+04	0.00000E+00	0.00000E+00	0.00000E+00
17	G	5.56774E-03	-1.17625E-02	4.00010E+04	0.00000E+00	0.00000E+00	0.00000E+00
20	G	0.00000E+00	0.00000E+00	4.00001E+04	0.00000E+00	7.32054E-03	0.00000E+00

BLAST ANALYSIS: BOUNDARY 1, TIME = 1.0000000E-01

D I S P L A C E M E N T   V E C T O R

POINT ID.	TYPE	T1	T2	T3	R1	R2	R3
5	G	8.20425E-03	-1.13775E-02	4.00047E+04	0.00000E+00	0.00000E+00	0.00000E+00
11	G	8.32891E-03	-1.12934E-02	4.00045E+04	0.00000E+00	0.00000E+00	0.00000E+00
17	G	8.52409E-03	-1.13581E-02	4.00044E+04	0.00000E+00	0.00000E+00	0.00000E+00
20	G	0.00000E+00	0.00000E+00	4.00036E+04	0.00000E+00	1.45867E-02	0.00000E+00

BLAST ANALYSIS: BOUNDARY 1, TIME = 2.0000003E-01

D I S P L A C E M E N T   V E C T O R

POINT ID.	TYPE	T1	T2	T3	R1	R2	R3
5	G	-2.32357E-03	2.20284E-03	4.00086E+04	0.00000E+00	0.00000E+00	0.00000E+00
11	G	-2.39051E-03	2.19695E-03	4.00086E+04	0.00000E+00	0.00000E+00	0.00000E+00
17	G	-2.40159E-03	2.22623E-03	4.00087E+04	0.00000E+00	0.00000E+00	0.00000E+00
20	G	0.00000E+00	0.00000E+00	4.00088E+04	0.00000E+00	-6.49708E-03	0.00000E+00

Figure 75. Abridged Output for the Blast Response Test Case

APPENDIX

MODIFYING THE ASTROS RUN TIME LIBRARY

One of the key features of the ASTROS software architecture is the ease with which a user may modify the system. The resultant ability to closely interact with the data resident on the ASTROS data base is a powerful addition to the set of tools that ASTROS provides for a user. The level of interaction with the existing system is entirely dependent upon the level of effort a user wants to expend to provide an additional capability to the system. As is discussed in Section IV of the User's Manual, these levels vary in complexity from simple modification of the standard executive sequence to the installation of new user application modules (sets of FORTRAN subroutines), bulk data, etc. This appendix introduces the mechanisms by which these more complex interactions are performed. It describes how additional modules may be added to the "Run Time Library" (the set of modules that can be called from MAPOL), additional bulk data entries may be defined, additional data base relational entities may be created and additional error messages may be installed for the system error message utility.

While the program developer may modify the ASTROS system through the modification of existing source code, the "user" is typically not prepared or able to go to such lengths. The features related to expanding the ASTROS run time library, however, are addressed through the inputs to the system generation program, SYSGEN. This standalone program creates a system data base which is used at run time by certain ASTROS system modules to obtain data to direct their action. In this way, the system may be grossly modified without direct modification of any existing software. Subsection 3.2 of the Programmer's Manual describes SYSGEN, its inputs, and the input formats and the formats in which the data are stored on the ASTROS system data base. Further, it indirectly documents which particular ASTROS utilities and application modules make use of these data to allow their "open-ended" operation. The Programmer's Manual is complete from the point of view of mechanics. However, to better illustrate the utility of the SYSGEN features to an advanced user (as opposed to the program developer), this appendix explicitly details the

installation of a new feature that requires an additional module, a new bulk data entry and a new relational entity. In addition, two new error messages are installed to handle possible error conditions that can occur in the new module. The additional module generates ELIST bulk data.

Subsection 3.2 of the Programmer's Manual should be read prior to the remainder of this document, since, without the Programmer's Manual, many of the particular aspects of this example may be obscure. A careful reading of the Appendix, however, in combination with the source code for the example module should provide the information needed to attempt similar modifications.

A.1 AUTOMATED SHAPE FUNCTION GENERATION

The shape function design variable linking in ASTROS requires the user to generate a coefficient associated with each finite element that is to be linked to a design variable. These coefficients define the "shape" that the global design variable controls. The user must manually determine the set of elements and their corresponding coefficients for each shape that is desired. One could, however, write a FORTRAN program which is directed by bulk data inputs to compute a set of coefficients for some set of standard shapes to ease the burden of input preparation.

As an example of this type of enhancement, such a FORTRAN program was written. The subroutine, called SHAPGN, to perform this preprocessor task is shown in Figure A-1. The code is designed to generate shapes in the form of completed ELIST bulk data entries based on a bulk data entry called SHPGEN, shown in Figure A-2. This bulk data input defines a design variable identification number, a set of finite elements to be linked to the design variable, a "shape" to be generated, and it provides inputs defining a new origin for the basic coordinate system to better generate the desired normalized coefficients. In this routine, the "shape" is limited to one of 27 combinations of the zeroth, first and second order basic coordinates of the center of the finite element. The SHAPGN subroutine interprets the SHPGEN data, along with the finite element summary data of element nodal coordinates and the ELEMLIST bulk data which is used to provide the list of associated elements.

```
      SUBROUTINE SHAPGN
C
C***********************************************************************
C     SHAPGN SUBROUTINE         AUTOMATED ELIST GENERATOR
C                               DJN
C             LASTMOD           14 JUNE, 1988
C***********************************************************************
C
C     GENERATES A SET OF ELIST ENTRIES FOR USE IN ASTROS BASED ON THE
C     ELEMENT CENTROIDS OF THE SPECIFIED ELEMENTS FROM:
C
C           1.  ELEMENT SUMMARY DATA PREPARED BY THE MAKEST MODULE AND
C               STORED IN THE RELATIONS:
C
C                    BEAMEST         BAR       ELEMENTS
C                    CONM2EST        CONM2     ELEMENTS
C                    QUAD4EST        QUAD4     ELEMENTS
C                    QDMM1EST        QDMEM1    ELEMENTS
C                    RODEST          ROD       ELEMENTS
C                    SHEAREST        SHEAR     ELEMENTS
C                    TRMEMEST        TRMEM     ELEMENTS
C
C               NOTE THAT ELAS1,2 AND MASS1,2 ARE NOT SUPPORTED SINCE
C               THEY HAVE NO SPATIAL COORDINATES
C
C           2.  THE SHPGEN RELATION OF INPUTS DEFINING THE DESIGN
C               VARIABLE ID, LIST OF ASSOCIATED ELEMENTS AND THE SHAPE
C               TO BE GENERATED BASED ON THE COORDINATES OF THE ELEMENT
C               CENTROID
C
C           3.  THE ELEMLIST RELATION CONTAINING THE LISTS OF ELEMENT
C               SETS.  THE SHPGEN RELATION TUPLES WILL REFERENCE THESE
C               ALREADY EXISTING BULK DATA ENTRIES.  THE ELEMENT TYPES
C               ON ELEMLIST ENTRIES THAT ARE SUPPORTED BY THIS ROUTINE
C               ARE:
C                      BAR
C                      CONM2
C                      QDMEM1
C                      QUAD4
C                      ROD
C                      SHEAR
C                      TRMEM
C
      CHARACTER*2      CONN1
      CHARACTER*4      SHAPE,       RO
      CHARACTER*8      BARNME,      BARSUM(7),   CM2NME,     CM2SUM(4),
     1                 QD4NME,      QD4SUM(13),  QD1NME,     QD1SUM(13),
     2                 RODNME,      RODSUM(7),   SHRNME,     SHRSUM(13),
     3                 TRMNME,      TRMSUM(10)
      CHARACTER*8      SHPGEN,      SHPLST(6)
      CHARACTER*8      ETYPE1(7),   ETYPE2(7),   ERR(2),     ETYPE,
     1                 OLDTYP,      BK,          NOFL,       SUMNAM,
     2                 CONNI,       CONNO,       STRING
```

Figure A-1. A FORTRAN Module for Generating ELIST Bulk Data Entries

```
      INTEGER          INFO(20,2), SG,         EL,          DVID,
     1                 ELMLID,     EID,        ETYPN,       ORDER,
     2                 SHPVAL,     SHPV0,      OLDEID
      REAL             RKOR(1),    SUMDAT(13), MAXREF
      LOGICAL          ABORT,      GETFLG
C
      COMMON /SHPKOR/  IKOR(1)
      COMMON /UNITS/   IREAD,      IRITE,      IDUM(12),    IPUNCH
C
      EQUIVALENCE      ( IKOR(1),  RKOR(1) )
      EQUIVALENCE      ( EID,      SUMDAT(1) )
C
      DATA             BK / ' ' /, RO / 'RO' /,
     1                 NOFL / 'NOFLUSH' /
      DATA             CONN1/ '+A' /
C
C     NAMES AND PROJECTION LISTS FOR ELEMENT SUMMARY DATA
C
      DATA       BARNME / 'BEAMEST' /,    LBAR / 7 /,
     1           BARSUM / 'EID',  'X1', 'Y1', 'Z1', 'X2', 'Y2', 'Z2' /
      DATA       CM2NME / 'CONM2EST' /,   LCM2 / 4 /,
     1           CM2SUM / 'EID',  'X', 'Y', 'Z' /
      DATA       RODNME / 'RODEST' /,     LROD / 7 /,
     1           RODSUM / 'EID', 'X1', 'Y1', 'Z1', 'X2', 'Y2', 'Z2' /
      DATA       QD1NME / 'QDMM1EST' /,   LQD1 / 13 /,
     1           QD1SUM / 'EID', 'X1', 'Y1', 'Z1', 'X2', 'Y2', 'Z2',
     2                          'X3', 'Y3', 'Z3', 'X4', 'Y4', 'Z4' /
      DATA       QD4NME / 'QUAD4EST' /,   LQD4 / 13 /,
     1           QD4SUM / 'EID', 'X1', 'Y1', 'Z1', 'X2', 'Y2', 'Z2',
     2                          'X3', 'Y3', 'Z3', 'X4', 'Y4', 'Z4' /
      DATA       SHRNME / 'SHEAREST' /,   LSHR / 13 /
     1           SHRSUM / 'EID', 'X1', 'Y1', 'Z1', 'X2', 'Y2', 'Z2',
     2                          'X3', 'Y3', 'Z3', 'X4', 'Y4', 'Z4' /
      DATA       TRMNME / 'TRMEMEST' /,   LTRM / 10 /,
     1           TRMSUM / 'EID', 'X1', 'Y1', 'Z1', 'X2', 'Y2', 'Z2',
     2                          'X3', 'Y3', 'Z3' /
C
C     NAME AND PROJECTION LIST FOR SHAPEGEN RELATION
C              DVID        DESIGN VARIABLE ID
C              ELMLID      ELEMLIST ID FOR LIST OF ASSOCIATED ELEMENTS
C              SHAPE       CHARACTER VARIABLE DEFINING DESIRED SHAPE
C                          A "NUMERIC" INPUT XYZ WHERE
C                              X = 0, 1, 2   ORDER OF X COORD. SHAPE
C                              Y = 0, 1, 2   ORDER OF Y COORD. SHAPE
C                              Z = 0, 1, 2   ORDER OF Z COORD. SHAPE
C
      DATA       SHPGEN / 'SHPGEN' /,     LSHP / 6 /
     1           SHPLST / 'DVID', 'ELMLID', 'SHAPE', 'X0', 'Y0', 'Z0' /
C
C     NAMES FOR ELIST ELEMENT TYPES.  FOR THIS ROUTINE, THE
C     "ELEMENT NUMBER" WILL CORRESPOND TO THE POINTER INTO THE ETYPE1
C     ARRAY.  NOTE THAT ALL ROD ELEMENTS WILL BE CONSIDERED CRODS
C     FOR PURPOSES OF THIS ROUTINE.  A MIXTURE OF CONRODS AND CRODS WILL
```

Figure A-1. A FORTRAN Module for Generating ELIST Bulk Data Entries (Continued)

```
C     REQUIRE MANUAL SEPARATION OF ELIST TERMS OR ALL CONRODS WILL
C     REQUIRE THE ETYPE ENTRY ON THE OUTPUT ELIST ENTRIES BE CHANGED TO
C     "CONROD" FROM "CROD"
C
      DATA        NSELM / 7 /
      DATA        ETYPE1 / 'CBAR',   'CONM2',   'CQUAD4',   'CQDMEM1',
     1                     'CROD',   'CSHEAR',  'CTRMEM' /
      DATA        ETYPE2 / 'BAR',    'CONM2',   'QUAD4',    'QDMEM1',
     1                     'ROD',    'SHEAR',   'TRMEM' /
C
C     SET SOME "TUPLE" LENGTHS FOR SOME IN-CORE TABLES
C
      DATA        LELST / 3 /,       LELM / 3 /
C
C     SET THE BASE OPEN CORE ADDRESS IN THE MEMORY MANAGER FOR LATER
C     MEMORY REQUESTS
C
      CALL MMBASE ( IKOR(1) )
C
C     OPEN THE SHAPEGEN RELATION, DETERMINE THE NUMBER OF TUPLES.
C     IF NONE,  RETURN
C
      CALL DBOPEN ( SHPGEN, INFO(1,1), RO, NOFL, ISTAT )
      NSHPGN = INFO(3,1)
      IF ( NSHPGN .LE. 0 ) THEN
         CALL DBCLOS ( SHPGEN )
         RETURN
      END IF
C
C     GET A MEMORY BLOCK TO HOLD SHAPEGEN TUPLES
C
      CALL MMGETB ( 'SHAP', 'RSP', LSHP*NSHPGN, 'SGP1', SG, ISTAT )
C
C     RETRIEVE ALL TUPLES INTO MEMORY BLOCK AND CLOSE RELATION
C
      CALL REPROJ ( SHPGEN, LSHP, SHPLST )
      CALL REGB ( SHPGEN, IKOR(SG), NSHPGN, ISTAT )
      CALL DBCLOS ( SHPGEN )
C
C     USE THE OFP UTILITY PRELEM WITH ENTRY POINTS ELMOE AND ELSRCH TO
C     INITIALIZE THE ELEMLIST DATA FOR RETRIEVAL.
C
      CALL PRELEM ( 'SGP1', IKOR(1) )
C
C     BEGIN GRAND LOOP ON SHAPEGEN BULK DATA ENTRIES.  EACH SHAPEGEN
C     ENTRY WILL GENERATE ONE ELIST BULK DATA ENTRY FOR EACH ELEMENT
C     TYPE IN THE CORRESPONDING ELEMLIST SET.
C
      ABORT = .FALSE.
      DO 8000 I = SG, SG + NSHPGN*LSHP - 1, LSHP
C
C        SET THE DESIGN VARIABLE ID, ELEMLIST ID AND CONVERT THE
C        SHAPE FROM HOLLERITH TO CHARACTER USING MACHINE DEPENDENT
```

Figure A-1. A FORTRAN Module for Generating ELIST Bulk Data Entries (Continued)

```
C        UTILITY
C
         DVID   = IKOR(I)
         ELMLID = IKOR(I+1)
         CALL DBMDHC ( IKOR(I+2), SHAPE, 4 )
         SHPV0 = 0
         IF ( SHAPE .NE. BK ) CALL XXSTOI ( *7999, SHAPE, SHPV0 )
         X0S    = RKOR(I+3)
         Y0S    = RKOR(I+4)
         Z0S    = RKOR(I+5)
         NPREF = 0
C
C        RETRIEVE THE POINTER "EL" TO THE PROPER ELEMLIST FROM ELMOE
C        NELM = -1 IF NO MATCHING ENTRY.  THIS IS A FATAL ERROR
C        THE PRELEM DATA IS IN THE FORM:
C                  ETYPE (2 HOLLERITH WORDS), EID
C
C        FOR EACH ELEMENT IN THE ELEMLIST.
C
         CALL ELMOE ( ELMLID, EL, NELM, IKOR(1) )
         IF ( NELM .LT. 0 ) THEN
C           *** USER FATAL ERROR ***
C           ELEMLIST $, REFERENCED ON SHAPEGEN ENTRY FOR D.V. $, DOES
C           NOT EXIST
            CALL XXITOS ( ELMLID, ERR(1) )
            CALL XXITOS ( DVID, ERR(2) )
            CALL UTMWRT ( 4, '30.1', ERR )
            ABORT = .TRUE.
            GO TO 8000
         END IF
C
C        ELEMLIST DATA SUCCESSFULLY FOUND, CONTINUE WITH THE PROCESSING.
C        GET A BLOCK OF MEMORY IN WHICH WE CAN STORE SIX WORDS FOR
C        EACH ELEMENT:
C                EID,  ETYPE #, PREF
C                ETYPE # IS THE ELEMENT TYPE NUMBER(POINTER TO ETYPE1,2)
C                PREF IS THE SHAPE FUNCTION COEFFIENT
C
         CALL MMGETB ( 'ELST', 'RSP', NELM*LELST, 'SGP2', L, ISTAT )
C
C        NOW LOOP ON EACH ELEMLIST ENTRY.  OPEN THE APPROPRIATE RELATION
C        AND SET THE PROJECTION LIST.  COMPUTE THE CENTROID FOR EACH
C        REFERENCED ELEMENT AND STORE EID, AND ETYPE # IN LIST.
C        NOTE THAT PRELEM HAS SORTED THE ELEMLIST DATA BY ELEMENT TYPE
C        AND BY EID.  ALSO, THE EST DATA ARE SORTED BY EID SO THAT WE
C        CAN USE LOGIC RELATED TO TWO SORTED LISTS
C
         OLDTYP = BK
         L1     = L
         MAXREF = 0.0
         DO 3000 J = EL, EL + LELM*NELM - 1, LELM
C
C           CONVERT THE ETYPE ON THE ELEMLIST TO CHARACTER
```

Figure A-1. A FORTRAN Module for Generating ELIST Bulk Data Entries (Continued)

```
C
          CALL DBMDHC ( IKOR(J), ETYPE, 8 )

          IF ( ETYPE .NE. OLDTYP ) THEN
C
C            CLOSE THE OLD EST IF NECESSARY
C
             IF ( OLDTYP .NE. BK ) CALL DBCLOS ( SUMNAM )
C
C            OPEN THE EST RELATION FOR THE NEW ELEMENT TYPE
C
             DO 100 K = 1, NSELM
                IF ( ETYPE2(K) .EQ. ETYPE ) GO TO 110
100          CONTINUE
C
110          CONTINUE
C
C            COMPUTED GOTO BRANCHING TO APPROPRIATE EST OPEN
C
             ETYPN  = K
             OLDTYP = ETYPE2(K)
             GETFLG = .TRUE.
             OLDEID = 0
             GOTO ( 1100, 1200, 1300, 1400, 1500, 1600, 1700 ), K
C
1100         CONTINUE
C
C               BAR ELEMENT
C
                CALL DBOPEN ( BARNME, INFO(1,1), RO, NOFL, ISTAT )
                CALL REPROJ ( BARNME, LBAR, BARSUM )
                FACTR  = 0.50
                LISTL  = LBAR
                SUMNAM = BARNME
                GO TO 2000
C
1200         CONTINUE
C
C               CONM2 ELEMENT
C
                CALL DBOPEN ( CM2NME, INFO(1,1), RO, NOFL, ISTAT )
                CALL REPROJ ( CM2NME, LCM2, CM2SUM )
                FACTR  = 1.0
                LISTL  = LBAR
                SUMNAM = CM2NME
                GO TO 2000
C
1300         CONTINUE
C
C               QUAD4 ELEMENT
C
                CALL DBOPEN ( QD4NME, INFO(1,1), RO, NOFL, ISTAT )
                CALL REPROJ ( QD4NME, LQD4, QD4SUM )
```

Figure A-1. A FORTRAN Module for Generating ELIST Bulk Data Entries (Continued)

```
          FACTR  = 0.25
          LISTL  = LQD4
          SUMNAM = QD4NME
          GO TO 2000
C
1400    CONTINUE
C
C         QDMEM1 ELEMENT
C
          CALL DBOPEN ( QD1NME, INFO(1,1), RO, NOFL, ISTAT )
          CALL REPROJ ( QD1NME, LQD1, QD1SUM )
          FACTR  = 0.25
          LISTL  = LBAR
          SUMNAM = QD1NME
          GO TO 2000
C
1500    CONTINUE
C
C         ROD ELEMENT
C
          CALL DBOPEN ( RODNME, INFO(1,1), RO, NOFL, ISTAT )
          CALL REPROJ ( RODNME, LROD, RODSUM )
          FACTR  = 0.50
          LISTL  = LBAR
          SUMNAM = RODNME
          GO TO 2000
C
1600    CONTINUE
C
C         SHEAR PANEL
C
          CALL DBOPEN ( SHRNME, INFO(1,1), RO, NOFL, ISTAT )
          CALL REPROJ ( SHRNME, LSHR, SHRSUM )
          FACTR  = 0.25
          LISTL  = LBAR
          SUMNAM = SHRNME
          GO TO 2000
C
1700    CONTINUE
C
C         TRMEM ELEMENT
C
          CALL DBOPEN ( TRMNME, INFO(1,1), RO, NOFL, ISTAT )
          CALL REPROJ ( TRMNME, LTRM, TRMSUM )
          FACTR  = 0.333333
          LISTL  = LBAR
          SUMNAM = TRMNME
C
2000    CONTINUE
      END IF
C
C     MERGE HERE AFTER ELEMENT DEPENDENT OPEN OPERATION
C     LOOP THROUGH THE EST RELATION AND FIND EID MATCHING
```

Figure A-1. A FORTRAN Module for Generating ELIST Bulk Data Entries (Continued)

```
C          THE ELEMLIST EID ( IKOR(J+2) ).  PROVIDE LOGIC TO ALLOW
C          NON-EXISTENT ELEMENTS TO BE REFERENCED
C
2100       CONTINUE
              IF ( GETFLG ) THEN
                 CALL REGET ( SUMNAM, SUMDAT, ISTAT )
                 IF ( ISTAT .NE. 0 ) GO TO 3000
                 IF ( EID .EQ. OLDEID ) GO TO 2100
                 OLDEID = EID
              END IF
C
C             CHECK IF EID'S MATCH
C
              IF ( EID .LT. IKOR(J+2) ) THEN
                 GETFLG = .TRUE.
                 GO TO 2100
              ELSE IF ( EID .GT. IKOR(J+2) ) THEN
                 GETFLG = .FALSE.
                 GO TO 3000
              END IF
C
C          MATCHING ENTRY, COMPUTE CENTROID AND STORE IN MEMORY
C
           GETFLG = .TRUE.
           X0     = 0.0
           Y0     = 0.0
           Z0     = 0.0
           DO 2200 NODE = 2, LISTL, 3
              X0 = X0 + FACTR * SUMDAT( NODE )
              Y0 = Y0 + FACTR * SUMDAT(NODE+1)
              Z0 = Z0 + FACTR * SUMDAT(NODE+2)
2200       CONTINUE
           X0          = X0 - X0S
           Y0          = Y0 - Y0S
           Z0          = Z0 - Z0S
C
C          NOW COMPUTE THE PREF VALUE BASED ON THE SHAPE
C          SAVE THE MAXIMUM VALUE FOR SUBSEQUENT NORMALIZATION
C
C             SHPVAL          SHAPE
C
C                0            UNIFORM
C                1            Z
C                2            Z*Z
C               10            Y
C               11            Y*Z
C               12            Y*Z*Z
C               20            Y*Y
C               21            Y*Y*Z
C               22            Y*Y*Z*Z
C              100            X
C              101            X*Z
C              102            X*Z*Z
```

Figure A-1. A FORTRAN Module for Generating ELIST Bulk Data Entries (Continued)

```
C               110             X*Y
C               111             X*Y*Z
C               112             X*Y*Z*Z
C               120             X*Y*Y
C               121             X*Y*Y*Z
C               122             X*Y*Y*Z*Z
C               200             X*X
C               201             X*X*Z
C               202             X*X*Z*Z
C               210             X*X*Y
C               211             X*X*Y*Z
C               212             X*X*Y*Z*Z
C               220             X*X*Y*Y
C               221             X*X*Y*Y*Z
C               222             X*X*Y*Y*Z*Z
C
      PREF = 1.0
C
C     DETERMINE ANY X CONTRIBUTION
C
      SHPVAL = SHPV0
      ORDER  = SHPVAL/100
      IF ( ORDER .GT. 0 ) THEN
         IF ( ORDER .EQ. 1 ) THEN
            PREF = PREF * X0
         ELSE IF ( ORDER .EQ. 2 ) THEN
            PREF = PREF * X0 * X0
         ELSE
            GO TO 7999
         END IF
      END IF
      SHPVAL = SHPVAL - ORDER*100
C
C     DETERMINE ANY Y CONTRIBUTION
C
      ORDER = SHPVAL/10
      IF ( ORDER .GT. 0 ) THEN
         IF ( ORDER .EQ. 1 ) THEN
            PREF = PREF * Y0
         ELSE IF ( ORDER .EQ. 2 ) THEN
            PREF = PREF * Y0 * Y0
         ELSE
            GO TO 7999
         END IF
      END IF
      SHPVAL = SHPVAL - ORDER*10
C
C     DETERMINE ANY Z CONTRIBUTION
C
      ORDER = SHPVAL
      IF ( ORDER .GT. 0 ) THEN
         IF ( ORDER .EQ. 1 ) THEN
            PREF = PREF * Z0
```

Figure A-1. A FORTRAN Module for Generating ELIST Bulk Data Entries (Continued)

```
            ELSE IF ( ORDER .EQ. 2 ) THEN
               PREF = PREF * Z0 * Z0
            ELSE
               GO TO 7999
            END IF
         END IF
C
         MAXREF = MAX ( MAXREF, ABS(PREF) )
C
         NPREF       = NPREF + 1
         IKOR( L1 ) = EID
         IKOR(L1+1) = ETYPN
         RKOR(L1+2) = PREF
         L1         = L1 + LELST
C
3000  CONTINUE
      IF ( OLDTYP .NE. BK ) CALL DBCLOS ( SUMNAM )
C
C     NORMALIZE THE PREF VALUES BY THE MAXIMUM PREF VALUE, MAXREF
C
      DO 3500 J = L+2, L+NPREF*LELST-1, LELST
         RKOR(J) = RKOR(J) / MAXREF
3500  CONTINUE
C
C     NOW ALL THE COEFFICIENTS ARE COMPUTED.  FOR EACH SEPARATE
C     ETYPN, WRITE AN ELIST ENTRY TO THE PUNCH FILE (UNIT IPUNCH)
C
      L1     = L
      LASTL  = L + NPREF*LELST - 1
      OLDTYP = BK
4000  CONTINUE
         ETYPN = IKOR(L1+1)
         ETYPE = ETYPE1(ETYPN)
C
C        ON FIRST ENCOUNTER OF NEW ETYPE, DETERMINE THE NUMBER OF
C        PREF VALUES AND WRITE THE PARENT ELIST BULK DATA ENTRY
C
         NPREF1 = 0
         DO 4100 KK = L1+1, LASTL, LELST
            IF ( IKOR(KK) .EQ. ETYPN ) NPREF1 = NPREF1 + 1
4100     CONTINUE
C
C        USE THE PREF COUNT TO SET THE PROPER CONTINUATION
C        NO CONTINUATION IS NEEDED IF LESS THAN 4 ENTRIES
C
         IF ( NPREF1 .GT. 3 ) THEN
            NE    = 3
            CONNO = CONN1
            WRITE (IPUNCH, 9000) DVID, ETYPE,
     1         (IKOR(JJ),RKOR(JJ+2),JJ=L1,L1+NE*LELST-1,LELST), CONNO
         ELSE IF ( NPREF1 .EQ. 3 ) THEN
            NE    = 3
            WRITE (IPUNCH, 9003) DVID, ETYPE,
```

Figure A-1. A FORTRAN Module for Generating ELIST Bulk Data Entries (Continued)

```
     1            (IKOR(JJ),RKOR(JJ+2),JJ=L1,L1+NE*LELST-1,LELST)
            ELSE IF ( NPREF1 .EQ. 2 ) THEN
               NE    = 2
               WRITE (IPUNCH, 9002) DVID, ETYPE,
     1            (IKOR(JJ),RKOR(JJ+2),JJ=L1,L1+NE*LELST-1,LELST)
            ELSE IF ( NPREF1 .EQ. 1 ) THEN
               NE    = 1
               WRITE (IPUNCH, 9001) DVID, ETYPE, IKOR(L1),RKOR(L1+2)
            END IF
C
C           WRITE THE REMAINING ENTRIES, IF ANY
C
            L1    = L1 + NE*LELST
            ITEST = NPREF1 - 4
            IF ( ITEST .GT. 0 ) THEN
               NCRDS = ITEST / 4 + 2
               DO 4200 KK = 2, NCRDS
                  CONNI = CONNO
                  CALL XXITOS ( KK, STRING )
                  CONNO = CONN1 // STRING
                  NE = 4
                  IF (KK .EQ. NCRDS) THEN
                     CONNO = BK
                     NE    = MOD ( NPREF1-3, 4 )
                     IF ( NE .EQ. 0 ) NE = 4
                     IF ( NE .EQ. 3 ) THEN
                        WRITE (IPUNCH, 9103) CONNI, (IKOR( JJ ),
     1                     RKOR(JJ+2),JJ=L1,L1+NE*LELST-1,LELST)
                     ELSE IF ( NE .EQ. 2 ) THEN
                        WRITE (IPUNCH, 9102) CONNI, (IKOR( JJ ),
     1                     RKOR(JJ+2),JJ=L1,L1+NE*LELST-1,LELST)
                     ELSE IF ( NE .EQ. 1 ) THEN
                        WRITE (IPUNCH, 9101) CONNI, IKOR(L1),RKOR(L1+2)
                     END IF
                  END IF
                  IF ( NE .EQ. 4 ) THEN
                     WRITE (IPUNCH, 9100) CONNI, (IKOR( JJ ),
     1                     RKOR(JJ+2),JJ=L1,L1+NE*LELST-1,LELST), CONNO
                  END IF
                  L1 = L1 + NE*LELST
 4200          CONTINUE
            END IF
C
C           LOOP BACK IF MORE DATA
C
            IF ( L1 .LT. LASTL ) GO TO 4000
C
C        FREE ALL MEMORY BLOCKS IN THE GROUP "SGP2"
C
         CALL MMFREG ( 'SGP2' )
         GO TO 8000
C
 7999    CONTINUE
```

Figure A-1. A FORTRAN Module for Generating ELIST Bulk Data Entries (Continued)

```
C
C          *** USER FATAL ERROR ***
C          ILLEGAL SHAPE $ SELECTED ON SHPGEN ENTRY FOR D.V. $
           ERR(1) = SHAPE
           CALL XXITOS ( DVID, ERR(2) )
           CALL UTMWRT ( 4, '30.2', ERR )
           ABORT = .TRUE.
C
8000  CONTINUE
C
C     FREE ALL MEMORY BLOCKS IN THE GROUP "SGP1"
C
      CALL MMFREG ( 'SGP1' )
C
C     IF A FATAL ERROR HAS OCCURRED, STOP THE PROGRAM USING THE EXIT
C     UTILITY
C
      IF ( ABORT ) CALL UTEXIT
C
C
C
9000  FORMAT ( ' ELIST', 2X, I8, A8,  3(I8, F8.5), A8 )
9001  FORMAT ( ' ELIST', 2X, I8, A8, I8, F8.5 )
9002  FORMAT ( ' ELIST', 2X, I8, A8,  2(I8, F8.5) )
9003  FORMAT ( ' ELIST', 2X, I8, A8,  3(I8, F8.5) )
9100  FORMAT ( A8, 4(I8, F8.5), A8 )
9101  FORMAT ( A8, I8, F8.5 )
9102  FORMAT ( A8, 2(I8, F8.5) )
9103  FORMAT ( A8, 3(I8, F8.5) )
      RETURN
      END
```

Figure A-1. A FORTRAN Module for Generating ELIST Bulk Data Entries (Concluded)

Input Data Entry SHPGEN Automated Shape Function (ELIST) Generation

Description: Defines the design variable id, the list of associated elements and the shape to be generated via the Shape Generation Utility, SHAPEGEN.

Format and Examples:

1	2	3	4	5	6	7	8	9	10
SHPGEN	DVID	ELMLID	SHAPE	X0	Y0	Z0			
SHPGEN	10	1000	201	100.0	0.0	0.0			

Field	Contents
DVID	Design variable identification number (Integer > 0)
ELMLID	ELEMLIST set identification number for associated elements (Integer >0)
SHAPE	The desired shape (Text) (see remark 1.)
X0	X-coordinate in the basic system of the new origin for shape generation
Y0	Y-coordinate in the basic system of the new origin for shape generation
Z0	Z-coordinate in the basic system of the new origin for shape generation

Remarks:

1. The shape is a character input that consists of one to three digits, xyz, where

   x is 0, 1 or 2 and denotes the order of the contribution of the element centroid's x-coordinate to the shape: 1, x or x*x

   y is 0, 1 or 2 and denotes the order of the contribution of the element centroid's y-coordinate to the shape: 1, y or y*y

   z is 0, 1 or 2 and denotes the order of the contribution of the element centroid's z-coordinate to the shape: 1, z or z*z

2. The ELMLID refers to an ELEMLIST bulk data entry that is normally used for element output requests. The associated element set provides the list of elements to be included in the ELIST entries that are generated.

Figure A-2. The SHPGEN Bulk Data Entry

Obviously, this is not the sort of enhanced feature that the novice user could devise without the Programmer's Manual to provide information on the form of the element data and the module which computes it. This feature does, however, serve to illustrate the installation of a module and, further, the module that is installed has some utility outside the scope of this appendix. Also, the source code of the SHAPGN routine can serve as a brief introduction to the application programmer's interface to the ASTROS data base.

A.2 INSTALLATION OF THE NEW RELATIONAL ENTITY

The bulk data entry shown in **Figure A-2** is the data format that the user must provide. As discussed in Subsection 3.2.3 of the Programmer's Manual, the Input File Processor (IFP) module translates the user input and stores it in data base relations as directed by the bulk data templates. In the process of designing the SHAPGN routine, the form of any bulk data entries and their associated data base relations have to be defined. In this case, it is a simple task to define a relational data base entity that has one "attribute" for each of the fields of the bulk data entry. The relation is given, for convenience, the same name as the bulk data entry and each attribute is named after a field. **Figure A-3** shows the resultant lines that must be inserted into the Relation Definition file for SYSGEN.

It is not necessary to declare this relational schema in the SYSGEN file; it merely avoids the complication of defining the schema at run time via the MAPOL sequence. This latter alternative is documented in Appendix B of the ASTROS User's Manual. By defining the schema in the SYSGEN input, the user need only declare the relational variable in the MAPOL sequence.

A.3 INSTALLATION OF THE NEW BULK DATA ENTRY

The ASTROS bulk data template for the SHPGEN bulk data entry is shown in **Figure A-4**. Unlike entries in all the other SYSGEN input files, the template definition must be installed in a particular location in the Template Definition file. The IFP module requires that the templates be defined in alphabetical order by bulk data entry name. In this case, the SHPGEN entry must be defined after the SET2 bulk data entry and before the SPC entry. Since there are no continuation lines for this bulk data entry, the template consists of a single template set of six lines. The first, LABEL, line

SHPGEN	6	
DVID	INT	0
ELMLID	INT	0
SHAPE	STR	4
X0	RSP	0
Y0	RSP	0
Z0	RSP	0

Figure A-3. Definition of the SHPGEN Relation

```
SHPGEN  |DVID    |ELEMLID|SHAPE   |X0      |Y0      |Z0      |        |        |        |
CHAR     INT      INT     CHAR     REAL     REAL     REAL
DEFAULT                   0
CHECKS   GT 0     GT 0
         1        2       3        4        5        -6
SHPGEN   DVID     ELMLID  SHAPE    X0       Y0       Z0                         290      $
```

Figure A-4. The SHPGEN Bulk Data Template

identifies the fields by name so that IFP can label the fields in any error messages. The second, DATA TYPE, line defines the data type associated with each bulk data field. In this case, each field is uniquely integer (INT), real (REAL) or character (CHAR). The third, DEFAULT, line is labeled as such in the first eight character field and is blank thereafter except for the SHAPE field since there are no defaults for any other data fields. The SHAPE field defaults to the character "0", which implies that a uniform shape is generated by default. The absence of defaults in the remaining fields means that the data defaults to 0 or 0.0, depending on the data type of the field. The fourth, CHECKS, line contains the requirements that IFP will impose on the data in each field. In this case, the design variable identification number, DVID, and the ELEMLIST identification number must both be greater than 0. The other data have no requirements placed on their values. However, there are explicit requirements on the SHAPE field. As a matter of definition, the software designer has determined that it must be a character string containing one to three characters, each of which must be 0, 1 or 2. Clearly, IFP could check the data in this field for its validity, but it would not be one of the standard checks so that it was expedient to put the validity check in the SHAPGEN routine.

The fifth, LOAD POSITION, line and the sixth, PROJECTION, line are closely related. The load position indicates the location in the data base loading array where the data are to be stored prior to performing the "write" operation to the data base. The sixth line defines the data base entity name and the relational "projection" to be used by the data base. These two lines are interrelated in that the projection (or set of attributes to be included in the data base operations) defines the order in which the data must be stored. For example, the DVID attribute appears first in the projection list, so that any data base read or write operations will have DVID values in the first word of the relation "row" that is read or written. Since there are no multiple data type fields, eight character data fields or other special cases, there is a one-to-one correspondence between the load positions, the attribute names and the data fields of the template. This particular example is very simple in this respect, but numerous standard examples in the ASTROS SYSGEN input files show some of the other features.

A.4 INSTALLATION OF THE NEW MODULE DEFINITION

The new module is defined to ASTROS through modifications to the Module Definitions file that is one of the SYSGEN inputs. **Figure A-5** shows eight lines of data that are required in this file to enable the addressing of the SHAPGN routine by the MAPOL code. The first line defines the MAPOL addressable module name, SHAPEGEN. It is not necessary that the MAPOL name have any correspondence with the FORTRAN name and the MAPOL name can be up to eight characters long. The second argument on the first line of the module definition indicates that there are no arguments to the MAPOL module. The next line indicates that the routine is a MAPOL procedure (equivalent to a FORTRAN subroutine) rather than a function. If the module had any arguments, their valid types would also be given on this line. The third line contains a single integer which gives the number of lines that follow that are FORTRAN program lines to be written to the XQDRIV subroutine. (The XQDRIV subroutine referred to is the SYSGEN output that provides a link between the MAPOL calls and the FORTRAN routines that are invoked.) In this case, there are three comment lines (that assist in keeping the Module Definition file documented) and two executable FORTRAN lines. The first FORTRAN line calls the subroutine, SHAPGN, while the second sets the module name that the ASTROS executive system will use in the execution timing summary. Whenever the Module Definition file is modified, the new XQDRIV routine must be linked into ASTROS.

A.5 INSTALLATION OF THE NEW ERROR MESSAGES

The SHAPEGEN module requires two additional error messages in the error message text file. These are added to the SYSGEN Error Message Text file as shown in **Figure A-6**. The choice of module number, 30, is arbitrary except that it must be unique (i.e., currently unused) and the module number in the Error Text file must match that used in the UTMWRT utility module calls in the source code. A quick study of the source code along with information in the Programmer's Manual and **Figure A-6** should be sufficient to understand how error messages are defined to ASTROS and used by UTMWRT. This capability is of lesser importance in any event, since a simple FORTRAN write statement to the proper unit would clearly suffice. In this example, however, the SHAPGN module is sufficiently useful to the program developers that it has been completely integrated as a "special feature."

```
SHAPEGEN   0
 102
   5
C
C      PROCESS 'SHAPEGEN' MODULE TO GENERATE ELIST ENTRIES
C
       CALL SHAPGN
       MODNAM = 'SHAPEGEN'
```

Figure A-5. Definition of the SHAPGEN Module

```
*MODULE 30      SHAPE GENERATION MESSAGES
'ELEMLIST $, REFERENCED ON THE SHPGEN ENTRY FOR DESIGN VAR. $, DOES NOT EXIST.'
'ILLEGAL SHAPE $ WAS SELECTED ON SHPGEN ENTRY FOR DESIGN VARIABLE $.'
```

Figure A-6. Error Messages for the SHAPGEN Module

A.6 USING THE NEW FEATURE

After the above modifications have been made to the SYSGEN inputs, the SYSGEN program must be executed and the new XQDRIV module linked into the system. At this point, the standard execution of ASTROS is completely unaffected by any changes made. In order to invoke the new module, the MAPOL sequence must be modified in the appropriate manner to include the call to the SHAPEGEN module. "The appropriate manner" means that the user must know where in the sequence to call the new module. This knowledge is the limiting factor for new users who wish to make modifications to the system. In this case, the MAPOL sequence up to and including the call to MAKEST on Line 199 of the standard sequence (as shown in Appendix C of the User's Manual) generates all the data needed by the SHAPEGEN module. Therefore, to invoke the module, a simple insert of the MAPOL line:

```
CALL SHAPEGEN;
```

after Line 199 causes the module to interpret any SHPGEN bulk data entries and write the ELIST bulk data to the ASTROS punch file.

Figure A-7 shows an example input deck based on the Intermediate Complexity Wing model of Subsection 4.7 and 4.8. It includes all the changes needed to invoke this new feature as a "preprocessor" function. This is done by running the standard input deck modified to include the SHPGEN bulk data entries through the MAKEST module and then calling the SHAPEGEN module to punch the ELIST entries. Following the execution, the user would add the appropriate DESVAR entries to complete the design variable linking and then rerun ASTROS to perform the desired optimization task.

```
ASSIGN DATABASE ICWCU PASS NEW DELETE
EDIT NOLIST
INSERT 7
$                                                                   $
$        DECLARE THE RELATIONAL ENTITY FOR THE SHAPEGEN            $
$        BULK DATA ENTRY                                            $
$                                                                   $
RELATION     SHPGEN;
$                                                                   $
$        REPLACE THE ENTIRE SEQUENCE AFTER MAKEST WITH A            $
$        CALL TO OUR SHAPEGEN MODULE                                $
$                                                                   $
REPLACE 200, 1531
CALL SHAPEGEN;
SOLUTION
TITLE = INTERMEDIATE COMPLEXITY WING
SUBTIT = QUAD4 ELEMENTS WITH 153 DESIGN VARIABLES
OPTIMIZE STRATEGY = 57
 PRINT DCON
   BOUNDARY SPC = 1
      STATICS ( MECH = 1  )
      STATICS ( MECH = 2  )
      LABEL = COMPOSITE STRUCTURE WITH FIBER ORIENTATIONS (0,90,+45,-45)
END
BEGIN BULK
$         .
$         .
$     OMITTED BULK DATA FOR THE INTERMEDIATE COMPLEXITY WING MODEL
$         .
$         .
$ BULK DATA FOR SHAPE GENERATION OF INTERMEDIATE COMPLEXITY WING
$
$ D.V. 1 -- UNIFORM OVER UPPER AND LOWER SURFACE
$
SHPGEN, 1, 100, 0
$
$ D.V. 2 -- LINEAR IN Y OVER UPPER AND LOWER SURFACE
$
SHPGEN, 2, 100, 10
$
$ D.V. 3 -- LINEAR IN X OVER UPPER AND LOWER SURFACE
$
SHPGEN, 3, 100, 100
$
$ D.V. 4 -- QUADRATIC IN X OVER UPPER AND LOWER SURFACE
$
SHPGEN, 4, 100, 200
$
$  SINGLE ELEMLIST ENTRY CONTAINING ALL SKIN ELEMENTS ON UPPER
$  AND LOWER SURFACES
$
ELEMLIST, 100, TRMEM, 1, 2
ELEMLIST, 100, QUAD4, 3, THRU, 64
```

Figure A-7. A Sample Input Data Stream for Generating ELIST Bulk Data Entries